Design, Development and Analysis of a Sustainable Drinking Water Scheme – Storage, Filtration, and Sludge Disposal

THESIS

Submitted in partial fulfillment of the requirements for the degree of

DOCTOR OF PHILOSOPHY

By

SOUMYA KAR

(2016PHXF0405P)

Under the supervision of

Dr. RAJIV GUPTA

Senior Professor, Department of Civil Engineering

BIRLA INSTITUTE OF TECHNOLOGY AND SCIENCE

PILANI-333031 (RAJASTHAN), INDIA

2023

BIRLA INSTITUTE OF TECHNOLOGY AND SCIENCE

PILANI-333031 (RAJASTHAN), INDIA

CERTIFICATE

This is to certify that the thesis entitled **"Design, Development and Analysis of a Sustainable Drinking Water Scheme – Storage, Filtration, and Sludge Disposal"** and submitted by **Ms. Soumya Kar**, ID No. **2016PHXF0405P** for the award of Ph.D. of the Institute embodies original work done by her under my supervision.

(Signature of the Supervisor)

Name: **Prof. Rajiv Gupta**

Department: **Department of Civil Engineering**

BITS Pilani, Pilani Campus

Date:

ACKNOWLEDGEMENTS

This study results from the unconditional cooperation and steadfast support of my supervisor, parents, and friends.

This aspiration would not have been possible without the knowledge and expertise shared by my professor, Senior Professor Rajiv Gupta. His invaluable patience, feedback, and critical insights have supplied the foundations of the present work. Prof. Rajiv Gupta was extraordinarily encouraging and instrumental in developing various arguments for the thesis. His constant motivation throughout the journey instilled confidence to undertake my research journey.

During my research, various individuals and institutions have been generous with their support. I extend my deepest gratitude to my defense committee, Associate Professor Suvendu Narayana Patel, Department of Civil Engineering, and Profesor Prabhat Nath Jha, Department of Biological Sciences, who generously provided knowledge and expertise. Additionally, I am thankful to the Department of Science and Technology, Government of India, for the financial assistance for my work. Further, I express my gratitude to the CSIR - Institute of Minerals and Materials Technology, Bhubaneswar; State Water Testing Laboratory, RWSS, Khandagiri, Bhubaneswar; and the Department of Chemistry, Utkal University, Bhubaneswar for allowing the usage of their laboratory facilities for conducting characterization studies.

I am also grateful to all other faculty members of the Department of Civil Engineering for their valuable comments through the different stages of my work. I am immensely thankful to Professor Anshuman, Professor Anupam Singhal, and Professor Ajit Pratap Singh for providing the necessary institutional support at various stages of my work.

I am also grateful to my colleagues for their editing help, late-night feedback sessions, and moral support. I want to take this opportunity to thank, in a personal capacity, my seniors, batchmates, and juniors, Dr. Gaurav Kumar, Dr. Makrand Wagale, Dr. Vidhi Vyas, Dr. Harish Pupalla, Dr. Vidumasetthi Shudir, Dr. Rahul Daundotiya, Lt. Col. (Dr.) Virendra Singh Phoghat, Dr. Raya Raghavendra, Mr. Akshay Kumar, and Mr. Deshbhushan Patil for their constant encouragement on this long journey.

Thanks should also be extended to the librarians, research assistants, and participants from the study areas, who impacted and inspired me. Mr. Shivpal Saini, Mr. Jaspal, Mr. R D Soni, and

Mr. Suresh Saini have provided all required assistance during the experiments. Mr. Ramesh and Mr. Sultan have been helpful during the survey and implementation stages of the study.

I would be remiss in not thanking my family for their constant emotional support and unyielding patience through my Ph.D. journey. My parents, Mr. Santosh Kumar Kar and Mrs. Pravati Kumari Mohapatra, have been my support and significant source of encouragement during this long and arduous journey. I extend special appreciation to my uncles, aunts, cousins, and grandparents from both my paternal and maternal sides for their unspoken support through the journey. Their beliefs have kept my spirits and motivation unwavering during this process.

Lastly, I thank the Almighty, whose blessings guided me from inception to complete this research work. Each moment during this work, I experienced the Grace of God, who continuously enhanced my intelligence even in moments of despair, inspired me to move forward, opened before me unexpected avenues, and enlightened my thoughts with His/her wisdom.

ABSTRACT

India is one of several countries facing increasing scarcity, as more than two billion people live in areas with a high level of water stress. With evolving urban areas and a booming economy, the destructive impacts of both physical and economic water scarcity loom in the distance. Apart from anthropogenic activities, climatic changes leading to reduced and uneven rainfall over the country's landmass further aggravate the problem of water stress. Aside from recent efforts to connect rural areas to piped water, most of the country relies on groundwater to meet its needs. Groundwater reserves in the country contribute significantly to the agriculture and industrial sectors. However, groundwater pollution is a persistent area of concern.

Persistent fluoride poisoning is endemic in several states in India due to the excess quantity of Fluoride in drinking water sources. Rural areas especially suffer where this health problem is relatively more prevalent. The lack of infrastructure for water storage from an alternate source and the unavailability of low-cost household water treatment systems further reinforces the public health issue. While the financial burden is recognized as a significant barrier to rural water infrastructure, the lack of a sense of ownership and participation among the local community further exacerbates the problem of water-related scarcity and health issues.

The work carried out in this study starts with the hypothesis of establishing an efficient water infrastructure system, with water storage, water treatment, and disposal of sludge produced as integrated and interrelated components. The proposed approach is designed to aid the existing water infrastructure system at a rural household level. The provision, distribution, and management of water resources in rural areas constitute rural water management. Rural water management guarantees that rural populations can access safe and dependable water supplies for drinking, agriculture, and other critical uses. Due to a lack of infrastructure and limited resources, water management systems in many rural locations are neglected more than in urban areas. Rural populations rely primarily on traditional water sources, such as wells and springs, due to the lack of access to contemporary water treatment and delivery systems, reducing water supply and quality and increasing susceptibility to several diseases.

In the initial phase of the study, water samples were collected from selected study areas in Rajasthan, India, and evaluated for fluoride concentrations. With analyte concentrations exceeding permissible thresholds, fluoride toxicity was determined through Health hazard risk assessment (HHRA). A worrying situation was observed with reported Ingestion hazard quotient (IHQ) values exceeding one. The sample analysis results were corroborated by literary

evidence of high fluoride concentration in the study region. The prevalent issue of fluoride toxicity pushes decision-makers to achieve a paradigm toward sustainable water infrastructure through the inclusion of alternate sources of water.

Rainwater is one of the safest sources of alternate water, with rainwater harvesting (RWH) as one of the most accessible and widely accepted water-harvesting techniques. Typical rainwater harvesting systems include a catchment area, such as a roof, a gutter system to collect the water, a storage tank or cistern, and a distribution system to carry the water to where it is required. The rainwater harvested can be stored in various facilities, including above-ground tanks, underground cisterns, and subsurface aquifers. Household water storage facilities form an integral part of water management systems and play a critical role in guaranteeing a stable and regular water supply for different purposes. Nonetheless, storage facilities may have an adverse effect on water quality, making the study of storage structure materials crucial.

In this study, two RWH tank materials were proposed. Jute and Glass fiber-reinforced polymer (JFRP and GFRP) composites were evaluated for their suitability as a storage infrastructure by physio-chemical water analysis. Plastic migration of tank material, water absorption, and determination of Bisphenol A from the water sample were other tests performed on the proposed composite tank material. The GFRP was further commissioned for installation as a household RWH structure in the study region due to the encountered disadvantages with JFRP. Strength analysis was performed on the fabricated tank samples to understand their durability on site.

Access to low-cost household water-treatment systems (HWTs) has a vital role in improving the health of residents, although an RWH system reduces dependence on groundwater resources. Fluoride sequestration through locally available bio-adsorbents and low-cost gravity filters is a novel area covered in this study. The locally available plant, Khejri (*Prosopis cineraria*), was used to develop a low-cost, reusable, and effective adsorbent. A rapidly growing subject in the modeling of adsorbent performance is machine learning. It is a subfield of artificial intelligence dealing with developing data-learning and prediction systems. In modeling adsorbent performance, machine learning can be used to analyze huge volumes of data from multiple sources, such as laboratory tests, simulations, and field investigations, to uncover patterns and correlations between different parameters that influence adsorbent performance. With the advantages accorded, machine learning techniques formed a characteristic part of the study assisting in the predictive modeling of the performance of the developed adsorbent.

Low-cost water filters constitute an essential part of robust HWTs. The filters analyzed in this study were prepared from cement and ceramic as raw materials, in addition to sugarcane, potato slurry, and activated carbon. Women and girl children are majorly responsible for fetching water for a household. Water collection activities are intended to supplement scarce household resources and improve the family members' well-being. This time taking and tedious activity takes a negative toll on the role of women and girls in decision-making. The provision of an on-site RWH structure will comparatively reduce the pressure of water collection though not completely eradicated. A functioning, low-cost, and energy-efficient water filter will further alleviate the burden of boiling water and re-contamination owing to improper storage. Participation of the households, especially female members, fosters a sense of ownership in the community, which enriched our discussion and comprehension of the ground reality and the needs of the people.

Concurrent with the fabrication of the water filters lies the inherent need for the safe disposal of fatigued filter plates. Safe disposal aims to prevent contamination of groundwater sources, justifying the primary hypothesis of an efficient rural water management system assisting a household. Monitoring the soil fluoride levels in replicated disposal conditions through experimental simulations and predictive models provided an intrinsic view of the efficiency of the proposed disposal system.

A sustainable water management system plays a critical role in ensuring the availability of clean and safe water for communities, agriculture, and industry. Implementing such a system involves multiple steps, such as design, fabrication, and experimentation. Through the study, an operational water management system focused on sustainability was developed.

Keywords: Fluoride, Health hazard risk assessment (HHRA), Household water treatment systems, Machine learning, Rainwater harvesting

TABLE OF CONTENTS

LIST OF FIGURES

LIST OF TABLES

LIST OF ABBREVIATION

AARE – Absolute average relative error

ADD – Average daily dose

AI – Artificial intelligence

ANFIS - Adaptive neuro-fuzzy inference system

ANN – Artificial Neural network

ASTM – American Society for Testing and Materials

Bgl - Below ground level

BIS – Bureau of Indian Standards

BPA – Bisphenol A

BW – Body weight

CGWB – Central Groundwater Water Board

CH_3COOH – Acetic Acid

Cl^- – Chloride

CWF – Ceramic water filter

DO – Dissolved Oxygen

DSC – Differential Scanning Calorimeter

EC - Electrical Conductivity

EDTA - Ethylenediamine tetraacetate

EDX – Energy dispersive X-Ray

EF – Exposure factor

F^- - Fluoride

FIS – Fuzzy Inference System

FTIR – Fourier transform infrared spectroscopy

GA – Genetic Algorithm

GEC - Groundwater estimation committee

GFRP – Glass fiber reinforced polymer

HCL – Hydrochloric Acid

HHRA – Human health risk assessment

HI – Hazard Index

HWTs – Household water treatment systems

HYBRID – Hybrid fractional error function

IHQ – Ingestion Hazard quotient

IR – Daily intake rate of contaminated water or ingestion rate

IWRM - Integrated Water-Related Management

JFRP – Jute fiber-reinforced polymer

KNO_3 – Potassium Nitrate

l/day – liters per day

l/hr – liters per hour

LC-MS - Liquid chromatography-mass spectrometry

MAE – Mean absolute error

MARE – Mean absolute relative error

mg/l – milligram per liter

ML – Machine learning

MOS – Margin of safety

Mpa – Megapascal

MSE – Mean square error

Na^{2+} – Sodium

NaF – Sodium Fluoride

NaOH – Sodium Hydroxide

NDT – Non-destructive testing

NTU – Nephelometric Turbidity Units

OVAT – One-variable-at-a-time

PCWF – Porous cement water filter

POUWT – Point of use water treatment

ppm – Parts per million

R^2 – Coefficient of regression

RCC – Reinforced cement concrete

R_fD – Reference dose

RMSE – Root mean square error

RO – Reverse Osmosis

Rpm – Rotations per minute

RWH – Rainwater harvesting structures

RWRM – Rural Water Resource Management

SDG – Sustainable Development Goal

SEM – Scanning electron microscope

SODIS – Solar Disinfection

SSE – Sum of the squares of the errors

TDS – Total Dissolved Solids

TGA – Thermogravimetric Analysis

TH – Total Hardness

UN - United Nations

UPV - Ultrasonic pulse velocity

USEPA - United States Environmental Protection Agency

UTM – Universal Testing Machine

UV – Ultra-violet

WHO – World Health Organization

WQI – Water quality index

WTS – Water treatment sludge

XRD - X-ray powder diffraction

μm – micro-meter

1 INTRODUCTION

The only planet that appears blue from space is Earth, a striking indication of water's ubiquitousness. Water is the most extraordinary resource, yet frequently being viewed as very pervasive. Humans desire to possess land masses from the moment they are born, yet overlook water resources, considering it an ever-flowing entity. Water bodies have been a part of the human cycle for thousands of years. Besides being culturally significant, water bodies have assisted the human population by supporting the growth of industries, farming, transportation, and recreation. Besides humans, every living creature directly or indirectly depends upon water.

The seas control 97.5% of the water cycle on Earth. Excluding the 1.7% frozen water, a mere 1% of our water stock consists of fresh liquid and atmospheric water, supporting terrestrial life. Besides its life-sustaining distinction, water is a subtle and delicate balancing entity within a much bigger system (Grey et al., 2013).

While dangers associated with water threaten society on a local, national, and international level, they are increasingly doing so globally because of the fast changes in the economy, population, and environment. These changes increase the urgency to understand better how more significant global changes may influence freshwater supply, even if we are not "running out of water."

The nation-states can no longer serve as the primary foundation for water management since water does not respect national boundaries or sovereignty (Milly et al., 2008). To safeguard and conserve our "one blue planet," "water security" must be achieved at all scales as part of risk management for the water sector. While most of the poor suffer from severe water insecurity and are exposed to acute water-related hazards by complicated hydrology, the wealthier people in the world have fewer threats from water and less complex hydrology. A split world results from the inverse link between hydrological complexity and prosperity. To attain global water security, scientists, policymakers, and water managers must address this divide.

Over the past century, nation-states and urban jurisdictions surrounding water bodies have evolved to manage water-related risks, developments, and trade-offs, resulting in beneficial effects on health, productivity, and ecological management. These favorable results have given individuals, primarily women, greater control over the risks of unstable systems (Grey et al.,

2013). However, water-related risks remain very high and unmanaged in many developed and underdeveloped nations.

While sufficient freshwater is available globally to fulfill all present and future water needs, its territorial and temporal distributions are not homogeneous. There are several regions where the lack of clean water for drinking and sanitation is a peruse of constraint on human health and productivity, economic development, and the maintenance of a clean environment and healthy ecosystems (Cosgrove & Loucks, 1974). Pollutants, broadly categorized as anthropogenic and natural, pose a severe threat to human health and the aquatic ecosystem (Madhav et al., 2020). Besides water scarcity, polluted water poses a significant barrier to universal access to safe drinking water perturbing Sustainability Development Goal-6.

Adopted by all the United Nations Member States in 2015, the 2030 Agenda for Sustainable Development provides a road map for peace and prosperity for people and the planet in the present and the future. At its center are the seventeen Sustainable Development Goals (SDGs), an urgent call to action for all rich and developing countries in a global partnership based on the goals laid down in the agenda. It is established that alleviating poverty and other deprivations must be accompanied by programs that promote health and education, reduce inequality, and drive economic growth, all while tackling climate change and conserving our oceans and forests.

SDG-6 is one of the seventeen goals with the official wording “Ensure availability and sustainable management of water and sanitation for all.” At its heart, the SDG contains six outcome-oriented targets, expressly, safe and affordable drinking water; end to open defecation and improved access to sanitation and hygiene; improve water quality by reducing pollution, efficient wastewater treatment and safe reuse; increase water-usage efficiency and assure sustainable withdrawals and supply of freshwater; employ integrated water resources management (IWRM) and protect and restore water-related ecosystems.

India is a vast country with multifaceted topography and climatic zones. The country witnesses an uneven spatial distribution of water resources, from the drier northwest, where rainfall is scarce (in the range from 100 to 574 mm), to the northeast, the highest rainfall-receiving region on the planet (averaging over 2000 mm) (Goyal & Surampalli, 2018). Rainfall in the mainland is primarily dependent upon the southwest and northeast monsoons. The nation is gifted with a river system comprising more than 20 significant rivers, perennial and seasonal (Kumar et al., 2005). Besides a vast river network, groundwater resources form an extensive part of the

Indian subcontinent. Groundwater has emerged as a crucial democratic water supply and poverty alleviation tool, significantly contributing to India's economic growth and is a vital accelerator for its socioeconomic development (Jha & Sinha, 2009). However, groundwater behavior across the Indian subcontinent is highly complex due to varied geological formations with significant lithological and historical variations, a complex tectonic framework, climatological variables, and distinct hydro-chemical situations.

As per international norms, if the water availability of a region is less than 1700 m^3 and the per capita availability is less than 1000 m^3, then the country is categorized as water-stressed and water scarce, respectively. Though India receives a yearly average of 4000 km^3 of rainfall, by 2050, India's overall water supply is expected to be lower than the forecast demand, with per capita surface water availability projected at 1191 m^3. Low rainfall, poor water management, lack of storage, and decrepit infrastructure will lead to 65 % of the country's reservoirs running dry (NITI Aayog, 2018). Therefore, adopting an efficient, cost-effective, and robust water management system to meet current and future water demands is indispensable.

While rivers are polluted due to dumping waste from industries, refineries, sewage treatment plants, and runoff from agricultural fields, aquifers are susceptible to over-drawing, leading to reduced water tables primarily during non-monsoon or drier periods.

As per an assessment report by the Groundwater Estimation Committee (GEC)-1997, of the 5723 assessment units, 14.7%, 3.9%, 9.61%, and 71.25% were categorized as over-exploited, critical, semi-critical, and safe, respectively (Jha & Sinha, 2009).

Recent estimates for groundwater level data (Pre-monsoon 2019) indicate that out of the total 14555 monitoring wells analyzed, 751 (5%) wells are showing water levels less than 2 m bgl (meters below ground level). Whereas 3433 (24%) wells indicate a water level of 2-5 m bgl, followed by 5933 (41 %), 3402 (23%), 786 (5%), and 250 (2%) wells showing water levels in the range of 5-10 m bgl, 10-20 m bgl, 20-40 m bgl, and > 40 m bgl, respectively (Central Ground Water Board, 2020).

Due to the significance of groundwater to India's water supply system, its availability and quality must be carefully monitored. Although groundwater typically lacks the microbiological contamination found in surface waters, natural or geogenic chemical contaminants are a problem (Podgorski et al., 2018; Saha et al., 2016).

The country's groundwater reserves are classified as calcium bicarbonate type when the total salinity of the water is below 500 mg/l, and electrical conductance corresponds to 750 μS/cm.

The groundwater represents a mix of cationic and anionic types when electrical conductance is between 750 and 3000 μS/cm. While for conductance above 3000 μS/cm, groundwater is classified as Na-Cl type. Further, some pockets of the country have observed high concentrations of physicochemical parameters such as chloride, Fluoride, iron, arsenic, and nitrate (Central Ground Water Board, 2010).

Contaminant sequestration in drinking water and safe access to and storage of contaminant-free water is the foundation of a society's overall sustainability. In the subsequent sections of the chapter, a concise overview of the thesis's central theme is provided through a brief discussion covering every component of storage, filtration, and sludge disposal.

1.1 Adequate water storage infrastructure in rural areas

Since water consumption varies, the drinking water supply requires storage for efficiency, safety, and uninterrupted access. Especially in non-piped and intermittent supply systems, storage is essential in ensuring water quality and public health. However, improper storage involves a risk of contamination before use (Slavik et al., 2020), nullifying the effect of the household storage paradigm.

Domestic drinking water storage tanks differ in their sizes, positions, construction materials, and operation depending upon their locations and usage. Storage of drinking water implies a change in its quality, physio-chemical and microbiological, during the residence time (US Environmental Protection Agency, 2002). In the same vein, it is paramount to maintain water quality as high as possible when designing domestic water storage tanks to reduce public health risks.

1.1.1 Household rainwater harvesting

With increasing pollution, the over-exploitation of groundwater resources, rapid urbanization, and climate change effects, water shortages occur more often than estimated. Searching for alternate sources of water and promoting its rational use to abate the problems of water shortages and secure a stable water supply is of paramount importance (Ghisi et al., 2006). Decentralized approaches address the issues of quality and quantity of water and advocate the use of alternative water sources.

Rainwater harvesting has re-emerged as one of the essential tools for water conservation, which can ensure safe, accessible, and affordable water for drinking and other domestic uses,

agriculture, livestock, and small-scale industries, besides its significant contribution to the augmentation of groundwater resources. There are several other benefits of rainwater harvesting, such as no excessive runoff, flood control in the downstream catchment, improved soil moisture availability, and water conservation.

Rainwater harvesting and treatment provide water directly to households, allowing family members to control their water system completely, significantly reducing centralized operation and maintenance costs (Naddeo et al., 2013). A significant part of an RWH system is safe storage, wherein two proposed alternate water storage materials are discussed in subsequent sub-sections.

1.1.2 Jute fiber reinforced polymer water tank (JFRP)

The applications of natural fiber-reinforced polymers are growing rapidly in numerous engineering fields. Jute, hemp, kenaf, and bamboo have applications in different industries, such as automotive, structural components, packing, and construction. Jute's application as a Rainwater harvesting storage structure piqued the curiosity in this study due to its relatively high strength, low production cost, biodegradable characteristics, availability, and renewability compared to synthetic fibers. On the flip side, there is the physical disadvantage of Jute composites being susceptible to moisture absorption and uneven surface finish, limiting their performance (Mohammed et al., 2015).

1.1.3 Glass fiber reinforced polymer water tank (GFRP)

GFRP enjoys widespread applicability in manufacturing because of its competitive cost, on-site/ off-site fabrication, and relatively good mechanical properties (Huang & Sun, 2007). Simões et al. (2016) highlighted that polymer composites have the least negative environmental and economic impacts and a superior life cycle environmental profile (Simões et al., 2016). Existing GFRP water tanks have a higher price advantage over stainless steel, increased life expectancy in storing corrosive liquids, lower density than steel, and greater tensile strength (Mohamed & Benmokrane, 2014; Newberry & Putri, 2005). The adaptation and household usage of a GFRP tank as a rainwater harvesting infrastructure is an area of novel exploration.

1.2 Prevalence of fluoride pollution in the study region

The Indian state of Rajasthan has known recorded high concentrations of F^- (Choubisa, 2018).

Fluorine (F^-), the most electronegative and reactive of all elements, is not found in elemental form and readily reacts to form F^- (Manahan, 2003). F^- has geogenic origins with a high likelihood of co-occurrence in aquifers characterized by unconsolidated calcareous sediments (Kumar et al., 2020; Rasool et al., 2017). F^- contamination is predominant in semi-arid and arid climates having alkaline soil and crystalline igneous rocks. The element can enter into groundwater due to geochemical interactions with fluoride-bearing minerals such as mica, hornblende, pyroxene, and apatite in the rocks and sediments, as well as from atmospheric deposition (Podgorski et al., 2018). Anthropogenic sources of high F^- concentrations result from using pesticides, applying phosphate-based fertilizers, and increased industrial activities (Ayala et al., 2018; Chaney, 2012). Besides India, high F^- levels in the groundwater are endemic to several countries, including the USA, Tanzania, Kenya, Ethiopia, Chile, Taiwan, Bangladesh, Pakistan, Mexico, Hungary, and China (Demelash et al., 2019; Gebrewold et al., 2019; Getachew et al., 2015; Rasool et al., 2017; Yadav et al., 2013).

While F^- is an essential constituent for human health, it can be beneficial or detrimental depending on its level in drinking water. The Bureau of Indian Standards (BIS) and the World Health Organization (WHO) have defined the maximum allowable amount of F^- consumption at 1.5 ppm (parts per million) or 1.5 mg/l, mandating the removal of excess F^- from drinking water (BIS, 2012; WHO, 2022). Both lower (< 0.5 mg/l) and higher (> 1.5 mg/l) limits of F^- pose dangers of dental and skeletal fluorosis, nervous system damage, reduced fertility, intellectual impairment, and urinary tract diseases in children and adults (Izquierdo-Vega et al., 2008; Jha et al., 2011; Kaoud & Kalifa, 2010; Maguire, 2014; Shivaprakash et al., 2011).

1.2.1 Removal of Fluoride through adsorption

Although investigations on the removal of F^- ions from aqueous solutions using various adsorbents have received a significant deal of attention, each unique material requires a specific investigational emphasis due mainly to the material composition of the suggested adsorbent. Preparing adsorbents from locally adaptable bio-sorbents, minimal treatment, spreading knowledge, and encouraging community participation will enable rural residents to use the adsorbent and access F^- free water (Getachew et al., 2015).

A novel adsorbent prepared from ***Prosopis cineraria*** (vernacular name: **Khejri**) has been explored in the current study. Being rich in calcium and phosphorous, Khejri has been advocated as a good candidate for Ca-based F^- adsorbent (Rathore, 2009).

1.3 Adaptation of household water treatment systems (HWTs)

Several studies have suggested that the key to reducing or even eradicating the burden of water-borne disease is through appropriate sanitation facilities and piped water systems. In the absence of such facilities, primarily in rural areas, point-of-use water treatment (POUWTs)/ Household water treatment (HWTs) systems which are simple to use and economically friendly, have been shown to reduce the microbial and contaminant load of household stored water, thereby reducing the risks of water-borne and associated diseases (Agrawal & Bhalwar, 2009; Clasen & Cairncross, 2004). The most promising and accessible technologies for household water treatment are filtration with ceramic filters, chlorination with storage in an improvised vessel, solar disinfection in clear bottles by the combined action of UV radiation and heat, thermal disinfection (pasteurization) in opaque vessels with sunlight from solar cookers or reflectors and combination systems employing chemical coagulation-flocculation, sedimentation, filtration, and chlorination.

1.3.1 Low-cost filters for water treatment

Of the several low-cost filtration techniques available, ceramic water filters (CWFs) have been widely promoted and used, primarily in low- and low-middle-income countries. CWFs are efficiently manufactured in the countries of intended use, mainly consisting of clay firing material, water, and often a silver additive. CWF shapes range from plate/ disc, candle, and pot to granules having micropores varying from 0.10 to 10 µm (Tchobanoglous et al., 2003).

A novel method used for the current work explored the usage of cement in preparing low-cost water filters. Though a few studies have reported porous concrete purification capabilities, F^- remediation remains unexplored.

The experimental viability of a low-cost cement and ceramic water filter with bio-mass-based adsorbent as a constituent material was explored during this research work. Studied adsorbents such as sugarcane bagasse, potato slurry, and activated carbon were evaluated in fabricating water filters for F^- removal.

1.4 Household water treatment Sludge disposal

The robustness of a system is the baseline for efficiency and sustainability. Water storage and treatment system are being established at a household level in this research work.

Figure 1-1 demonstrates the schematic representation of the various elements involved in a comprehensive water delivery system. The highlighted portions are the areas focused on in this thesis.

An integral part of the water treatment industry is the sustainable disposal of waste generated during the process. Existing water sector institutions are primarily structured for traditional approaches and generate a significant amount of residue or sludge, almost 100,000 tons/per year, necessitating efficient disposal (Bourgeois et al., 2004). Water treatment sludge (WTS) is classified as the by-product generated after raw water is allowed to pass through multiple stages of treatment and predominantly consists of precipitate hydroxides of chemicals used for treatment in addition to sediments and debris in the water (Titshall & Hughes, 2005). If not efficiently disposed of, the WTS can leach into the environment and re-contaminate water sources. WTS generated at a household level is not much in volume but needs efficient disposal to encourage adapting HWT systems and prevent on-site re-contamination of water sources.

Land application of liquid or dry sludge is a low-cost and most common alternative for disposal. Meng et al. indicated that the generated sludge might not have much impact on the environment if disposed of adequately in the soil in designated and restricted areas (Meng et al., 2001). With the motive of designing a self-sufficient system, exploring the sludge disposal method and associated risks to the immediate environment forms an integral part of the study.

1.5 Use of machine learning in mapping input-output relationships and prediction modeling

Artificial intelligence (AI), which includes machine learning, is the scientific field that employs computer algorithms to learn from data, recognize patterns, and make predictions. Implementing AI results in a flexible mathematical structure that identifies non-linear and complex input-output data correlations.

Machine learning methods have contributed significantly to the advancement of prediction systems to mimic the complex relationships of contaminant remediation's physical and

chemical processes, providing better performance and cost-effective solutions (Yetilmezsoy & Demirel, 2008).

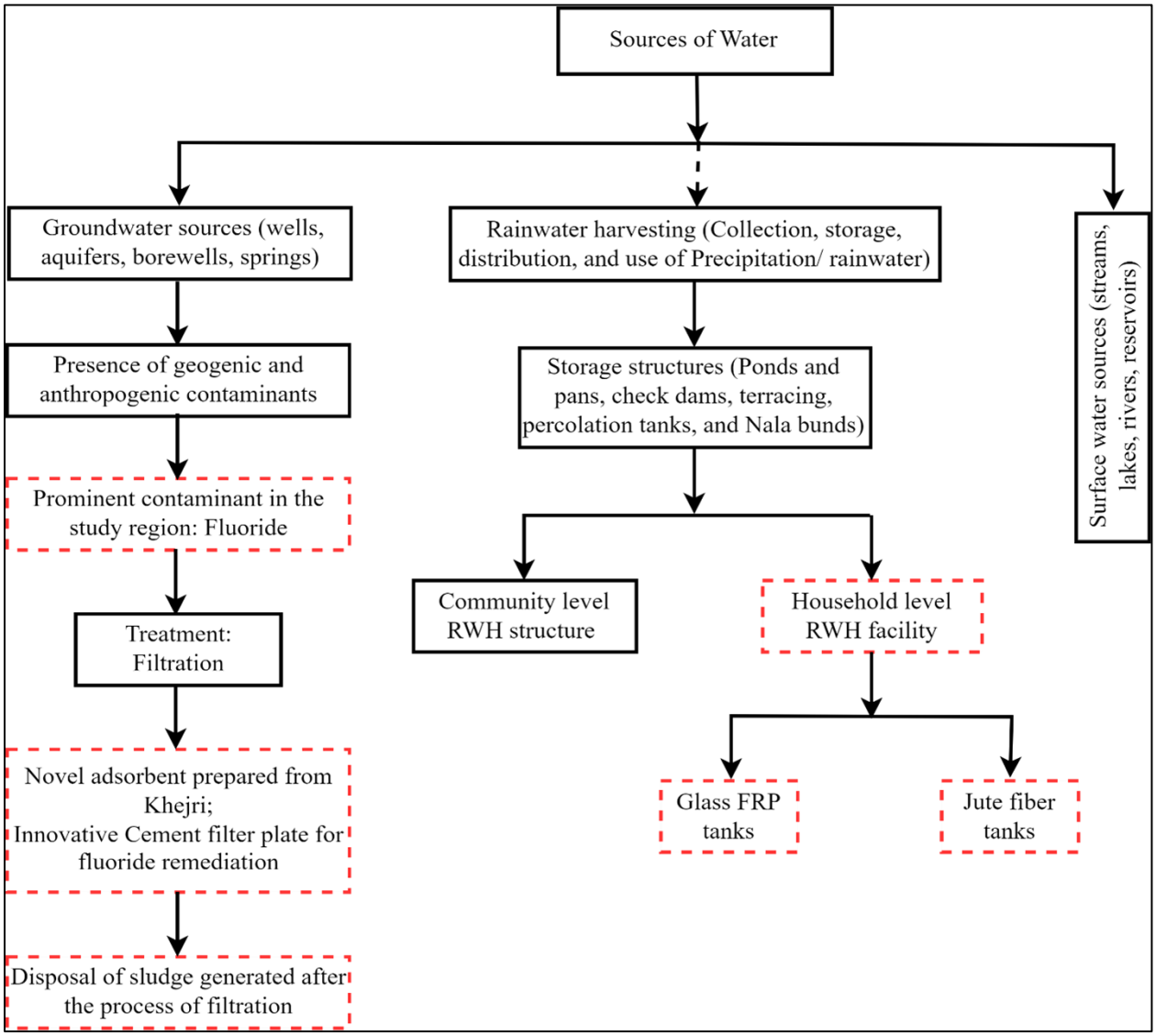

Figure 1-1 Integrated and systematic representation of water flow from source to the user (includes water treatment, storage, and disposal of sludge)

Modeling pollutant movement in soil is another application of ML techniques. The effects of effluent leachate on soil's physical and chemical properties and its propagation depth have been investigated, and mathematical techniques have been devised to describe the observed patterns (Yousefi Kebria et al., 2018).

Traditional statistical algorithms effectively map out correlations between dependent and independent factors that regulate a system. However, they fail when there is no logical association between data or an apparent non-linear relationship exists. In this view, soft computing methods like artificial neural networks (ANN), fuzzy logic (FL), artificial neural

fuzzy inference systems (ANFIS), and genetic algorithms (GA) are better suited for system identification and adapted in the present study.

1.6 The hypothesis of the proposed study

The Merriam-Webster dictionary describes a system as a regularly interacting or interconnected group of elements constituting a cohesive whole. A fundamental premise of a system is that it is greater than the summation of its components (Arnold & Wade, 2015). The three chief components of a system constitute: elements (here, units of water storage and treatment, separately), interconnections (the way these elements relate to and feed back into each other), and an operational purpose (Meadows, 2008).

In this study, the chief aim was to establish a water infrastructure system in a rural household to meet the water demands of the inhabitants and uplift living standards. The hypothesis of the study is highlighted in Figure 1-2.

Even though significant work is being carried out in urban sectors by improving existing water infrastructures and commissioning new ones to meet the exponential demand increase, rural communities are on the back burner and experience multiple confronts such as inadequate quality water, food, storage, and transport infrastructures. Encouragement of community participation in the rural water supply sector acts as a catalyst to gradually replace the government-oriented, centralized, supply-driven, and non-people-participating water program with a people-oriented decentralized, demand-driven, and community-based, robust infrastructure. Poor quality RWH structures, non-participation of people in the design/operation/maintenance of assets, and fast depletion of groundwater levels lead to problems of enhanced contaminant content. The above situation necessitates addressing the issues of control on groundwater withdrawal, water harvesting and soil and water conservation, and community participation in managing drinking water as an economic asset.

Participants' lives, primarily women and girl children aim to improve with improved rural water infrastructure. These systems increase their participation in decision-making and reduce the risk of violence against the fair gender (Dickin et al., 2020; Graham et al., 2016).

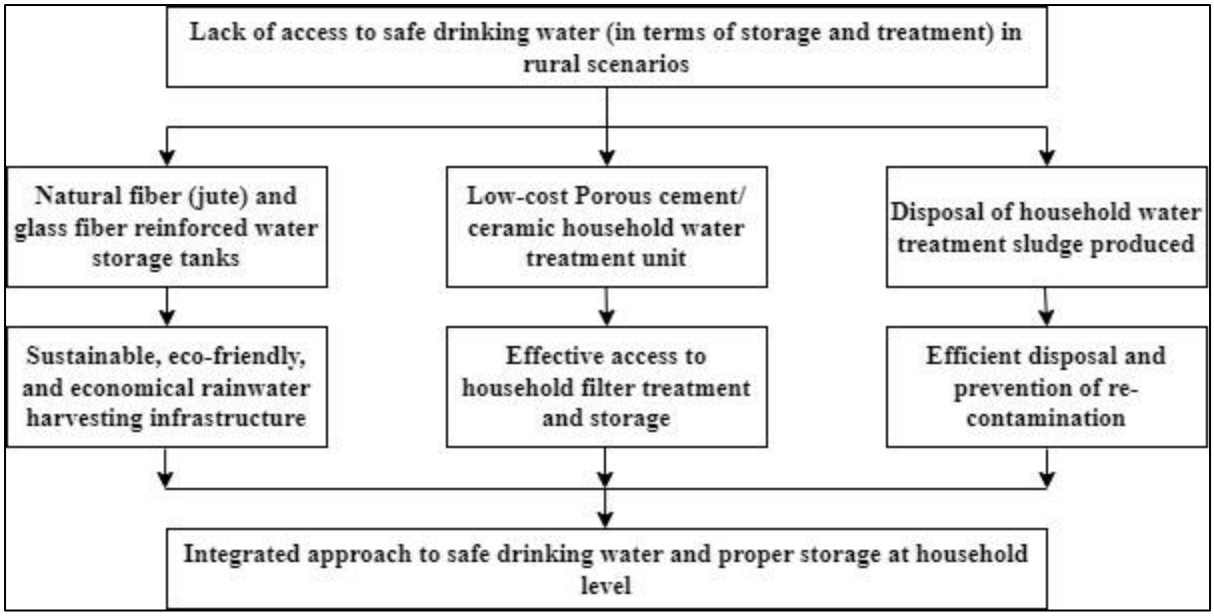

Figure 1-2 The hypothesis of the current study

1.7 Outline of the thesis

A summary of the eight chapters of the dissertation has been presented hereafter. Chapters three to seven cover the methodology, documented results, and detailed analysis of individual objectives.

Chapter 2: Literature review

This chapter covers the various components that form a part of the rural water infrastructure system. The literature review identifies the research gaps discussed in subsequent chapters.

Chapter 3: Evaluation of fiber-composite material for suitability as rainwater harvesting tank

Advocating for rainwater harvesting highlights the need for safe storage structures. For the current work, two composites, JFRP and GFRP, were proposed as alternative tank materials. The effect of tank materials on the rainwater was experimentally documented and analyzed. Upon selecting the preferred composite, i.e., GFRP, a strength analysis was performed on the composites, and the field installation was documented.

Chapter 4: Synthesis and experimental verification of *Prosopis cineraria* carbon (PCC)

This chapter covers the synthesis, characterization, isotherm, and kinetic studies conducted to understand the mechanisms governing the removal efficiency of Khejri, a novel adsorbent. Regression, neural network, and fuzzy inference system predictive models have been used with

the experimental data to model the non-linear relationship between the input and output parameters. The genetic optimization algorithm was applied to the developed neural network to derive optimum experimental conditions.

The experimental analysis was followed with a field application of prepared PCC. The F^- removal capacity from field groundwater samples was monitored without altering the initial water quality.

Chapter 5: Assessment of water quality from Hurda block villages; preparation and performance evaluation of low-cost water filters

Human health risk assessment on groundwater F^- concentrations from literature covering the state of Rajasthan was performed. To corroborate literary data, groundwater samples collected from selected villages from Hurda Block were tested, and F^- levels were monitored to highlight the toxicity issue.

Low-cost household water filters made of ceramic, cement, sugarcane bagasse, activated carbon, and potato slurry were fabricated, and their performances were monitored experimentally. Discharge rate and F^- removal efficiency were the prioritized selection criteria for choosing the optimum filter material combination.

Chapter 6: Water quality assessment in selected villages of Chirawa tehsil and on-ground performance evaluation of developed water filters

The selected villages in Chirawa tehsil were identified for the study implementation. The chapter also covers household surveys conducted in the villages, followed by the distribution of fabricated household water filter systems. The follow-up surveys after three and six months are also reported. Positive and negative feedback obtained through the study has been discussed.

Chapter 7: Experimental analysis of soil fluoride concentration subject to the disposal of exhausted filter plates

This chapter covers the lab-scale experiments conducted for the proposed exhaust filter disposal system. Qualitative parameter variations were monitored with time and depth of observation. Neural methods used to predict F^- concentrations using pH, TDS, depth, and time of observation as input parameters have been covered in the chapter.

Chapter 8: Conclusion

This chapter concludes with the findings of the research work based on the methodology and validations carried out. Besides, the chapter outlines the study's limitations and future scope.

Chapter Summary

An introduction concerning the proposed hypothesis for the current work has been highlighted. Concise descriptions of the individual interconnected components of the proposed sustainable drinking water scheme, covering storage, filtration, and sludge disposal, have been covered.

2 LITERATURE REVIEW

Overview of Rural Water Resource Management

Water resource management (WRM) encompasses all facets of planning, developing, and managing water resources for all water users with regard to both water quality and quantity. Institutions, infrastructure, incentives, and information systems are included. In addition, WRM attempts to thrive on the benefits of water by providing sufficient water of acceptable standard for drinking and sanitation facilities, food production, and energy generation while supporting a healthy water-dependent ecosystem. WRM also involves the management of risks associated with water, such as drought and contamination. The complexity of the relationships between water and families, economies, and ecosystems necessitates an integrated approach to water management that considers the synergies and tradeoffs between water's numerous uses and values.

While urban WRM has received significant attention and funding, Rural WRM (RWRM) remains disregarded, which encourages looking into the existing gaps in attending a sustainable RWRM. Of the several components involved in a successful WRM system, lack of infrastructure and contamination-related risks play a pivotal role. Sustainability in the water sector focuses primarily on maximizing the use of water to meet existing economic, ecological, and social needs without negatively impacting the nearby environment through waste generation.

In developing nations, the failure of rural water infrastructure is frequently the result of the systemic interaction of technical, social, financial, institutional, and environmental issues (Walters, 2015). Poor quality construction, lack of community participation, rent-seeking, poor pricing, and tariffs have been identified as reasons hindering the success of RWRM. A “demand-driven” consensus for rural water programs has proven effective (Whittington et al., 2009). The essential components of a demand-driven process include 1) identification of participatory households and updating on the usage of technology and fiscal arrangements; 2) giving women a more prominent role in decision-making; and 3) encouraging community participation through share-holding and operation and maintenance of installed water supply infrastructure.

Recognizing the fundamental components required in the successful implementation of RWRM, this chapter sequentially evaluates the existing literature and offers discussions to aid

in identifying the research gaps and formulating the research objectives. To ensure and study the viability of the proposed sustainable drinking water scheme, all components involved - storage, treatment/ filtration, and sludge/ waste disposal are studied in depth and analyzed.

2.1 Alternative sources of water

In rural locations, the lack of robust water storage infrastructure inhibits the proper implementation of RWRM. It is essential to investigate alternative water sources to reduce the reliance on groundwater or contaminated surface water sources. In the given scenario, rainwater acts as a successful alternative.

2.1.1 Rainwater harvesting structures

Rainwater Harvesting (RWH) structures are well-connected infrastructure systems for intercepting and storing rainwater. These structures play critical roles in adapting to water shortages and future demands, alleviating anthropopressure on existing water resources (Musz-Pomorska et al., 2020). Rainwater harvesting enables the efficient use/ re-use of treated water that would otherwise go down the drain, playing a significant role in water security. Further, intercepting rainwater reduces the chances of flooding in public storm drains. RWH systems notably alleviate the problem of water scarcity in arid and semi-arid regions (Domènech & Saurí, 2011; Freni & Liuzzo, 2019; Tamaddun et al., 2018).

RWH is an age-old concept practiced worldwide along with India for centuries. However, the importance associated with RWH structures today is paramount with substantial work and associated research (Kumar et al., 2006). RWH can broadly be classified as surface or rooftop water harvesting, depending upon the abstraction surface. RWH uses a simple storage tank, gutters, and a network of interconnected pipes to collect the precipitation and contains it for future use. The facilities can be community-level designated infrastructure or closely situated facilities for individual households (GhaffarianHoseini et al., 2016). Collected rainwater has also been directed to recharge aquifers through check dams and infiltration ponds (Brunner et al., 2014).

Though rainwater is generally considered one of the cleanest forms of water, high concentrations of metals, nutrients, and other pollutants acquired through precipitation, atmospheric deposition, and the material of the abstraction surface substantially impact its quality. Heavy metal concentrations are accounted for in areas of intensive human activities

(Melidis et al., 2007). Gases, aerosols, and suspended particulates of dust and ash are dissolved, absorbed, and collected as rain droplets while descending through the atmosphere (Huston et al., 2009). Apart from being susceptible to the material of construction, rooftop rainwater can be polluted with germs from bird and animal droppings, contaminating the collected water and limiting its use for non-potable purposes, such as flushing toilets, cleaning sidewalks, laundry, and gardening (Lupia & Pulighe, 2015; Melville-Shreeve et al., 2016; Musz-Pomorska et al., 2020; Sepehri et al., 2018; Vialle et al., 2015). However, in developing countries with pronounced water scarcity, rainwater is adopted for potable and non-potable uses with increased risk to human health, making it necessary to monitor the quality of collected and stored rainwater and contrive ways and methods to improve the quality of collected and stored rainwater (Silva et al., 2015). Rainwater is preferable to piped water because of the volume collected, its capacity to qualify the majority of municipal water quality criteria, and its cost-effectiveness (Rahman et al., 2014).

A significant part of an efficient RWH system is storage, guaranteeing a complete and uninterrupted water supply. Domestic drinking water storage tanks differ in their sizes, positions, construction materials, and operation depending upon their locations and usage. However, storage involves a risk of contamination before use (Slavik et al., 2020). Storage of drinking water implies a change in its quality, physio-chemical and microbiological, during the residence time (US Environmental Protection Agency, 2002). When designing domestic water storage tanks to reduce public health risks, maintaining water quality as high as possible should be the prime objective.

2.1.2 Commercially available water storage tanks

Commonly used domestic water storage tanks include Reinforced Cement Concrete (RCC), masonry, Poly Vinyl Chloride (PVC), glass fiber reinforced polymer (GFRP), high-density polyethylene, fiber cement, plastic, and metal (Steel, GI, cast iron) water tanks (Al-Bahry et al., 2011; Chalchisa et al., 2018; Evison & Sunna, 2001; Olorunnisola & Alaka, 2018; Richards et al., 2021; Schafer & Mihelcic, 2012; Schafer, 2010). Slavik et al. have conducted a comprehensive study covering water quality in conjunction with storage tank material considering current standards and guidelines (Slavik et al., 2020). However, tank materials show degradation over time due to corrosion, leaching, and degradation by microbial presence. A tank's temperature, color, diaphaneity, and location significantly affect material deterioration structurally and aid microbial and fungal growth (Chia et al., 2013). In a recent study,

degradation of the concrete tank was recorded due to water-transported fungal presence (Babič & Gunde-Cimerman, 2021). Compromise in the structural integrity of concrete tanks is a regular sight with age and exposure to harsh environmental substances (Sangiorgio et al., 2020). Metal tanks are prone to corrosion and require galvanization, where the zinc breaks over time and leaches into the water (Manga et al., 2021). The tank material and existing user practices affect the water quality in metal tanks. While PVC and plastic tanks are the most spotted household tanks, these are susceptible to UV radiation, affecting water quality. Dark-colored plastic tanks are standard. Nevertheless, dark colors absorb more light than light-colored tanks encouraging bacterial growth (Graham & VanDerslice, 2007; Manga et al., 2021). In a similar vein, *Heterotrophic bacteria, Total coliform, Enterococci,* and *Escherichia coli* were determined in HDPE water tanks studied in Nigeria (Nnaji et al., 2019).

2.1.3 Jute-fiber reinforced polymer (JFRP) composites

Due to their superior qualities, natural fibers have recently captured the interest of scientists and engineers. Natural fibers are characterized by their lightweight, low cost, environmental friendliness, high flexibility, renewability, biodegradability, high specific strength, good thermal characteristics, high toughness, reduced wear, lack of skin irritation, and ease of processing (Gupta et al., 2015). Bio-composites can be described as a composite of a biodegradable polymer matrix reinforced with natural fibers (Ray et al., 2001). Using natural fibers such as Jute, hemp, flax, sisal, and bamboo as reinforcement in polymer composite material has increased and found usage in several industries, including automobile, defense, building, and construction. However, due to inherent drawbacks, including high moisture absorption and poor adhesion between the matrix and fiber, the wide-scale application of natural fibers is a field of study.

Jute (*Corchorus olitorius*) is a cheap natural fiber found in abundance in India and Bangladesh. These fibers have been used for manufacturing bags, ropes, and mats. The adaptation of untreated jute fibers of varying thicknesses for making water storage tanks a potential RWH structure highlights the application of eco-friendly materials in water storage. However, being a class of natural fiber, jute is hydrophilic and requires chemical modifications such as alkaline, acetylation, silane, and peroxide treatment to improve its overall quality (Kabir et al., 2012; Li et al., 2007). Untreated jute was finalized through the study, taking cognizance of the size of the proposed water storage tank and ease of construction.

2.1.4 Glass Fiber-reinforced polymer (GFRP) composites

Fiber-reinforced polymer (FRP) enjoys widespread applicability because of its competitive cost, on-site/ off-site fabrication, and relatively good mechanical properties (Huang & Sun, 2007). FRP composites also resist weathering, chemical degradation, blast, and ballistic impacts (Wei & Hadigheh, 2022). Further, reported literature highlights that polymer composites have the least adverse environmental and economic effects and a superior life cycle ecological profile (Simões et al., 2016). In FRP, synthetic fibers, such as carbon and glass, are generally embedded in a resin matrix. Depending upon requirements, the resin used is epoxy, vinyl ester, and unsaturated polyester, combined with a hardener and catalyst to aid polymerization. Epoxy resin is the most commonly used, as it is readily available in the market and is easy to use. These resins are a class of thermosetting polymers widely used as protective coatings due to their excellent corrosion resistance, stable chemical properties, outstanding adhesion, low shrinkage, higher price advantage over stainless steel, lower density, and high tensile strength (Yu *et al.*, 2015; Kongparakul *et al.*, 2017; Pourhashem *et al.*, 2017). Several studies have highlighted the usefulness of a GFRP tank for storing oil, acids, and water (Mohamed & Benmokrane, 2014; Newberry & Putri, 2005).

Prior studies have focused on the curing kinetics, mechanical, thermal, and moisture absorption/ degradation properties of the glass fiber-reinforced polymer composite (Braga & Magalhaes, 2015; Hardis, 2012; Hardis et al., 2013; Leman et al., 2008; Zuhri et al., 2010). A significant step in the fabrication of composite is curing. The structural property of a composite considerably varies depending upon the curing process. The general methods adopted are radiation, thermal, pressure, and self-curing. Due to limitations in the study area regarding the cost and quality available, self-curing was selected (Abliz et al., 2013; Carbas et al., 2014; Celikbag et al., 2017; Tang et al., 2019).

Previous literature has pointed out that the focus of studies concentrating on the environmental component of the GFRP tanks has been physio-chemical and micro-biological (Agensi et al., 2019; Al-Bahry et al., 2011; Chalchisa et al., 2018; Chia et al., 2013; Evison & Sunna, 2001; Graham & VanDerslice, 2007; Manga et al., 2021; Mohanan et al., 2017; Nnaji et al., 2019; Schafer & Mihelcic, 2012). A compiled list of parameters evaluated in previous studies has been presented in Table 2-1. However, a significant issue in GFRP tanks is the potential leaching of chemicals from resin and hardeners in case of inadequate curing.

Table 2-1 Description of some of the studies conducted on FRP

Material of Water storage tanks (rainwater and otherwise)	Parameters tested	References
Cast iron, polyethylene, fiberglass	Temperature, pH, turbidity, residual chlorine, TOC, HPC	Evison & Sunna, 2001
Polyethylene, fiberglass, fiber cement	Temperature, conductivity, TDS, DO, pH, turbidity, TC, E.coli	Schafer & Mihelcic, 2012
Glass-reinforced plastic, polyethylene, galvanized iron	Microbial populations, free chlorine, turbidity, TON, Color	Al-Bahry *et al.*, 2011
Plastic	pH, turbidity, temperature, TC, and FC	Chalchisa et al., 2018
Cement-bonded composites storage	Color, pH, salinity, TH, conductivity, turbidity, TDS, TSS, density, thermal conductivity	Olorunnisola & Alaka, 2018
Reinforced concrete	pH, conductivity, turbidity, alkalinity, BOD, TP, TN, TOC, Residual chlorine, total coliforms, E.coli	Richards *et al.*, 2021
Plastic Tanks	Microalgal and cyanobacterial, TDS, TP, BOD, pH, DO, EC, temperature	Chia Ahii et al., 2013
High-density polyethylene	Heterotrophic bacteria, TC, E.coli, pH, DO.	Nnaji et al., 2019

55-gallon drums	Turbidity, residual chlorine, TC, E.coli	Graham & VanDerslice, 2007
Plastic, glass, brass, copper, aluminum, steel, and clay	pH, TDS, alkalinity, EC, salinity, DO, BOD, temperature, THB, coliform	Mohanan et al., 2017
Open jerrican	Bacteriological contamination, TC, E. coli	Agensi *et al.*, 2019

TOC: Total Organic Carbon, HPC: heterotrophic plate count; TDS: Total dissolved solids; DO: Dissolved Oxygen; TC: Total coliforms, TON: Threshold Odour Number; FC: Fecal coliform; TH: Total Hardness, TSS: Total Suspended solids, BOD: Biological Oxygen Demand, TP: Total Phosphorus, TN: Total Nitrogen, EC: Electrical Conductivity, THB: Total Heterotrophic Bacteria

2.1.5 Qualitative analysis and Health hazard risk assessment

Physio-chemical parameters such as pH, Total Dissolved Solids (TDS), and Total Hardness (TH) are essential water quality indicators. Apart from these selected parameters, the leaching of BPA was studied. An epoxy-based composite's primary component is a pre-polymer. The pre-polymer is known as Bisphenol A diglycigyl ether (DGEBA), produced by the alklyzation of Bisphenol A and Epichlorohydrin. Bisphenol A (BPA, 4,40-isopropylidine diphenol, CAS Registry No. 80-05-7) is a commercially important industrial chemical. However, the chemical has been identified as an endocrine disruptor that causes obesity, thyroid dysfunction, and cancer by imitating or interfering with hormone production and metabolism, affecting wildlife and humans alike (Selvaraj et al., 2014; Tabb & Blumberg, 2006). BPA is widely used to manufacture polycarbonates, epoxy resins, and other plastics and is reportedly detected at low concentrations in receiving water near such manufacturing facilities (Staples et al., 2000). BPA can also be found in baby bottles, food containers, water bottles, electrical insulation, and pipes (Moghadam et al., 2015). Leaching of BPA from old water pipe's epoxy coatings has been reported earlier (Rajasärkkä et al., 2016). The maximum acceptable dose (tolerable daily intake) of BPA established by USEPA, 1988; Health Canada, 2008; and the European Food Safety Authority 2015 are 0.05 mg/kg-bw/day, 0.025 mg/kg-bw/day, and 0.004 mg/kg-bw/day, respectively (European Food Safety Authority, 2015; Health Canada, 2008; US Environmental Protection Agency, 1988). Human exposure to BPA has been evaluated by characterizing the concentration of BPA in media such as diet, dust, air, and water ingestion, though a minor

source (Arnold et al., 2013). Health risk assessment is a well-established approach for assessing possible hazards to human health associated with long-term exposure to particular substances over a while (United States Environmental Protection Agency, 2011). Health risk assessments with chemicals typically follow the general paradigm of four steps—hazard identification, dose-response assessment, exposure assessment, and risk characterization (Wilkinson et al., 2000). This study evaluated the population's potential health risk of BPA concentration by estimating the Ingestion Hazard Quotient (IHQ) of possible BPA leachate from the GFRP and JFRP tanks. Theoretically, a hazard quotient (HQ) is the ratio of the potential exposure to a selected compound relative to the level at which no adverse effects are expected (Pongpiachan et al., 2018). Potential exposure or Average Daily Dose (ADD) of BPA was calculated for different age groups by multiplying the measured concentration of BPA by the average daily intake (consumption rate) of water by each age group and dividing it by the average body weight of the concerned group (Moghadam et al., 2015). The villagers' age, weight, and daily water intake rate were adopted from previous studies (Chen & Chang, 2018; Chen et al., 2016; Hossain et al., 2013). Estimated intakes were then verified against existing oral toxicity benchmarks, and the margin of safety was determined (Arnold et al., 2013).

2.2 Contaminant remediation

Rural households generally lack water treatment units and depend directly upon raw water. Even groundwater consumed is polluted with geo-genic contaminants unique to a given area, warranting tailored treatment methods. For a sustainable RWRM, a sturdy methodology involving contaminant monitoring and treatment is essential.

2.2.1 Presence of fluoride in groundwater in Rajasthan, India

High fluoride (F^-) levels in groundwater are endemic to several countries affecting 260 million people globally. 24.8% of the exposed are in India, with the potential risk of developing fluorosis. The Indian state of Rajasthan is particularly vulnerable to a high F^- problem. Before the guinea worm eradication effort began in 1986, ponds, lakes, rivers, and streams were the main supply of drinking water for the inhabitants of Rajasthan (Choubisa, 2018). However, with the advent of the aforementioned national health program, reliance on surface water was reduced with a simultaneous increase in the number of bore/ tube wells. With increased dependence on groundwater, Rajasthan led the charts for the highest number of individuals

impacted by excessive F^- levels (Muralidharan et al., 2002; Singh et al., 2011). Reported F^- levels in the state range from <1 mg/l to > 20 mg/l (Choubisa, 2018).

2.2.2 Fluoride sequestration from groundwater

Several conventional de-fluoridation techniques such as precipitation-coagulation, membrane separation (reverse osmosis, nano-filtration, and electrodialysis), solar distillation, and adsorption onto activated alumina, modified alumina, and aluminum-based adsorbents, carbon nano-tubes, zeolites, calcium-based adsorbents, soils and clays, bio-polymers, and bio-adsorbents have been reported in the past (Jagtap et al. 2012; Meenakshi & Maheshwari, 2006). The requirement of large dosages of salts, a skilled workforce, concentrated brine discharge reject, significant water loss, fouling of membranes, generation of secondary pollutants, high initial investment, maintenance, and operating cost, and energy demand are identified limitations restricting the adaptation of techniques described above in rural areas. However, only a few techniques are applied at large scale in rural areas of developing countries due to the high initial investment, maintenance, operating cost, and production of toxic by-products that require further disposal.

Water treatment units governed through technology such as nano-filtration, reverse osmosis, and direct-contact membrane distillation have proven highly effective in F^- removal. Nonetheless, these technologies are scarce in actual practice due to the absence of continuous electricity and water supply, infrastructure facilities, and operational skills. Though solar distillation showed approximately 97% F^- removal, installing these distillers proves expensive. Another major drawback of the nano-filtration technique is the fouling of membranes and filters due to inorganic compounds such as $CaCO_3$. The negative aspects of precipitation and coagulation processes are the generation of high amounts of secondary pollutants, high costs, and unavailability of coagulants in F^--affected areas. In villages where any technique is practiced in actual, the techniques though able to perform satisfactorily, fail due to a lack of cooperation among community members, proper monitoring, and maintenance (Antwi et al., 2011; Gebrewold et al., 2019; Hou et al., 2010; Jagtap et al., 2012; Sehn, 2008; Tahaikt et al., 2007; Yadav et al., 2013).

Adsorption processes using biomass waste products such as activated coconut fiber, sugarcane bagasse, rice straw, tamarind, bone charcoal, and banana peel are becoming the new alternatives for removing F^- from an aqueous solution. The mechanisms underlying the adsorption process include (1) solute transfer from the aqueous solution to the adsorbent

surface, (2) transfer from the surface to the active structural positions via ion exchange, and (3) uptake on the active site via complexation, sorption, precipitation, and hydrolysis (Pyrgaki et al., 2018).

The performance of the adsorbents has been evaluated as functions of pH, contact time, initial adsorbent concentration, adsorbate dosages, temperature, and co-ion interference, showing good F^- removal efficiency (Bashir et al., 2015; Bhaumik & Mondal, 2015, 2016; Cengeloglu et al., 2002; Chakrabarty & Sarma, 2012; Gebrewold et al., 2019; Getachew et al., 2015; Ramanaiah et al., 2007; Ray et al., 2020; Sivasankar et al., 2012; Yadav et al., 2013). Even though pH and the presence of co-ions are critical elements in determining the efficacy of an adsorbent, significant modifications are possible. A few adsorbents studied for F^- removal efficiency has been cataloged in Table 2-2.

Table 2-2 The fluoride adsorption capacity of selected adsorbents through literature

Studied adsorbent	Optimum pH	Capacity (mg/g)	Maximum removal efficiency (%)	Reference
Rice husk	4.0	7.9	91	Gebrewold et al., 2019
Corn cob	6.0	5.83	89	
Wheat straw	6.0	1.93	40.2	Yadav et al., 2013
Sawdust	6.0	1.73	49.8	
Activated bagasse carbon	6.0	1.15	57.6	
Banana peel (*Musa paradisiaca*)	2.0	0.3123	85	Getachew et al., 2015
Coffee husk (*Coffee arabica*)	2.0	0.2946	86	
Thermally Basic Oxygen Furnace Slag	6.0 to 10.0	8.07	93	Islam & Patel, 2011
Alum-impregnated activated alumina	6.5	40.68	99	Tripathy et al., 2006

Brick powder	6.0 to 8.0	-	51.0 to 56.8	Singh et al., 2008
Tamarind (*Tamarindus indica*) {Virgin}	7.05	-	91	Sivasankar et al., 2012
Tamarind (*Tamarindus indica*) {Activated}	7.05	12.91 to 214.28	83	
Waste fungus (*Pleurotus ostreatus* 1804)	7.0	1.272	70	Ramanaiah et al., 2007

Reusability, environment-friendly, and small initial costs are advantages of using biomass adsorbents (Getachew et al., 2015). However, limitations are galore. For example, bone charcoal as an adsorbent has an F^- uptake capacity of 97.9%; however, the manufacturing process has certain environmental constraints and involves higher costs (Ray et al., 2020). Also, large-scale acceptance of the said raw material is not feasible. Further, access to low-cost adsorbents, more straightforward process development, sufficient availability at or near F^--affected areas, a high F^- removal efficiency on actual groundwater samples, and convenient form for easy usage are certain impediments restricting mass usage of adsorbents in developing and underdeveloped nations.

Even though F^- removal with bio-sorbents has received much attention, the adsorbents have a long way to go before being used substantially. Preparing adsorbents from locally adaptable bio-sorbents, spreading knowledge, and encouraging community participation will enable increased usage of the adsorbent and access to F^--free water, primarily in rural areas.

During this work, several adsorbents were studied in the lab. However, sugarcane bagasse and potato slurry from the available literature were selected for further work (Singh et al., 2016; Singhal et al., 2019; Yadav et al., 2013). The low cost and abundance in availability significantly influenced the selection of these adsorbents.

A limited number of studies have reported the efficiency of Khejri in removing textile dye, lead, and cadmium from water and wastewater (Eshraghi et al., 2016; Garg et al., 2004; Natarajan & Manivasagan, 2020; Shahmaleki et al., 2020). However, a literature survey showed the absence of studies covering the F^- adsorption efficiency of Khejri. After additional research, Khejri was evaluated as a potential F^- remediation adsorbent.

Prosopis cineraria forms an integral part of the Indian desert ecosystem because of its hard-climatic adaptation. Also referred to as "King of Desert," this species represents all five F, i.e., Forest, Fiber, Fuel, Fodder, and Food, justifying its extensive use in dryland agroforestry and significance in the economy of Thar Desert (Krishnan & Jindal, 2015). These plants effectively stabilize dunes and can withstand periodical burial. Khejri holds an important place in the rural economy of Rajasthan. A nutritionally rich food source, every part of the plant is used for food preparation and medicines.

Further, the plant is a source of fodder for cattle and firewood for the inhabitants. The agro-forestry system involving Khejri reported higher biomass and soil moisture status under the canopy, high micro-nutrient in the plant vicinity, improved crop yield, and soil erosion control (Duhan et al., 1992; Purohit et al., 2002). The chemical composition of Khejri and its adaptation to the local population and environmental conditions encouraged the authors to investigate its potential as an adsorbent.

Elemental calcium and phosphorus are abundant in Khejri (Rathore, 2009). Studies have validated the behavior of calcium-enriched adsorbents showing improved defluoridation activity as they react with F^- to form insoluble compounds such as CaF_2 and $Ca_5(PO_4)_3F$ and avoid the associated health risk of metal leaching (Sivasankar et al. 2012; Tchomgui-Kamga et al., 2010). Therefore, developing an environmentally friendly, inexpensive, and effective Ca-based adsorbent would benefit F^- removal (Choi et al., 2022).

2.3 Water treatment and contaminant remediation

Providing water from long distances is unfeasible in a rural scenario. Access to low-cost household treatment units for water deals with the contaminant segment of an RWRM. In the following sections, the importance of HWTs has been discussed.

2.3.1 Low-cost Household water treatment systems (HWTs)

With much of India comprising arid and semi-arid regions, the country depends heavily on groundwater to support its growing economy and population (Podgorski et al., 2018). Unsafe drinking water, poor sanitation, and hygiene result in many diseases and deaths—poor water hygiene results in frequent diarrheal disease transmission (Quick et al.,1999). In India alone, 9.1% of all deaths in children younger than 6 years of age (Clasen et al., 2008a) are attributed

to diarrheal disease. Besides waterborne diseases, groundwater-related diseases are prevalent in the Indian sub-continent, particularly the F^- endemic.

Safe drinking water is still a distant dream for most people, stressing the importance of an affordable water treatment system and secure storage. Much of the disadvantaged global population consume untreated water with no protection from further contamination (Rosa & Clasen, 2010; Sobsey et al., 2003a). An inconsistent power supply and lack of water treatment facilities make the availability of potable water difficult for community consumption, primarily in rural areas (Ankidawa & Tope, 2017). In such dismal scenarios, household water treatment systems (HWTs) or point of use (POU) water filters prove superior in ensuring potable water. Several practical and affordable methods have been identified and implemented worldwide to treat and safely store non-piped gathered household water (Sobsey et al., 2003). Further, there is convincing evidence that accessible, acceptable, low-cost interventions at the household and community level dramatically improve the microbial quality of household stored water and reduce diarrheal disease risks (Clasen & Cairncross, 2004).

Standard techniques adopted for household water treatment include filtration, chlorination, solar disinfection (SODIS), thermal disinfection, the Ion-exchange method, Reverse osmosis (RO), adsorption, and systems employing coagulation-flocculation, sedimentation, filtration, and chlorination (Agrawal & Bhalwar, 2009). Re-contamination, fuel procurement, health hazards, unfavorable weather, turbid source water, ignorance regarding causes of waterborne disease, absence of water sources near the user, and economic and electric constraints limit the scalability of HWT (Bitew et al., 2020; Kurmi & Ayres, 2010; Martínez et al., 2020; Rehfuess et al., 2006).

The adaptability of HWT is 66.8% in Western Pacific and 45.4% in Southeast Asian regions, while less common in Eastern Mediterranean regions and Africa. The subsequent sections provide a brief discussion concerning common everyday HWTs.

2.3.2 Boiling or thermal disinfection

Boiling is one of the most common means of treating water at home. Boiling or heating water effectively destroys all classes of waterborne pathogens and can be effectively applied to all waters, including those high in turbidity (Agrawal & Bhalwar, 2009). Non-spore-forming bacterial pathogens, viruses, and parasites have been known to be effectively reduced when heating at 60°C for 10 minutes or 55° for several hours. Clasen et al. (2008) reported an

assessment of boiling practices in semi-urban India. After treatment, the water sample showed a 2.1 log10 reduction in fecal coliforms (Clasen et al., 2008a). Similar results were observed in Vietnam (Clasen et al., 2008). Despite its extensive use, boiling presents certain disadvantages that may limit its scalability, such as recontamination, fuel procurement, health hazards (air pollution and burning), and the involved cost (Kurmi & Ayres, 2010; Luby et al., 2000; Rehfuess et al., 2006; Wright et al., 2004).

2.3.3 Solar Water Disinfection (SODIS)

SODIS was developed in the 1980s to treat water inexpensively with oral rehydration solutions. It is a simple and cheap method using natural sunlight to treat contaminated water filled into transparent plastic bottles or containers and exposed to sunlight for up to 6 hours (Borde et al., 2016). Encouraging trends in the impact on the health of SODIS consumers have been reported in Kenya, India, and Cameroon (Conroy et al., 1999). Bitew et al. (2018) verified the SODIS intervention's role in substantially reducing diarrhea among under-five children in a rural community in northwest Ethiopia, highlighting the SODIS intervention as an invaluable strategy, particularly for rural communities (Bitew et al., 2018). Regardless of its efficiency and ease of use, several factors inhibit the mass-scale implementation of SODIS. Cold or cloudy weather, fear of leaching in plastic bottles, turbid water, the users' accustomed attitude, ignorance regarding causes of waterborne disease, and absence of water sources near the user have documented reasons for low dissemination of SODIS (Bitew et al., 2020; Borde et al., 2016; Martínez et al., 2020; Tamas & Mosler, 2011). Besides, the accumulation of plastic waste in the environment upon discarding the bottles adds to the plastic load.

2.3.4 Water Filtration

Water filtration is the process of removing impurities from water by using a physical barrier, chemical process, or biological process. Many water filtration systems are available, ranging from simple pitcher filters to complex reverse osmosis systems.

2.3.4.1 Granular filter media

Granular media filtration (GMF) removes suspended or colloidal particles; for example, removing suspended solids remaining after sedimentation clarification. It reduces turbidity and

improves clarity by removing particles ranging from coarse sediment down to particles in the range of 10.0 μm (Gray, 2013).

2.3.4.2 Membrane filtration

Membrane filtration is a sophisticated physicochemical separation process that employs thin semi-permeable membranes for particles < 1 μm. Membrane filters are broadly classified into four main types depending upon the nominal size of the pore on order of magnitude basis; micro-, ultra, nano-, and reverse osmosis. Membrane systems are further classified according to how raw water is introduced to the membrane, dead-end, and cross-flow systems (Gray, 2013).

2.3.4.3 Bio-sand filters

Bio-sand filters (BSFs) are point-of-use/ decentralized potable water filtration systems used in low-income communities at the household level, ensuring a safe drinking water supply. The principal filtration mechanisms involved are physical, chemical, and biological, and studies have corroborated the positive impact of BSFs in reducing diarrheal diseases (Kabir et l., 2016; Mutsvangwa & Matope, 2017). Iron-assisted BSF has shown appreciable performance in removing coliforms and arsenic from the water sample (Mueller et al., 2021; Mutemi et al., 2020; Te et al., 2018). Denitrification was observed after applying external carbon sources to conventional BSF (Mutsvangwa & Matope, 2017).

2.3.4.4 Reverse Osmosis

Despite their relatively high operational costs and energy consumption, pressured membrane techniques, particularly reverse osmosis, have been utilized in water treatment companies and utilities. However, new pollutants are present in more significant amounts in reverse osmosis concentrate than in feed water, posing issues for concentrate treatment (Joo & Tansel, 2015). The scarcity of fresh water in Middle East regions, industrial waste in developed areas, and scarcity of rains in arid regions have mobilized countries to adopt and revolutionize RO.

RO system separates dissolved solutes (including single charged ions, such as Na^+, Cl^-) from the water via a semipermeable membrane that passes water in preference to the solute. The RO membrane is very hydrophilic; water readily diffuses into and out of the membrane's polymer structure.

Reverse osmosis (RO) is a leading technology for producing fresh water from saline water (Shenvi et al., 2015). Primarily used in large desalination plants and industries, efficient disposal of the plant reject and old RO modules is becoming a critical challenge (Lawler et al., 2012). Some reuse options include directly applying old membranes in lower throughput systems, chemical conversion into porous filters, recycling module components, and incineration (Baker, 2011; Johnke, 1991). Recently, the use of RO and UV filtration units in individual households has significantly increased. Such portable wall-mounted units provide families with their daily potable water requirements. A majority of commercial devices available run on electricity and require water to flow under gravity. A significant drawback of RO units is the rejected water. Low-income households in developing countries cannot access continuous electricity or piped water connection. Most families depend upon the manual collection of water and are unfavorable towards excessive wastage of water. On the other hand, the UV lamp is at a disadvantage when organic matter, turbidity, and specific dissolved contaminants are present in significant concentrations (Gadgil, 1998; Naddeo et al., 2013).

2.3.4.5 Ceramic water filters (CWF)

A commonly adopted HWT is ceramic-based filters, also ceramic water filters (CWF). These water filters have been traditionally used throughout the world for their suitability for the removal of pathogens, in addition to the removal of dyes, toxic metals, and F^- (Ghosh et al., 2013; Jana et al., 2011; Kim et al., 2007).

CWFs are generally manufactured from clay mixed with burn-out materials (sawdust and milled rice husk) and sintered at temperatures of 500–1000 °C to prevent shrinkage and cracking (Farrow et al., 2018). CWF shapes range from plate, candle, and pot to granules having micropores varying from 0.10 to 10 µm (Tchobanoglous et al., 2003).

Many ceramic filters are impregnated with colloidal silver to inactivate certain classes of microbes (van Halem et al., 2007). The 3-Kolshi System, developed by the SONO Diagnostic Center in Bangladesh, has successfully removed arsenic from potable water (Ngai et al., 2007b). Though ceramic filters have many advantages, such as ease of use, longer shelf life, and low cost, several drawbacks are attached. Lack of residual protection, a low flow rate, and user behavior to keep the clean filters decrease the adaptability of the filters (Lantagne et al., 2006). Disposal of these filters after their life cycle needs to be given attention. Though the sludge volume is not large, the discarded filters can pollute the environment.

2.3.4.6 Porous cement water filter (PCWF)

Using adsorbents to develop low-cost filters for de-fluoridation increases the necessitous population's chance to access F^--free water and improves well-being. Nevertheless, studies have not yet explored cement usage in preparing HWTs. Few studies have reportedly highlighted porous concrete's purification capabilities by removing total phosphorous and nitrogen in test water (Park & Tia, 2004). In a separate study, the effectiveness of vertical porous concrete was compared with horizontal sand filters, where the feasibility of porous concrete as an acceptable water treatment method in small communities was highlighted (Taghizadeh et al., 2007). In another study, Tanji et al. reported using plain, grain, porous, and wet concrete to estimate the self-cleaning purification of sewer pipes (Tanji et al., 2006). A heterogeneous biofilm grew on the surface of each block after 79 days of sewage exposure. The blocks' self-purification capabilities were calculated by monitoring the decrease in substrate concentration in simulated sewage. The suitability of two bacteria groups from the family of *Bacillaceae*, namely *Bacillus licheniformis* and *Bacillus subtilis*, were studied for their potential to produce potable water by forming a biofilm (Gupta, 2020). Recent studies have documented the efficiency of portland pozzolana cement, cement granules, and red mud cementitious composites for removing F^- and heavy metals, respectively (Shyamal & Ghosh, 2019; Ray et al., 2020; Sevgili et al., 2021).

Nonetheless, every technology has certain advantages and disadvantages. However, on the whole, HWT proves to have a positive impact through aesthetic appeal, cost-saving, improved health and gender equality, and social status.

2.4 Sustainability of drinking water scheme

The sustainability of an implemented WRM system ensures affordable and safe water to meet current and future needs. Disposal of the water treatment sludge (the used and exhausted filter plates) is essential in limiting the contamination of the immediate environment. The disposal of sludge generated at a household level is accorded equal weight to create a sustainable system with components establishing a rural water management system.

2.4.1 Disposal of household water treatment sludge

Existing water sector institutions are primarily structured for traditional approaches and generate a significant amount of residue or sludge, almost 100,000 tons/per year, necessitating

efficient disposal (Bourgeois et al., 2004). Water Treatment Sludge (WTS) is the by-product of flocculation, filtration, and coagulation during potable water production; in simple terms, the waste is generated when raw water is passed through different treatment processes. The constituents of the WTS vary primarily depending on the raw water quality and the chemicals used for treatment consisting mainly of the precipitated hydroxides added to remove dissolved and suspended material in the raw water source (Titshall & Hughes, 2005). The chemical properties of WTS are variable and depend on impurities in the water flowing into the treatment facility (Benlalla et al., 2015; Heil & Barbarick, 2010).

With an increasing number of water treatment plants, India regularly produces large amounts of waste at their WTPs. However, due to a lack of efficient sludge management strategies, most WTS is discharged back into nearby drains or disposed of directly in landfills. The produced sludge serves as a reservoir for heavy metals, which can contaminate soils or nearby streams (Ahmad et al., 2016; Dahhou et al., 2016).

The wastewater generated during backwashing and chemical cleansing of the filters in water treatment plants contains rejected particles, including algae, clay particles, precipitated solids, chemical residuals, inorganic colloids, and microbes, and needs proper disposal (Kline, 2009). Apart from the rejection, the membranes in use pose a critical challenge for their disposal.

These challenges direct us toward the next area of discussion, i.e., household water treatment sludge disposal. Understanding the transport and sorption process through sub-surface porous media is critical to protect the sub-surface groundwater from reactive contaminants. Advection, diffusion, dispersion, and sorption processes often describe the flow of reactive pollutants through subsurface porous media (Sharma et al., 2015). In conjunction with the current study, when a great deal of F^- pollutants are drained into the soil, and the proportion of pollutants exceeds the capacity of self-purification, pollutants continue to travel downwards with water. Therefore, it is critical to understand the migration and transformation of F^- in the soil-water system through the experimental study on the transport of high- concentration F^- (Zhang & Su, 2006).

In a pilot study conducted for the remediation of arsenic and pathogen from water, the Kanchan Arsenic Filter (KAF) was used. Particles and dirt deposited on the top layer of the sand progressively clog the filter after a period of use. When the user notices that the filtration rate is insufficient to fulfill the family's needs, it is time to clean the filter. Cleaning frequency ranges from once a month to six months, depending on the turbidity of the influent water,

consumption, and season (Ngai et al., 2007). The wasted iron nails (used in the filters) were buried in a marked area and kept under oxic conditions to prevent arsenic remobilization. However, no leaching studies were conducted further.

2.5 Use of Machine learning in the field of prediction modeling

The use of soft computing in modeling adsorbents and removing pollutants is a field gaining adequate attention. Several studies have explored the techniques of ANN, RSM, and linear regression to model the contaminant removal efficiency. SVM and ANFIS are relatively new among researchers in a similar field. Without being solely programmed, machine learning (ML) equips computers to assimilate data and is broadly classified as supervised and unsupervised learning (Khan *et al*., 2018). In supervised learning, an endeavor is carried out to learn an outcome hinged on a labeled training dataset comprising a set of input-output pairs. Predictive modeling is a proven and accepted engineering approach helping understand the contaminant removal process of numerous developed adsorbents (Ghaedi *et al.*, 2016; Hu *et al.*, 2017). ML-assisted predictive modeling is an increasingly employed tool to solve sustainable water engineering and management issues (Noori et al., 2011). The quantity and quality of the data determine the suitability of the machine learning technologies. Selecting the best method of the prediction model for case-specific experimental research is a key thrust area in this field due to the features of various methods (Sahu et al., 2022). In the same vein, though several investigations have been conducted on removing F^- ions from aqueous solutions using different adsorbents, every unique material needs to be given a particular focus, primarily due to varying material composition (Yetilmezsoy & Demirel, 2008). To aid the ML-assisted prediction models, sensitivity analysis is performed to understand the relative importance of individual input parameters on output efficiency. The best-related input parameters are then adopted for finer designing of the experiment and on-field applications.

Soil pollution or contamination happens when humans transfer dangerous materials, chemicals, or substances into the soil, either directly or indirectly. Typical pollutants include agricultural chemicals (over pesticide, herbicide, or fertilizer application), heavy metals, industrial activities, improper waste disposal, and seepage from a landfill. The movement of contaminants in soil is described by dispersion and diffusion processes. ML algorithms have been applied successfully in the area of soil property and target contaminant modeling. Emamgholizadeh et al. have determined soil dispersivity using ML (Emamgholizadeh et al., 2017). Field capacity (FC) and permanent wilting point (PWP) are two essential properties of

the soil when soil moisture is concerned. Since determining these parameters is expensive and time-consuming, Vaheddoost et al. developed and evaluated a hybrid artificial neural network model coupled with a whale optimization algorithm (ANN-WOA) as a meta-heuristic optimization tool (Vaheddoost et al., 2020). Another separate study applied a supervised committee machine with artificial intelligence (SCMAI) method on four ML techniques such as Sugeno fuzzy logic, Mamdani fuzzy logic, artificial neural network (ANN), and neuro-fuzzy to predict F^- concentration in soil (Nadiri et al., 2013).

Recent studies have furthered the application of machine learning algorithms to predict the concentration of pollutants in soil and soil temperature at various depths. For multi-step soil temperature forecasting, ML techniques such as KStar, instance-based K-nearest learner (IBK), and locally weighted learner (LWL) were designed and evaluated, with resampling algorithms of bagging (BA) and dagging (DA) (Khosravi et al., 2022). Dar et al. used ANNs to address F^- contamination in the Mamundiyar basin in India (Dar et al., 2012). In a separate study, several hybrid methods for groundwater F^- modeling using a global database combined two classification techniques, classification tree and knowledge-based clustering, and three predictive techniques (multiple regression, logistic regression, and adaptive neuro-fuzzy inference system) (Amini et al., 2009). Chitsazan et al. used hierarchical Bayesian model averaging to aggregate several artificial neural networks (ANNs) predictions for F^- contamination in the Maku area (Chitsazan et al., 2015). As demonstrated, AI/ML algorithms can successfully model and predict contaminant concentration in groundwater and soil through varying positions and depths (Barzegar et al., 2017).

Research gaps identified

The following gaps spanning all aspects of water storage, filtration, and sludge disposal were found based on the thorough literature survey conducted, and the literary evidence gathered:

i. In conjunction with economic barriers, the lack of appropriate and performing water storage infrastructure in rural areas often discourages the habitants from exploring alternate water sources and depending heavily on groundwater sources or irregular supply of tap water.
ii. Relying excessively on groundwater leads to a decline in groundwater levels and an increase in illness risk due to the presence of geo-genic contaminants in the groundwater.

iii. Unavailability and user displeasure in adapting to low-cost household water treatment units forces habitants to consume fluoride-laden water, which is significant to the study region of rural Rajasthan.

iv. Many studies conducted in contaminant remediation are limited to lab-scale experiments, creating a demand for economic and energy-efficient water filters in the field that are prepared with abundantly available and low-cost materials.

v. Given the preceding gap, the usage of Khejri has not been reported as an adsorbent for the removal of F^-. Though few reported studies have studied the purification of cement for applicability in the water industry, no study was found exploring the usage of cement in the preparation of a water filtration unit.

vi. Few studies in water filtration have addressed the inherent necessity to properly dispose of used filters and membranes and keep track of the impact these materials have on the environment.

Research objectives

i. For the first objective of the work, an in-depth study was carried out regarding the materials generally adopted for a household water storage facility. The advantages and disadvantages of the reviewed materials functioned as the guide to deciding the study's preferred tank materials. The objective included exploring two materials, jute, and glass, as composites due to their inherent advantages compared with regularly used tank materials. The proposed tank material was studied, focusing significantly on composites' effect on water quality. Health risk assessments for the proposed tanks were in tandem with the first objective.

ii. As a fluoride-prone region, developing and evaluating a low-cost adsorbent was addressed as the second objective. Considering the objective, an adsorbent was synthesized from Khejri, characterized, and studied for F^- removal efficiency.

iii. The third objective included studying the prevalence of Fluoride (F^-) in the study state of Rajasthan, India. Apart from data gathered from the literature, field collection and testing of groundwater was an area of focus. The toxicity of increased levels of F^- in the water was established through health risk assessments. Low-cost water filters were fabricated from cement and ceramic and extensively studied in the laboratory for their performance.

iv. The fourth objective primarily covered the distribution of filters among the participatory households from the study region, field visits, and surveys, participants'

acceptance toward the developed HWTs, and interactions with them. A component of the goal was to assess filter performance via follow-up surveys.

v. The disposal of the household sludge generated subject to exhausted filter plates, and soil quality monitoring constituted the final objective of the thesis.

Physical water quality parameters such as pH, turbidity, TDS, conductivity, hardness, and dissolved oxygen refer to the characteristics of water that can be observed or measured without changing its chemical composition. These parameters are important indicators of water's overall health and quality and can impact its suitability for various uses, such as drinking, irrigation, or industrial processes. Turbidity is an important parameter referring to the presence of suspended particles in water. The pH of water refers to its acidity or basicity, which can affect the solubility of pollutants. While Electrical conductivity (EC) is an indirect measurement of the concentration of ions in water, Total dissolved solids (TDS) refer to the total concentration of inorganic and organic substances in water. EC is controlled by the concentration of dissolved ions and mineral contamination, whereas TDS refers to the total concentration of inorganic and organic substances in water. EC and TDS values beyond prescribed limits guarantee the unsuitability of water for drinking or irrigation. Hardness is another significant physical parameter used to assess the water quality caused by calcium and magnesium.

It is important to note that these parameters can vary depending on the source of the water and the surrounding environment and can change over time due to natural processes or human activities. During the current study, a focus on the physical parameters was given due to the importance of studied parameters and their ability to affect users' health and safety directly. Further, physical parameters indicate the presence of other significant pollutants critical to human health (Sevgili et al., 2021).

Throughout the investigation, predictive modeling and optimization approaches were used to assess the performance of the selected adsorbent and the influence of disposal of exhausted HWTs on the soil and water quality. All of the objectives stated are interrelated to aid in establishing an effective rural water infrastructure system at a household level and aid existing water supply systems.

3 EVALUATION OF FIBER-COMPOSITE MATERIAL FOR SUITABILITY AS RAINWATER HARVESTING TANK

Chapter Overview

To reduce the dependence on groundwater sources, the need to explore alternate sources of water increases. Rainwater harvesting is a viable option to augment water scarcity. Appropriate storage structures are integral to the robust rural water management system and RWH. Given the identified gap pertaining to storage structures, an in-depth discussion has been provided regarding the construction and methodology adopted during the construction of the proposed polymer tanks, Jute fiber, and Glass fiber-reinforced polymers as suitable alternatives for rainwater harvesting structures.

The chapter further covers the methodology for fabricating fiber tank specimens and associated water quality tests. The experimental observations and concluding remarks are discussed in the subsequent sections of the chapter.

3.1 Jute fiber reinforced polymer (JFRP) composite preparation

The inherent importance associated with environmental friendliness and sustainability increased usage of eco-friendly materials as a replacement for conventionally available materials is the need of the hour. Environmental concerns and the social issue of renewable and biodegradable products have boosted interest in utilizing natural fibers in composites as an alternative to synthetic fibers (Chandramohan et al., 2019; Mathur, 2006). The idea of the Jute Fibre reinforced polymer (JFRP)Water Tank arose by considering all kinds of possible advantages of jute, like durability and high strength in nature. For the JFRP, a different approach was selected to fabricate and test specimens. Prototype tanks with a 20-liter capacity were erected using a plastic mold. For the lab-scale experiments, a plastic container was used as the mold. The mixture of epoxy resin and hardener was thoroughly weighed and mixed in a ratio of 10:1, respectively. Initially, the external coat of the mixture was applied, and the mold was removed after complete curing. Later the inner coat was applied. The base of jute fiber was made separately and fixed to it using the same coat of epoxy hardener mixture. A total of 3 coats were applied on both the inside and outside surfaces. After complete curing, rainwater was filled in the models.

The jute fiber prototypes could hold water up to its total volume. The models were prepared with different thicknesses of jute rope, like 2 mm, 10 mm, 20 mm, and 30mm. Physio-chemical variations observed in rainwater were monitored and evaluated to verify the credence of JFRP as a water storage structure. Figures 3-1 to 3-4 represent the fabrication of the JFRP prototypes figuratively. Parameters such as pH and total dissolved solids (TDS) were monitored at regular time intervals throughout the study. In addition, water absorption, plastic migration, and the presence of BPA were also monitored for pre-determined durations. The associated risk to human health was verified by evaluating ADD and IHQ for the recorded BPA values.

Figure 3-1 Dia of jute rope – 30mm and the size of the model – 1.5ft dia & 2ft height

Figure 3-2 Dia of jute rope – 20mm and the size of the model – 1.5ft dia & 2ft height

Figure 3-3 Dia of jute rope – 10mm and the size of the model – 1.5ft dia & 2ft height

Figure 3-4 Dia of twine rope (sutli) – 2mm and the size of the model – 1.5ft dia & 2ft height

3.2 Glass fiber reinforced polymer (GFRP) composite preparation

GFRP specimens are prepared from synthetic glass fibers as reinforcements and a resin-hardener mixture as the matrix. For the study, the resin and hardener were initially mixed in the ratio of 10-part resin to 1-part hardener by weight until a clear mixture was achieved in a beaker at room temperature. Fiber sheets were laid in the silicon mold layer by layer (Table 3-1), and resin was poured on each layer. Excess resin and trapped air bubbles were removed by moving a roller over the sheets. Sheets with a cross-sectional area of 300 mm * 300 mm were fabricated with varying thicknesses : 0 sheets for neat epoxy specimen, followed by 2, 3, and 5 layers of sheets corresponding to S2, S3, and S4, respectively. It took approximately 20

minutes to work with the mixture until polymerization started. The specimens were left and cured for 24 hours at room temperature under no external pressure. The curing duration was as per the specifications provided by the supplier. After complete curing, the specimens were released from the molds and cleaned with a cloth.

The samples were cut into test samples, 250*15 (ASTM D 3039, 2000; Singh et al., 2018), 105*10 (ASTM D3410, 2000), 100*100 (IS 9845 : 1998, 1998), 250*25(for pH, TDS, TH, BPA, and moisture absorption) [all dimensions are in mm]. Samples were divided into different groups corresponding to different immersion periods. The weights of samples were measured on a weighing balance accurate to 1mg. Subsequently, the cured specimens were dipped in the rainwater stored in a large container (collected during the active rainfall cycles) and kept at a temperature of 28±3 °C. Except for the tensile test, when samples were evaluated in quintuplicates, all specimens were prepared and tested in triplicates.

Table 3-1 The material composition of the composite specimen

Sample Designation	Glass fiber Layered laminates [No of layers]
S1	0 (Control; pure epoxy)
S2	2
S3	3
S4	5

Physio-chemical variations observed in rainwater were monitored and evaluated. Parameters such as pH, total hardness (TH), and total dissolved solids (TDS) were monitored at regular time intervals throughout the study. The recorded values were compared with rainwater quality stored in an RCC RWH tank. BPA concentration was monitored, followed by an assessment of ADD and IHQ. Aside from the physicochemical parameters, the structural endurance of the GFRP tank is required for extended service life. The water absorption, plastic migration, compressive strength, and tensile strength test further enhance our understanding of the adaptability of the GFRP composite as an RWH tank, structurally and qualitatively. The effect of water has been shown to reduce tensile properties and increase the bending behavior of composite with increased time because of interphase capillarity (Ji Hua & Sheng, 2004). Therefore, structural tests are essential to establish the suitability of the composite as a water

storage tank in the long run. Figure 3-5 sequentially highlights all the tests carried out during the completion of objective 1.

3.3 Tests conducted on the composite specimens

3.3.1 pH, Total Hardness, and Total Dissolved Solids

A small water sample was taken from the test container in a beaker, and the parameters were recorded. The electrode probe method determined pH and TDS. TH was measured by the volumetric method using EDTA (Ethylenediamine tetraacetate) according to the guidelines laid by the Bureau of Indian Standards (2008) (IS 3025 (Part 46): 1994, 2008).

All the recorded water quality data were monitored for the four jute specimens fabricated. Rope thicknesses of 2, 10, 20, and 30 mm were used for prototype fabrication. pH and TDS tests were successively performed on the four specimens for 24 days. For the GFRP specimens, pH, TH, and TDS were recorded continuously for the first 14 days. After that, tests were performed on days 15 and 30, and 60. The final readings were noted on day 180 [six months] (approx.).

Freshly collected rainwater was regularly added to the storage container, replicating an actual rainfall event to counter the problem of stagnant water and emulate a real RWH scenario on the field. The above method was achieved by capturing fresh rainwater during a rain event and adding the water to the specimen's storage container.

3.3.2 Presence of Bisphenol A

The water samples were collected in clean 25 ml sampling bottles after days 60 and 180 to understand the long-term effect of JFRP and rainwater interaction. On the contrary, for the GFRP specimen, the water samples were extracted and tested for BPA on days 15, 60, and 180. The extracted water sample was stored at 4°C until transportation and chemical extraction. The samples were tested at the State Water Testing Laboratory, Bhubaneswar, Odisha, India. Waters Xevo Triple Quadrupole Mass Spectrometer identified and quantified the target compounds. System control and data acquisition were achieved through Waters MassLynx V4.2. LC-MS. The samples were compared against Millipore water and BPA standards. ADD, and IHQ were determined for BPA to monitor the adverse health effect on consumers.

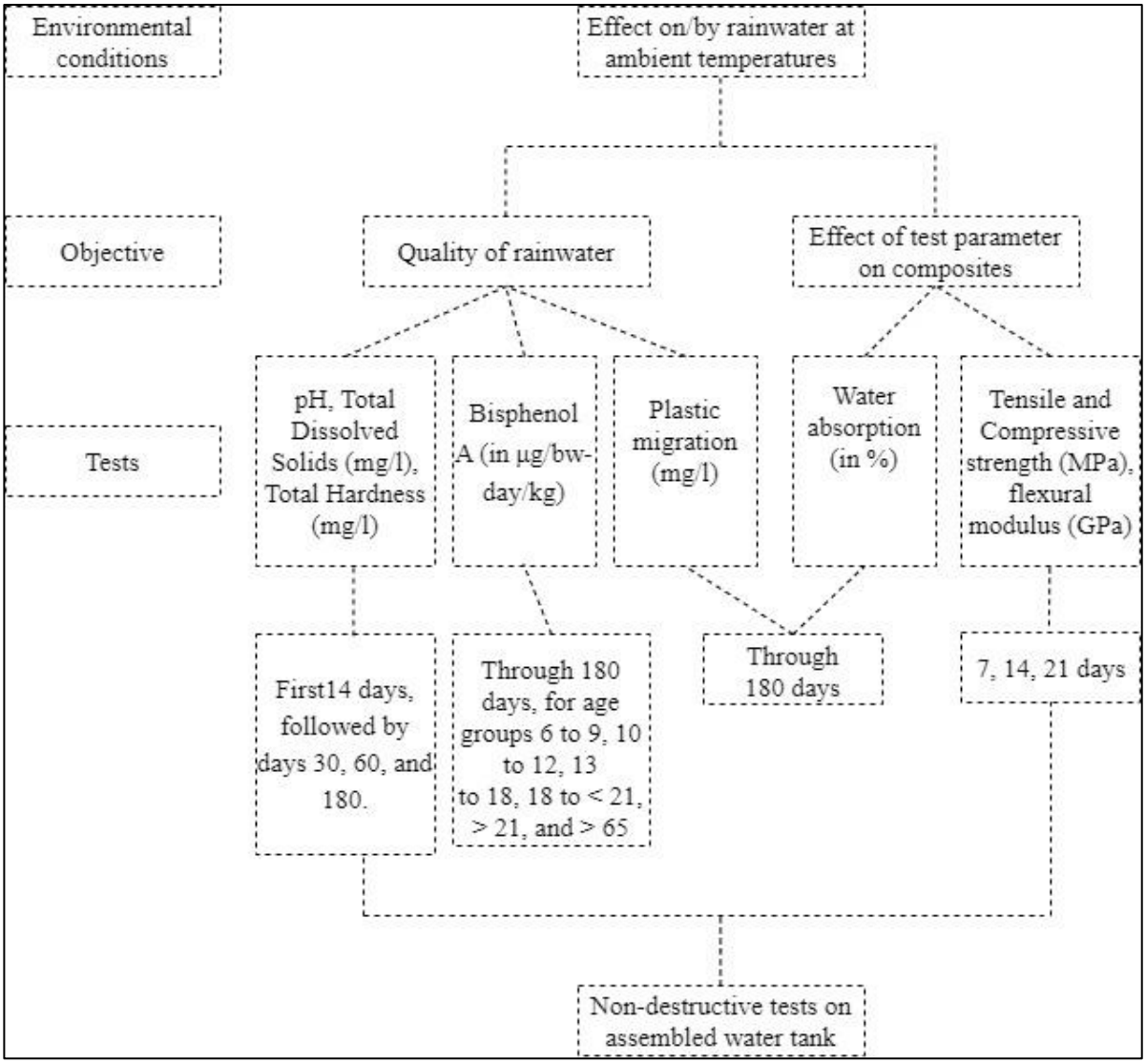

Figure 3-5 Flowchart outlining the objective and experiments conducted on the GFRP specimens

3.3.2.1 Human Health Risk Assessment (HHRA)

Health risk assessment is a verified paradigm adopted extensively for evaluating potential hazards to human health after exposure to certain chemicals over a period (United States Environmental Protection Agency, 1989). Health risk evaluations of chemicals adhere to the paradigm set forth by the National Research Council (NRC, 1983), with hazard identification, dose-response assessment, exposure assessment, and risk characterization being the four processes in the methodology. Ingestion, dermal, and inhalation are common pathways by which human populations are exposed to specific contaminants. Ingestion was considered the dominant pathway in the current work.

The results obtained from the HHRA highlight the associated harm to human health. The hazard quotient (HQ) is a non-cancer risk evaluation calculated using the ratio between the average daily dose (ADD) of a contaminant and the reference dose (Rfd) below which there will not be any appreciable risk (Khandare et al., 2020). While the average daily dose (ADD) is computed from the actual element content per the exposure scenarios defined, i.e., site and population-specific, the reference dose (RfD) is established for particular elements or pollutants in the standards and literature.

Average daily doses (ADD) of BPA ingestion were calculated for different age groups by multiplying the measured concentration of BPA by the average daily intake (consumption rate) of water by each age group and dividing it by the corresponding body weight (Chen & Chang, 2018). ADD can be calculated as in Equation 3.1,

$$\text{ADD} = \frac{C*IR*EF}{BW} \tag{3.1}$$

where ADD = average daily exposure dose (mg/kg-bw/day); C = fluoride concentration in the sample water (mg/l); IR = daily intake rate of contaminated water or the ingestion rate (l/day); EF = exposure factor (unitless) [The exposure factor (EF) is equal to 1 representing a daily exposure to the contaminant]; BW = body weight of specific age group (kg).

The Ingestion Hazard Quotient (IHQ) is used to determine the health risk of a chemical agent. The IHQ of F- exposure via ingestion was calculated as in Equation 3.2,

$$\text{IHQ} = \frac{ADD}{RfD} \tag{3.2}$$

where RfD is the reference dose. The reference doses (RfD) of BPA used were 0.05, 0.025, and 0.004 mg/kg-bw/day. While evaluating the IHQ values for the ingestion of Bisphenol A (BPA), the water ingestion rates, as discussed in Table 3-2, are adopted. For the specific case of water storage tanks, it is assumed that the water consumption primarily concerns the water consumed directly from the rainwater harvested and stored in the tank.

In addition to the health quotient, the Hazard Index (HI) evaluates the health risk of toxic chemicals in the water sample. All IHQs are combined to produce the composite number HI for the complete water sample. It is logical that if IHQ is greater than 1, the water sample is unfit for ingestion concerning that chemical.

The HI was calculated considering the parameters of TDS, TH, BPA, and plastic migration and calculated from Equation 3.3,

$$HI = \sum_{i=1}^{n} IHQ_i \quad (3.3)$$

Table 3-2 The village population's average age, weight, and water consumption range for the composite tanks

Average Age	Average weight (in kg)	Water consumption (in liters)
6 to ≤9	25	0.447
≤9 to ≤12	42	0.606
≤12 to ≤18	51	0.731
≤18 to ≤21	59	0.826
≥21	60	1.104
≥65	60	1.127

3.3.3 Moisture Absorption test

The samples' moisture absorption test was performed to evaluate their suitability when immersed in water to understand swelling behavior and matrix degradation (ASTM D570-98, 1998).

The specimens were dried in an oven for 24 hours at 50 ± 3°C, mellowed to room temperature, and immediately weighed to the nearest 0.001 g. Subsequently, specimens were placed in a container of rainwater sample water for 24 hours, rested on the edge, and immersed entirely.

At the end of 24+1⁄2 h, the specimens were removed from the water one at a time; the adhered water on the surface of the composites was wiped off with a dry cloth, weighed to the nearest 0.001 g immediately, and kept in water. The amount of time needed to remove the samples from the water bath and complete the weight measurement is relatively fast, presuming there is no water desorption during this time. While for the JFRP specimen, the weighing was carried out for 24 consecutive days, for the GFRP specimen, the weighing was continued and recorded for days 1-14, 30, 60, and 180. The weight difference calculated the moisture absorption.

Absorption determined as %M is expressed as (Equation 3.4):

$$\% M = \frac{w_t - w_o}{w_o} \times 100 \quad (3.4)$$

Where, w_t, and w_o are the weight of the composite samples after and before water immersion, respectively. When a sample's periodic weight change is less than 0.1 percent, it is said to reach equilibrium.

3.3.4 Migration of plastics from composites

The migration of plastics is an essential test when a particular composite is designed to be in contact with foodstuff or drinking water. The test was performed according to the Bureau of Indian Standards (1998) (IS 9845 : 1998, 1998). For the tests, two simulants, A and B, were used, where simulant A was deionized water, and simulant B was 3% acetic acid (w/v) in an aqueous solution. The composite samples were kept in a predetermined volume of simulants. The entire assembly was held in a water bath at 70°C for 2 hours for both the simulants. The specimens were then removed from extracted simulant with tongs, washed with a small amount of fresh simulant, and combined with extracted simulant. Blank was also conducted without the specimen. The entire beaker's content was then evaporated to about 50 to 60 ml and subsequently transferred into a clean-tared stainless-steel dish after three washings of the beaker with a small amount of fresh simulant. The concentrate in the container was then further evaporated to dryness in an oven at 100±5°C. After cooling the dish with the extractive in a desiccator for 30 minutes, the residue was weighed to the nearest 0.1 mg.

The amount of extractive (in mg/l) was computed from (Equation 3.5)

$$\textit{Amount of extractive (Ex in mg/l)} = M \times TSA \times \frac{1000}{A \times V} \quad (3.5)$$

where M (in mg) = mass of residue minus the blank value, A (in cm^2) = surface area exposed in each replicate, TSA (in cm^2) = total surface area of the container, V (in cm^3) = total volume of the container.

3.3.5 Strength test of composite and SEM analysis

The strength tests were primarily carried out for GFRP specimens. The GFRP samples prepared were immersed in rainwater and distilled water for 7, 14, and 21 days to study the detrimental effect of moisture on the epoxy-fiber interface. Distilled water was taken as the reference.

The tensile test was performed in the universal testing machine (UTM) with load cells having 100 kN capacity with a hydraulic grip pressure maintained at 3.5 MPa, and the crosshead displacement rate was fixed at 2 mm/min. A flat rectangular cross-section-shaped specimen

250 mm* 15 mm (length × width) wide was tested as per guidelines mentioned in ASTM D3039. The specimens were gripped between the wedge grips so that the entire grip length covered the face of the grips with enough pressure to prevent the sample from slippage and failure during tension. The grip length was maintained at 50 mm on both ends, while the gage length was kept at 150 mm.

The compressive test was performed on the UTM at a displacement rate of 1.5 mm/min and a grip pressure of 3.5 Mpa per guidelines established in ASTM D3410.

SEM analysis was performed to observe the matrix deterioration after the tensile test. After sputtering with gold, the surface morphology was studied using a field emission scanning electron microscope (FEI, Nova Nano FE-SEM 450, Oxford Instruments, UK).

3.3.6 Non-destructive testing of the GFRP tank

Flaws in FRP composites must be found and assessed throughout the structure's service life to ensure the structure's functionality. According to this viewpoint, non-destructive testing (NDT) can meet the demand for in-the-moment characterization and evaluation of flaws and damages (Dong & Ansari, 2011).

Numerous NDT techniques have been developed for evaluating the integrity or quantitatively measuring properties of materials, components, or structures. The Ultrasonic pulse velocity (UPV) test examines the homogeneity, quality, and defects, and the hydrostatic test checks for leaks and tightness of a water tank.

GFRP generally exhibits large thickness variations according to the size of the structure and its applications. The ultrasonic pulse-echo velocity results were obtained for tank wall cast panels to investigate thickness measurement errors. The obtained thickness values were compared with the values obtained using a Vernier caliper to calculate the measurement errors (Han et al., 2021). The panel was divided into rectangular grids for the study, 36 in number. At each marked location, three readings were recorded, and the average was reported. The average over the 36 points was compared with the vernier caliper reading to determine the error.

For the hydrostatic test, the completely assembled tank was filled with clean/ irrigation water to capacity, and the load was maintained for 24 hours to visualize leaks and damages.

Results and Discussions

3.4 Water quality and strength analysis of Rainwater harvesting tanks

This sub-section of the chapter covers the water qualitative analysis of the proposed rainwater storing facility.

3.4.1 Jute fiber reinforced polymer (JFRP) composite preparation

All the recorded water quality data were monitored for the fabricated specimens. Four specimens of varying rope thicknesses of 2, 10, 20, and 30 mm were fabricated. pH, TDS, plastic migration, and water absorption tests were performed on the four specimens for 24 days. However, the BPA leaching tests were conducted at the end of 60 and 180 days to understand the long-term effect between water and JFRP interaction. Apart from qualitative monitoring of water quality parameters, an essential aspect is the suitability of the proposed material for safe human exposure. The Human Health Risk Assessment paradigm, comprising the Ingestion Hazard quotient (IHQ) and Hazard index (HI), was used for material evaluation depending on the monitored water quality data.

3.4.1.1 Determination of pH and Total Dissolved Solids

The water sample was taken from the sample fabricated jute tanks and tested in the laboratory. The water quality was continuously monitored for 24 days.

The recorded pH values ranged from a minimum of 8.06 to a maximum of 8.54, averaging over 8.36 for the 2mm thick tank. It is noted that the pH value of 8.54 exceeded the threshold of 8.5 for a single recorded incidence.

For the tanks with rope thicknesses of 10mm, 20 mm, and 30 mm, the recorded minimum and maximum pH values were 8.0, 8.13, and 8.09, and 8.5, 8.46, and 8.44, respectively. The mean pH values were 8.28, 8.31, and 8.31 for the three samples sequentially. All the recorded pH values have been presented in Figure 3-6.

With TDS values averaging over 899.98, 891.29, 879.03, and 882.52 through the specimens in increasing order of their rope thickness, it was evident that the recorded values lay within the threshold limit of 2000 mg/l.

As reported in Figure 3-7, the TDS values for the samples followed a homogenous pattern and increased over the test days.

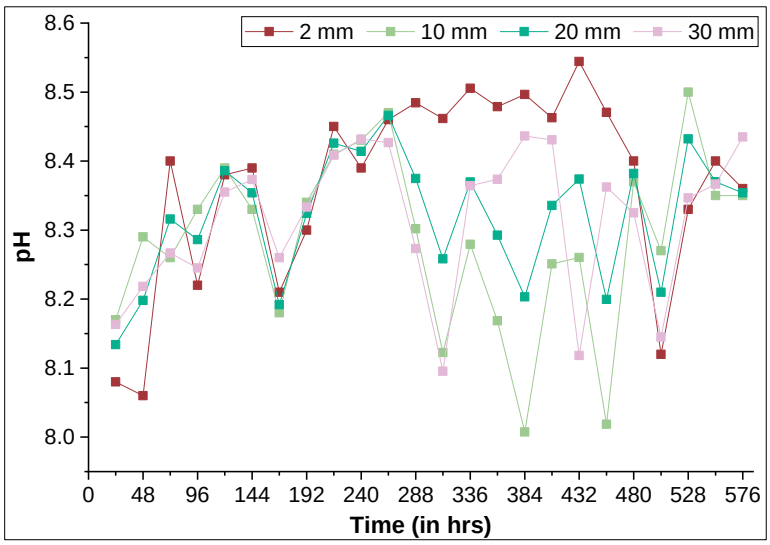

Figure 3-6 Observed variation of pH for all fabricated samples

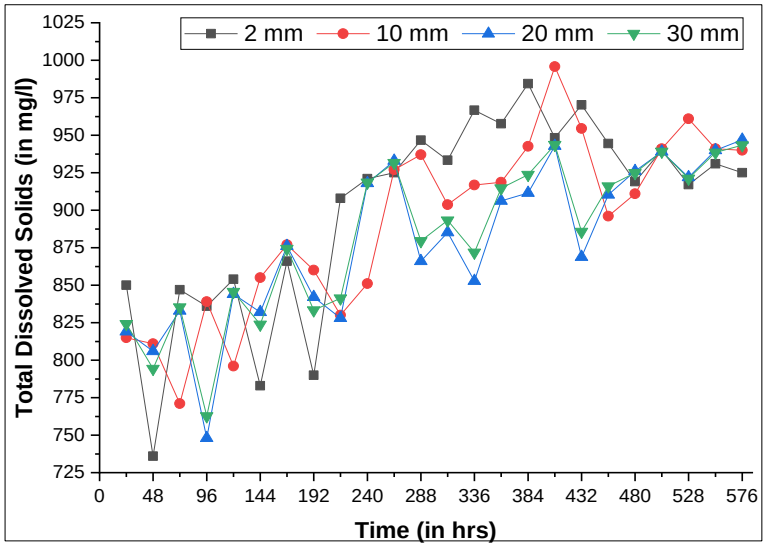

Figure 3-7 Observed variation of TDS for all fabricated samples

3.4.1.2 Presence of Bisphenol-A

By methodically analyzing the obtained experimental BPA values in stored rainfall samples, the proportional contributions of drinking water to overall exposure and potential human health risk were estimated for the jute fiber samples.

Results reported an average of 3 readings over the test duration of 60 and 180 days. An increased value of BPA was detected for all the jute samples for test day 180. After the test day 60, the 10 mm thickness specimen had the least recorded BPA, 1.65 µg/ml. The 2 mm, 20 mm,

and 30 mm prototypes have recorded BPA readings of 4.92, 9.91, and 8.97 µg/ml. For test day 180, the observed BPA concentrations for the samples in sequence are 28.3, 28.3, 28.4, and 38.34 µg/ml.

Figure 3-8 represents the calculated ADD for intended users on day 60. With 100% absorption, the 10 mm specimen performs better, followed by 2 mm, 30 mm, and 20 mm specimens in sequence. A homogenous sequence is recorded for all the specimens. Age groups 10 to 12, 13 to 18, and 18 to 20 have the least recorded ADD.

In another observation, the ADD values recorded on day 180 highlight the similar readings recorded for 2 mm, 10 mm, and 20 mm in Figure 3-9. However, it is appreciable to note that all the values derived were below the permissible value of the tolerable daily intake (TDI) of 0.004 mg/kg-bw/day by EFSA.

The calculated IHQ values for the three global reference dosages are documented in Tables 3-3 and 3-4. The ratio between the exposure doses for each age group and the RfD values for US EPA, EFSA, and Health Canada standards were all <1, signifying that exposure doses are lower than reference doses. The safety of the proposed JFRP tank as a water storage infrastructure is justified.

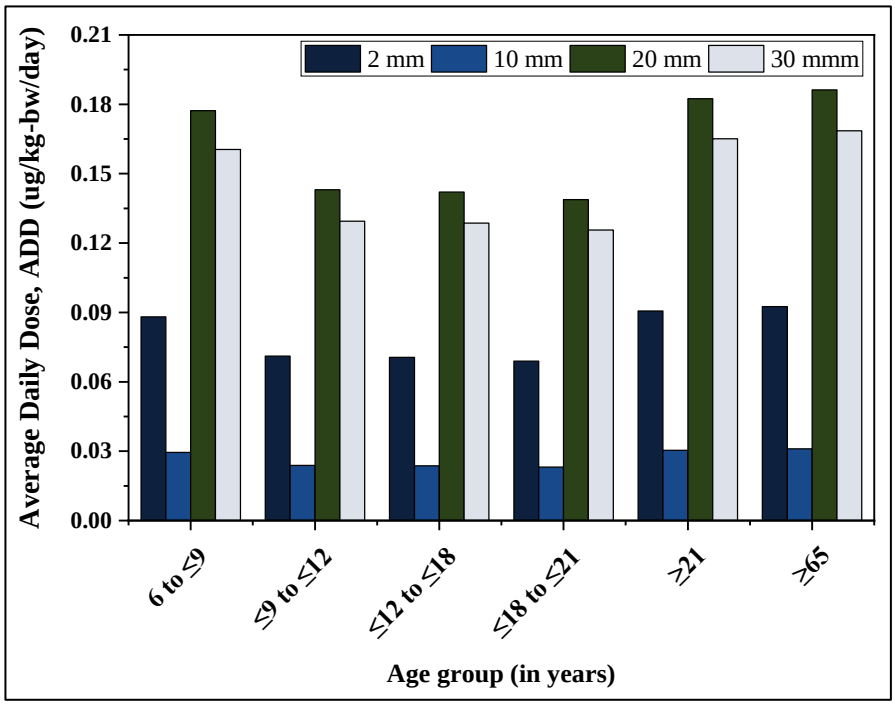

Figure 3-8 ADD values for the jute specimens on test day 60

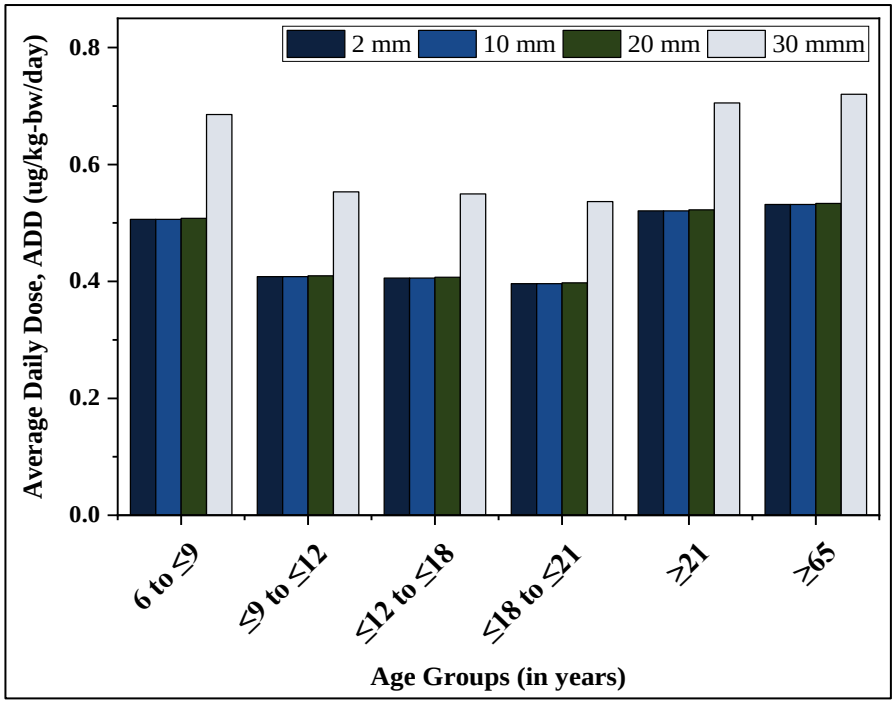

Figure 3-9 ADD values for the jute specimens at test day 180

Table 3-3 Age-specific and specimen-specific calculated IHQ values for test Days 60

Age groups	RfD = 50 (µg/kg/day)				RfD = 25 (µg/kg/day)				RfD = 4 (µg/kg/day)			
	2	10	20	30	2	10	20	30	2	10	20	30
6 to ≤9	0.0018	0.0006	0.0035	0.0032	0.0035	0.0012	0.0071	0.0064	0.0220	0.0074	0.0443	0.0401
≤9 to ≤12	0.0014	0.0005	0.0029	0.0026	0.0028	0.0010	0.0057	0.0052	0.0178	0.0060	0.0358	0.0324
≤12 to ≤18	0.0014	0.0005	0.0028	0.0026	0.0028	0.0009	0.0057	0.0051	0.0177	0.0059	0.0355	0.0322
≤18 to ≤21	0.0014	0.0005	0.0028	0.0025	0.0028	0.0009	0.0056	0.0050	0.0172	0.0058	0.0347	0.0314
≥21	0.0018	0.0006	0.0036	0.0033	0.0036	0.0012	0.0073	0.0066	0.0227	0.0076	0.0456	0.0413
≥65	0.0019	0.0006	0.0037	0.0034	0.0037	0.0012	0.0074	0.0067	0.0231	0.0078	0.0466	0.0421

***All dimensions are in mm**

Table 3-4 Age-specific and specimen-specific calculated IHQ values for test Days 180

Age groups	RfD = 50 (µg/kg/day)				RfD = 25 (µg/kg/day)				RfD = 4 (µg/kg/day)			
	2	10	20	30	2	10	20	30	2	10	20	30
6 to ≤9	0.0101	0.0101	0.0102	0.0137	0.0202	0.0202	0.0203	0.0274	0.1265	0.1265	0.1269	0.1714
≤9 to ≤12	0.0082	0.0082	0.0082	0.0111	0.0163	0.0163	0.0164	0.0221	0.1021	0.1021	0.1024	0.1383
≤12 to ≤18	0.0081	0.0081	0.0081	0.0110	0.0162	0.0162	0.0163	0.0220	0.1014	0.1014	0.1018	0.1374
≤18 to ≤21	0.0079	0.0079	0.0080	0.0107	0.0158	0.0158	0.0159	0.0215	0.0991	0.0991	0.0994	0.1342
≥21	0.0104	0.0104	0.0105	0.0141	0.0208	0.0208	0.0209	0.0282	0.1302	0.1302	0.1306	0.1764
≥65	0.0106	0.0106	0.0107	0.0144	0.0213	0.0213	0.0213	0.0288	0.1329	0.1329	0.1334	0.1800

***All dimensions are in mm**

3.4.1.3 Moisture Absorption test

The relation between the moisture absorption content of the composites and immersed time is reported in Figure 3-10. Specimens with 10 mm and 20 mm rope widths witnessed a homologous trend. Till 192 hours, a sudden increase in water absorption was witnessed. Thereby, the water absorption was even till achieving an equilibrium stage.

2 mm and 30 mm thick specimens followed a similar trend, with a significant increase in water absorption observed till 288 hours. After that, the moisture absorption rate decreased until achieving an equilibrium stage.

The initial absorption phase of all the fibers is caused due to the wetting of the fibers and the capillary absorption process, where the water diffuses into the fibers until it reaches maximum absorption. A diminishing trend in water absorption happens when the immersion period increases, attributed to physical damage, chemical reactions, or material hydrolysis (Nayak & Mohanty, 2019).

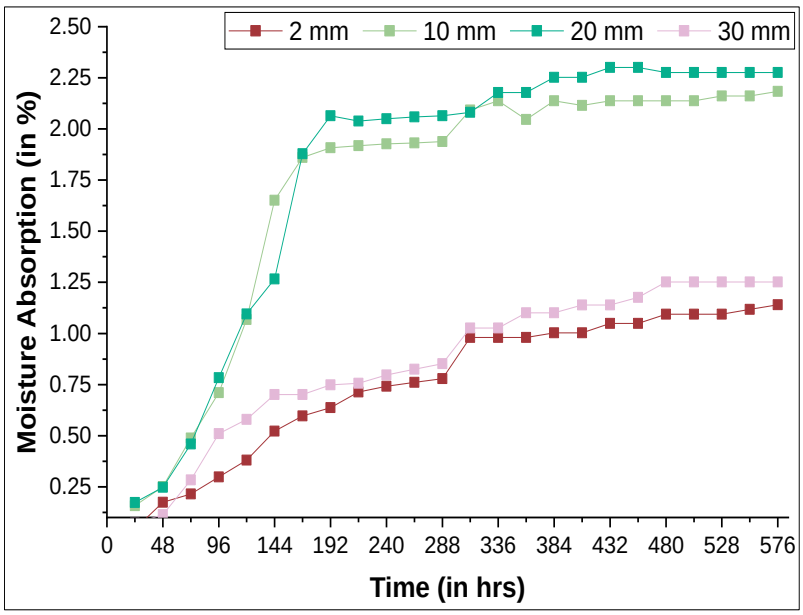

Figure 3-10 Moisture absorption observed over test duration for the fabricated JFRP specimens

3.4.1.4 Migration of plastics from composites

The specimens exhibit an increasing pattern for all the observations, as reported in Figure 3-11. 20 mm thick specimen showed the highest plastic migration when the simulants were switched from A to B. For 10 mm and 2 mm specimens, the plastic migration varied from 0.039 mg/l to 0.095 mg/l and 0.035 mg/l to 0.081 mg/l, respectively. The overall percentage increase was 132.57 % and 142.93 % for the 2 mm and 10 mm specimens.

The plastic migration was within comparable ranges for the first three specimens, with the largest variation of 18.93 % between 2 mm and 20 mm specimens.

The documented plastic migration was highest for the 30 mm specimen. The values were 0.057 mg/l and 0.11 mg/l for simulants A and B. However, the total increase when switching simulants was lowest for the specimen, at 92.13%.

Because of the corrosive nature of the acidic medium and the displacement of individual composite particles owing to increasing temperature, the values obtained in simulant B were more significant than those obtained in simulant A for all the samples. The total plastic migration for all samples was significantly below the authorized limits of 60 mg/l, demonstrating that the proposed JFRP is appropriate for a rainwater collecting tank construction (IS:10146-1992).

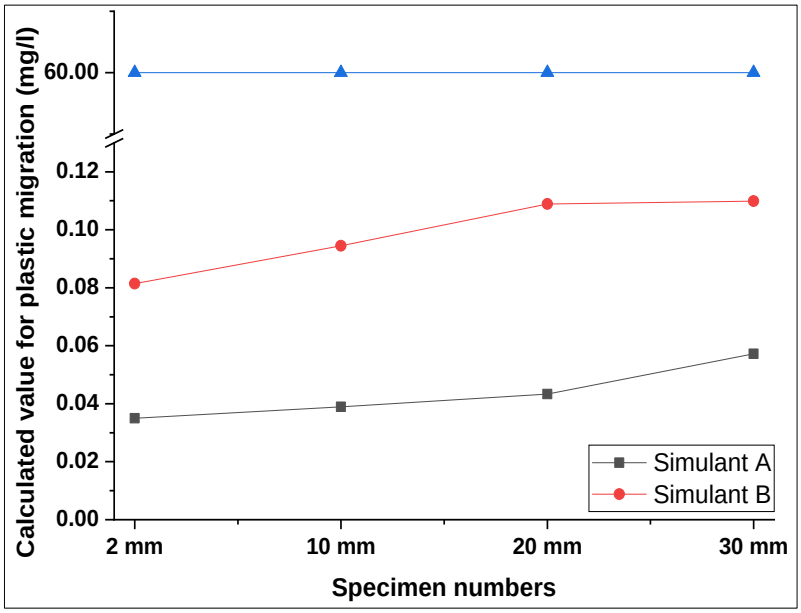

Figure 3-11 Migration of plastic in water for Simulant A (distilled water) and Simulant B (Acetic Acid) over the experimental period for individual specimens

3.4.1.5 Fabrication of a full-scale JFRP tank

After the experimental analysis and water quality monitoring were completed, a full-scale JFRP tank of capacity 20 m^3 and dimension 3.05 m*3.05 m was fabricated. The 2 mm and 10 mm thick rope specimens had better qualitative analysis among the four rope specimens. Therefore, these two ropes were used for JFRP tank construction. In the first step, a hollow metal frame was used for wounding the jute. Subsequently, the resin-hardener mixture was applied to the upright structure, externally and internally. A base from a similar thickness fiber was prepared separately and bonded to the tank's walls. After complete curing, the tank was filled with water and inspected for leakages -- minor leakages from the base portion were controlled by applying a few coats of the resin hardener at precise points. The fabrication process of the JFRP tank is represented in Figures 3-12 and 3-13.

(a)  (b) 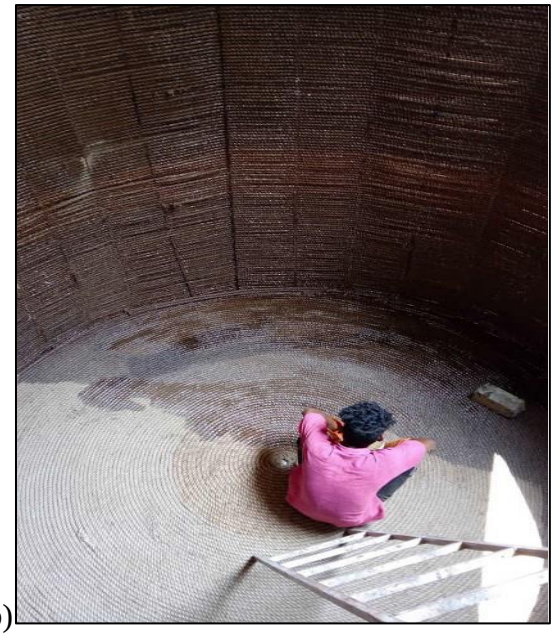

Figure 3-12 a) Winding of jute fiber around the frame b) internal application of the resin-hardener coat

(a)  (b) 

Figure 3-13 a) Removal from the frame after complete curing of the tank b) Final JFRP tank of capacity 20 m^3

With the issues encountered during the fabrication of JFRP tanks, a lightweight alternative was explored.

3.4.2 Glass fiber reinforced polymer (GFRP) composite tanks

All the recorded water quality data were monitored for the fabricated specimens. pH, Total Dissolved Solids, Total Hardness, Plastic migration, and water absorption tests were performed on the four specimens, i.e., S1, S2, S3, and S4. After a successful qualitative evaluation of the specimens, the best combination was selected for the strength tests and subsequent on-site fabrication.

The recorded water physicochemical parameters for the GFRP tanks were compared qualitatively with the water stored in the Concrete RWH structure.

3.4.2.1 Determination of pH, Total dissolved solids, and Total hardness

Continuous qualitative parametric readings were recorded for the first 14 days, followed by days 15, 30, 60, and 180. Rainwater quality data corresponding to both composites and concrete are represented in Figures 3-14 and 3-15.

The recorded pH values ranged from a minimum of 8.16 to a maximum of 8.46 for sample S1 averaging over 8.36. All recorded values lay within the acceptable range of 6.5 to 8.5. The maximum and minimum recorded pH values for samples S2, S3, and S4 were 8.79, 8.54, 8.44; 7.73, 8.06, and 8.02, respectively. Evison and Sunna recorded a pH of 7.7 to 8.3 for a fiberglass water storage tank (Evison & Sunna, 2001). pH ranging from 7.23 to 6.81, averaging over 7.05, was observed for fiberglass tanks in Bolivia (Schafer & Mihelcic, 2012). pH varied from 6.75 to 7.1 for HDPE tanks in a select city in Nigeria (Nnaji et al., 2019). For S1 and S4, all recorded pH was below the threshold of 8.5. While 42.1% (n=8) of recorded pH values for S2 exceeded the permissible limit of 8.5 concentrated in the first week of recording water quality, only 5.26 % (n=1) of recorded readings exceeded 8.5 for S3. Observed pH values for water stored in the concrete tank varied from 7.2 to 8.63, averaging 7.49.

According to WHO (2022) and Indian (2012) guidelines, all TH readings for S1 and S3 were below the 200 mg/l thresholds (WHO, 2022; IS 10500, 2012). 21.05% readings for S2 had hardness higher than 200 mg/l. The mean hardness values were 134.64, 179.52, 187.78, 155.1, and 146.1 mg/l for S1, S2, S3, S4, and concrete samples. With TDS values averaging over 881.43, 709.94, 876.68, and 714.35 mg/l through samples S1 to S4, it was evident that the recorded values lay within the threshold limit of 2000 mg/l. Concrete water samples performed better with maximum, minimum, and average recorded values at 224, 115, and 188.68 mg/l.

The maximum TDS of a fiber cement tank was recorded at 0.2 g/l with a standard deviation of 0.1 g/l (Schafer & Mihelcic, 2012).

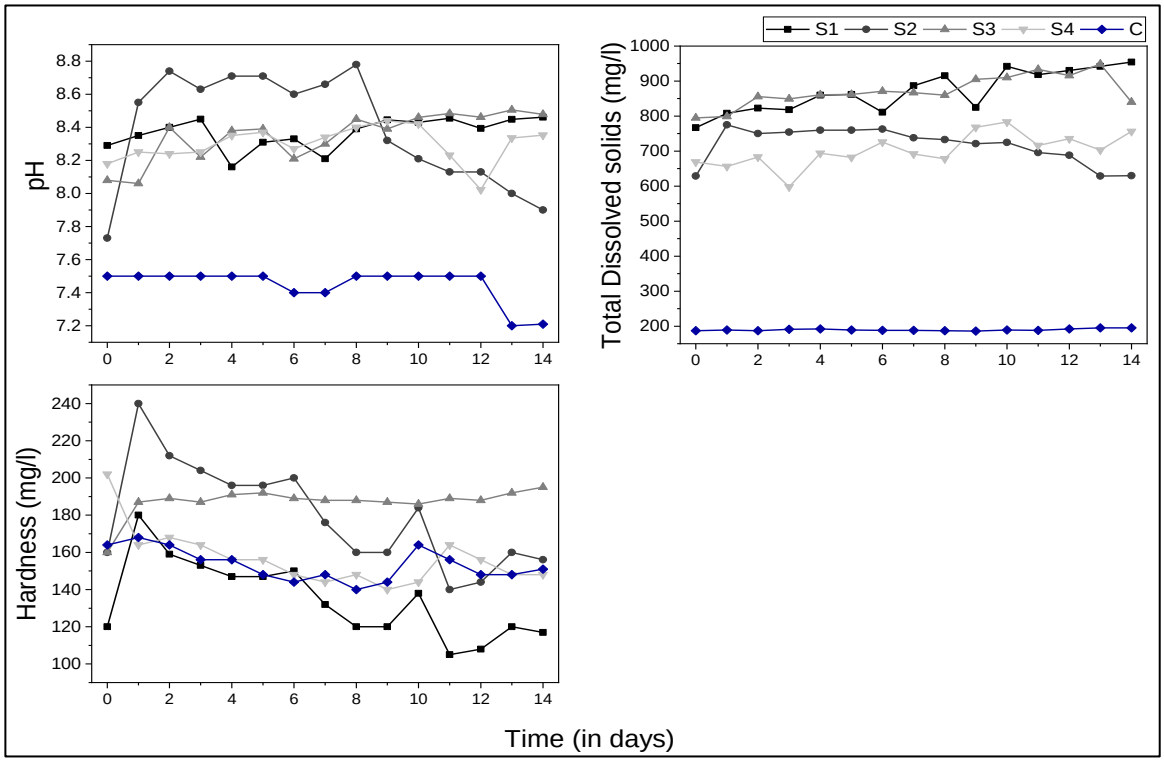

Figure 3-14 pH, Hardness, and Total Dissolved Solids of specimens S1, S2, S3, S4, and concrete for the initial 14 days

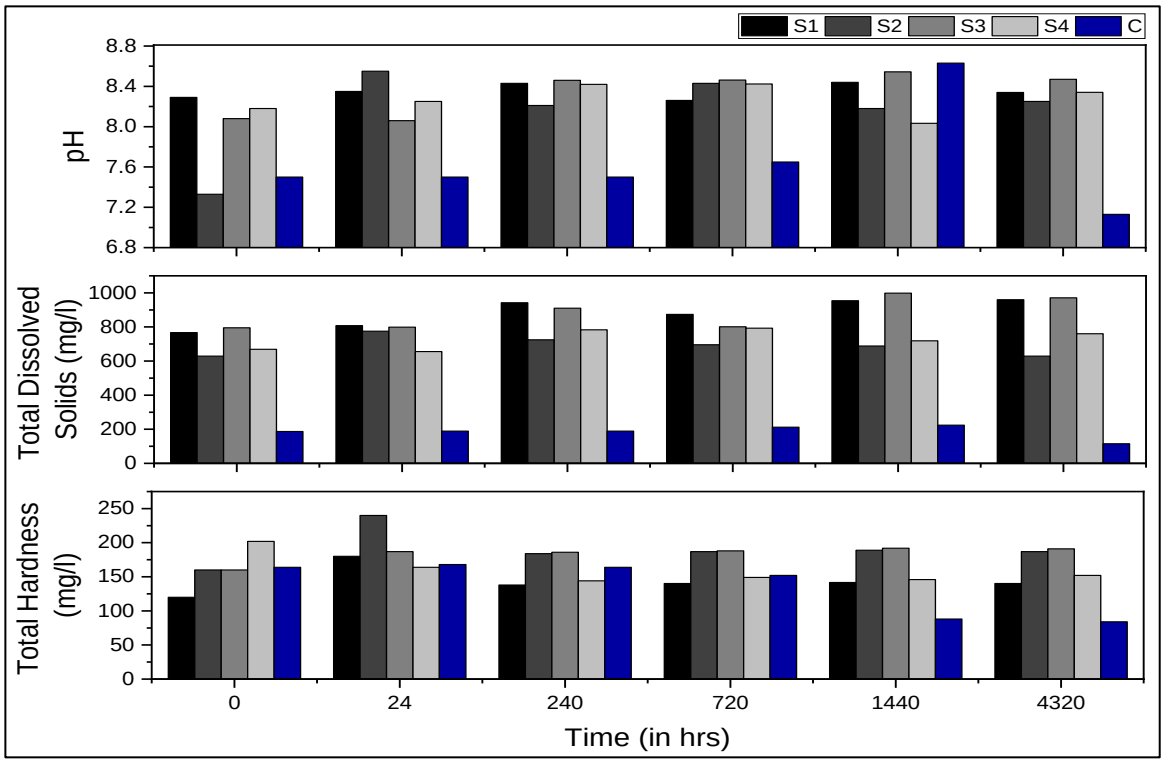

Figure 3-15 Parameters recorded throughout the experiment duration of 180 days

3.4.2.2 Presence of Bisphenol-A

The proportional contributions of drinking water to overall exposure and possible human health risk were determined by systematically evaluating the obtained experimental BPA values in stored rainfall samples.

BPA concentration was detected in the specimens from ND (not detected) to 56.6 μg/l with a detection rate of 86.1% (n=31). Results reported an average of 3 readings over the test duration of 180 days (Figure 3-16a). While an increased value of BPA was detected for S4, S3 had the most negligible concentration of BPA. As observed, BPA concentration was proportional to the number of test days. For day 60, the median and standard deviation values for S2, S3, and S4 were reported at 5.81,7.06, 7.74μg/l, and 2.42, 1.9, and 1.99 μg/l. For test day 180, the observed median values for S2 through S4 varied from 28.5 to 45.28 μg/l. The corresponding standard deviations for S2, S3, and S4 are 13.42, 1.91, and 7.53 μg/l.

Figure 3-16b represents the calculated ADD from Equation 3.1 for intended users on day 180. The observed performance of the specimens was S3> S2> S4. Based on the determined concentration of BPA and 100% absorption, the estimated median BPA intake for S2 on day 180 is 0.35, 0.29, 0.28, 0.28, 0.36, and 0.37 ug/kg-bw/day for ages 6 to ≤ 9, ≤9 to ≤ 12, ≤12 to ≤18, ≤ 18 to ≤ 21, ≥ 21, and ≥ 65, respectively. The values derived were below the permissible value of the tolerable daily intake (TDI) of 0.004 mg/kg-bw/day by EFSA.

IHQ was derived from Equation 3.2. The ratio between the exposure doses for each age group and the RfD values for US EPA, EFSA, and Health Canada standards were all <1, signifying that exposure doses are lower than reference doses (Table 3-5).

The lowest available oral reference dose or oral toxicity benchmark was used to determine the Margin of safety (MOS) calculated by dividing the oral toxicity standard by the ADD, with the target MOS ≥1. The current study adopted an oral toxicity benchmark of 16 μg/kg-bw/day (Willhite et al., 2008). Compared with the lowest oral toxicity benchmark, the MOS for ADD ranges from 18 to 138 (Figure 3-17). The percentile values of MOS show that the BPA dosages identified have no harmful impact on human health.

Figure 3-18 represents the cumulative hazard index calculated for test days from Equation 3.3. All other calculations determining the ADD, IHQ, and MOS for days 15 and 60 have been detailed in Appendix 1, from Table i to iv.

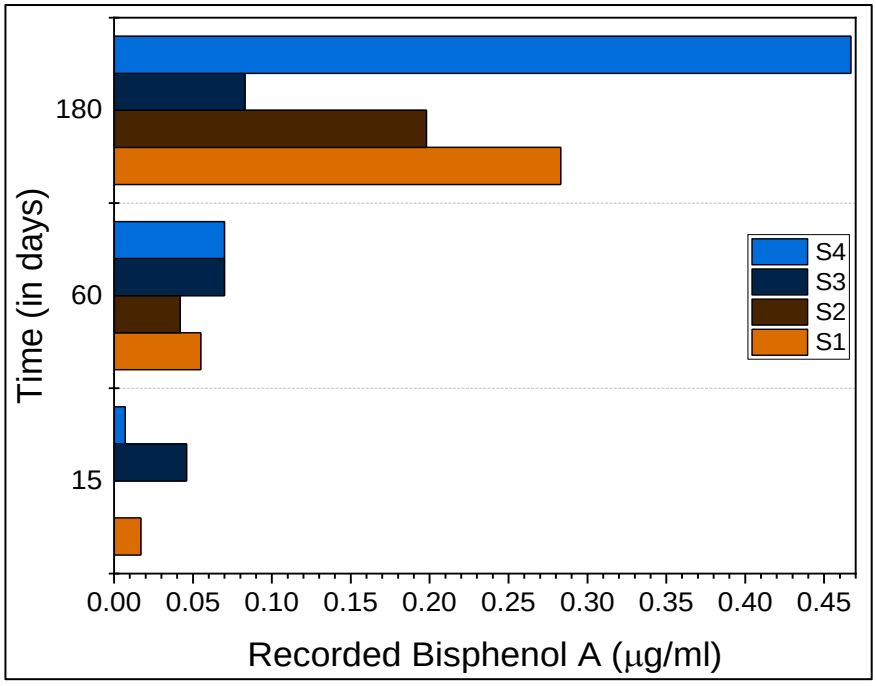

(a)

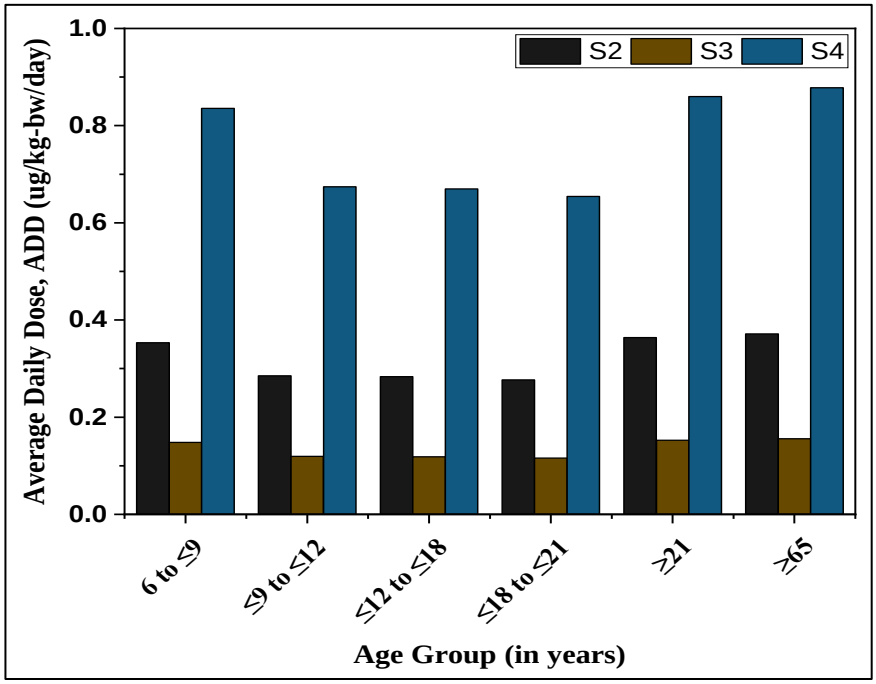

(b)

Figure 3-16 a) BPA concentrations determined for the specimens through 180 days b) ADD calculated for different age groups at day 180

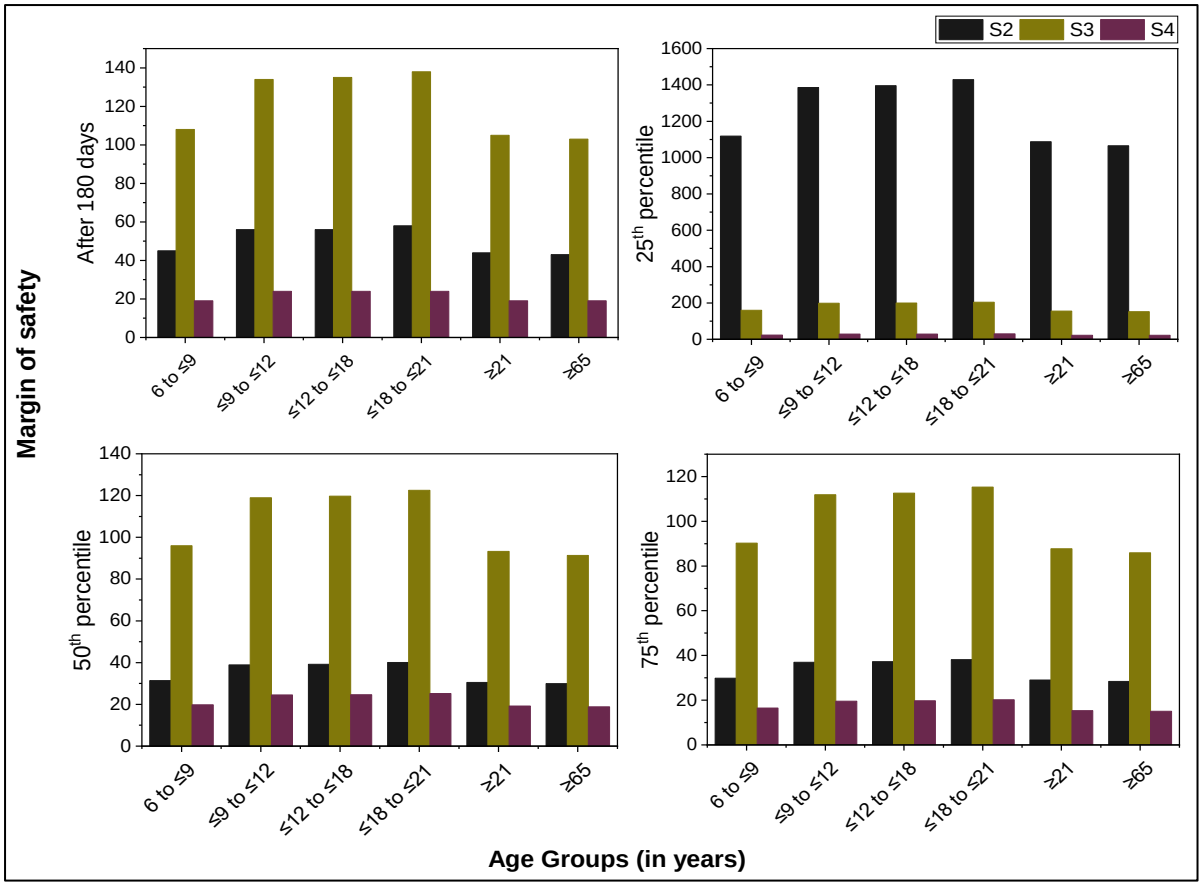

Figure 3-17 Margin of safety calculated for specimens S2, S3, S4

Table 3-5 Age-specific and specimen-specific calculated IHQ values for test Days 180

Age Groups	R_fD = 50 (µg/kg/day)			R_fD = 25 (µg/kg/day)			R_fD = 4 (µg/kg/day)		
	S2	S3	S4	S2	S3	S4	S2	S3	S4
6 to ≤9	0.0071	0.003	0.0167	0.0141	0.0059	0.0334	0.0884	0.037	0.2089
≤9 to ≤12	0.0057	0.0024	0.0135	0.0114	0.0048	0.0269	0.0713	0.0299	0.1686
≤12 to ≤18	0.0057	0.0024	0.0134	0.0113	0.0047	0.0268	0.0708	0.0297	0.1675
≤18 to ≤21	0.0055	0.0023	0.0131	0.0111	0.0046	0.0262	0.0692	0.029	0.1636
≥21	0.0073	0.003	0.0172	0.0145	0.0061	0.0344	0.0909	0.0381	0.215
≥65	0.0074	0.0031	0.0176	0.0149	0.0062	0.0351	0.0928	0.0389	0.2195

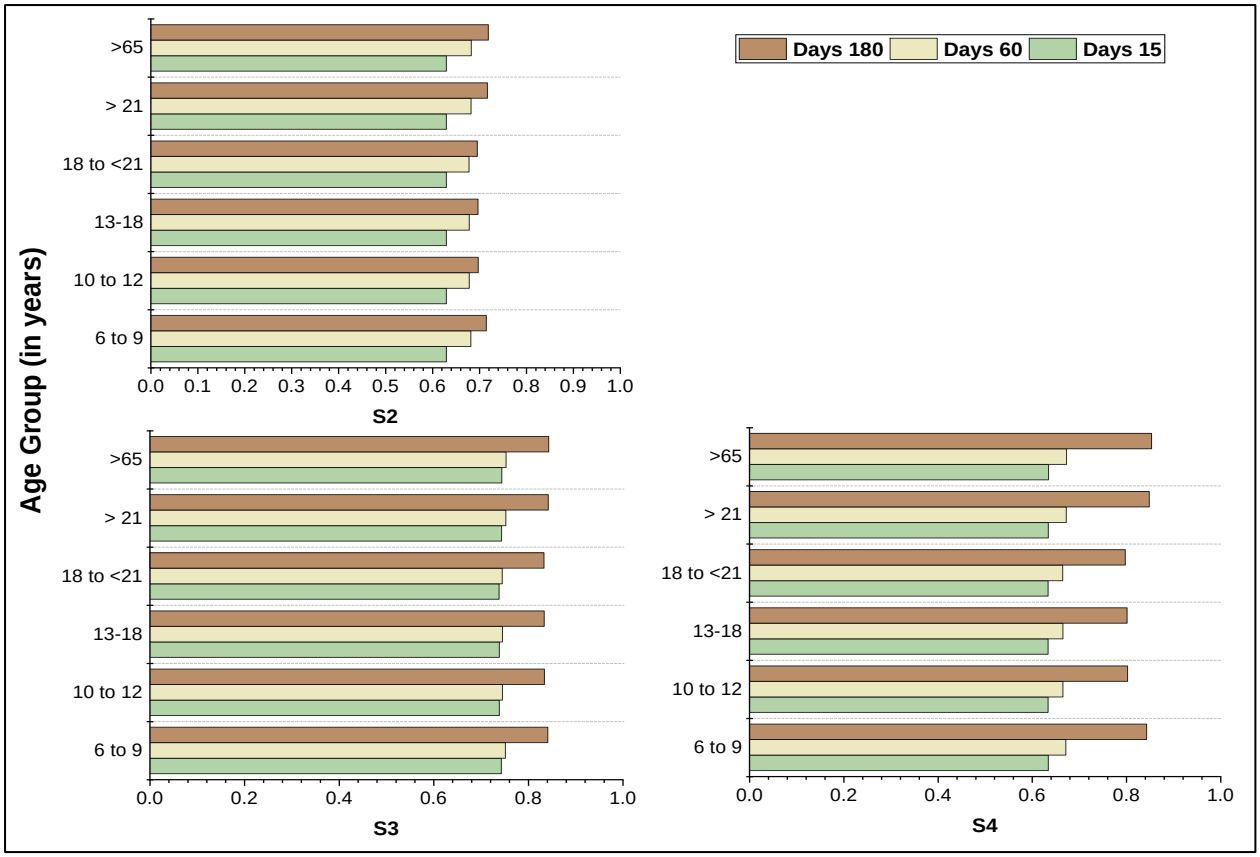

Figure 3-18 Hazard index (HI) values for all the samples recorded on different test days

3.4.2.3 Migration of plastics from composites

For Simulants A and B, the specimens exhibit a consistent pattern (Figure 3-19). S4 showed the largest plastic migration of any sample, with readings for simulants A and B of 0.042 and 0.099 mg/l, respectively. However, when the simulants were switched, the overall increase was the smallest, at 135.71%.

Plastic migration rose in the range of 275% for S1 upon varying the simulant from A to B, affected by incomplete curing or displaced particles. Plastic migration in S2 and S3 is 0.03 and 0.033 mg/l in Simulant A; and 0.084 and 0.089 in Simulant B, respectively. The values were within comparable ranges, indicating an increase of 180 and 169.7% in total plastic migration. The values obtained in simulant B were more significant than A for all samples due to the acidic medium's corrosive character and the displacement of individual composite particles due to increased temperature. The overall plastic migration for all the samples was far below the permitted limits of 60 mg/l, indicating the composite structure suitable for a rainwater harvesting tank (IS:10146-1992).

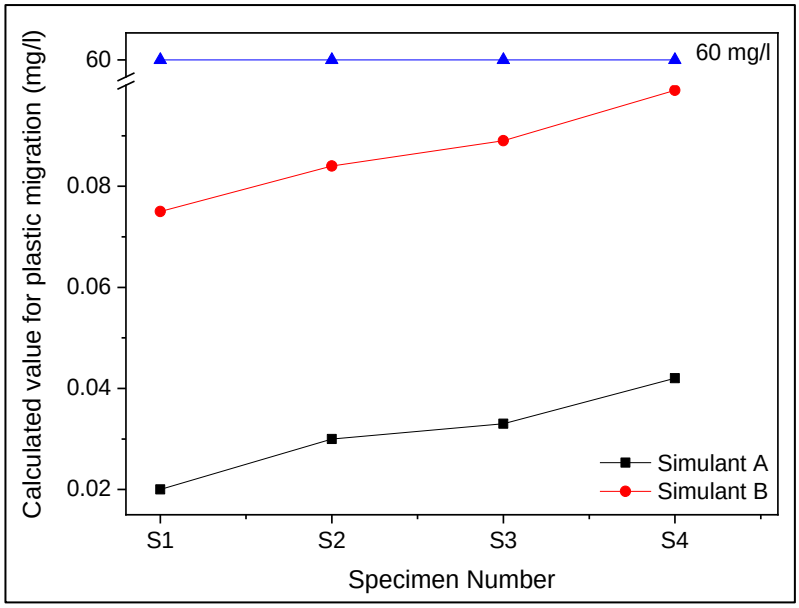

Figure 3-19 Migration of plastic in water for Simulant A (distilled water) and Simulant B (Acetic Acid) over the experimental period for individual specimens

3.4.2.4 Moisture absorption for composites

The relation between the moisture absorption content of the composites and immersed time is reported in Figure 3-20, starting after 24 hours. Water absorption is a significant factor degrading the mechanical strength of FRP composites. The weak interface between the fiber and the matrix is particularly prone since water can travel through the interface due to the fiber's capillarity (Oskouei et al., 2018). Pure epoxy control specimen showed a higher water absorption than GFRP composites, indicating moisture is primarily absorbed into epoxy as glass fiber is hydrophilic. The affinity of functional groups in epoxies having high polarity towards water molecules results in higher water uptake by S1 through the epoxy network.

The moisture absorption behavior of the composite is broadly divided into four stages. Till 360 hours, a sudden increase in weight is observed for S1. An increasing trend in water absorption is observed in parts B, C, and D at 12.61, 11.2, and 25.89%. S3 follows an increasing trend in A and B, followed by a decreasing trend resulting from leaching out of material until equilibrium (Akil et al. 2010).

S2 and S4 followed a very similar trend throughout the test duration, with an initial negative slope in A followed by an increasing trend in B. A significant increase is observed in Part C until equilibrium. Cumulative moisture uptake reported was 5.62, 0.81, 2.54, and 0.96% for samples S1 through S4.

Capillarity would conduct the water molecules to the material; voids and cracks in the composites are ideal spaces to accept the water, as voids inside the material were the main water-storage pathway. S3 has a higher water absorption rate than S2 and S4, preferably due to the formation of defects/voids during composite manufacturing, allowing more water to be absorbed.

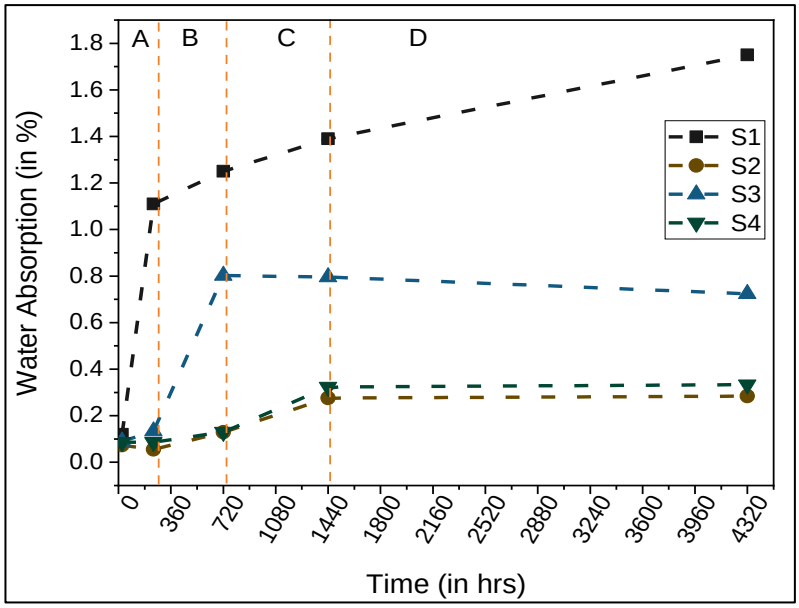

Figure 3-20 Moisture absorption observed over 180 days

3.4.2.5 Strength test for composites

Though the water absorption recorded for Specimen S3 was the highest among S2, S3, and S4, reported plastic migration and detected BPA concentration was the lowest. Therefore, the S3 composition was selected for further testing. Standard-sized specimens were immersed in deionized and rainwater, with the tensile and compressive test carried out on days 7, 14, and 21. After removing the test specimens from the water samples, the samples were thoroughly dried, followed by the strength tests.

The specimens' strength results are represented in Figures 3-21 to 3-23. 88.2 Mpa, 5.12 Gpa, and 60 Mpa were the dry specimen's recorded tensile strength, Young's modulus, and compressive strength. Similar results were observed in a previous study designed for GFRP composites with similar applied usage (Raya & Gupta, 2022). For the test days, composite tensile strength witnessed an increasing trend apart from Day 14. The compressive strength, however, witnessed an increasing trend through the test days. However, a cumulative increase

in tensile strength was reported for rainwater at around 7.09%. The compressive strength witnessed a collective strength increase of 19.96% in rainwater.

Due to the composite's molecular chain structure changing to a more stable condition with enough time, a progressive improvement in tensile strength was observed with the increasing immersion period (Wang et al., 2021). The SEM images (Figure 3-24) highlight the reported structural damages. Damages observed through the specimens include matrix cracking, fiber breakage, fiber pull-out, and matrix-fiber delineation. Similar failure characteristics were reported by Kini et al. (Kini et al., 2018).

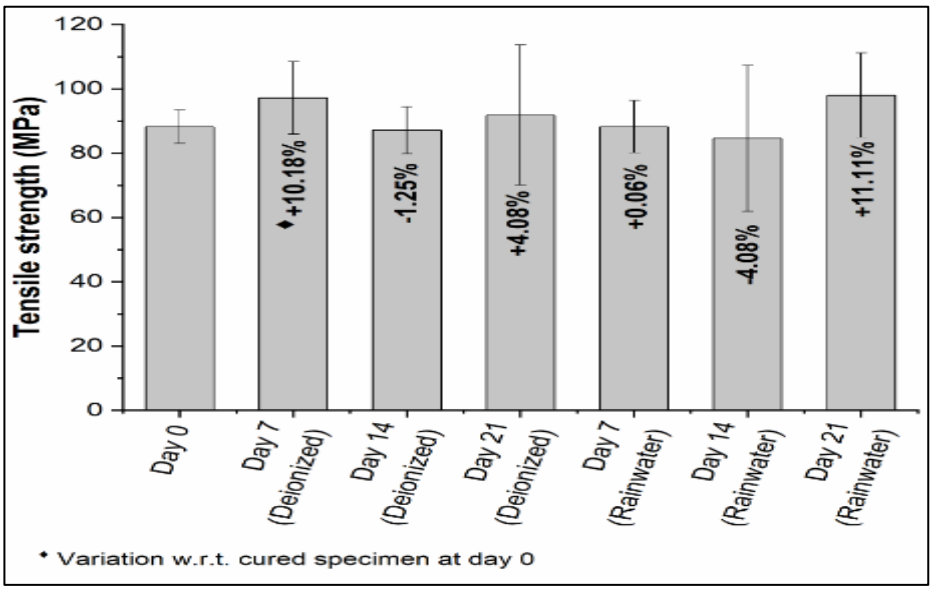

Figure 3-21 Tensile strength of specimens immersed in deionized water and rainwater

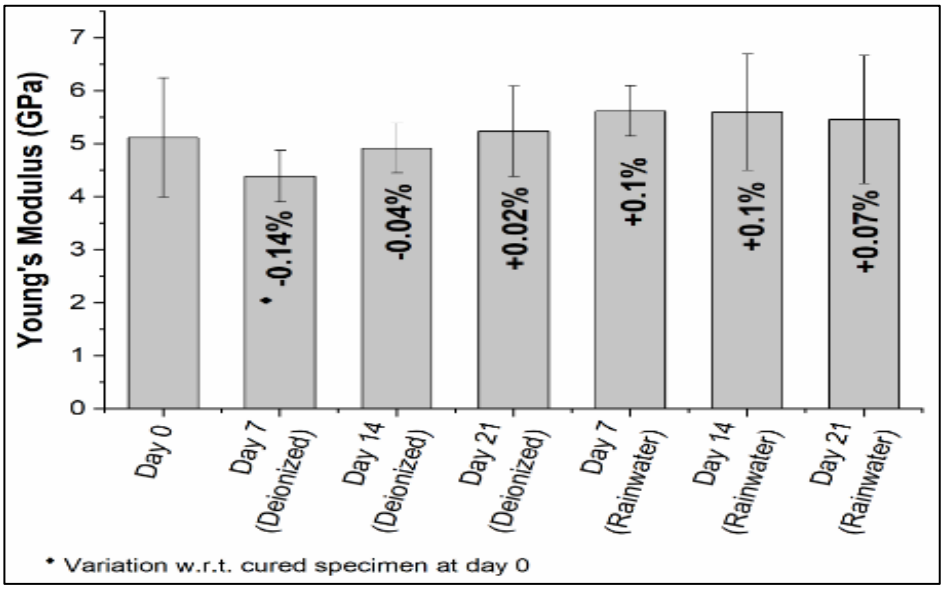

Figure 3-22 Young's modulus of samples measured over the test duration of 21 days immersed in deionized water and rainwater

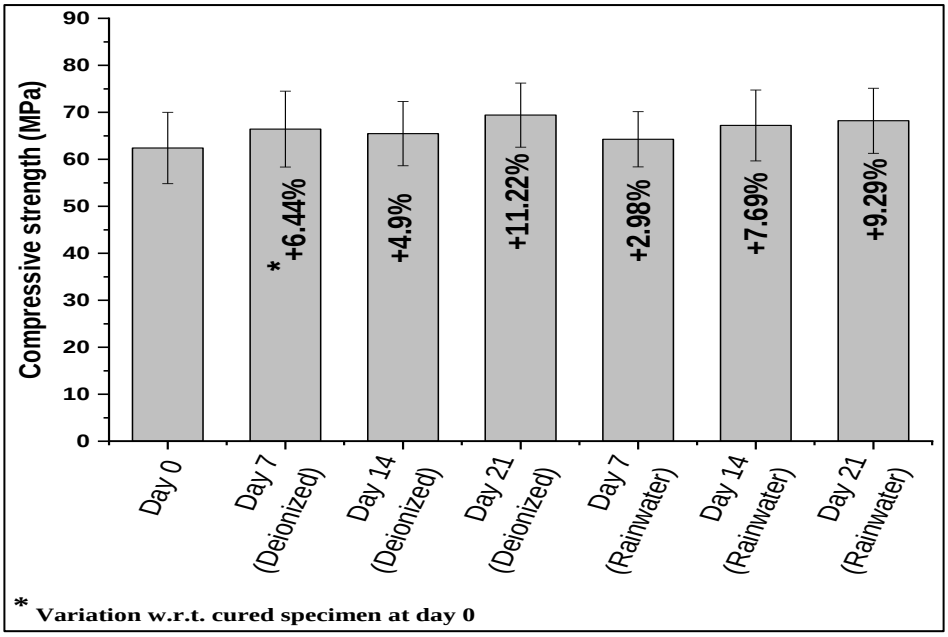

Figure 3-23 Compressive strength of specimens immersed in deionized water and rainwater

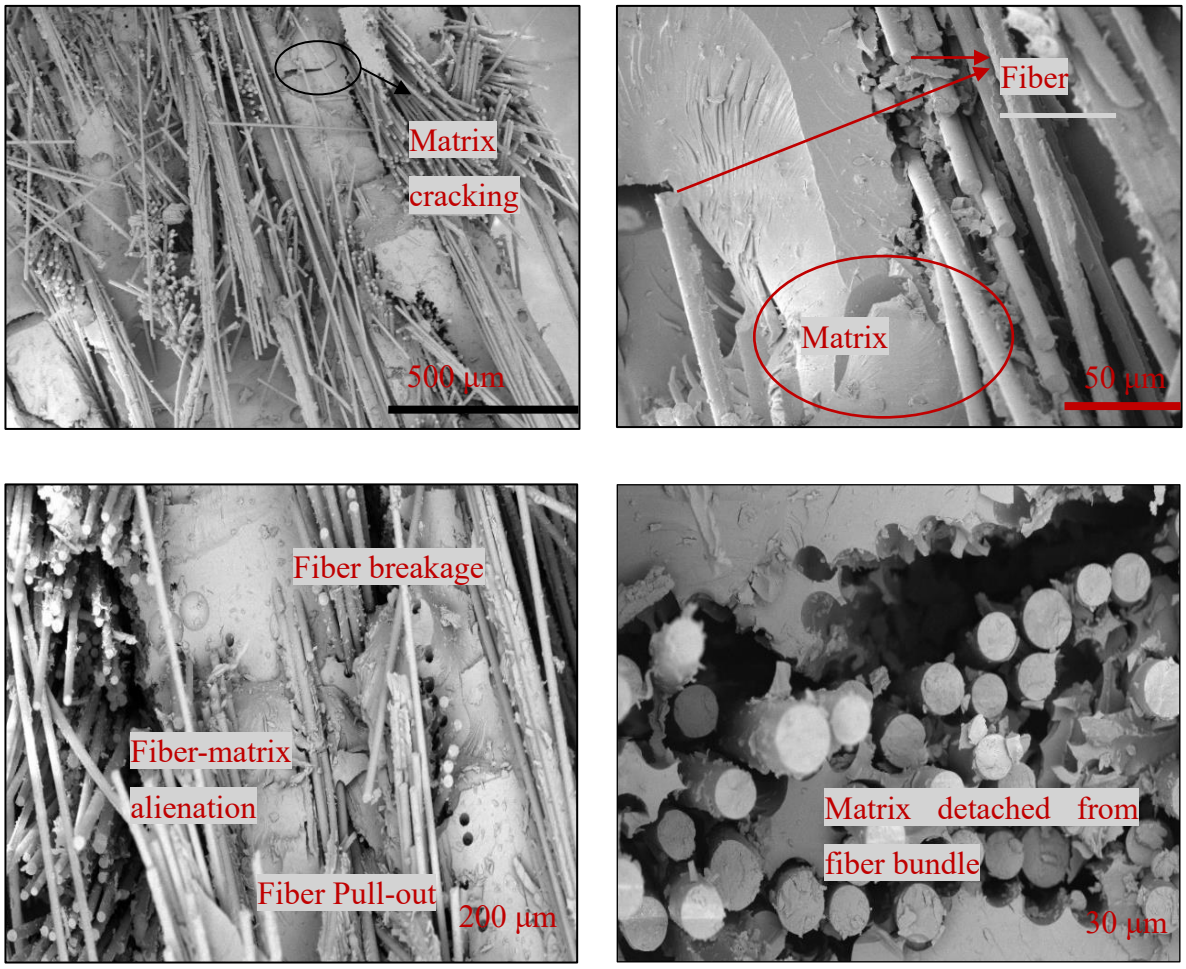

Figure 3-24 SEM images showing fiber-matrix degradation after the immersion period and tensile test

3.4.2.6 Field Implementation

Owing to its considerable weight and magnitude, the conveyance of the JFRP tank proved cumbersome for field application. In consequence, GFRP was considered suitable for field implementation.

The capacity of the proposed RWH tank was fixed at 20,000 liters and designed to be an underground tank, with a meter above the ground and provided with pipe connections to facilitate rooftop rainwater collection.

For field applications, the job was outsourced to a local workshop. Every water tank comprised eight panels with a height of 3.05 meters. Wood molds were prefabricated and used as a framework for casting the panels. The panels were assembled and hoisted into place at the installation site. Once the complete installation was over, other necessary arrangements were facilitated to establish an efficient rooftop rainwater harvesting system. The conveyance system was laid from the roof to the tank through the inlet. The rooftop connection was made with gutters and downspouts, which allowed rainwater to flow into the domestic tanks. The first flush connection has been incorporated into the residential tanks because it collects settlable sediments and debris. The tank was installed with a solar pump to minimize energy needs during water pumping, achieving a sustainable RWH system. The step-by-step procedure for preparing and installing the tanks is depicted in Figures 3-25 through 3-28. After the GFRP tanks were finally fabricated and assembled, NDT testing was carried out.

3.4.2.6.1 Non-destructive testing of GFRP

While the lab-scale fabricated specimens' thickness averaged 4.59 mm, full-sized panels averaged 4.72 mm with an error of 2.83%. The recorded values for the 36 points of the three specimens are compiled in Table v in Appendix 1—figure 3-29 reports the UPV tests conducted on the GFRP panels. No visible leakage or damages were observed in the assembled tanks after 24 hours of the hydrostatic test conducted.

Figure 3-25 Fabrication of the GFRP tank panels in the workshop

Figure 3-26 Assembly of GFRP tanks at the site of installation

Figure 3-27 Installation of GFRP RWH tanks in a participatory household

Figure 3-28 Fixing of a solar pump to the GFRP tank to draw water and ensure sustainable energy

Figure 3-29 NDT testing using the Ultra Pulse Velocity instrument

Chapter Summary

Glass and jute fibers were explored in this chapter for their suitability for the construction of a rainwater water harvesting tank. Since rainwater is generally considered one of the purest forms of water, the effect of the tank material plays a significant role in ensuring optimum water quality. JFRP specimens were analyzed for qualitative parameters and evaluated. Though the JFRP had acceptable performance, with improved pre-treatment o the fibers, the efficiency of the tanks can be enhanced. Further, a comparison was made between the water quality stored in a pre-constructed concrete RWH tank and GFRP specimens. The qualitative parameters recorded for GFRP were higher than the concrete tank but were within the limits of Indian and

international standards. Following lab testings, on-site fabrication for JFRP and GFRP was undertaken. Subsequently, the GFRP tanks were fabricated and installed in study locations.

The proposed RWH is designed to aid the existing water resource system in a rural scenario and not completely eradicate the dependence on groundwater. For the rural population relying on groundwater, an alternative method for removing contaminants needs to be developed.

4 SYNTHESIS AND EXPERIMENTAL VERIFICATION OF *PROSOPIS CINERARIA* CARBON (PCC)

Chapter Overview

The Fluoride problem is not unknown in the study region. F^- sequestration is essential to ensure safe water for habitants depending on groundwater. Removal through adsorbent is a cost-effective and environmentally friendly method. In the current chapter, the complete process for the synthesis of the adsorbent derived from Khejri (*Prosopis cineraria*) is discussed. In addition, the characterization tests are also covered. The PCC's fluoride removal mechanism is understood through batch tests. The experimental data is then fitted with four AI models to predict the removal efficiency of PCC. Sensitivity analysis and Genetic algorithm optimization identify the significant input parameter affecting the removal efficiency and the optimum operating conditions, respectively.

4.1 Preparation of Prosopis cineraria carbon (PCC)

Khejri leaves, stems, and pods were collected locally from Pilani, Rajasthan, India, during the annual pruning of the khejri tree for maintenance purposes between January to March. After gathering, decaying leaves were physically excerpted. The collected foliage was then thoroughly washed under running tap water. A final wash was done with distilled water to remove the remaining dirt and dried under the sunlight until all the moisture was evaporated. After drying, the leaves were soaked in the 0.1N acetic acid solution for 10 hours. After proper washing until neutral pH, the material was air-dried for another 24 hours, then heated at 300° C in a muffle furnace for 6 hours. The resulting material was grounded, sieved through a 150 µm sieve, and subsequently placed in an airtight container for further use. Figure 4-1 represents the step-by-step preparation of the PCC. The reagents used [acetic acid (CH_3COOH), sodium fluoride (NaF), sodium hydroxide (NaOH), potassium nitrate (KNO_3), hydrogen chloride (HCL), Fluoride test kit (catalog number 1.14598.0002] in the study were of analytical grade and acquired from Merck. All the solutions were made with deionized water. The tests conducted on the PCC have been represented in Figure 4-2.

4.2 Preparation of adsorbate solution

A fluoride stock solution of 100 mg/l was prepared by dissolving 221 mg of sodium fluoride (NaF) in distilled water. The final volume was made up to 1 L with distilled water. The stock solution was diluted to obtain synthetic fluoride-contaminated water with concentrations ranging from 3 to 15 mg/l.

Figure 4-1 Step by step process of adsorbent preparation

4.3 Setup for batch experiments

The adsorption experiments were performed in batch mode using the "one-variable-at-a-time" (OVAT) method, keeping all but one-factor constant to attain the optimum operating conditions. Ghosal and Gupta have highlighted the merits of OVAT (Ghosal & Gupta, 2016). Batch F^- experiments were carried out using synthetic samples prepared in the laboratory with characteristics as stated: pH (4-9), contact time (10-240 minutes), initial F^- concentration (3-15 mg/l), and PCC dosage (0.5 – 10 g/l).

The pH of the synthetic test solutions was maintained with the addition of 0.1N HCL and 0.1N NaOH. All the batch tests were carried out in 250 mL conical flasks with 100 mL test solution at 30 ± 3º C. The flasks, test solution, and adsorbent were shaken in an orbital shaker at 50 rpm with a holding capacity of 16 flasks to study the influence of various parameters like pH, contact time, initial F^- concentration, and adsorbent dosage on PCC's F^- removal efficiency. After each experimental run, the test solution was filtered using the Whatman filter paper size

41Φ. The amount of adsorbed F^- was determined using the UV Spectrophotometer to calculate the removal rate of F^- and contaminant concentration on the PCC surface.

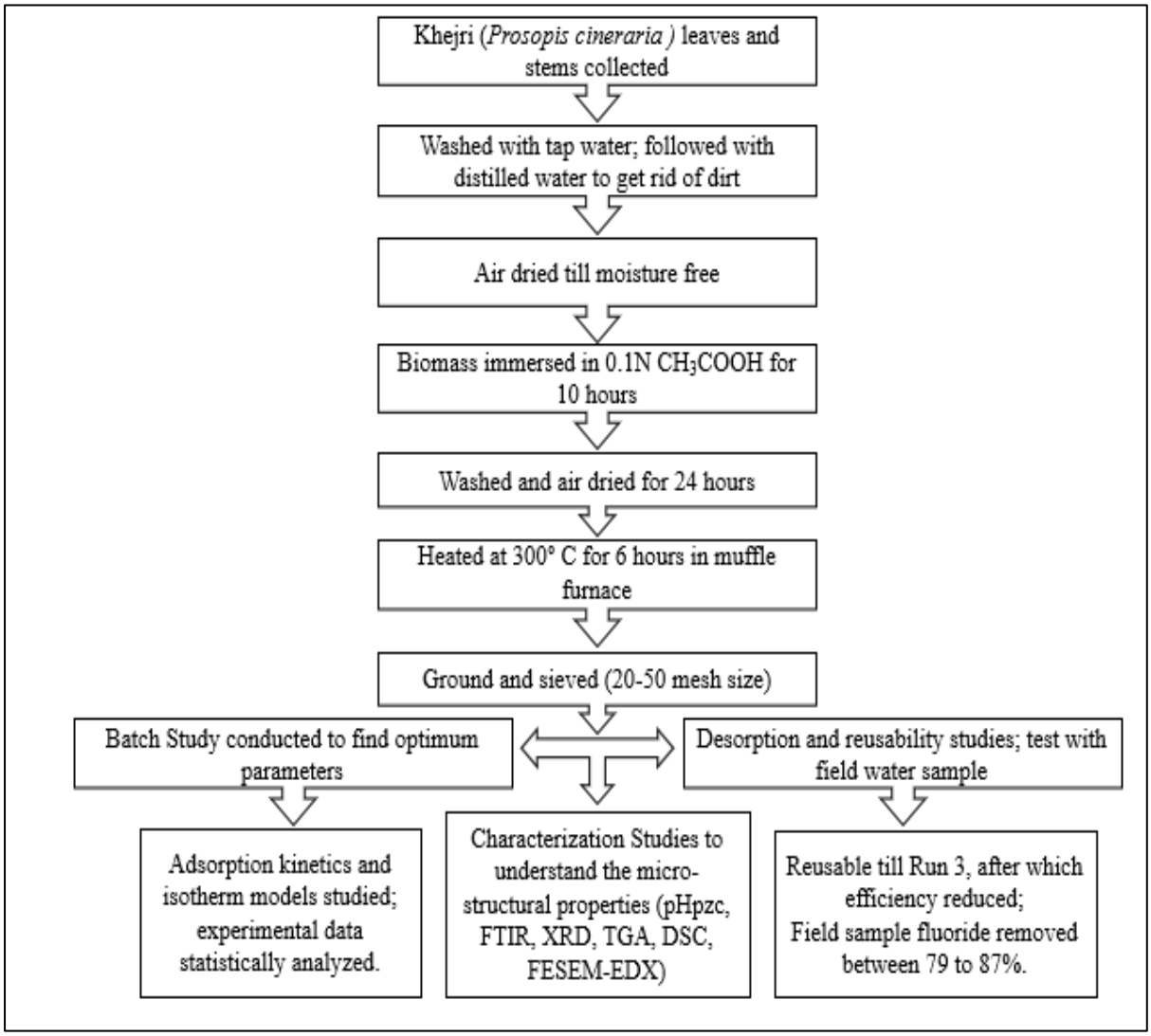

Figure 4-2 Schematic representation of steps involved in the adsorbent study

The amount of contaminant adsorbed (mg/g) at equilibrium (q_e) and at any given time t (q_t) on the PCC surface and the removal efficiency of the F^- ion from the aqueous phase were calculated using Equations 4.1, 4.2, and 4.3, respectively

$$q_e = \frac{(C_i - C_e)}{m} * V \quad (4.1)$$

$$q_t = \frac{(C_i - C_t)}{m} * V \quad (4.2)$$

$$\% \text{ sorption} = \frac{(C_i - C_e)}{C_i} * 100 \quad (4.3)$$

where,

C_i = liquid phase concentration of F- at the initial time (mg/l)

C_t = liquid phase concentration of F- at any time t (mg/l)

Ce = F^- concentrations at equilibrium (mg/l)

V = volume of the solution (l)

m = mass of the adsorbent (g)

4.4 Characterization of Prosopis cineraria carbon (PCC)

The PCC's point-zero charge (pHpzc) was determined based on the pH drift method. The experiments were conducted in 100 ml conical flasks containing 25 ml of 0.1M KNO_3 solution. Initially, the pH value was varied from 2 to 12 at intervals of 1, adjusting with 0.1M NaOH or 0.1M HCl, noted for each flask as the initial pH (pH_i). Then 0.2 g of PCC was added to each flask, shaken manually, and kept in a dark place for 48 hours. After the fixed duration, the final pH was measured (pH_f). The relation between the initial and final pH was plotted, with pH_i on the x-axis and ΔpH ($=pH_f - pH_i$) on the y-axis. Further, the zeta potential of PCC was measured with a Zetasizer Ver.7.12 (Malvern Instruments Ltd.) with the PCC suspended in distilled water.

The PCC's surface morphology and elemental distribution were studied using a field emission scanning electron microscope (FEI, Nova Nano FE-SEM 450, Oxford Instruments, UK) equipped with an energy dispersive X-ray spectrometer (EDX, SAPPHIRE SEM). ImageJ analysis software was used for particle size distribution calculation (before and after adsorption). The surface chemistry covering the functional groups and bonds was determined via FTIR spectra acquired using PerkinElmer (Frontier) by mixing samples in KBr and obtaining the spectra in the 400 – 4000 cm^{-1} range. X-ray diffraction (Rigaku Miniflex II, CuKa, λ= 1.5406 Å, 30 kV, and 15 mA) was performed within the 2θ range of 10° to 70° with a scanning rate of 2°/min to find the phase composition and probable chemical composition of the prepared adsorbent. The crystallite size was calculated using the Scherrer equation. A UV-Vis spectrophotometer (Evolution 201, Thermo Scientific) was used to determine the F- concentration in the filtrate. The thermal behavior of PCC was studied through differential scanning calorimetry (DSC), and the adsorbent's thermal gravimetric analysis (TGA) was performed using NETZSCH STA 449F5, with the temperature range from 0 to 800°C with a heating rate of 10°C/min.

4.5 Statistical analysis of the adsorption data

A research hypothesis is a predicted assertion that can be tested scientifically and associates an independent variable with a dependent variable (Kothari, 2004). Null and alternative hypotheses are frequently discussed in the context of statistical analysis. While a null hypothesis represents the hypothesis we are trying to reject, an alternative hypothesis represents all other possibilities. First, a null hypothesis (H_o) is defined, assuming true. An alternative hypothesis (H_a) is next defined simultaneously, assuming that the alternative hypothesis is accepted if the null hypothesis is rejected, or vice-versa (Kaushal & Singh, 2017).

4.6 Adsorption Isotherms

An isotherm is an invaluable curve that describes the retention of a substance on a solid surface at different concentrations, thereby illustrating the relationship between adsorbate equilibrium concentration and adsorbent adsorption capacity (Gandhimathi, 2022). It is an effective tool for demonstrating the phenomenon governing the substance's mobility (retention or release) from an aqueous porous media or aquatic environment to a solid phase at constant operational parameters (Limousin et al., 2007; Pyrgaki et al., 2018). The isotherm provides a relationship between F^- adsorbed on the solid phase and its concentration in the solution when both phases are in equilibrium. Adsorption isotherms, namely Langmuir (1 and 2), Freundlich, and Temkin, were tested to fit the experimental data and determine the equilibrium data of the adsorption system (Table 4-1). The isotherm constants were obtained from the intercept and slope of their respective isotherm plots.

Table 4-1 The equation of isotherm models employed for Fluoride (F^-) adsorption

Model	Governing equation	Linear Form	Plot
Langmuir 1	$q_e = \frac{Qmax\ K_L\ Ce}{1+K_L\ Ce}$	$\frac{Ce}{qe} = \frac{Ce}{Qmax} + \frac{1}{K_L * Qmax}$	C_e/q_e versus C_e
Langmuir 2		$\frac{1}{q_e} = (\frac{1}{K_L\ q_m})\frac{1}{C_e} + \frac{1}{q_m}$	$\frac{1}{q_e}$ versus $\frac{1}{C_e}$
Freundlich	$q_e = K_F\ C_e^{1/n}$	$\log(q_e) = \log K_F + (\frac{1}{n})\log C_e$	$\log q_e$ versus $\log C_e$
Temkin	$q_e = B\ln(AC)$	$q_e = B\ (\ln A_T) + B\ (\ln C_e)$	$\ln C_e$ versus q_e

KL= the constant of Langmuir's equation, related to the enthalpy of the process; KF = constant related to the adsorption capacity; n = adsorption intensity or surface heterogeneity; AT = equilibrium constant corresponding to maximum binding energy; B = Temkin isotherm constant

4.7 Adsorption Kinetics

Kinetic models are fitted to experimental data primarily to examine the adsorption process controlling mechanisms, such as mass transfer and chemical reaction. Since the sorption process is a function of several parameters, such as structural properties of adsorbent, nature, and concentration of adsorbate, and adsorbate-adsorbent interactions, the study of kinetics is significant (Sadaf & Bhatti, 2014). Kinetics plays an imperative role in scaling up the process. Adsorption primarily occurs through the following steps: i) transport of the solute from the bulk aqueous phase to the film of the adsorbent molecules, (ii) diffusion of the solute from the film to the adsorbent's pores, and (iii) adsorption of the solutes onto the inner surface of the pores (Nethaji & Sivasamy, 2014). The current study tested the experimental data with pseudo-first-order, pseudo-second-order, and intra-particle diffusion models. The governing expressions and concurrent linearized forms are compiled in Table 4-2.

Table 4-2 The equation of kinetic models employed for Fluoride (F^-) adsorption

Model	Linear Form	Plot
Pseudo-first-order Reaction	$\ln (q_e - q_t) = \ln q_e - k_1 \frac{t}{2.303}$	$\ln(q_e - q_t)$ versus t
Pseudo-second-order Reaction	$\frac{t}{qt} = \frac{1}{k_2 q_e 2} + \frac{1}{q_e} t$	t/q versus t
Intraparticle Diffusion	$q_t = X_i + K_p t^{0.5}$	q_t versus $t^{0.5}$

k1 (min−1) and k2 (g/mg/min) are pseudo-first- and second-order rate constants, respectively; Kid (mg/g/min0.5) is intra-particle diffusion rate constant; c is the intercept

4.8 Desorption studies and recyclability of adsorbent

Desorption experiments were carried out to assess the recovery of F^- from the adsorbent and subsequent reusability. Recyclability provides insights into the continuous usage of the

adsorbent efficiently. With a focus on rural applications, the recyclability of adsorbents is essential from an economic aspect.

In this study, six runs were carried out successively to investigate the reusability of the PCC at the optimum operating conditions. After each run, the test solution's remaining F^- concentration was determined. The exhausted adsorbent was then dried and reused for another F- removal cycle with no chemical treatment.

Subsequently, to perform the desorption studies, distilled water, 0.1N NaOH, and 0.1N NaCl were used as eluents to desorb F^-. The regenerative studies were carried out by mixing 50 mL of the aqueous solution with the saturated PCC. The setup was agitated for 30 mins at 40°C. The desorbed adsorbent was then separated from the filtrate and reused for F^- removal. A total of five experimental runs were performed.

4.9 Field study

Field groundwater samples were collected from localized villages around the campus and treated with the adsorbents to verify the PCC's field applicability and practical effectiveness. Physio-chemical parameters such as pH, TDS, TH, and F^- were recorded before and after defluoridation. For ease of understanding, the water quality level was represented as a single number, or the water quality index (WQI). The water quality index (WQI) is an effective tool for evaluating water quality for domestic usage (Panneerselvam et al., 2020). The WAWQI index methodology uses the most commonly measured water quality variables and incorporates those into a mathematical equation, thereby classifying the water quality with a number (García-Ávila et al., 2022).

The calculation of WAWQI is performed using Equation 4.4:

$$\text{WAWQI} = \frac{\sum_{n=1}^{n} q_n w_n}{\sum_{n=1}^{n} w_n} \quad (4.4)$$

Where,

n = the number of parameters

q_n = quality rating of the n^{th} parameter

w_n = relative weight of the n^{th} parameter

$$q_n = 100[\frac{V_n - V_{id}}{S_n - V_{id}}] \quad (4.5)$$

where,

S_n = standard value of n^{th} water quality parameter

V_n = observed value of n^{th} water quality parameter

V_{id} = ideal value of n^{th} water quality parameter

$$W_n = \frac{K}{S_i} \quad (4.6)$$

Where K = constant proportionality, calculated from equation 7:

$$K = \frac{1}{\sum_{i=1}^{n} \frac{1}{S_i}} \quad (4.7)$$

∴ In equation 4.5, V_{id} is considered as 7 for pH, and $V_{id} = 0$ for the remaining parameters.

The calculated WAWQI values were classified as excellent, good, fair, poor, very poor, inadequate, or unsuitable for human consumption, represented in Table 4-3. The WHO standard values for drinking water quality are given in Table 4-4.

Table 4-3 Water quality rating as per WAWQI method

WQI value	Grading	Rating of water quality
0-25	A	Excellent
26-50	B	Good
51-75	C	Fair
76-100	D	Poor
101-150	E	Very poor
Above 150	F	Unfit for drinking purposes

Table 4-4 Drinking water quality standards used in the calculation of WAWQI

Physio-chemical Parameters	WHO standards
pH	8.5
Total Dissolved Solids (mg/l)	1000
Total hardness (mg $CaCO_3$/L)	200
Fluoride (mg/l)	1

4.10 Machine learning predictive modeling

Without being solely programmed, machine learning (ML) equips computers to assimilate data and is broadly classified as supervised and unsupervised learning (Khan et al., 2018). In supervised learning, an endeavor is carried out to learn an outcome hinged on a labeled training dataset comprising a set of input-output pairs. Predictive modeling is a proven and accepted engineering approach helping understand the contaminant removal process of numerous developed adsorbents (Ghaedi *et al.*, 2016; Fan, Hu *et al.*, 2017). ML-assisted predictive modeling is an increasingly employed tool to solve sustainable water engineering and management issues (Noori et al., 2011). The quantity and quality of the data determine the suitability of the machine learning technologies. Selecting the best method of the prediction model for case-specific experimental research is a key thrust area in this field due to the features of various techniques (Sahu et al., 2022). In the same vein, though several investigations have been conducted on removing F- ions from aqueous solutions using different adsorbents, every unique material needs to be given a particular focus, primarily due to varying material composition (Yetilmezsoy & Demirel, 2008). The present study highlights and compares four algorithms modeling the adsorption potential of Khejri (*Prosopis cineraria*) in F- sequestration from aqueous solutions. The effects of various operational parameters, such as pH, contact time (in minutes), adsorbent dosage, and initial concentration of F- ions, were investigated for removal effectiveness. SPSS (Statistical package for the social sciences) and MATLAB (ver. 2019b) environment were used for the predictive modeling. All the data (input and output) were normalized between 0 and 1, improving the training quality (Krauss et al., 1997). The normalization is performed over the experimental data by applying Equation 4.8.

$$\mathbf{y} = \left(\frac{x_i - x_{min}}{x_{max} - x_{min}}\right) \quad (4.8)$$

where y is the normalized value corresponding to x_i, and x_{max} and x_{min} are the maximum and minimum values of x_i, respectively [x signifying the inputs].

4.10.1 Multiple Linear Regression

Regression analysis is one of the most effective approaches for describing how one or more independent (predictor) variables affect a response variable. In linear regression, the function is a linear equation representing a straight line expressed in the form:

$$Y = b_0 + b_1X_{i1} + b_2X_{i2} + b_jX_{ij} + \ldots + b_pX_{ip} \quad (4.9)$$

Where Y is the dependent variable, b_0 to b_p are the equation parameters for the linear relation, and X_{i1} to X_{ip} are independent variables for this system.

Cevik proposed using step-wise regression as a robust approach for identifying the best subset models, i.e., the combination of best independent variables (Cevik, 2007). Subset models are selected based on the addition or elimination of the variable(s) that significantly influence the residual sum of squares. Step-wise regression is a forward selection method that, at each step, reevaluates the significance of all previously added variables (Bilgili & Sahin, 2010).

The connection between the F^- concentration of water and soil was examined by Naik et al. using multiple linear regression (Naik et al., 2017). To assess the quality of fits and adsorption efficiency for F- removal from aqueous solutions, linear regression analysis has frequently been used (Yadav & Singh, 2017).

4.10.2 Non-linear Regression

In non-linear regression, observational data are described by a function that depends on one or more independent variables and is a non-linear combination of the model's parameters. Non-linear regression may estimate models with arbitrary connections between independent and dependent variables, in contrast to classic linear regression, which can only estimate linear models.

The general representation of a non-linear equation is expressed as in Equation 4.10:

$$Y = \alpha_0(X_{i1}^{\alpha 1})\,(X_{i2}^{\alpha 2})\,\ldots.\,(X_{ip}^{\alpha p}) \qquad (4.10)$$

where α_0 to α_p are the equation parameters for the non-linear relation.

For easy comprehensibility, non-linear regression models can be moved to a linear domain by a suitable linear transformation. Taking the log of Equation 4.10, the governing relationship is transformed into the linear form (Equation 4.11):

$$\log(Y) = \log(\alpha_0) + \alpha_1 \log(X_{i1}) + \alpha_2 \log(X_{i2})$$

$$+\ldots. + \alpha_p \log(X_{ip}) \qquad (4.11)$$

Subsequently, the parameters of $\alpha_0, \alpha_1, \ldots$, and α_p are estimated by the linear regression of log(Y) on log (X_{i1}), log (X_{i2}), ….., log(X_{ip}) (Cankaya, 2009; Yadav & Singh, 2017).

4.10.3 Artificial Neural Network

Artificial neural networks (ANNs), often traced back to McCulloch and Pitts, are a popular tool in the data mining and research arena that has witnessed adaptation in engineering, nuclear science, biology, medical and space applications (McCulloch & Pitts, 1943; Dehghani et al., 2021). The tool's salient feature of mimicking the working of the brain and nerve systems in biological organisms with a capability for self-learning and automatic abstracting is a reason for its broad applicability. Further, ANNs are an alternative tool for complex process modeling that captures and generates linear and non-linear complex relationships between independent and dependent variables (Ghosal & Gupta, 2016). While ANN modeling is an empirical approach, it can easily account for undefined non-linearities without additional computational burden with adequate data through training the multiple input-output systems algorithm (Li *et al.*, 2017; Onu *et al.*, 2021). Moreover, once the ANN model is trained, it takes very little time to predict the properties, and hence it is very suitable for online use (dan Suditu et al., 2013).

A neural network consists of many simple processing elements called neurons, capable of processing a local memory and carrying out localized information (Haykin, 1994). Generally, an artificial neural network (ANN) can be defined as a system or mathematical model which consists of many non-linear artificial neurons running in parallel and which may be generated as one layer or multiple layers. Most ANNs have three layers: input, output, and hidden. Each neuron computes a weighted sum of the inputs it receives and adds it with a bias (b) to form the net input (x), as demonstrated in Figure 4-3.

A multilayer feed forward-back propagation training network containing the input layer, the output layer, and one or more hidden layers is the most frequently used ANN architecture. Backpropagation (BP) is the method in which the gradient is computed for non-linear multilayer networks. The neural model includes an externally applied bias, denoted b_k. The bias increases or lowers the activation function's net input, depending on whether it is positive or negative.

The input to the hidden layer U is determined from input variables as follows:

$$v_k = \sum_{j=1}^{m} w_{im}\, x_m \qquad (4.12)$$

The output signal y_k is computed as follows:

$$y_k = \Phi(v_k + b_k) \qquad (4.13)$$

x_1, x_2,….,x_m are the input signals; w_{k1}, w_{k2},…,w_{km} are the synaptic weights of the neuron k, b_k is the bias; Φ(.) is the activation function, and y_k is th output signal.

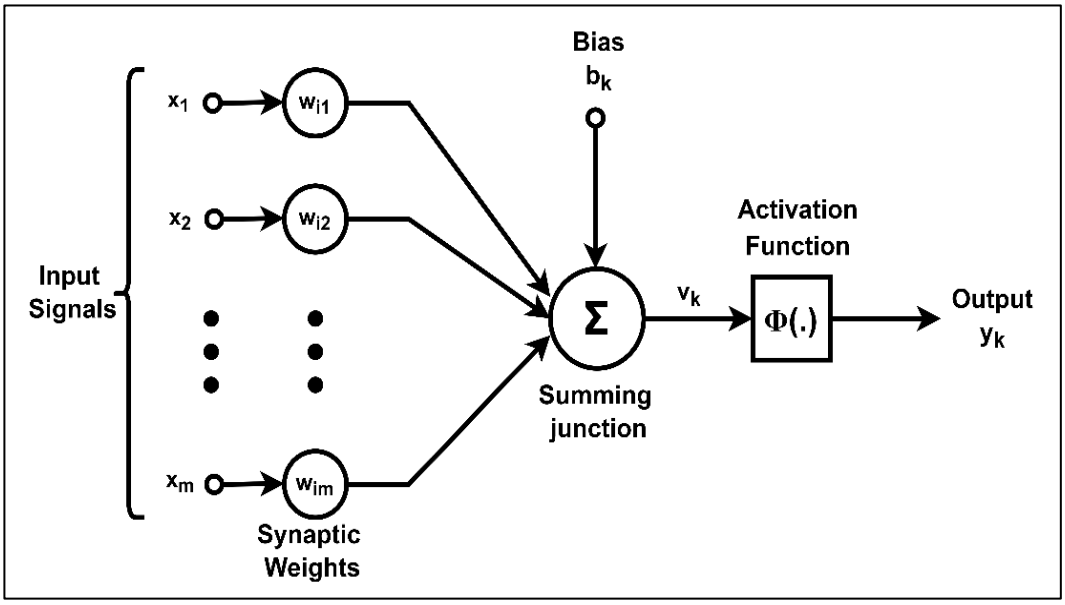

Figure 4-3 The general layout of the Artificial neural network

4.10.4 Fuzzy Inference system

Fuzzy logic is a multi-valued logic, allowing intermediate values to be formulated mathematically, like true/false, yes/no, and high/low, to apply more human-like thinking in the programming. Based on the fuzzy set theory, fuzzy systems include partial membership ranging between 0 and 1, in contrast to their crisp membership and logic.

A general fuzzy system has four components: fuzzification, fuzzy rule base, fuzzy output engine, and defuzzification, as presented in Figure 4-4. The model architecture used for the current study consists of four inputs and one output.

i. Fuzzification converts each piece of crisp input data to varying degrees of membership by perusing one or more different membership functions. Each fuzzy set is represented by a membership function (MF), where a membership function may have different shapes, such as Gaussian, triangular, trapezoidal, or sigmoid, among others. A membership function can represent partial belonging to a set, which assumes values between 0 and 1. Triangular and trapezoidal membership functions were employed for the inputs and output variables during the study.

ii. A fuzzy rule base includes all possible fuzzy relations between inputs and output. The rules are expressed in the IF-Then statement format covering model parameters, uncertainties,

and non-linear relationships. For this study, the authors constructed a Mamdani-type rule base. Considering the following IF-Then fuzzy rule:

$$\text{Rule k: IF, } x_1 \text{ is } A_{k1}, x_2 \text{ is } A_{k2}, \ldots . x_n \text{ is } A_{kn}, \text{ THEN } y_1 \text{ is } B_k \qquad (4.14)$$

A_{k1} is a fuzzy set corresponding to a portioned course of input variable x_1 in the k^{th} IF-Then rule, n is the number of input variables, and y_k is the output corresponding to the inference rule. The parts of the rule between IF and THEN, and after THEN are called the antecedent and consequent parts, respectively.

iii. The fuzzy inference engine consists of several components and operations, considering all the fuzzy rule base transforms a set of inputs into corresponding outputs. In this study, we employed the product (prod) inference method.

iv. Defuzzification converts the resulting fuzzy outputs from the fuzzy inference engine to a crisp number. The input for the defuzzification process is a fuzzy set (the aggregated output), and the output is a single crisp number. Of the many defuzzification methods, the centroid method was used for this study. It returns the center of the area under the curve, as expressed:

$$J_x^* = \frac{\sum_i \mu(K_{xi}) K_{xi}}{\sum_i \mu(K_{xi})} \qquad (4.15)$$

Where J_x^* is the defuzzified output value, K_{xi} is the output value in the i^{th} subset, and $\mu(K_{xi})$ is the membership value of the output value in the i^{th} subset.

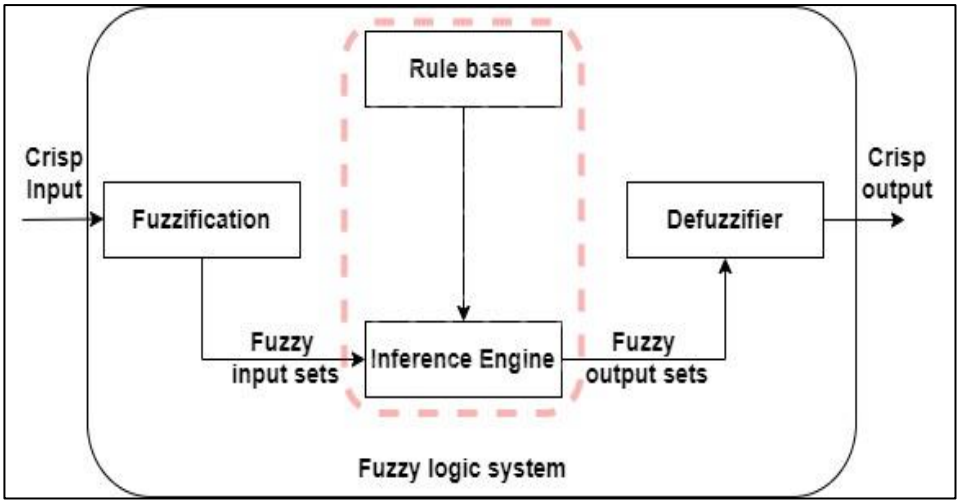

Figure 4-4 The general layout of the Fuzzy Inference system

4.10.5 Model performance indices: Evaluation of predictive models

An extensive error function assessment was conducted to identify the best-fitted soft computing model having the best predictive ability concerning the experimental results. The sum of the squares of the errors (SSE), mean absolute error (MAE), Absolute average relative error (AARE), Mean absolute relative error (MARE), hybrid fractional error function (HYBRID), chi-square test ($\chi 2$), and adjusted R^2 values were used. The lower the numerical value of an error function, the better the model's fit. The best-fit predictive model was selected based on the error functions that produced minimum error distribution between the experimental and predicted databases (Chowdhury et al., 2011).

Table 4-5 Statistical Error Functions

Error functions	Governing Equation	Reference
Sum of the squares of the errors (SSE)	$\sum_{i=1}^{n}\left(P_{exp}-P_{cal}\right)^2$	(Sahu et al., 2022)
Mean absolute error (MAE)	$\frac{1}{n}\sum_{i=1}^{n}\lvert(P_{exp}-P_{cal})\rvert$	(Bazoobandi et al., 2019)
Absolute average relative error (AARE)	$\frac{1}{n}\sum_{i=1}^{n}\left[\left\lvert\frac{P_{exp}-P_{cal}}{P_{exp}}\right\rvert\right]$	(Onu et al., 2021)
Mean absolute relative error (MARE)	$\frac{100}{n}\sum_{i=1}^{n}\left[\left\lvert\frac{P_{exp}-P_{cal}}{P_{exp}}\right\rvert\right]$	(Pinar et al., 2011)
Hybrid Fractional Error Function (HYBRID)	$\frac{100}{n-p}\sum_{i=1}^{n}\left[\frac{(Pexp-Pcal)^2}{P_{exp}}\right]$	(Sahu et al., 2022)
χ^2	$\sum_{i=1}^{n}[\frac{\left(P_{cal}-P_{exp}\right)^2}{P_{cal}}]$	(Sahu et al., 2022)
Adjusted R^2	Adj $R^2 = 1 - [(1-R^2)*\frac{N-1}{N-P-2}]$	(Onu et al., 2021)

Note: Pexp is the experimental values of the ith experiment; Pcal is the model predictions of the ith experiment; n is the number of experiments; p is the number of independent factors.

4.10.6 Optimization of operational parameters through Genetic Algorithm

Genetic Algorithms (GA) are a set of evolutionary optimization techniques which produce near-global solutions. GA is a population-based iterative method that primarily relies on three operators – selection, crossover, and mutation- to select the best solution.

The meta-heuristic optimization algorithm is based on an intelligent mechanism mimicking natural selection. The initial population refers to the initial set of solutions used by the algorithm. Every response is a chromosome (or individual in the population) that indicates a position in the search field. The genetic operators of selection, recombination, and mutation help the chromosomes grow through time or via repeated iterations or "generations." A fitness function is used as the criterion by the selection operator to choose some "desirable" solutions. The recombination operator (crossover operator) creates new solutions while keeping the parents' most vital attributes and enhancing population diversity. Mutation's function is to find a means to get around the local minima (dan Suditu et al., 2013). The method terminates after a convergence test has achieved its maximum (pre-determined) number of generations; a specific termination criterion is applied for a given work. The general layout of the applied GA is demonstrated in Figure 4-5.

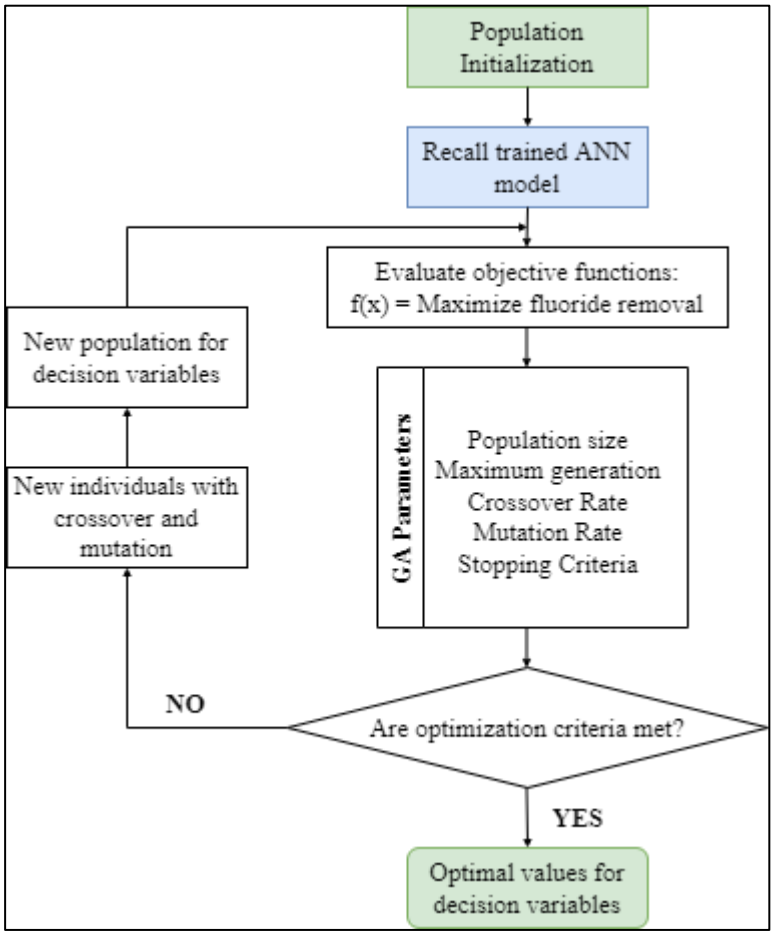

Figure 4-5 Methodology of the adopted Genetic algorithm optimization model

4.10.7 Sensitivity Analysis

Sensitivity analysis (SA) assesses how "sensitive" a model is to changes in the parameters' values and the model's structural parameters. A SA of the best predictive model was conducted to examine the "cause-and-effect" relationship between the input variables and the modeling outputs.

SA investigates how the variation in the output of a numerical model can be attributed to variations in input factors (Tenza-Abril et al., 2018). Three methods, namely Garson's equation, connection weights, and Perturbation method, were utilized to assess the relative importance of the dependent variables on the independent variable for the F^- removal efficiency (Olden & Jackson, 2002; Olden et al., 2004). The possible combination of variables method was utilized as the conservative method for performing the SA (Hu *et al.*, 2017).

4.10.7.1 Garson's algorithm

The algorithm concerns the portioning of the hidden-output connection weights into components associated with each input neuron using the absolute values of connection weights (Gevrey et al., 2003; Goh, 1995; Olden et al., 2004). Since the algorithm primarily uses the absolute values of the connection weights, the direction of the relationship between the direction of the input-output variable interaction is discredited. The Garson equation can be given as follows:

$$O_j = \frac{\sum_{f=1}^{n}\left(\frac{|w_{ef}|}{\sum_{i=1}^{m}|w_{if}|}|w_{fg}|\right)}{\sum_{e=1}^{m}\{\sum_{f=1}^{n}\left(\frac{|w_{ef}|}{\sum_{i=1}^{m}|w_{fg}|}|w_{fg}|\right)\}} \quad (4.16)$$

Where O_j is the relative effect of the e^{th} dependent variable on the g^{th} independent variable, w is the connection weight, and e, f, and g are the number of neurons in the input layer, hidden layer, and output layer, respectively.

4.10.7.2 Connection weights

The algorithm involved entails the calculation of the raw input-hidden and hidden-output connection weights between each input and output neuron. Subsequently, the product is summed up across all hidden neurons (Olden & Jackson, 2002). The obtained importance has positive and negative values, unlike Garson's algorithm (Nie et al., 2022). The proposed method by Olden et al. (2004) proved to be the most efficient overall methodology for accurately quantifying variable importance, i.e., the network's sensitivity to each input variable (Olden et al., 2004).

The contribution $O_{j,k}$ of neuron *i* to the output via hidden neuron *h* is defined as

$$O_{f,g} = w_{e,f}\, w_{f,g} \quad (4.17)$$

The importance I_i of input variable x_i is expressed as:

$$I_i = \sum_{f=1}^{F} O_{f,e} \quad (4.18)$$

4.10.7.3 Perturbation method

The variable perturbation method tries to evaluate the impact of minute adjustments to each input on the neural network's output. The method perturbs one variable's input value while all other variables remain unchanged. It is observed how the output variable reacts to changes in the input variable. The input variable with the most significant relative effect is the one whose modifications impact the output (Gevrey et al., 2003).

The changes are represented in the form $x_i = x_i + \delta$, where x_i is the selected input variable, and δ is the change/ noises. The model's response to input-value perturbations increases the understanding of the model behavior and reality representing capacity (Yao et al., 1998).

δ is usually varied in steps of 5 to 10% up to 50% of a particular input in both positive and negative directions. However, caution should be exercised so that the perturbed inputs do not take physically infeasible values (Dutta & Gupta, 2010). An average overall perturbation was taken for each variable, with input producing the maximum change in the output considered the most influential.

4.10.7.4 Possible combination of variables

In this conservative method, each input parameter was independently checked to see how it affected the objective, which was a higher F^- removal efficiency. The best-performing governing equations then verified every possible combination of two, three, and four input parameters, determining the one input parameter that significantly affected removal efficiency.

4.11 Characterization of Prosopis cineraria carbon (PCC)

4.11.1 Point of zero-charge and Zeta potential

The point of zero charges is a valuable characterization technique to ascertain the surface affinity of an adsorbent towards a specific pollutant in an aqueous medium. It is also described as the pH of net electrical neutrality (Mondal et al., 2021; Villela-Martínez et al., 2020). For pH< pH_{pzc}, the adsorbent has a positive surface charge, while for pH > $pH_{pzc,}$ the adsorbent surface has a net negative charge.

Figure 4-6 represents the pH_{pzc} curve of PCC. The pH_{pzc} of PCC was determined to be 9, implying appreciable defluoridation within the acidic and neutral range (pH < pH_{pzc}). Further, the total charge on the surface and the stability of the aqueous solution of PCC was assessed by zeta potential analysis (Indana et al., 2016). Zeta potential results show that our synthesized adsorbent had a net positive surface charge of +11.41 mV. A positively charged surface attracts negatively charged F^- ions (Hoang Lam et al., 2021). However, at a higher pH, the surface of the adsorbent changes to negative, impeding F^- adsorption.

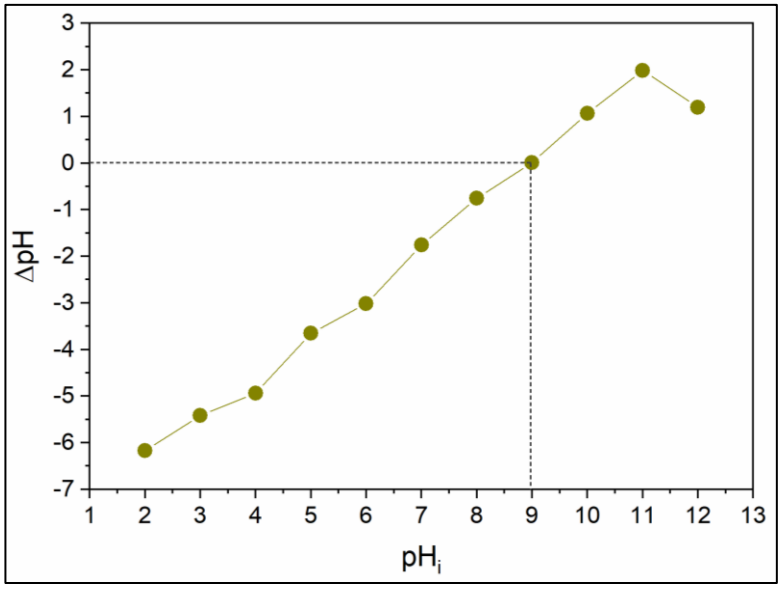

Figure 4-6 The pzc determination curve for PCC

4.11.2 Fourier transform infrared spectroscopy

FTIR spectroscopy was studied to investigate the bonds formed in the synthesized adsorbent. Figure 4-7. illustrates a broad range of stretch in the 3800-3000 cm^{-1} region attributed to the

water and hydroxyl group (Pouretedal & Sadegh,2014). The functional groups of the PCC observed at 1103 cm^{-1}, 1443 cm^{-1}, and 1799 cm^{-1} corresponded to the C-O stretching vibration, S=O stretching vibration, and carboxylate stretching vibration, respectively (Granbohm et al., 2017; Shahmaleki et al., 2020). The bands at 713 cm^{-1} and 875 cm^{-1} are fingerprints of $CaCO_3$, further confirmed in the XRD analysis (2θ: 29.808° and 43.24°) (Ramasamy et al., 2018). The general shift in the absorption bands for pre-and-post-sorption accredits to F- adsorption onto the PCC (Naga Babu et al., 2018).

4.11.3 X-ray diffractometer

The XRD phase analysis for 2θ diffraction angles from 10° to 70° is shown in Figure 4-8. Crystalline phases are identified accordingly with the Match Software. The peak obtained at 2θ of 35.95° indicates Calcium (C) (PDF- 9012917). The most substantial peak observed at 29.8° could be indexed as $CaCO_3$ and $CaSi_2$. The diffraction peaks observed at 2θ of 43.24° and 47.34° were identified as $CaCO_3$ (PDF- 1010929) and $CaSi_2$ (PDF-1536815), respectively (Bux et al., 2010; Shahmaleki et al., 2020). The peak observed at 31.8° on the unspent PCC could be attributed to the existence of Ca_2SiO_4 (PDF- 1546029). A prominent peak at 31.8° on the loaded PCC acknowledges fluorapatite – $Ca_5(PO_4)_3F$ (PDF- 9006955), confirming defluoridation (Thole, 2013). The adsorbent's grain size (before and after adsorption) was calculated using the Scherrer equation and found 32.27 nm and 45.23 nm at 29.808° and 29.335°, respectively.

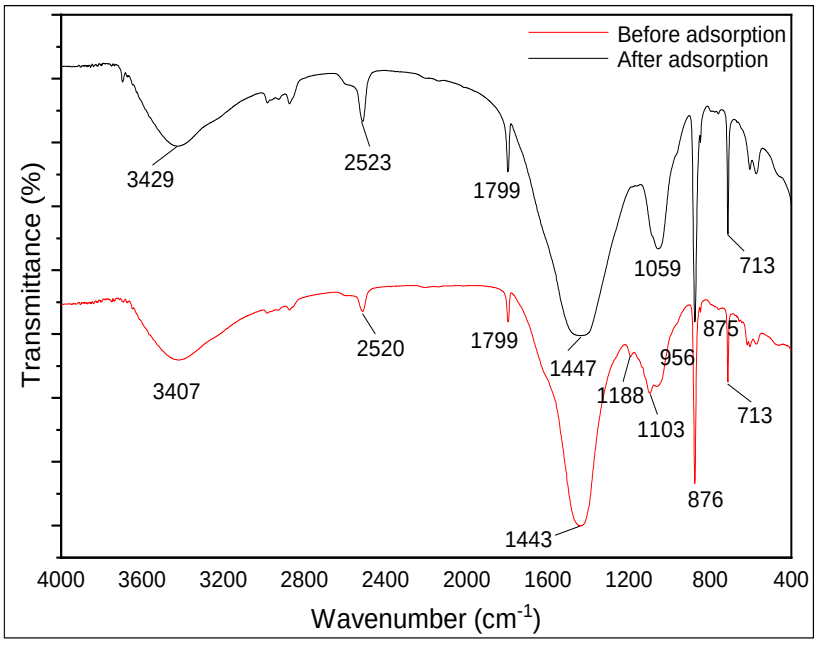

Figure 4-7 FTIR spectrum of PCC before and after adsorption

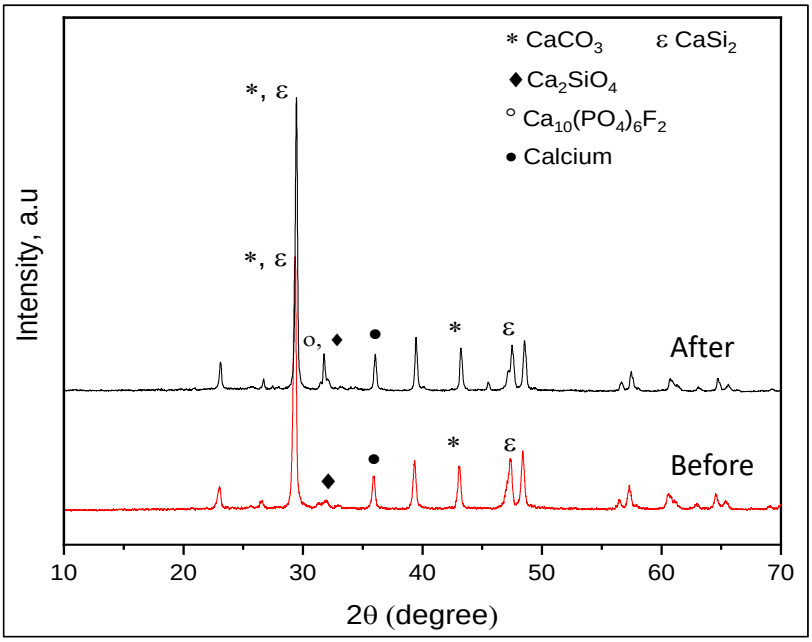

Figure 4-8 XRD spectrum of PCC before and after adsorption

4.11.4 Thermogravimetric and Differential Scanning Calorimetry

Thermogravimetric and heat flow profiles have been reported in Figure 4-9 a and b, recorded from 50° to 800° C. Both thermogravimetric (TG) and differential scanning calorimetry (DSC) analyses were conducted synchronically to examine the weight and enthalpy change (exothermic or endothermic). The TG curve of the adsorbent presented two mass loss steps. The first step in the 100-125°C temperature range is attributed to moisture elimination with a 3.4% mass loss. The above findings corroborate the result observed from the DSC curve, with an endothermic transformation observed in a similar temperature range, explaining the evaporation of water molecules (Khammour et al., 2021). The second step appearing at the 650-750° C range, corresponds to the mass loss caused by organic species with a mass loss of 9.46% (dos Reis Ferreira et al., 2018; Mothé & De Miranda, 2009).

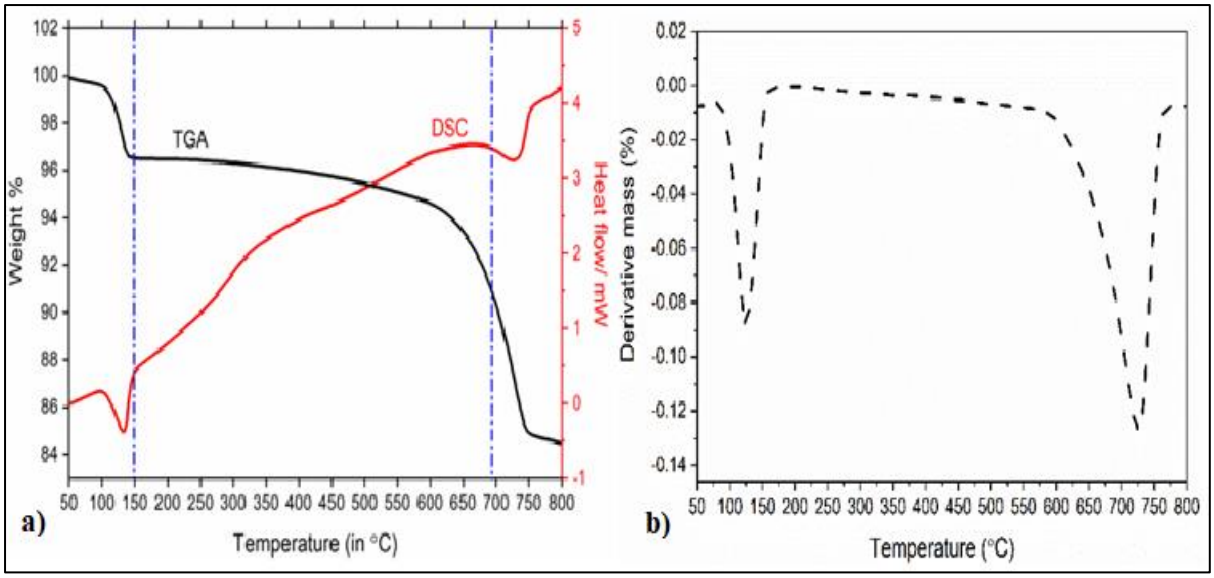

Figure 4-9 a) TGA and DSC profile of PCC b) DTG profile of PCC

4.11.5 FESEM, EDX, and EDS dot mapping

The surface morphology of PCC (before & after adsorption) is depicted in Figures 4-10 a and b. As illustrated from the FESEM plan images and insert frequency distribution graph, sorbent particle sizes have increased from 30-40 nm to 50-80 nm for the loaded adsorbent. The presence of F^- in the spent PCC is validated with the EDS elemental mapping, as shown in Figures 4-11 a and b. Table 4-8 shows the adsorbent surface's elemental composition percentage distribution before and after F^- deposition. Though the particle size distribution was almost in similar ranges, a minor discrepancy was observed between the particle size measured via the Scherrer equation and FESEM images. Similar results were observed in an earlier study and attributed to small agglomerations of the particles during PCC's synthesis and testing (Shahmaleki et al., 2020). As observed in Figure 4-11 c, the main elements in the EDX spectrum data corresponded to Ca, C, O, and P, along with Si and Mg. The detected essential elements have been reported in an earlier study by Nodushan et al. on *Prosopis cineraria*, including leaves, branches, and stems (Nodushan et al., 2020).

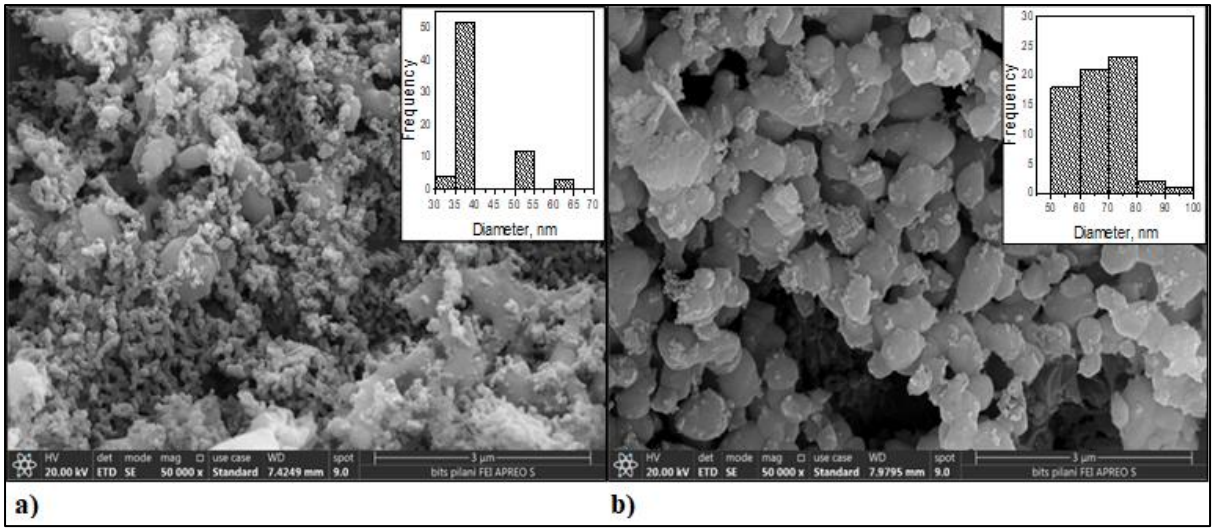

Figure 4-10 FESEM images of PCC and Frequency distribution of PCC particles a) before and b) after adsorption

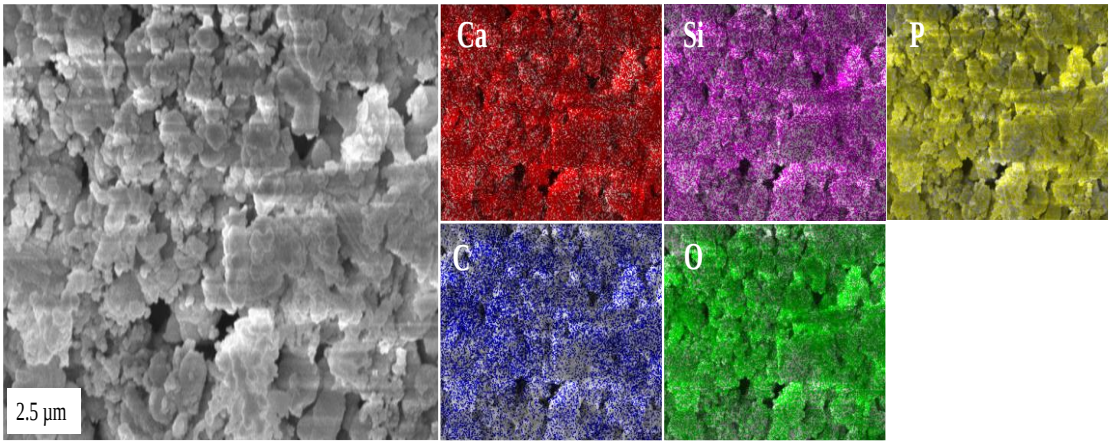

(a)

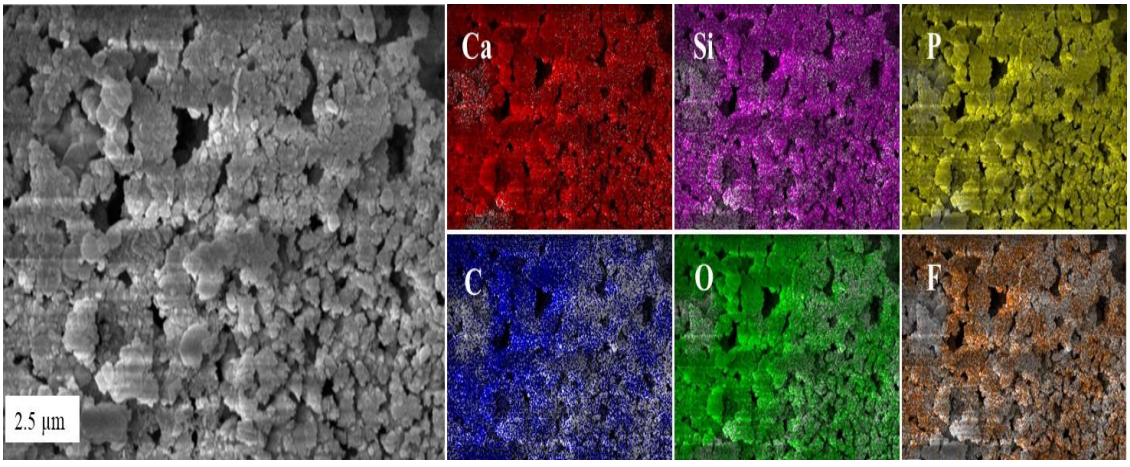

(b)

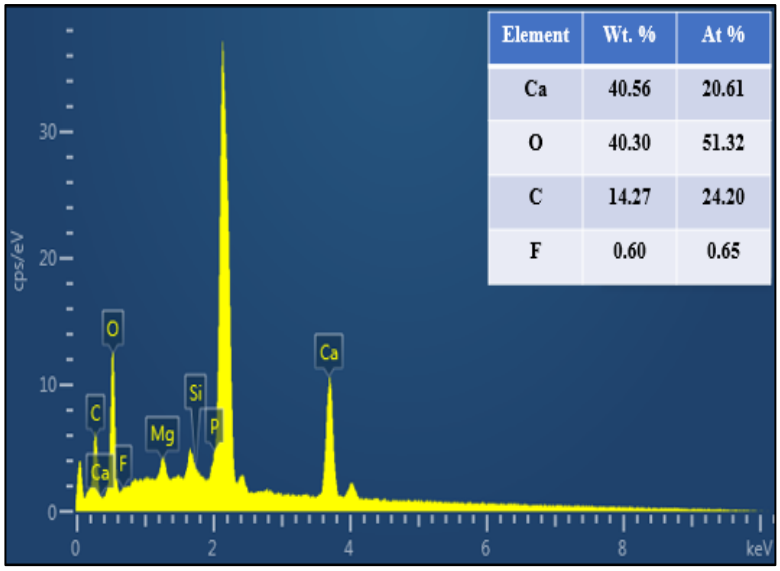

(c)

Figure 4-11 EDS dot mapping of PCC a) before b) after adsorption c) EDX spectrum of PCC after adsorption

Table 4-6 Elemental concentration on PCC surface in percentages

Elements	% Composition	
	Before adsorption	After adsorption
Calcium (Ca)	42.04	40.56
Silicon (Si)	1.18	0.57
Phosphorus (P)	0.64	1.64
Carbon (C)	12.24	14.27
Oxygen (O)	41.05	40.30
Magnesium (Mg)	2.85	2.06
Fluoride (F^-)	0	0.60

4.12 Sensitivity Analysis through batch tests

The sensitivity investigation systematically alters operational factors such as pH, contact time, initial F^- concentration, and PCC dose to determine their effect on the adsorption process at work. A large number of experimental studies were conducted by varying the operational parameters as a precursor examination.

In the present study, the operational parameters were varied in the following ranges: pH- 4 to 9; Time (in minutes)- 10,20,40,60,120,240; Dosage of adsorbent (g/l)- 0.5,1,2,5,7.5,10; and Initial F^- concentrations (mg/l)- 3,5,7,11,15.

4.12.1 Effect of pH

pH is essential for establishing the F^- removal mechanism in adsorption studies. The effect of pH on PCC was studied by varying the standard solution's initial pH concentration. The pH was studied in the range of 4.0-9.0. The pH range considerably impacts F^- removal; the lower the pH range, the H^+ ions' concentration increases, resulting in more F^- ion affiliation. The maximum removal efficiency of 38% was observed at pH 5 in Figure 4-12 a. However, at a lower pH value of 4, the removal efficiency was below 25%, which can be attributed to the fact that the solution's distribution of F^- and HF^- is pH-controlled (Tor et al., 2009).

Further, the positive charge of the PCC surface contributes to adsorbing F^- ions, supplemented by the pH_{pzc} results. At higher pH values, PCC's removal capacity was diminished due to the negative surface charge (Mondal et al., 2022). Hence, pH 5 was selected as the optimum pH for all the remaining experiments. Previous literature on *Prosopis cineraria's* malachite green, textile dye, and lead removal efficiency ranged in the pH range of 6-10, 10.5, and 2-6, respectively, primarily depending on the charge carried by the adsorbate (Garg et al., 2004; Natarajan & Manivasagan, 2020; Shahmaleki et al., 2020). The biosorption process strongly relies on the aqueous phase pH, the functional groups on the bio-sorbent, and their ionic states (Yadav et al., 2013). Biomass has been determined to contain biomacromolecules comprising several functional groups. The biosorption phenomena depend primarily on the protonation and deprotonation of these functional groups, which in turn depends upon the solution pH (Chen et al., 2020; Tüzün et al., 2005). For this work, the pH of the solution after treatment with PCC was accounted as well and represented in Figure 4-12 b. After treatment, pH was monitored to ensure a symbiotic relationship between F^- removal and drinkable water quality. The final pH of the solutions was maintained between 7.9 and 8.26, ensuring the drinkability of treated water with no further action. pH measurement after defluoridation is essential to ensure the cost-saving advantage and applicability of bio-sorbents in rural areas where pH adjustment is not preferable.

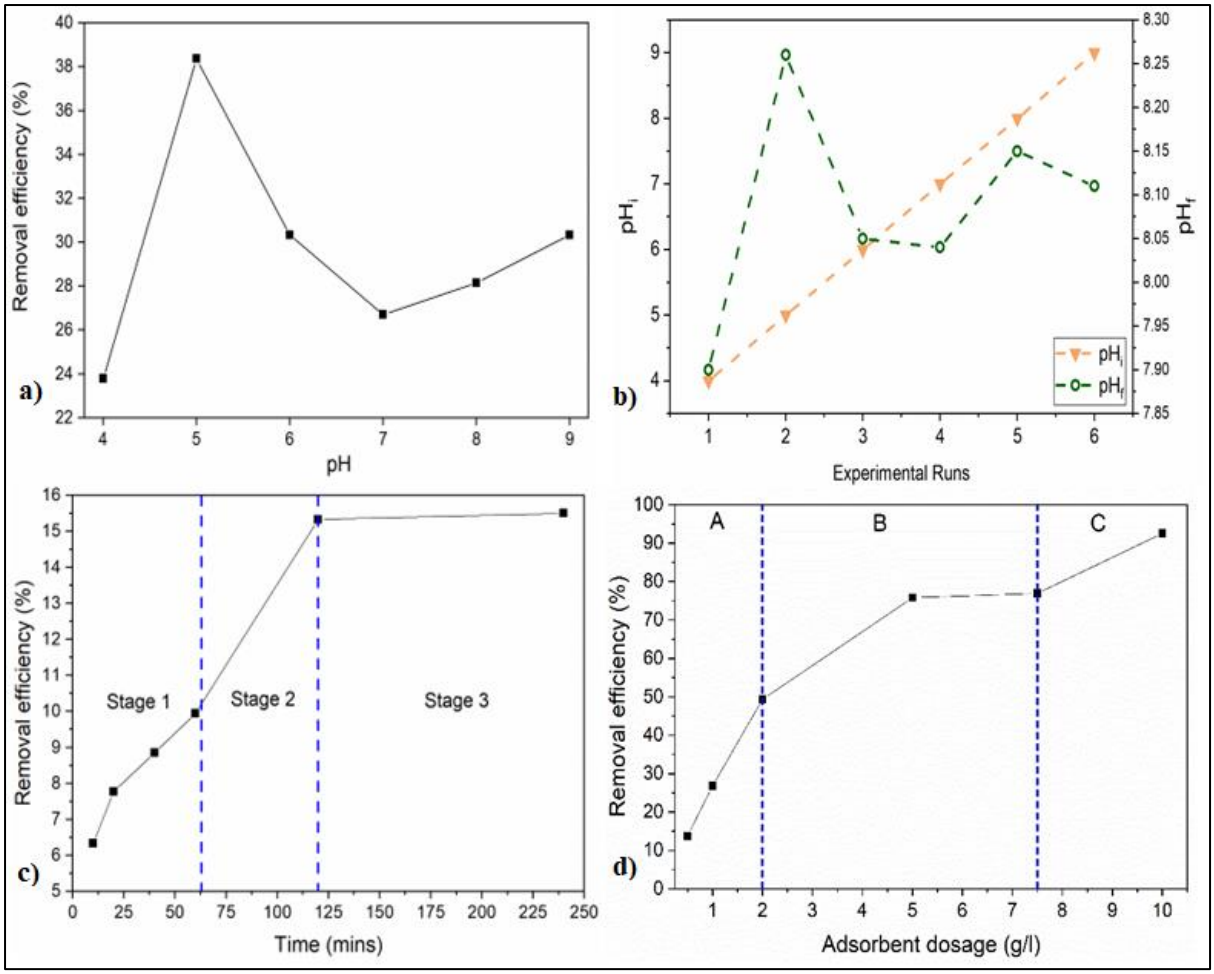

Figure 4-12 a) Effect of pH on the F^- removal efficiency b) Recorded pH values after treatment with PCC with an F^- concentration of 3 mg/l, contact time of 40 minutes, and dosage of 0.5 g/l) c) Effect of contact time (mins) on the F^- removal efficiency at pH 5, PCC dosage 0.5 g/l d) Removal efficiency observed for PCC with varying adsorbent dosage at pH 5, contact time of 120 minutes

4.12.2 Effect of Contact time

The removal of F^- as a function of contact time is shown in Figure 4-12 c, where contact time was varied from 10 minutes to 240 minutes. As contact time increased, the percentage removal increased, gradually approaching an almost constant value, denoting the attainment of equilibrium. In the current case, at a fixed adsorbent dosage of PCC, the removal efficiency of F^- increased with time and attained equilibrium after 120 minutes, with no significant changes till 240 minutes. As the contact duration rises, so does the interaction time between the ions and the active sites on the adsorbent. Hence, increased removal efficiency is observed. However, as equilibrium removal efficiency is reached, all the active sites are assumed to be saturated. Thus, no further fluoride adsorption is observed, even at a higher contact time of 240 minutes. F^- adsorption can be seen to be a triphasic occurrence.

Stage 1 shows an F^- reduction in the first 60 minutes, where the initial peak portion demonstrates an increased sorption uptake of F- ions. The second stage highlights an about-to-reach equilibrium stage, highlighting a slow uptake of F- ions, synonymous with the consumption of all sites over the adsorbents. Equilibrium was attained at stage 3, with sorption uptake relatively small. Ramanaiah et al., and Yadav et al., have reported homologous trends (Ramanaiah et al., 2007; Yadav *et al.*, 2013). The presence of functional groups and active surface sites is attributed to the observed initial fast adsorption. In contrast, the constant removal rate towards the end of the experiment indicates exhaustion of the active sites.

4.12.3 Effect of Adsorbent Dosage

The PCC dose was changed from 0.5 g/l to 10 g/l to establish the optimal adsorbent dosage while maintaining pH and time as constants. As observed in Figure 4-12 d, a three-phase process is observed for F- removal with varying adsorbent dosages. There is a significant increase in removal efficiency from 14% to 77% by increasing the adsorbent dosage from 0.5 to 7.5 g/l. An increase of 35.58% in removal efficiency was observed upon increasing the dose from 0.5 g/l to 2 g/l, supposedly due to the sudden availability of active adsorbent sites, surface area, and pore volume for F^- adsorption (Phase A). With increased PCC dosage from 2 to 7.5 g/l, a percentage increase of 27.6% was observed in reported removal efficiency (Phase B). While with an increase in PCC dose, increased adsorption was observed, the unit adsorption rate was decreased. A plausible explanation could be the overlapping of active sites or aggregation of adsorption sites at a higher dosage, thus reducing the net surface area. For Khejri's removal of malachite green dye, adsorption increased from 52.6 to 100%, with an increase in dose from 0.2 to 1 g/100ml (Garg et al., 2004). In a separate study, the COD removal efficiency of the thermally activated bio-sorbent increased from 28 to 72%, increasing the dosage from 0.25 to 4 g/l (Natarajan & Manivasagan, 2020). In this study, an increase of dose by another 2.5 g increased removal efficiency by 15.61% up to 92.52% observed in Phase C, following a similar trend as in Phase B. Considering an economic point of view, 5 g/l of dosage was adopted for further study.

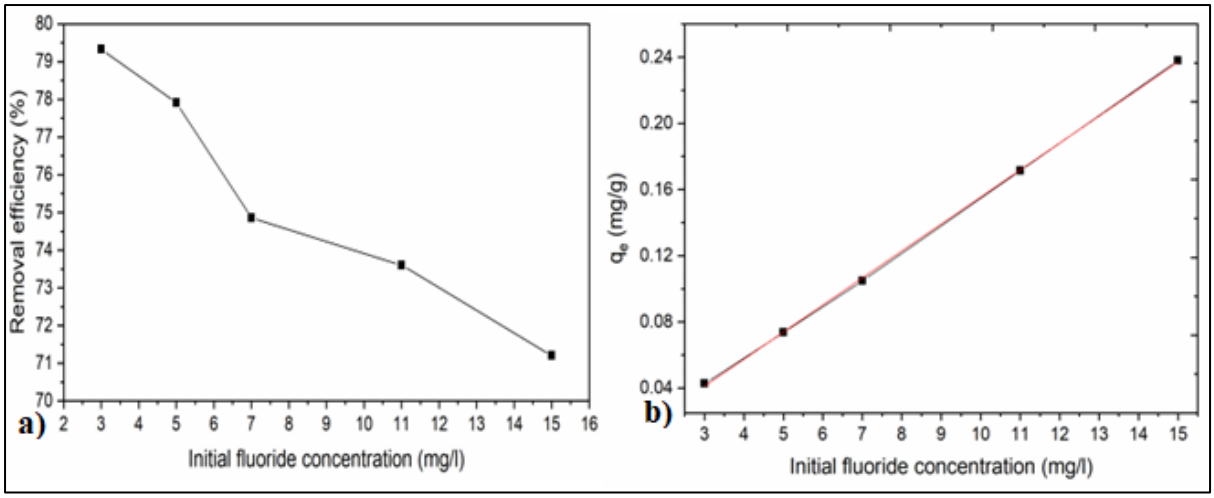

Figure 4-13 a) Effect of initial F- concentration on the removal efficiency and b) F- adsorption on the PCC (mg/g) at a pH of 5, contact time of 120 minutes, and dosage of 5 g/l

4.12.4 Effect of initial fluoride concentration

The initial F^- concentration effect was studied by adding a fixed amount of PCC (5 g/l) onto solutions having varied F^- concentrations (3, 5, 7, 11, and 15 mg/l) with pH and time maintained at optimum values at a temperature of 30 ± 3 ◦C. The range of Fluoride was adopted from the literature (Choubisa, 2018). As observed in Figure 4-13a, the removal efficiency of PCC decreased from 79.33% at 3 mg/l to 71.2 % at 15 gm/l. Natarajan and Manivasagan observed similar results for thermally activated *Prosopis cineraria* with an increased concentration of COD in dye wastewater (Natarajan & Manivasagan, 2020). The decrease in removal percentage can be attributed to the fact that the available sites are loaded with F^- from the solution, thereby exhausting the adsorbent material. The available adsorption sites were limited to a fixed adsorbent dose, which became saturated at a higher concentration (King et al., 2006). Figure 4-13b illustrates the deposition of F^- on the adsorbents. A positive relationship is observed between the initial F^- concentration and F^- deposited on the adsorbent (r = 0.99). It is evident from the experiments that though the percentage adsorption was decreased with an increase in initial F^- concentration, the actual amount of F^- adsorbed per unit of adsorbent was increased with an increase in F^- concentration in the test solution. F^- mass transfer resistances between the aqueous and solid phases were overcome due to the gradient's increased F^- concentration. Additionally, it caused an increase in equilibrium sorption up until sorbent saturation (Mondal et al., 2012).

4.12.5 Statistical analysis of the adsorption

The results of the statistical analysis on th experimental results are discussed in the subsequent sections.

4.12.5.1 Hypothesis testing to judge the optimum contact time for maximum F^- removal

A two-tailed t-test was applied to judge the optimum contact time value within a 1 % significance level.

Null hypothesis H_o:μ_{H_o} = Optimum contact time = 120 minutes

Alternative hypothesis H_a: Optimum contact time ≠ 120 minutes

For (n-1) degree of freedom,

$$t_{observed} = \frac{(Xavg - \mu)}{\frac{\sigma_s}{\sqrt{n}}} \quad (4.19)$$

where σ_s, X_{avg}, and n are the recorded experiments' standard deviation, average, and sample size. With σ_s = 3.9, n = 6, and X_{avg} = 10.62, from Equation 4.19, $t_{observed}$ is calculated to be -2.958. The $t_{tabulated}$ = -4.032 at a 1% significance level for 5 degrees of freedom for a 2-tailed t-distribution (Kothari, 2004).

As $t_{observed} < t_{tabulated,}$ the null hypothesis is accepted, approving 120 minutes as the optimum contact time in line with the experimental results obtained.

4.12.5.2 Hypothesis testing to conclude that higher adsorbent dosage had higher F^- removal efficiency

The Chi-square test was applied to the data collected from the experiments. An F^- concentration of 3 and 15 mg/l and adsorbent dosages of 5 and 10 g/l were selected for the study. Suppose the estimated value of $\chi 2$ is less than the table value at a specific significance level; in that case, the fit is regarded as satisfactory, implying that the difference between observed and predicted frequencies is due to sampling variations.

$$\chi^2 = \Sigma\frac{(O_{ij} - E_{ij})^2}{E_{ij}} \quad (4.20)$$

Oij and Eij are the observed and expected frequencies of the cell in the i^{th} row and j^{th} column.

Table 4-7 Observed fluoride ion removal for an initial F^- concentrations of 3 and 15 mg/l and PCC dosage of 5 and 10 g/l

		% Fluoride removed		Total
		IFC = 3 mg/l	IFC = 15 mg/l	
Adsorbent Dosage (g/l)	5	79	71	150 = A
	10	93	98	191 = a
Total		172 = B	169 = b	341

Table 4-8 Calculation for Chi-square

Groups	Oij	Eij	$(Oij-Eij)^2/ Eij$
AB	79	75.65	0.15
Ab	71	74.34	0.15
aB	93	96.34	0.12
ab	98	94.66	0.12

***AB, Ab, aB, ab represents the ion removal at the interjection of a given adsorbent dosage and initial F^- concentration**

Null hypothesis H_o: % removal is more significant with a higher adsorbent dosage

Alternate hypothesis: % removal decreases with increasing adsorbent dosage

From Equation 4.20, the calculated value of $\chi^2_{observed}$ = 0.53, whereas $\chi^2_{tabulated}$ = 3.841 at a 5% level of significance for 1 degree of freedom (Kaushal & Singh, 2017). Since $\chi^2_{observed} < \chi^2_{tabulated}$, null hypothesis signifying that a higher adsorbent dose results in higher removal of fluoride is accepted. The experimental results observed are statistically validated.

4.12.5.3 Testing hypotheses to determine the experiment's success

The paired t-test was used on the matched pairs, the concentrations of F^- ions in the solution before (Xi) and after (Yi) the adsorption experiment.

Null hypothesis H_o: The experiment did not change the solution's concentration of F^- ions.

Alternate hypothesis H_a: The adsorption experiment was successful.

For the paired t-test,

$$t_{observed} = \frac{(D_{avg} - 0)}{\frac{\sigma_{diff}}{\sqrt{n}}} \quad (4.21)$$

where n = number of matched pairs, D_{avg} = mean of differences, and σ_{diff} = standard deviation of differences.

With D_{avg}, σ_{diff}, and n values as 6.05, 3.33, and 5, respectively, from Equation 4.21, $t_{observed}$ = 4.06. $t_{tabulated}$ = 2.776 at a 5% level of significance for 4 degrees of freedom for 2-tailed t-distribution.

Since $t_{observed} > t_{tabulated}$, the null hypothesis that the experiment did not change the concentration of F^- ions in the aqueous solution was rejected. The alternative hypothesis supporting the experiment's success was simultaneously accepted in light of the experiment's findings.

4.13 Adsorption Isotherms

4.13.1 Langmuir isotherm

The Langmuir isotherm is based on the following assumptions: i) ions are chemically adsorbed at a fixed number of well-defined sites; ii) monolayer adsorption on a homogenous surface; iii) no lateral interaction and steric hindrance between adsorbed molecules; and iv) all sites are energetically equivalent (Nur et al., 2014). Langmuir adsorption isotherm, developed initially to describe gas-solid phase adsorption onto activated carbon, has been traditionally employed to investigate the potential and performance of various sorbents. The model resonates with the validity of solutes' adsorption from aqueous solutions through monolayer adsorption on a finite number of homogenous sites within the adsorbent surface. It has been reported that Langmuir isotherm could be linearized into different forms, with linear regression resulting in different parameter estimates. The authors adopted the most popular linear forms in the study: Langmuir 1 and Langmuir 2. All the reported results are tabulated in Table 4-9.

The Langmuir constants, Q_{max} and K_L are determined from the slope and intercept, respectively, from the plot between C_e and C_e/q_e for Langmuir model 1 and between $1/q_e$ and $1/C_e$ for Langmuir model 2. Figure 4-14 shows the Langmuir models' plots and the experimental data for the sorption of F^- onto PCC. The best fit was obtained using Langmuir-2 isotherm because of minimized deviations from the fitted equations (Yadav & Singh, 2017). The maximum adsorption capacity Q_{max} for PCC was 4.357 mg/g with a high R^2 value (0.997). To establish the feasibility of the isotherm, the Langmuir isotherm can be expressed in terms of a dimensionless constant separation factor R_L from Equation 4.22.

$$R_L = \frac{1}{1+bC_o} \qquad (4.22)$$

The separation factor R_L was 0.629 for an initial F- concentration of 3 mg/l. The adsorption phenomenon was favorable, with R_L less than 1 (Ayub et al., 2020).

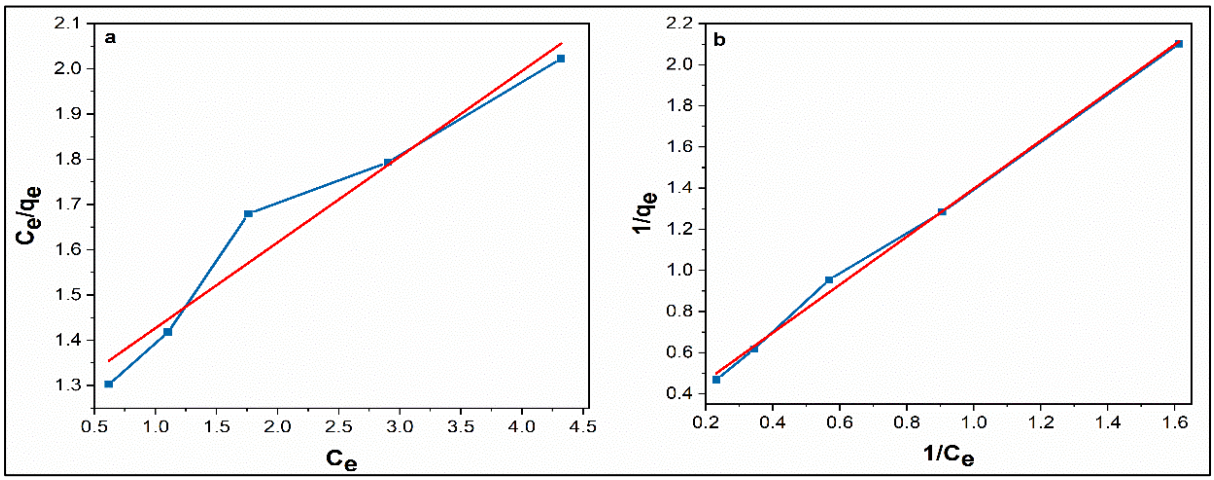

Figure 4-14 Representation of isotherms curve fit in this study a) Langmuir Isotherm 1, b) Langmuir Isotherm 2

4.13.2 Freundlich isotherm

Freundlich Isotherm is an empirical equation that describes non-ideal and reversible adsorption. It applies to multilayer adsorption with the interaction between adsorbed molecules. The isotherm further advocates that sorption energy exponentially decreases upon completion of the adsorption process (Ghorai & Pant, 2005). The Freundlich constants, K_f, and empirical parameter 1/n were determined from the intercept and slope of the linear plot of log q_e versus log C_e (Figure 4-15a), respectively. While K_f measures the adsorption capacity, 1/n is the adsorption intensity or surface heterogeneity. A value of 1/n below 1 indicates a favorable Freundlich isotherm, while 1/n above 1 indicates cooperative adsorption (Gebrewold et al.,

2019). A conducive condition for adsorption is confirmed with 1/n lying between 0.1 to 1.0 and the n value lying in the range of 1-10, at 0.77 and 1.296, respectively. Shahmaleki et al. reported n values in ranges similar to the current study (Shahmaleki et al., 2020). The recorded K_f value was 1.432 mg/g(l/mg). With an explicable high R^2 value (0.998), the Freundlich isotherm model fitted well with the experimental data, as demonstrated in Figure 4-15a.

4.13.3 Temkin isotherm

Temkin isotherm model presumes that the heat of adsorption (a function of temperature) of all the molecules in the layer would decrease linearly rather than logarithmically with coverage due to adsorbate–adsorbent interactions. A uniform distribution of binding energies further characterizes the adsorption process. From the slope and intercept of Figure 4-15b, the values of Temkin isotherm constants are determined, where A_T is 2.42 L/g and b (heat of adsorption) is 2.96 kJ mol-1. b is derived from Equation 4.23.

$$B = \frac{RT}{b} \tag{4.23}$$

Where R is the ideal gas constant (8.3145 J mol-1K-1), and T is the temperature (K).

The lower heat of adsorption value, b < 8, represents a weak interaction between the F- ions and adsorbent (Bhaumik & Mondal, 2015).

A significant finding from the isotherm models was the high degree of correlation value (R^2) observed for both Langmuir and Freundlich isotherms, at 0.997 and 0.998, respectively, indicating adsorption by combined mechanisms onto a heterogeneous surface. Previous studies have demonstrated the involvement of two adsorption processes (Asgher & Bhatti, 2012; Nethaji & Sivasamy, 2014).

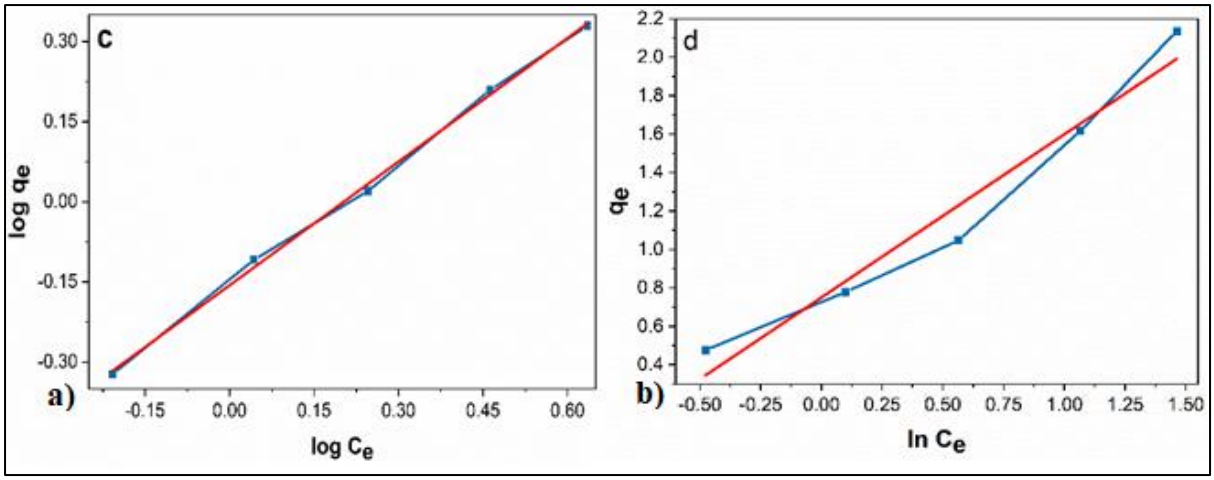

Figure 4-15 Representation of isotherms a) Freundlich Isotherm, and b) Temkin Isotherm

Table 4-9 Adsorption Isotherm Parameters

Langmuir 1	
Q (mg/g)	5.277
K_L (l/mg)	0.153
R_L	0.685
R^2	0.951
Langmuir 2	
Q (mg/g)	4.357
K_L (l/mg)	0.196
R_L	0.629
R^2	0.997
Freundlich	
K_f (mg/g(l/mg)$^{1/n}$)	1.432

n	1.296
R^2	0.998
Temkin	
A_T (l/mg)	2.42
b_T	2.96
R^2	0.957

4.14 Adsorption Kinetics

The pseudo-first-order reaction generally applies over the initial stages of adsorption. It is based on the assumption that the adsorption rate is proportional to the first power of free sites. It is an extensively used rate equation to describe adsorbate adsorption from the liquid phase. The pseudo-second-order model assumes that the rate-limiting step is chemical sorption and predicts the behavior over the whole range of adsorption. It is based on the presumption that the adsorption rate is proportional to the second power of the number of unoccupied sites (Gandhimathi, 2022).

It is essential to identify the rate-limiting step in adsorption investigations. The solute transfer process for the solid-liquid adsorption process is often characterized by exterior mass transfer (boundary layer diffusion), intraparticle diffusion, or both. As a consequence, the rate-limiting step was studied using the experimental results.

Figures 4-16 a to c, and Table 4-10, reported the kinetic curves and model constants. With an R^2 value of 0.99, the pseudo-second-order kinetic model best described the experimental results. For the first-order rate expression, the experimental q_e values do not agree with the computed ones derived from the linear plots. However, a good agreement is observed for the second-order model with the experimental data with $q_{e,cal}$ at 2.51 mg/g.

The intraparticle diffusion model presents multi-linearity, indicating that the adsorption process occurs in multiple steps, as observed in Figure 4-16 c. The first portion of the curve is attributed to the transport of adsorbate molecules from the bulk solution to the external adsorbent surface by diffusion through the boundary layer (film diffusion). The second portion

describes the adsorbate's diffusion from the external surface into the adsorbent's pores (pore or intraparticle diffusion). While the initial curve portion is attributed to the boundary layer diffusion effect, the final linear portion is intra-particle diffusion. Previous studies have depicted multi-linearity in the plot between q_t versus $t^{0.5}$, characterizing two or more steps involved in the adsorption process. Extrapolation of the linear portion of plots back to the Y axis provides intercepts proportional to the boundary layer thickness (Mahramanlioglu et al., 2002; Sun & Yang, 2003; Duran *et al.*, 2011). If the plot of q_t versus $t^{0.5}$ passes through the origin, then pore diffusion is the only rate-limiting step; if not, it is considered that the adsorption process is complex, where surface adsorption and intra-particle diffusion simultaneously contribute to the rate-determining step (Ghorai & Pant, 2005).

The isotherm and kinetic study results highlight PCC's appreciable F^- removal capacity as an alternative for F^- sequestration.

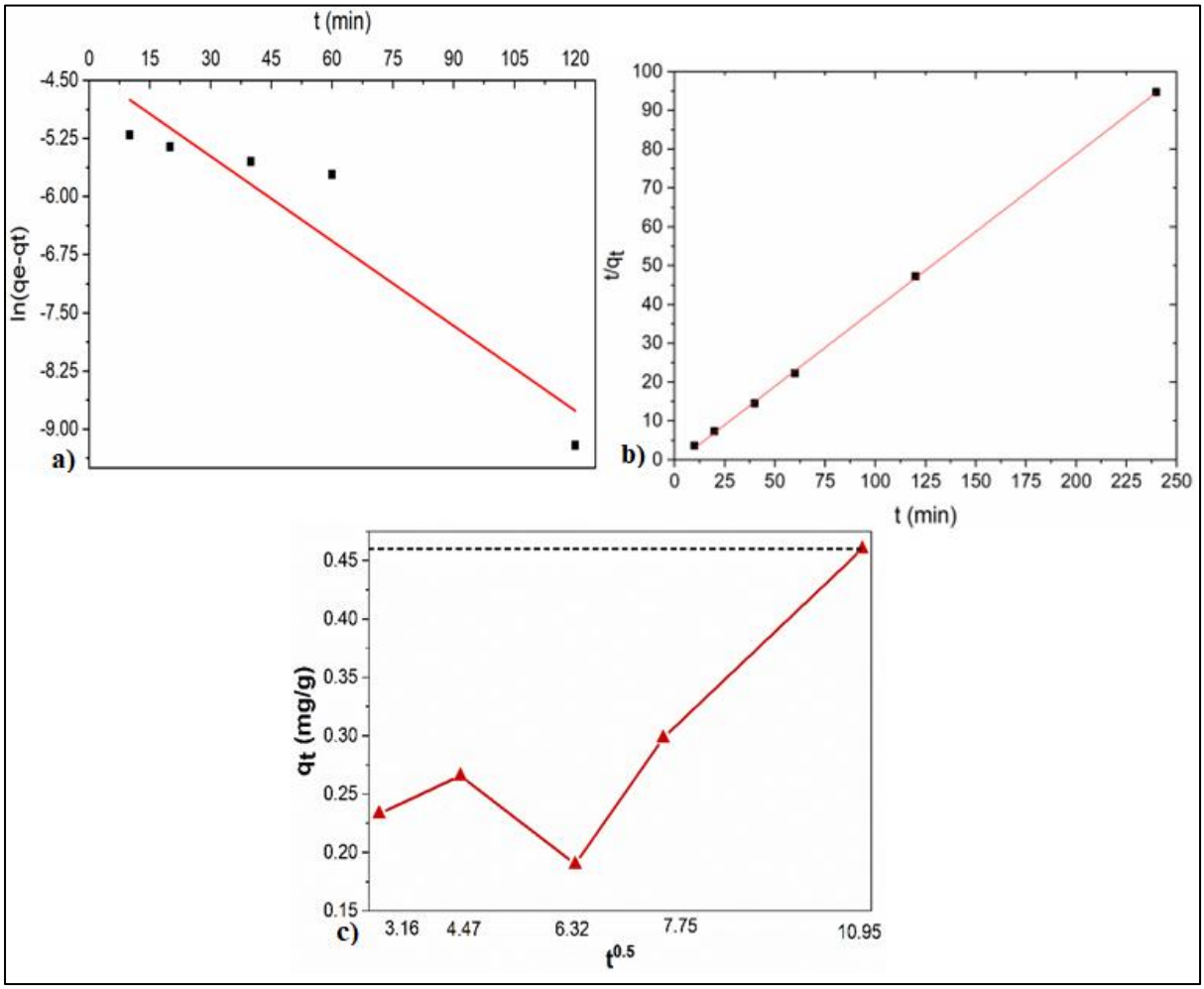

Figure 4-16 Fitting experimental data to kinetic curves to study the adsorption mechanism. a) Pseudo-first-order model, b) pseudo-second-order model, c) Intraparticle diffusion model

Table 4-10 Pseudo-first order, Pseudo-second order, and Intraparticle diffusion model Parameters for the adsorption of F- onto PCC

Model	Parameters	
Experimental Value	$q_{e,exp}$ (mg/g)	2.54
Pseudo-first-order kinetic model	k_1 (min^{-1})	0.037
	$q_{e,cal}$ (mg/g)	0.013
	R^2	0.887
Pseudo-second-order-kinetic model	k_2 (g/mg. min)	0.166
	$q_{e,cal}$ (mg/g)	2.51
	R^2	0.999
Intraparticle diffusion model	$K_{id,1}$ ($mg/g.min^{0.5}$)	0.0279
	c	0.46
	R^2	0.668

4.15 Recyclability of adsorbent

Better reusability of the developed adsorbent is essential in establishing its superior performance, particularly for large-scale applications. In this context, the authors conducted six experimental runs to investigate the PCC's reusability at the optimum operating conditions of 3 mg/l of F^- concentration, 5 g/l adsorbent doses, a pH of 5, and a contact time of 120 minutes. It is to be noted that while conducting this set of experiments, no regenerating solution was used on the adsorbents. Instead, the used adsorbents were dried and utilized repeatedly until the removal effectiveness was reduced—figure 4-17a shows PCC's efficacy at each cycle. The adsorbent performed satisfactorily till experimental Run 3, with efficiency falling from 79 to 58.7%. After that, the removal efficiency decreased sharply by 22.6% from Run 3 to Run 4. Thereafter, a declining trend in overall removal efficiency was observed, conceivably due to the loss of adsorbent during the recycling process and the blocking of active sites by F^- ions and other organics (Shahmaleki et al., 2020).

4.16 Regeneration of PCC

High regenerative capability further cements the economic performability of the adsorbent for application to remote areas. The current study used the eluents of distilled water, 0.1N NaOH, and 0.1N NaCl. The regenerative studies were carried out by mixing 50 mL of the eluent with the loaded PCC. The setup was agitated for 30 mins at 40°C; the adsorbent separated from the filtrate, then reusing the PCC for F- removal. Figure 4-17b reflects the pollutant removal potential of the treated PCC through a number of regeneration (desorption-adsorption) cycles. The removal percentage of NaOH varied from 60.01 to 68.05%, with a maximum of 75.44% exhibiting appreciable performance. The NaCl removal efficiency remained less than 60% for all five experimental runs concluding with moderate performance. Removing efficiencies above 80% for distilled water were observed at par with the original removal efficiency for the first three runs. For the last two runs, 4 and 5, the efficiency reduced to 75.2 and 55.6%, respectively. Overall, distilled water outperformed the remaining desorption solutions. Lee et al. reported the superiority of deionized water in the regeneration of thermally treated *Mytilus coruscus* shells, similar to our reported results (Lee et al., 2021).

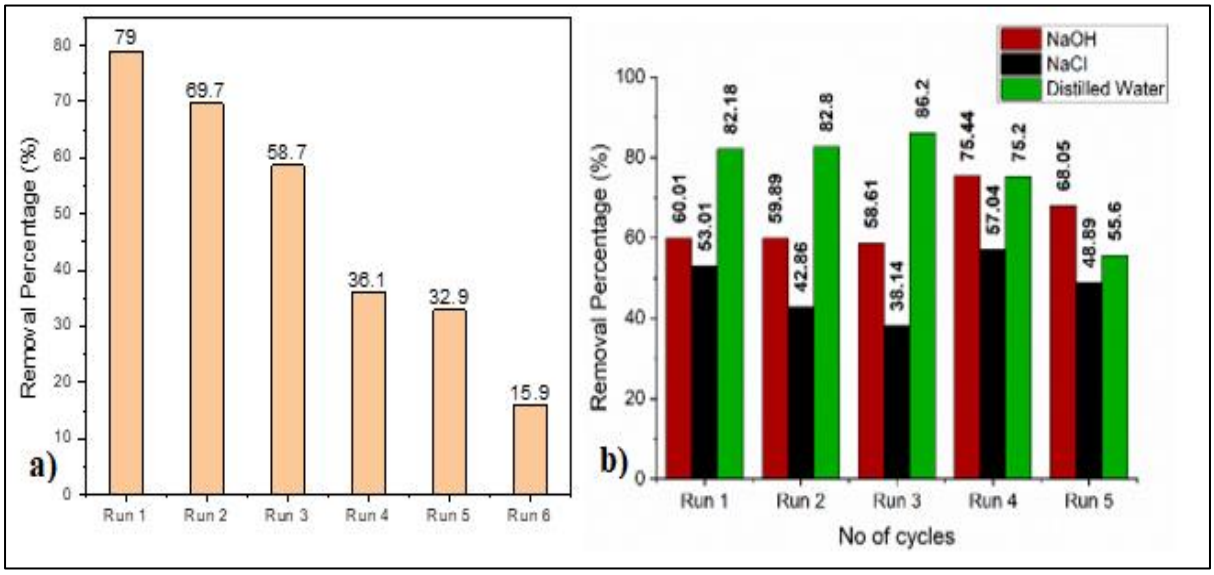

Figure 4-17 a) Reusability of PCC in the F- removal process over six cycles and b) Desorption studies carried out with three different solutions

4.16.1 Comparison with various adsorbents

The reported adsorbent for the present investigation, PCC, was contrasted with various currently available adsorbents in the literature, reported in Table 2-2. Compared to several bio-sorbents, PCC demonstrated good removal effectiveness in F^- remediation.

4.17 Field Study and WAWQI

The PCC bio-adsorbent developed was tested with five field groundwater samples collected from Jhunjhunu district, Rajasthan, India.

The influent treatment process maintained the optimum operating conditions of contact time (120 minutes) and dosage (5 g/l). The pH of the collected sample was unaltered to observe PCC performance under neutral conditions.

Table 4-11 presents the performance of PCC after defluoridation. pH was reduced by 4.21% to 12.02% for Villages 1 and 2. Villages 3, 4, and 5 had pH decreases in a similar range at 7.76, 7.45, and 7.72%, respectively. TDS for the village samples decreased in the range of 40.92, 59.53, 49.03, 60.99, and 55 % for the villages sequentially. The recorded TH value increased by 33.33% for village 1. However, a decrease in TH value was observed at 22.857,13.04, 13.04, and 8.64% across villages 2, 3, 4, and 5, respectively. It is further evident from these observations that the PCC developed could remove the F^- to a range of 79.7 to 87 % of its initial concentrations, confirming its potential as an effective F^- scavenger.

Table 4-11 pH and F^- values of villages after treatment with PCC

	Before Treatment	**Village 1**	**Village 2**	**Village 3**	**Village 4**	**Village 5**
Water Quality Parameters	pH	8.4	7.83	8.11	8.59	8.29
	TDS (mg/l)	452	598	720	685	856
	TH (mg/l)	120	140	322	230	185
	F^- (mg/l)	1.2	1.53	1.75	2.05	1.91
	After Treatment	**Village 1**	**Village 2**	**Village 3**	**Village 4**	**Village 5**
	pH	7.39	7.5	7.48	7.95	7.65
	TDS (mg/l)	267	242	367	267.2	385.2
	TH (mg/l)	160	108	280	200	169
	F^- (mg/l)	0.18	0.31	0.32	0.34	0.25

All previously obtained groundwater samples were deemed unfit for consumption with a WAWQI >150, as shown in Figure 4-18a; Fluoride is the primary contaminant. In addition to lowering the concentration of F^-, the study's novel adsorbent significantly impacted the other

parameters. The total WAWQI of the water samples decreased following defluoridation at the optimum dose and duration, keeping pH neutral. The groundwater samples were subsequently put into the good and fair categories following treatment.

The unsuitability of the collected water is aided with evaluated HI. As is demonstrated in Figure 4-18b, all village samples were categorized into medium-risk zone except Village 1. With a HI value of 0.97, Village 1 lies on the border of medium risk. All village samples were classified into the low-risk zone after treatment with PCC. The results signify PCC's health risk assessment results, highlighting the proposed adsorbent as a contender for effective F^- remediation.

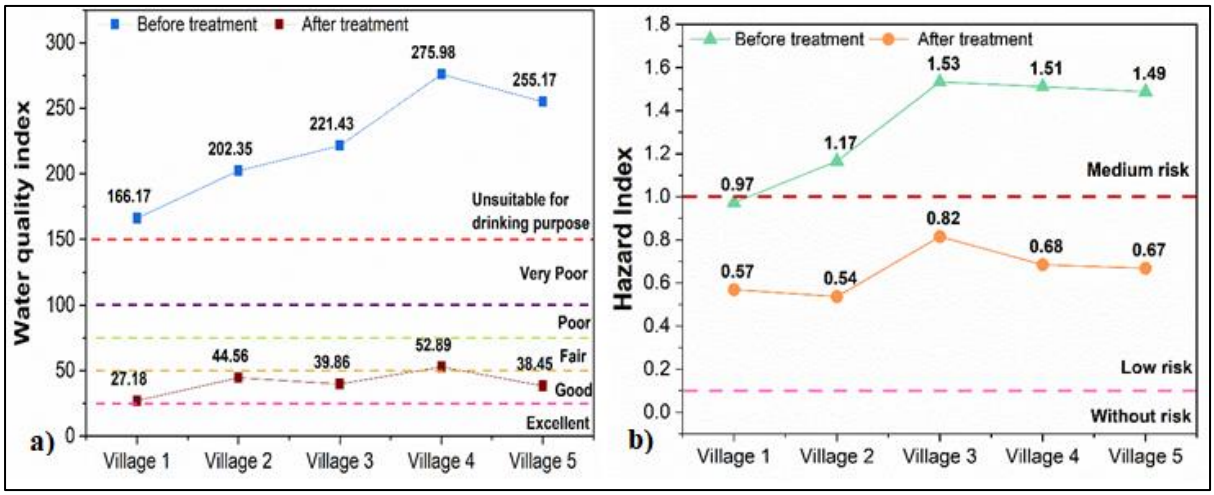

Figure 4-18 a) WAWQI of village water samples after treatment with PCC b) Hazard Index developed for the villages

4.18 AI algorithms as predictive models

A significant drawback of the OVAT approach is its incapability to provide any prediction model when more than one variable is varying. Machine learning models are used to efficiently derive the governing equation and provide a prediction model over varying input conditions to overcome the inconvenience and deal with the unfeasibility of conducting many experiments fundamental to OVAT.

4.18.1 Linear and Non-linear regression modeling

The essential step in the regression approach is choosing the predictor variables that offer the best prediction equation for modeling the dependent variables. Every independent variable was initially included in the simple regression model. Then, the best independent variables were

identified using the step-wise regression approach and selective elimination—the results of step-wise regression analysis for LR and NLR models are summarized in Table 4-12.

The basic regression model initially included all the independent variables (inputs). The stepwise regression technique was then employed. Suppose the partial sums of squares for any previously had variables do not reach a minimal condition to remain in the model; in that case, the selection phase switches to backward elimination, and variables are discarded one by one until all remaining variables match the minimum criterion. The SPSS software performed the regression analysis. The step-wise models for linear and non-linear regression were observed to have a lower fit to the experimental data. A similar trend was observed by Bilgili and Sahin (Bilgili & Sahin, 2010).

Since the simple regression methods had a higher correlation coefficient, the derived equations were used to predict the removal efficiencies. The corresponding predicted results and the actual output measurements are represented in Figure 4-19 to indicate the performance of all evaluated models. The residuals obtained are plotted in Figure 4-20. The residuals for the simple LR varied from -19.27 to 66.88, whereas the step-wise model ranged from -12.04 to 69.27. For the NLR models, the residuals recorded for the simple and step-wise models were 74.17 to 3.72 and 74.89 to 2.93. Low regression coefficients and high residuals highlight the inefficiency of the regression model in aptly modeling the complex process involved in the removal of F^-.

Table 4-12 The results of simple and stepwise regression analysis for the LR and NLR model

Model		Equation	R^2	Sig. levels for ANOVA	Significant levels of coefficients				
						1	2	3	4
Linear Regression Model	Simple	$Y = 0.358 - 0.278 \times X1 + 0.050 \times X2 + 0.065 \times X3 + 0.390 \times X4$	0.369	0.000^{**}	0.000^{**}	0.019^{**}	0.596	0.465	0.000^{**}
	Step-wise	$Y = 0.379 - 0.271 \times X1 + 0.439 \times X4$	0.357	0.000^{**}	0.000^{**}	0.011^{**}	-	-	0.000^{**}
	Simple	$Y=1.267X1^{0.105}X2^{0.202}X3^{-.039}X4^{0.376}$	0.484	0.000^{**}	0.001^{**}	0.194	0.019^{**}	0.596	0.000^{**}

Non-linear Regression Model	Step-wise	$Y = 1.34X2^{0.375}X4^{0.181}$	0.469	0.000**	0.000**	-	0.000**	-	0.029**

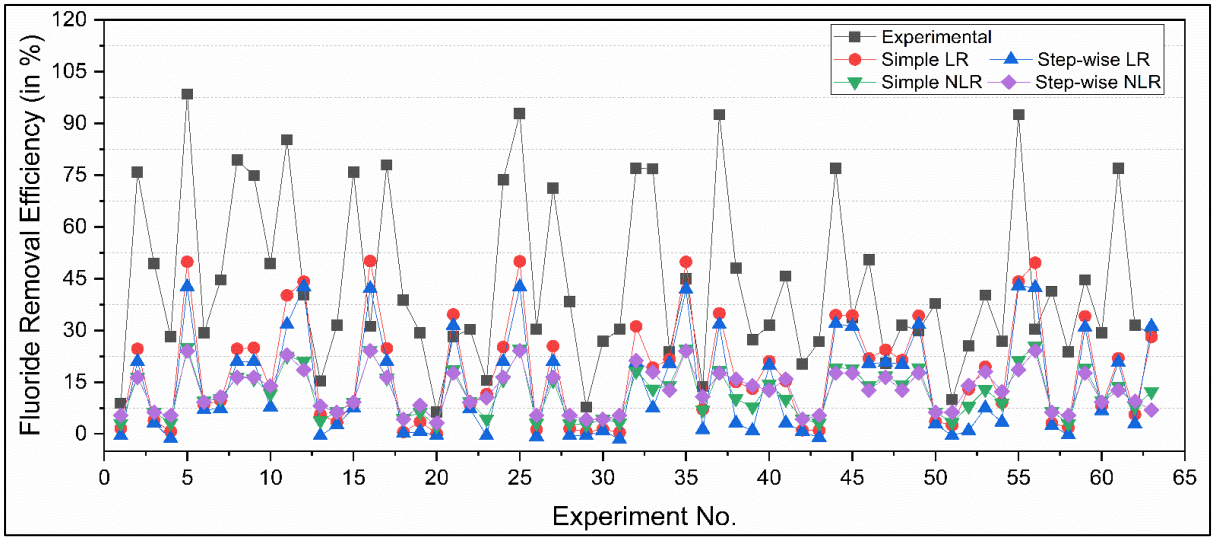

Figure 4-19 Comparison between experimental and predicted regression results for fluoride removal

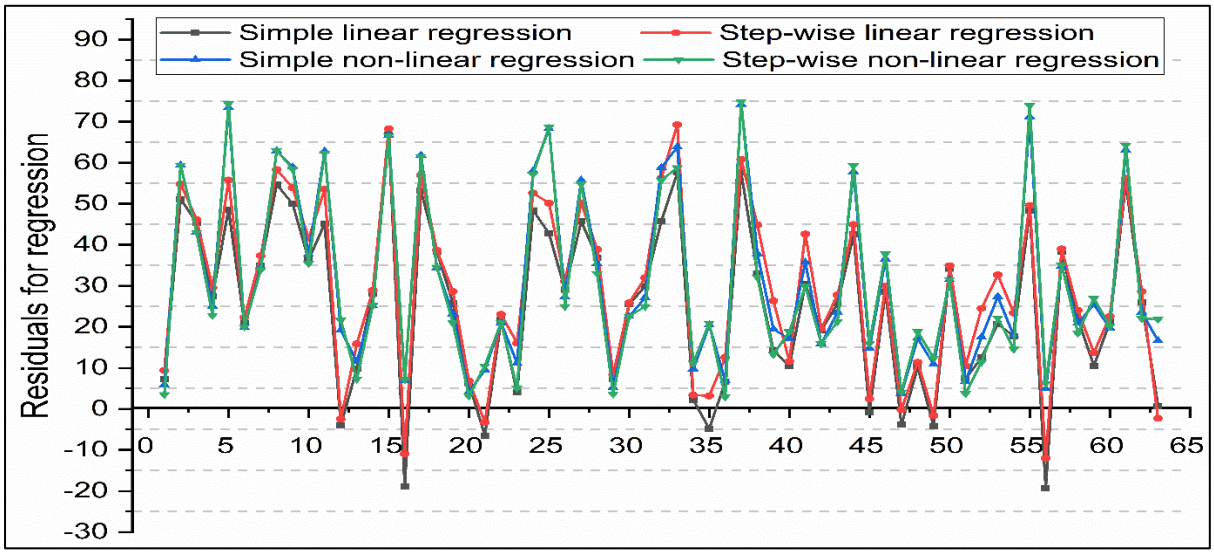

Figure 4-20 Residuals of linear and non-linear regression models

4.18.2 Artificial neural network (ANN)

Artificial neural networks are known for their ability to learn, simulate and predict data and mimic the functioning of the human brain (Elmolla et al., 2010). The inability of ANN to build

specific relationships between the input and output variables is a severe disadvantage, rendering the model a "black box."

The judgment about the efficiency of the ANN model is based on maximizing the R^2 value and reducing the MSE value of the testing set. The neural network consisted of the input layer, hidden layer (neurons), and output layer. The input variables were pH, contact time, dosage, and initial F^- concentration, while the output layer was the percentage removal of F^-.

Eight BP algorithms were studied to determine the best backpropagation (BP) training algorithm. For the first eight training models, 4-4-1 network architecture was used with tangent sigmoid transfer function as the activation function at both input-hidden and hidden-output layers. For the subsequent eight training algorithms, 4-4-1 network architecture with a log-sigmoid transfer function at the hidden layer and a linear transfer function (purelin) at the output layer was used. Tables 4-13 and 4-14 compile the comparison of different BP training algorithms. Levenberg–Marquardt backpropagation algorithm (LM) had the least mean square error (MSE) compared to other backpropagation algorithms. So, LM was considered the training algorithm for modeling the F^- removal efficiency.

The optimum number of neurons for the model was determined based on the minimum value of MSE of the training data set. The optimization was done using LM as a training algorithm with the 4-n-1 network architecture. 'n' represented the number of neurons in the hidden layer and varied from 1–20, as shown in Table 4-15. Optimizing the number of neurons was essential to ensure minimum deviation of predictions from experimental results and to reduce the possibility of over-fitting the model (Onu et al., 2021). About 70% of the data sets were used to train the network, while 15% each were used in testing the network and validating the result, respectively. Allocating more data to the training improved the model and decreased processing time.

MSE was 0.0264 when one neuron was used and decreased to 0.000182 when ten neurons were used—increasing the number of neurons by more than ten did not significantly reduce MSE. Based on the lowest mean square error, the best number of neurons for the hidden layer was ten in the trainlm algorithm. Therefore, the final network topology developed was designated as 4–10–1 (four input neurons representing pH, contact time, adsorbent dosage, and initial F-concentration; ten neurons in the single hidden layer, and one output neuron representing the percentage removal) for the optimal neural network with tangent sigmoid transfer function (tansig) at both hidden and output layers (represented in Figure 4-21 a and b). The R^2 value

obtained was 0.944 for the optimum network. The correlation obtained were 0.947 and 0.935 for the training and testing dataset, represented in Figures 4-22 and 4-23.

The correlation coefficients were better than those obtained for LR and NLR, indicating that the fit was appropriate for all the data sets. The complete ANN predicted removal percentage of F^- based on each experimental run could be assessed in Appendix 1 in Table vi. The ANN's superior correlation and predictive accuracy were attributed to its established ability to approximate the nonlinearity of the adsorption process.

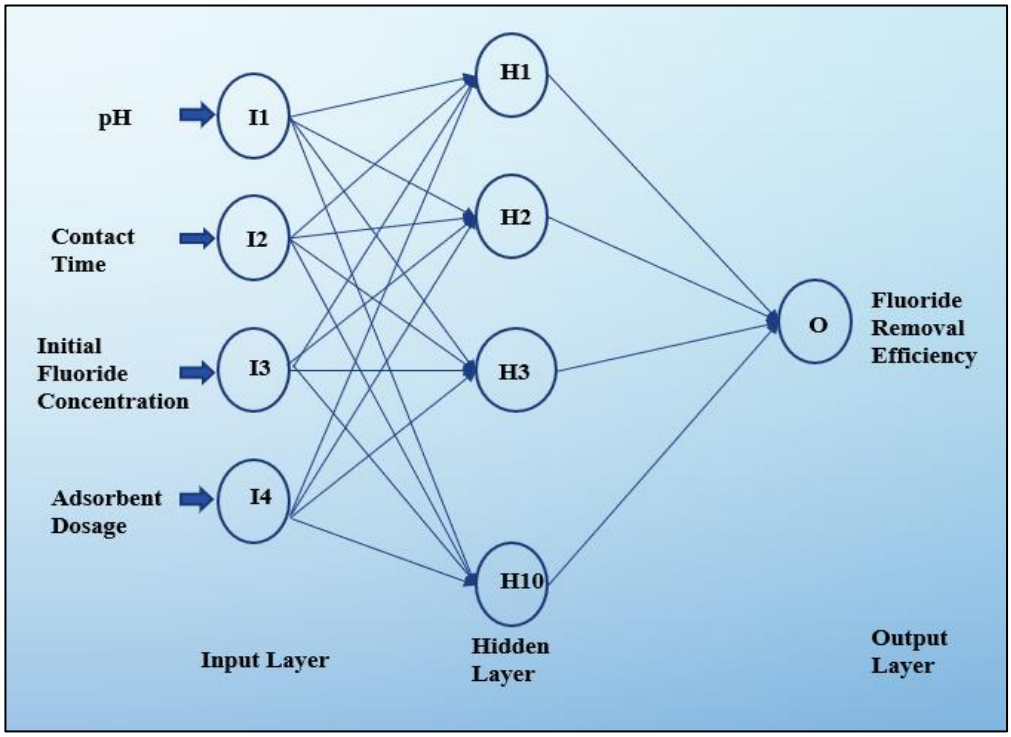

(a)

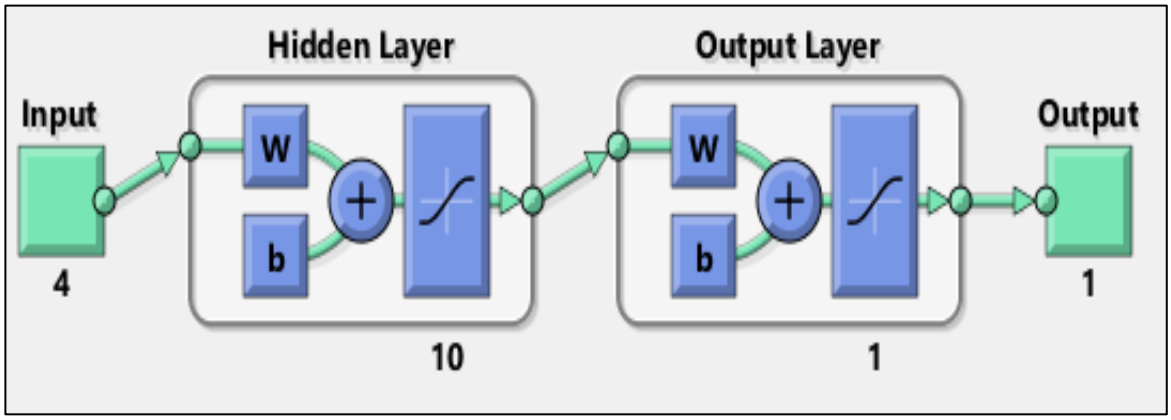

(b)

Figure 4-21 a) and b) The layout of the 4-10-1 architecture neural network

Table 4-13 Performance study of training algorithms of ANN models with 4-4-1 tansig-tansig network architecture

Sl no.	Training Algorithm	MSE	R^2	Linear Equation
1	**trainlm**	**0.00326**	**0.882**	**0.95x+0.0097**
2	trainbfg	0.0231	0.651	0.73x+0.11
3	traingd	0.0903	0.151	0.4x+0.31
4	traingdx	0.0566	0.138	0.16x+0.31
5	traingdm	0.046	0.511	0.68x+0.09
6	traincgf	0.0261	0.511	0.53x+0.19
7	traincgp	0.0133	0.745	0.81x+0.091
8	traincgb	0.0231	0.560	0.66x+0.14

Table 4-14 Performance study of training algorithms of ANN models with 4-4-1 logsig-purelin network architecture

Sl no.	Training Algorithm	MSE	R^2	Linear Equation
9	trainlm	0.0122	0.66	0.84x+0.1
10	trainbfg	0.0351	0.44	0.53x+0.19
11	traingd	0.0913	0.003	0.037x+0.39
12	traingdx	0.0482	0.267	0.18x+0.32
13	traingdm	0.0646	0.062	0.091x+0.34
14	traincgf	0.0253	0.478	0.38x+0.22
15	traincgp	0.0241	0.572	0.62x+0.15
16	traincgb	0.0299	0.517	0.5x+0.19

Table 4-15 Comparison of 20 neurons in the hidden layer for removal efficiency of Fluoride by the ANN model developed with the Levenberg-Marquardt algorithm

Sl no.	1 hidden layer Model Architecture	MSE	R^2	Linear Equation
1	4-1-1	0.0264	0.549	0.38x+0.26
2	4-2-1	0.0585	0.105	0.12x+0.33
3	4-3-1	0.0119	0.771	0.77x+0.073
4	4-4-1	0.00326	0.882	0.95x+0.0097
5	4-5-1	0.00426	0.876	0.89x+0.051
6	4-6-1	0.0126	0.462	0.46x+0.23
7	4-7-1	0.00386	0.689	0.7x+0.13
8	4-8-1	0.00171	0.885	0.89x+0.056
9	4-9-1	0.0032	0.795	0.82x+0.074
10	**4-10-1**	**0.000182**	**0.944**	**0.91x+0.038**
11	4-11-1	0.00373	0.653	0.77x+0.14
12	4-12-1	0.00162	0.876	0.9x+0.035
13	4-13-1	0.00258	0.440	0.39x+0.3
14	4-14-1	0.00175	0.809	0.92x+0.0084
15	4-15-1	0.0024	0.801	0.92x+0.045
16	4-16-1	0.00129	0.905	x-0.02
17	4-17-1	0.0013	0.856	x-0.0031

18	4-18-1	0.00141	0.826	0.84x+0.03
19	4-19-1	0.00126	0.534	0.54x+0.2
20	4-20-1	0.00197	0.819	0.86x+0.07

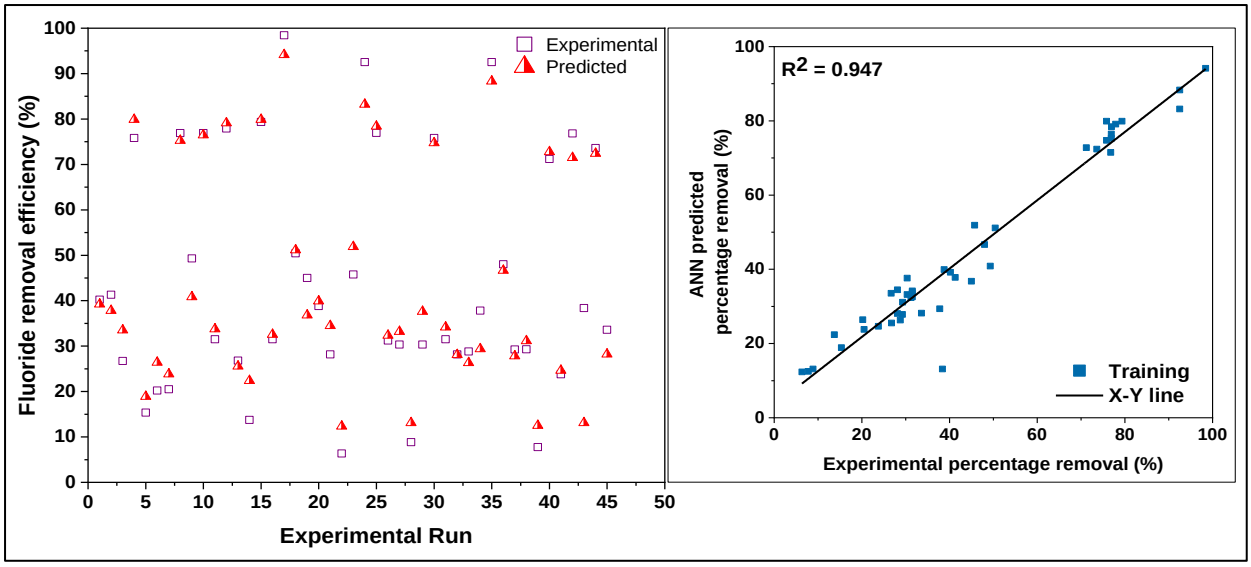

Figure 4-22 The graphical output of the ANN outputs plotted versus the corresponding targets for the training data

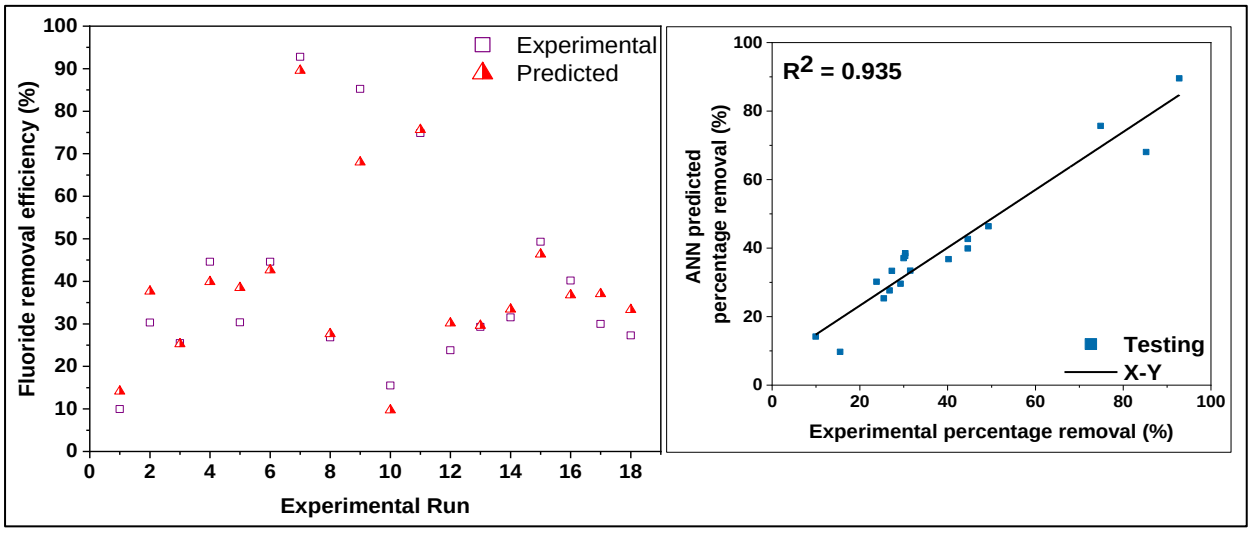

Figure 4-23 The graphical output of the ANN outputs plotted versus the corresponding targets for the testing data

4.18.3 Fuzzy inference system

Structure identification forms an integral part of developing a fuzzy system covering the problem of input-output space partition and the number of rules (Madaeni et al., 2012). To

create a fuzzy model for F^- removal efficiency, pH, contact time, adsorbent dosage, and initial F^- concentration represents the antecedent variables with one, three, three, and three fuzzy subsets, respectively. The output had nine membership functions to account for the distinctive distribution of recorded removal efficiencies. A combination of triangular and trapezoidal membership functions was used in the study to maintain the inclusivity of the range of input parameters represented in Figure 4-24. Sixty-three rules were established to address every discrepancy to map out the trial data adequately. The fuzzy logic-based algorithm was developed using the fuzzy logic toolbox in the Matlab software. The prod and centroid method were used as inference operators and defuzzification methods, respectively. Fuzzy logic as a predictive model was used for this study because of its inherent advantage over the black-box ANN model-- the ability to develop and write rules verbally, emulating human thoughts (Akkurt et al., 2004).

The predicted values for the FIS vs. the actual values for removal efficiencies were plotted in Figures 4-25 and 4-26 for training and testing data, respectively. The correlation obtained were 0.894 and 0.9037 for the training and testing dataset. According to Table 4-16, the fuzzy model predicts the measured data successfully, and its performance is comparable with that of ANNs.

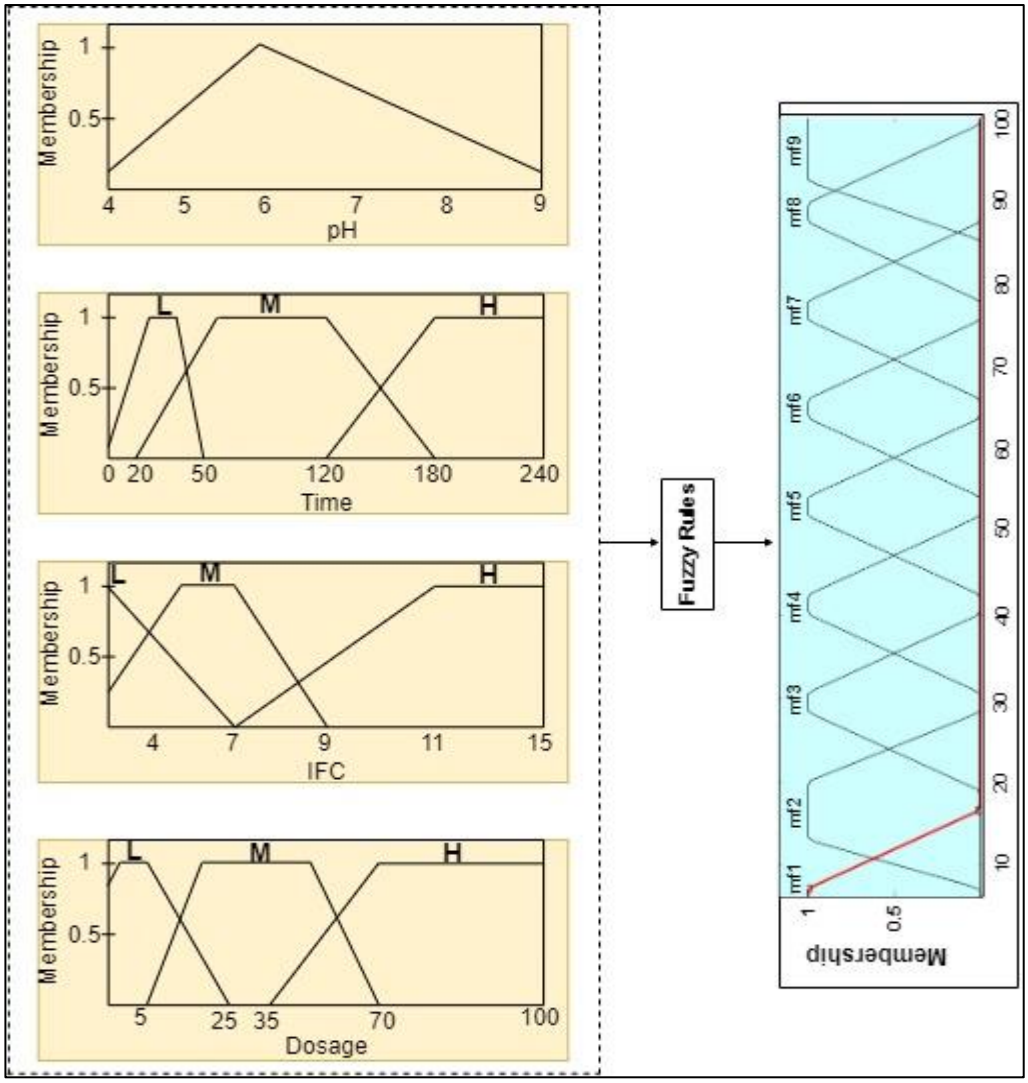

Figure 4-24 Membership functions for input and output parameters used for fuzzy modeling

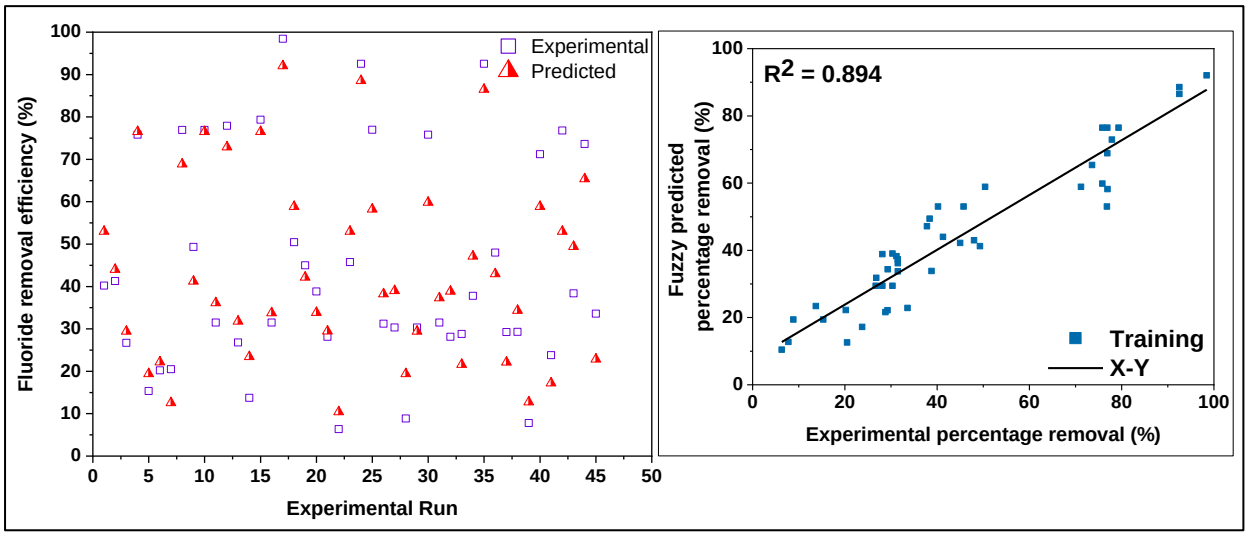

Figure 4-25 The graphical output of the FIS outputs plotted versus the corresponding targets for the training data

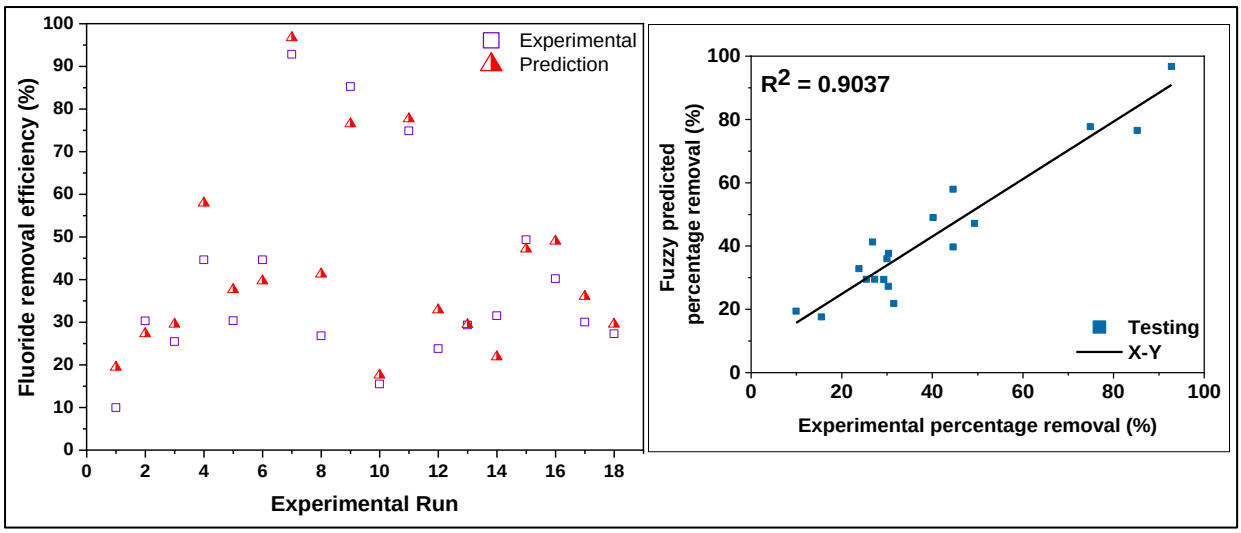

Figure 4-26 The graphical output of the FIS outputs plotted versus the corresponding targets for the testing data

4.19 Statistical error analysis

Eight statistical error functions were evaluated for each model. The functions are SSE, MAE, AARE, MARE, HYBRID, χ^2, and Adj. R^2. R^2 must not be less than 0.8 for reliable correlation involving predicted and experimental values (Joglekar & May, 1987). In general, the statistical results highlighted that both ANN and FIS performed comparatively in modeling the fluoride removal efficiency of Khejri. Madaeni et al. observed a similar pattern when modeling the chemical cleaning of microfiltration membranes (Madaeni et al., 2012). However, on verifying all the statistical errors, ANN was the best-performing model in predicting the accuracy of fluoride removal. Linear regression models were the least effective. With an R^2 value of 0.290, step-wise linear regression was the worst performing.

Although the accuracy of ANN is higher than that of FIS, as shown in Table 4-16, using prior knowledge about the considered system is complex, and explaining the behavior of the ANN system in a specific case is nearly impossible. The FIS model comprises fuzzy rules that, to a greater extent, describe real-world processes. The decreased accuracy of FIS could be attributed to fuzzy logic approximation reasoning and ANN's robust learning method. Furthermore, specialists' understanding of the system significantly impacts FIS model performance. All the predicted data values have been reported in Appendix Table vi.

Table 4-16 Statistical error indices of the studied models

Error Functions	Results					
	1	**2**	**3**	**4**	**5**	**6**
SSE	65589.250	79967.857	90041.586	87838.946	2157.735	4143.585
MAE	27.007	30.072	31.448	30.602	4.181	6.762
AARE	0.632	0.723	0.695	0.651	0.151	0.221
MARE	63.181	72.258	69.505	65.126	15.100	22.156
HYBRID	2054.215	2559.202	2548.638	2420.955	116.017	206.015
χ^2	1211.987	1509.929	1503.697	1428.363	68.450	107.934
R^2	0.312	0.290	0.372	0.354	0.944	0.895
Adj. R^2	0.252	0.228	0.317	0.297	0.939	0.884

1:Simple linear regression, 2: Step-wise linear regression, 3: Simple Non-linear regression, 4: Step-wise non-linear regression, 5: MLP network, 6: Fuzzy Inference system

4.20 Sensitivity Analysis

Modeling is a good alternative for investigating the effects of different parameters on contaminant sequestration efficiency. Since ANN fitted the experimental results efficiently compared to the other models, the developed ANN model was used for further work.

It is essential to assess the input variables' relative importance concerning the output variable, i.e., removal efficiency, wherein four evaluation processes were used. These methods were Garson's equation and connection weights methods depending upon the neural net weight matrix, input perturbation method, and the traditional method based on the possible combination of variables. For the latter, the performance of the groups of one, two, three, and four variables were tested by the optimal ANN network structure (4-10-1) using the LM algorithm.

The weight matrix obtained for the trained ANN model was used for the first two sensitivity analysis methods. Tables 4-17 and 4-18 show the weights obtained between the input and hidden layer; and the hidden and output layer, respectively. The relative importance of the input parameters for Garson's algorithm and connection weight approach is represented in Figure 4-27 and Appendix 1 Table vii. The adsorbent dosage had the most effect on both methods' F^- removal process. In the same vein, IFC came second for both sensitivity analysis methods. However, a certain discrepancy was observed for pH and contact time.

The input parameters were sequentially perturbed at ±5% and ±10% for the perturbation method, aiming to assess the effect of small changes in each input on the neural network output. The algorithm adjusts the input values of one variable while keeping all the others unaffected. The responses of the output variable against each change in the input variable are noted. The input variable whose changes affect the output most is the one with the most relative influence. The effect of this perturbation was monitored by observing the MAE and MSE values obtained after each perturbation (Gevrey et al., 2003). The perturbed effects are shown in Table vii in Appendix 1. From the determined MSE values, the adsorbent dosage is found to have the most effect on the output. For both 5 and 10 % perturbation, the homogeneous sequence of input parameters is followed, i.e., dosage > IFC > contact time > pH.

The fourth sensitivity analysis was based on the possible combination of input parameters taking X1, X2, X3, and X4 as pH, contact time, initial F^- concentration, and adsorbent dosage, respectively, as compiled in Table 4-19. With the least MSE, X4 (dosage) was the most influential variable among the variables. Sensitivity analysis is a critical study to identify the most significant parameter affecting output and guide the design of further experiments. Sensitivity analysis will further aid in improving the practical application of the proposed adsorbent in contaminant removal.

Table 4-17 Weight matrix, weights between input and hidden layers (W1)

Input Variables	Neuron	1	2	3	4	5	6	7	8	9	10
	pH	-1.899	0.057	0.846	1.792	-1.144	-2.86	-1.423	-0.087	-0.396	-1.644
	Contact Time (in minutes)	1.232	-1.373	-1.087	0.262	1.057	1.352	0.207	0.455	1.892	0.12

	Initial Fluoride Concentration (mg/l)	1.108	-0.42	1.3	-2.052	-0.899	1.541	-1.286	0.513	-0.64	-0.928
	Adsorbent Dosage (g/l)	0.486	1.512	-2.073	-0.849	-2.079	-4.57	-2.161	2.751	1.795	1.076

Table 4-18 Weight matrix, weights between hidden and output layers (W2)

Neuron	**1**	**2**	**3**	**4**	**5**	**6**	**7**	**8**	**9**	**10**
Output Variable	-0.453	1.474	-0.409	-0.779	0.138	1.1	0.168	1.336	-0.114	-2.448

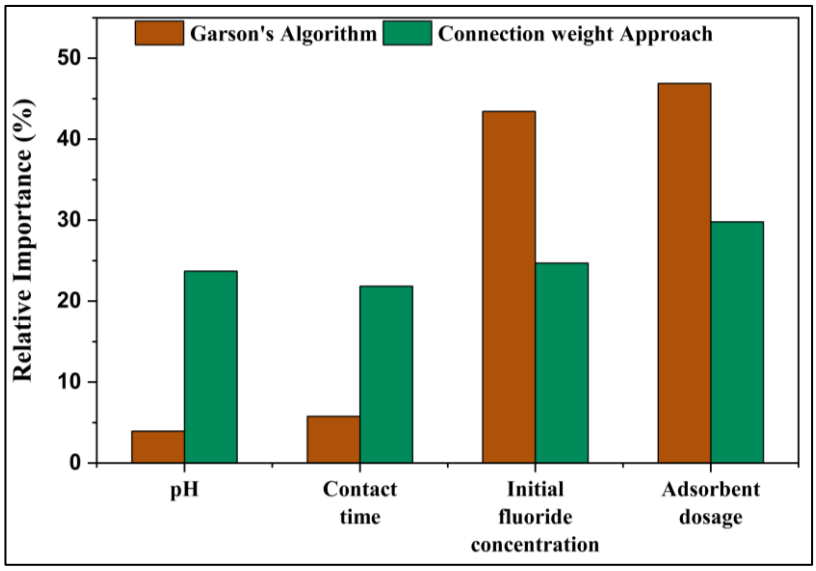

Figure 4-27 Relative importance (RI) of inputs for the predicted removal efficiency using the ANN model using Garson's algorithm and Connection weight approach

Table 4-19 Performance evaluation of combinations of input variables for the LM algorithm with 10 neurons in the hidden layer for sensitivity analysis

Combination	**Mean square error (MSE)**	**Correlation coefficient (R^2)**	**Best linear equation**
X1 (pH)	0.06	0.163	0.17x+0.36
X2 (Time)	0.0417	0.194	0.17x+0.29
X3 (IFC)	0.0588	0.048	0.061x+0.37

X4 (Dosage)	0.0402	0.378*	0.43x+0.23
X1+X2	0.0355	0.288	0.36x+0.26
X1+X3	0.0442	0.291	0.38x+0.32
X1+X4	0.0145	0.708*	0.74x+0.11
X2+X3	0.0479	0.215	0.28x+0.29
X2+X4	0.0306	0.501	0.53x+0.19
X3+X4	0.0244	0.411	0.47x+0.24
X1+X2+X3	0.0339	0.151	0.29x+0.12
X1+X2+X4	0.00753	0.687	0.71x+0.11
X1+X3+X4	0.00296	0.793*	0.87x+0.057
X2+X3+X4	0.0174	0.509	0.58x+0.19
X1+X2+X3+X4	0.000182	0.944*	0.91x+0.049

***Best group performance.**

4.21 Optimization using Genetic Algorithm

GA begins with a population of random solutions, each representing a chromosome. The input variables of pH, time, IFC, and adsorbent dosage are the optimization variables. The fitness function was obtained from the developed BP-ANN model, which can be expressed as follows:

$$F = \text{tansig}\,(JW * \text{tansig}\,(KW * [x1;x2;x3;x4] + b_j) + b_k) \quad (4.24)$$

Where F is the removal efficiency, JW and b_k represent the weight and bias in the output layer, and KW and b_j stand for the weight and bias in the hidden layer, respectively. The GA was developed with the objective of maximization of F- ion removal.

The values of GA-specific parameters used in the optimization technique were as follows: population size = 100, crossover probability = 0.8, and mutation probability = 0.01. The input

ranges were varied to cover every possible physical on-field scenario, and the optimization algorithm was run. Also, some constraints (limitations of the ranges of values for decision variables) were imposed based on practical considerations (dan Suditu et al., 2013). Figure 4-28 represents the optimized values and experimental results. The observed residual error varied from -6.56 to 4.97, confirming the validity of the ANN-GA model. The limitations applied to the simulations are presented in Table viii in Appendix 1.

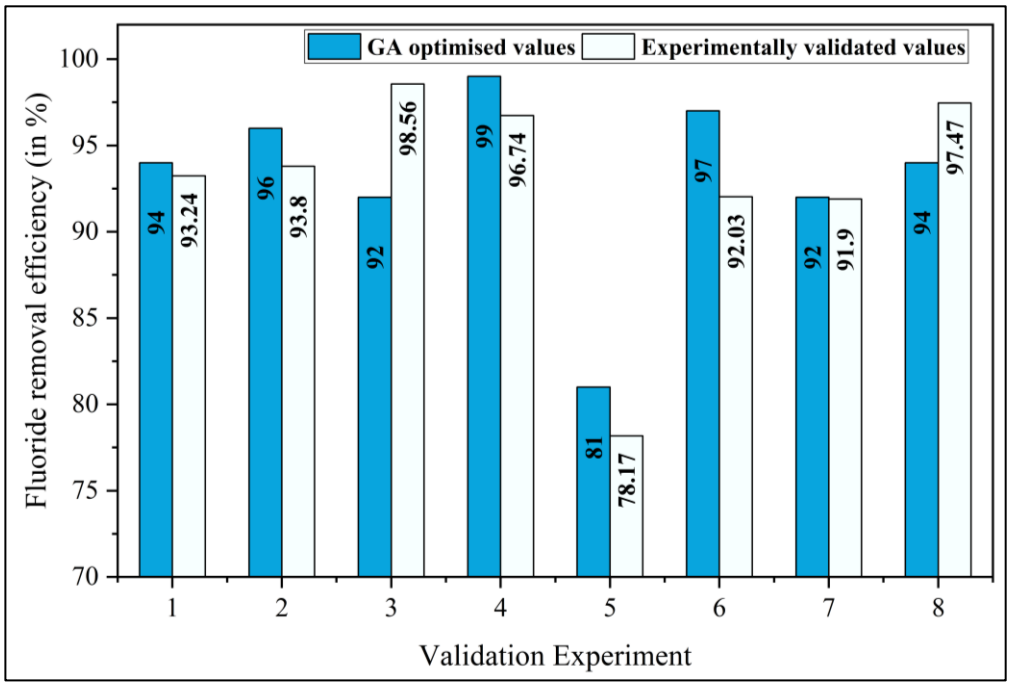

Figure 4-28 Optimization results obtained with limitations imposed on the simulations

Chapter Summary

The novel adsorbent PCC derived from the local fauna of Rajasthan, Khejri, was discussed in detail. With an observed fluoride removal efficiency in synthetic conditions at 79% and for field groundwater samples in the range of 79.7 % to 87 %, Khejri is a suitable agent for contaminant remediation. Further, the complex governing equation among the input and output parameters was successfully modeled with ANN. Sensitivity analysis highlighted the role of adsorbent dosage having a highly positive relation with F^- removal percentage.

With the conclusion derived, other studied adsorbents were evaluated directly in fabricating low-cost water filters. The selected adsorbents were readily available in large quantities at an economically feasible rate.

5 ASSESSMENT OF WATER QUALITY FROM HURDA BLOCK VILLAGES; PREPARATION AND PERFORMANCE EVALUATION OF LOW-COST WATER FILTERS

Chapter Overview

The current chapter starts with the fluoride toxicity evaluation through the health risk assessment paradigm for the state of Rajasthan. For the evaluation process, surveyed data from existing literature was used. To substantiate the data and overview the ground reality, nine villages from the Bhilwara district of Rajasthan were selected for water quality analysis. The results and associated health risks have been evaluated further in the chapter. The fabrication and performance evaluation of low-cost household water treatment systems have been discussed in detail. Cement, clay, ceramic, sugarcane bagasse, potato slurry, and activated carbon have been explored as raw materials. The raw material combinations, fabrication process, void ratio evaluation, and continuous water quality and discharge rate monitoring have been carried out.

5.1 An introduction to Rajasthan

Rajasthan is India's seventh most populous state, with the largest geospatial area at 342,239 km2. Nestled in the northwestern part of the country at a latitude of 27.39º and longitude of 73.43º, the state is divided into seven divisions comprising thirty-three districts. There are four major physiographic regions, namely (i) the western desert with rocky and sandy plains and barren hills; (ii) the mighty Aravalli hills flowing from southwest to north-east; (iii) the eastern lowlands with rich alluvial soils; and (iv) the southeastern plateau.

Three rivers—the Mahi, Chambal, and Banas—drain the state primarily. The climate varies throughout Rajasthan, from hot and dry in the west to humid in the east. On average, winter temperatures range from 8° to 28° C, and summer temperatures range from 32° to 46° C. Average rainfall is unevenly distributed through the state, associated with high risks of crop failure. While the western deserts accumulate about 100 mm (about 4 in) annually, the southeastern part of the state receives 650 mm (26 in) annually. Approximately 90% of rainfall is concentrated primarily through the monsoon, i.e., July through September. Two districts, Jhunjhunu and Bhilwara, were selected for the study. While the groundwater quality analysis was performed for the groundwater sampled from the Hurda block, Bhilwara district, the field

implementation proposed during the study was carried out in the Chirawa tehsil from Jhujhunu district. Nine and four villages were selected from the Bhilwara and Jhunjhunu districts, respectively. The field implementation part of the study covered installing GFRP tanks (described in Chapter 3), distribution of water filters in participatory households, and feedback generation from the four selected villages in Jhunjhunu. The Hurda district is treated in length in later sections, while the Jhunjhunu district is covered in the chapter after that.

5.2 Area of location for on-field water sample collection: Hurda block

The focused study region is the Hurda block of the Bhilwara district, which is located in central Rajasthan (Figure 5-1). The Hurda block comprises 90 villages that account for 80.37 % of the rural population. The Bhilwara district is situated between 25° 01' & 25° 58' North latitude and 74° 01' & 75° 28' East longitude covering a geographical area of 10,455 km^2 and is part of the distinctive Indian semi-arid zone experiencing scorching, dry summers to chilling winters, with the mean, recorded temperature as 26.9°C. The primary occupation of the residents is farming, with tube wells/bore wells supplementing as the principal water source.

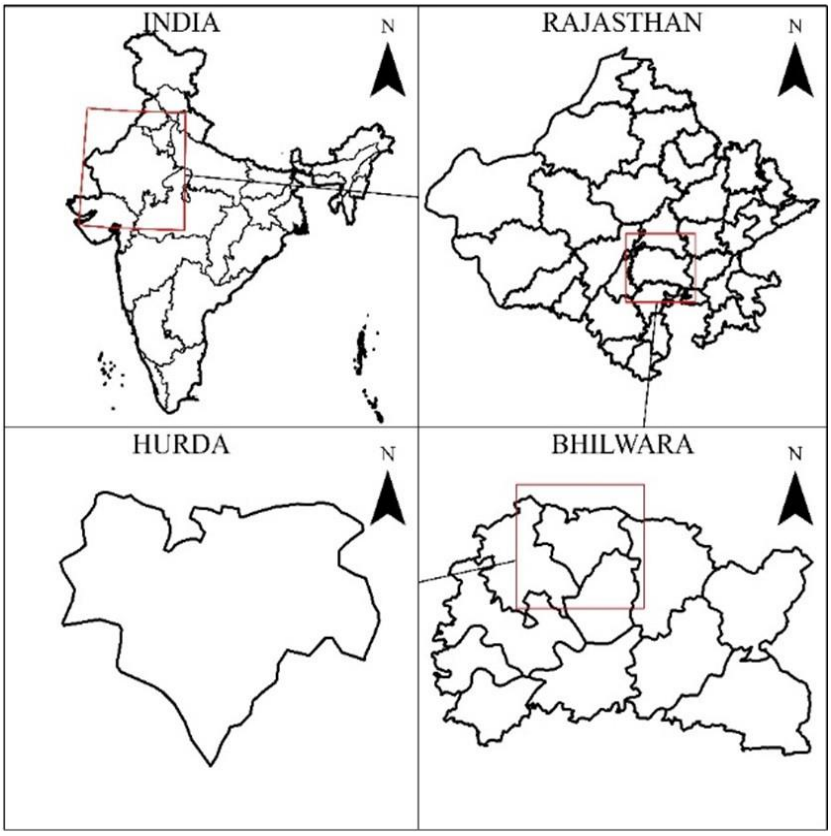

Figure 5-1 Representation of the study area, Hurda block, Bhilwara district, Rajasthan, India

5.2.1 Water sample collection and qualitative assessment

Nine villages—Murayla, Hajiyas, Patiyon ka Khera, Barantiya, Phalamada, Hurda, Balapura, Bharliyas, and Sanodiya—had predetermined well locations from which water samples were taken. During additional discussion throughout the research, the villages are referred to as V1, V2, V3, V4, V5, V6, V7, V8, and V9. The groundwater samples were collected in clean polyethylene and sterilized water storage containers with a capacity of 70 liters with necessary precautions and transported to the Public health engineering laboratory of the BITS Pilani campus for further qualitative analysis.

pH, Total dissolved solids (TDS), Electrical Conductivity (EC), Total Hardness (TH), Chloride (Cl^-), Fluoride (F^-), and Dissolved Oxygen (DO) were measured for the water samples. pH and TDS were measured with the Hi-media Soil analysis kit with specified electrodes. The standard colorimetric titration measured the TH with EDTA solution. Mohr's and Winkler's methods measured the Cl^- and DO concentrations. The F^- in the water sample was analyzed through the Fluoride test kit, with the catalog number 1.14598.0002 obtained from Merck. The test solutions were prepared according to the instructions provided in the kit manual and analyzed in the UV Spectrophotometer. Standard laboratory procedures were implemented to accomplish higher quality assurance. All samples were tested in triplicates, and the mean values were reported. The reagents used were of analytical grade and acquired from Merck.

5.3 Fluoride risk assessment

The risk assessment was carried out following the similar steps discussed in Chapter 3 under the human health risk assessment sub-section.

By multiplying the observed concentration of fluorides by the average daily intake (consumption rate) of water for each age group and dividing it by the corresponding body weight, average daily doses (ADD) of F^- ingestion were computed for various age groups.

The Ingestion Hazard Quotient (IHQ) is used to determine the health risk of a chemical agent and is determined from the ratio of ADD to reference dose (RfD). According to the US EPA's Integrated Risk Information System (IRIS) database, the RfD for F^- in a specific route is 0.06 mg/kg-day. An IHQ value > 1 implies a high potential for detrimental effects on human health and vice versa.

Different age groups have varying body weights, daily water consumption demands, and metabolic rates. Therefore, considering the behavioral and physiological characteristics of inhabiting age groups, the village or study area population is divided into different age categories. Age-based population division thoroughly explains the most affected demographic segment by contamination or toxicity.

In the first application, concerning evaluating fluoride toxicity in Rajasthan, generalized human body weight and water ingestion rate (WIR) were taken for ease of classification. These WIR were used to classify the state of Rajasthan district-wise and obtain ADD and IHQ values. The body weights and water intake values for both genders have been averaged as compiled in Table 5-1 to expedite calculations and reporting,

Table 5-1 Distribution of water intake rates of inhabitants for the statewide calculation of ADD and IHQ

Average age of inhabitants (in years)	Water ingestion rate (in l/day)
≤ 21	2.31
21 ≤ 65	3.51
≥ 65	2.45

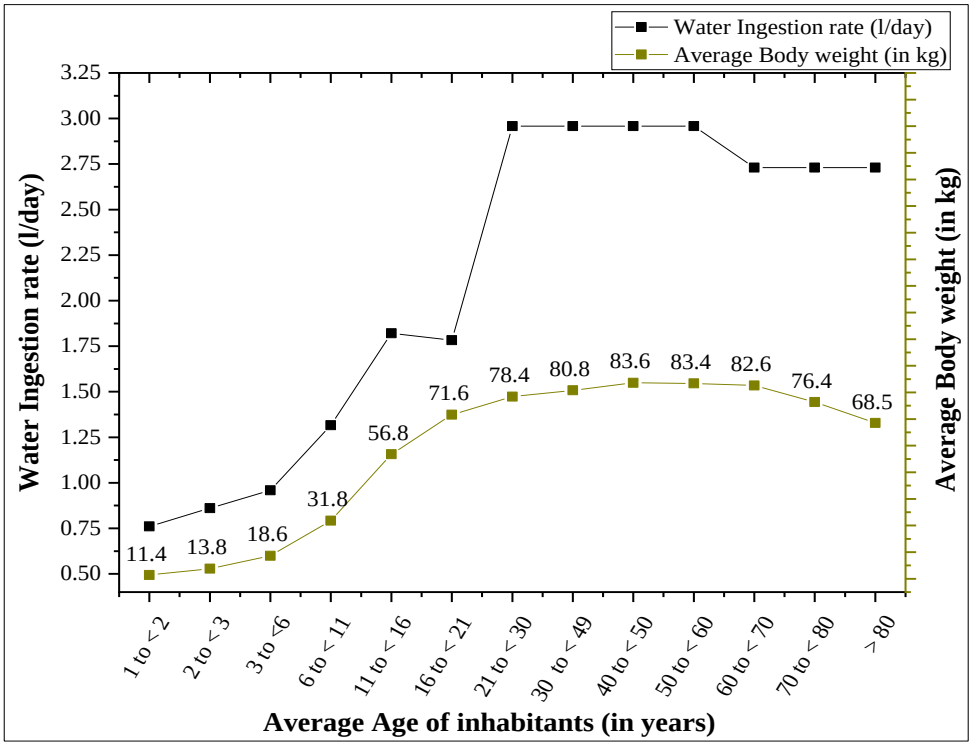

Figure 5-2 Water intake rate and average age versus body weight of inhabitants (taken for Hurda block)

For the second application, i.e., at the study area level, a more pronounced WIR distribution was determined. The participants in the study area were classified into 13 age groups, 1 to < 2, 2 to < 3, 3 to <6, 6 to < 11, 11 to < 16, 16 to < 21, 21 to < 30, 30 to < 40, 40 to < 50, 50 to < 60, 60 to < 70, 70 to < 80, and over 80. Figure 5-2 highlights the WIR of individuals and the average recorded body weight versus the age of the inhabitants in the selected study area. The weight and water ingestion rate obtained were averaged for both genders.

5.4 Filter plate preparation

Two phases make up the filter preparation method: preparation of the adsorbent and filter plate fabrication. The materials required during the study, such as cement, river sand (type 1 and type 2 correspond to two different locations), clay, and ceramic powder, were procured through local vendors. While sugarcane bagasse, sawdust, and potatoes were collected from within the university campus, the coconut-based activated carbon (AC) was procured online. The step-by-step procedure followed for the fabrication of water filters has been represented in Figure 5-3.

5.4.1 Adsorbent preparation

The process involving the adsorbent is described in the following section. As the adsorbent development methodology differs for sugarcane bagasse and potato slurry, two sections have been devoted to the procedures.

5.4.1.1 Sugarcane Bagasse

To remove dirt from the sugarcane bagasse surface, it was thoroughly washed with tap water until clear running water. A final wash was done with distilled water before further treatment. The material was soaked in 0.1N NaOH and 0.1N CH_3COOH solutions for 10 hours each after being thoroughly air-dried for 24 to 48 hours. After adequate washing to remove traces of basic and acidic solution, the material was air-dried for another 24 to 48 hours. The prepared material was heated for 6 hours at 300° C in a muffle furnace to produce the adsorbent. The resulting material was grounded, sieved in a size range of 20–50 mesh ASTM, and subsequently placed in an airtight container for further use.

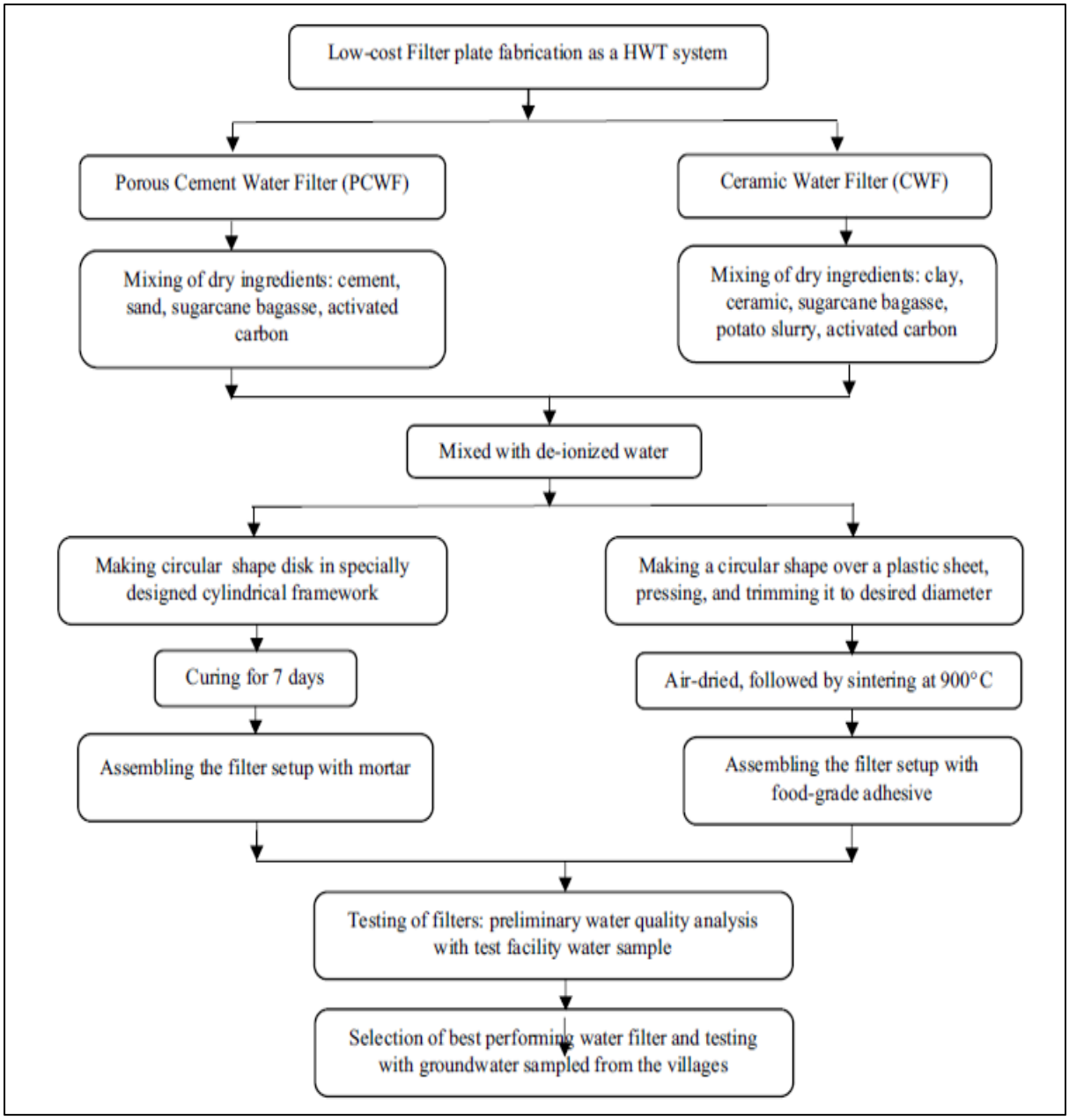

Figure 5-3 Schematic representation of filter preparation procedure

5.4.1.2 Potato Slurry

The potato adsorbent was prepared in the form of a slurry. The potatoes were cleaned thoroughly with running water, diced, and oven-dried at a temperature of 60±2 °C to remove excess moisture. After drying, a potato slurry was prepared by grinding the chopped potatoes. The slurry was suspended in distilled water in a beaker, followed by gentle heating and holding at 55-60°C for 24 hours (Singh, 2017). The prepared slurry was then allowed to cool to room temperature before fabricating filters.

5.4.2 Filter plate preparation

The first step was to mix raw materials in varying proportions, as shown in Table 5-2. Following preliminary testing (by varying the shapes of the filters) with underwhelming results, the filter was designed in a cylindrical shape with a diameter of 25 cm and a thickness of 1 cm for ceramic filters and 1.5 cm for cement filters.

For the Ceramic Water Filter (CWF), clay and ceramic powder were mixed with sugarcane bagasse, sawdust, and potato slurry. Upon combining the raw materials, distilled water was added to the dry mix to create a paste, subsequently pressed to the desired dimensions, and allowed to air-dry before firing in the kiln at 900°C. After discarding damaged filters, the prepared CWFs were soaked in test water (laboratory water), followed by thorough air drying to ensure complete saturation.

The PCWF followed the route of dry and wet mixing, air drying, and curing. The raw materials were weighed to the nearest 0.1 gm and mixed in a tray, followed by the addition of distilled water. Once the fresh batch of cement paste was prepared, a hollow cylindrical steel frame was used to give the required proportions to the plates. After air-drying for 48 hours, the PCWFs were released from the molds/ framework and cured for 7 days (in laboratory water). The schematic representation of the filter assembly is shown in Figure 5-4.

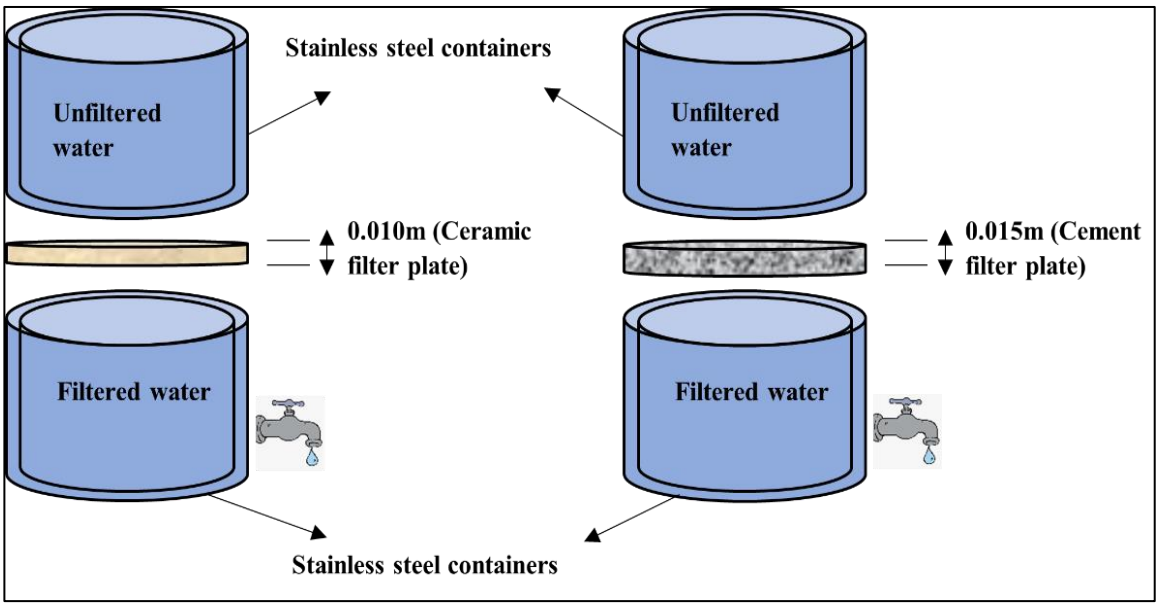

Figure 5-4 Filter setup assembly

Table 5-2 Raw material combination of different plates and given nomenclature

Materials	Weight Combination of raw materials (all values are in grams)							
	Plate Nomenclature							
	Plate 1	Plate 2	Plate 3	Plate 4	Plate 5	Plate 6	Plate 7	Plate 8
Cement	200	180	170	180	-	-	-	-
River sand (location 1)	360	1080	700	360	-	-	-	-
River sand (location 2)	720	-	350	720	-	-	-	-
Sugarcane bagasse	30	50	50	50	-	-	55	50
Sawdust	-	-	-	-	-	20	30	25
Potato gel	-	-	-	-	250	150	-	-
Activated carbon	40	-	40	-	-	-	-	-
Water	140	140	140	140	-	110	210	220
Clay	-	-	-	-	400	350	300	300
Ceramic	-	-	-	-	400	150	200	170

5.4.3 Filter Setup Assembly

Following the fabrication of the water filter plates, the next stage was to assemble the filtering apparatus or HWT system. As represented schematically in Figure 5-4, the system comprises two steel water storage containers with filter plates attached in between. A local merchant provided the steel containers with a 30-liter capacity. A 23 to 24-cm diameter round aperture was cut into the container's base. All the cutting work was completed in the Institute Workshop. To ensure proper adhesion, mortar and food-grade adhesive were used for the cement and ceramic plates, respectively. While the cement plates were mortared to the steel container and left to dry for 48 hours, a food-grade adhesive was used to adhere the ceramic plates to the containers. All the filters were air-dried until complete curing of the selected adhesive.

5.4.4 Water quality monitoring for filter performance evaluation

After assembling all the filter components, water from the testing facility (predetermined quality) was passed through the water filters, both CWF and PCWF. The filters were tested for 30 days continuously to test the passing water quality and performance of the fabricated plates. The study's findings are the averages of six pieces of each filter combination. Flow rate/discharge, pH, TDS, EC, Hardness, Cl^-, and F^- concentrations were monitored.

Following the initial water quality analyses, the best filter was identified (with a primary focus on higher F^- removal efficiency and sufficient flow rate). The chosen water filter was subsequently reproduced and tested with the nine village water samples collected from the Hurda block for 7 continuous days.

5.4.5 Economic Estimation

Costing is a significant step in the economic assessment of water-related undertakings and is used by decision-makers and users in selecting solutions to implement and adopt, respectively (Jagals & Rietveld, 2011). The cost of all the raw materials, including transportation charges, was included in the analysis. Cement, sand, clay, and ceramic prices were estimated per bag, whereas sugarcane bagasse, sawdust, and activated carbon costs were calculated per kilogram. The material composition, including energy, water, and sintering expenses, determined the plates' price.

5.5 Fluoride concentration and risk assessment of Rajasthan district-wise

Choubisa compiled a comprehensive dataset using previous literature on reported water quality from various villages, taluks, and rural centers in Rajasthan (Choubisa, 2018). Thereof, a single fluoride value was imitated by considering an average of all the reported and gathered data. Several districts had reported fluoride concentrations greater than 10 mg/l. For such specific cases, the average recorded fluoride concentration was derived using the highest reported fluoride concentration and the number of locations. When an average fluoride concentration was given for a district, the quoted number was assumed to be spread evenly across the district and accepted without modification.

As is seen in Figure 5-5, the calculated IHQ is greater than 1 for all districts except the eight districts falling under the highlighted red line of 1. It is further witnessed that children and young adults in the age group of ≤ 21 are the most affected by the high fluoride concentrations in drinking water. Table ix in Appendix 1 presents the calculated ADD and IHQ values for all the districts.

In Figure 5-6, the districts are classified into severity zones, i.e., low, medium, and severe. The districts classified into low, medium, and severe risk zones are 4, 21, and 8, respectively, for the age classification ≤ 21 years. For the age groups of 21 ≤ 65 and ≥ 65, the frequency of districts in the three severity classes are 7, 20, and 6, and 9, 22, and 2, respectively.

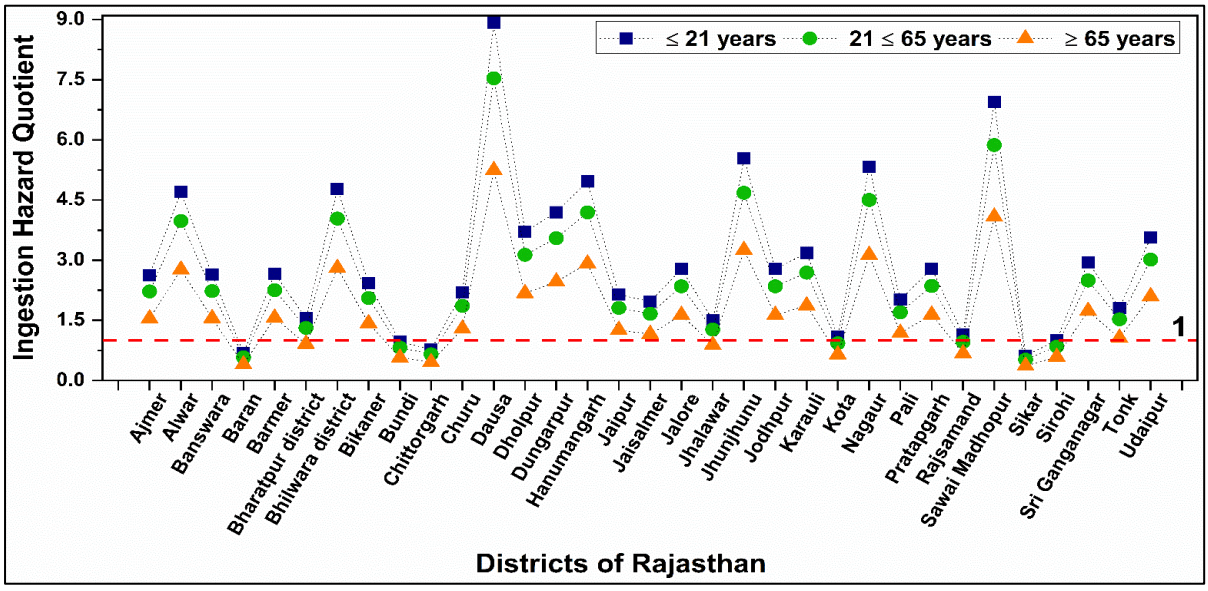

Figure 5-5 Ingestion Hazard Quotient for all the 33 districts of Rajasthan

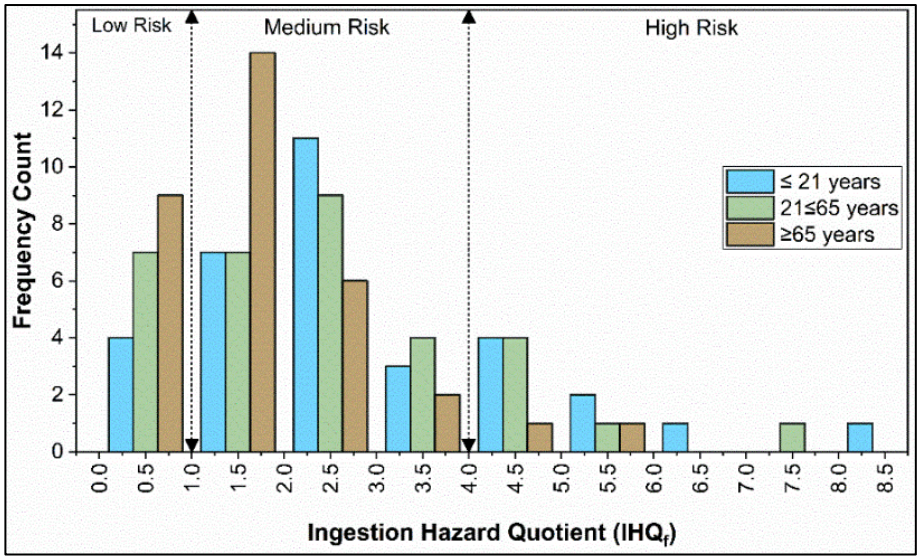

Figure 5-6 Classification of districts into risk zones for three different age groups

There have been reported cases of fluorosis from selected villages from the southern districts of Banswara, Dungarpur, and Udaipur (Choubisa, 2001). Suthar et al. studied the northern district of Hanumangarh for fluoride concentrations in the groundwater. The fluoride reportedly ranged from 1.01 to 4.78 mg/l averaging over 2.82 mg/l (Suthar *et al.*, 2008). Hussain et al. analyzed water samples of 1030 villages from central Rajasthan from nine tehsils: Asind, Banera, Bhilwara, Hurda, Mandal, Raipur, Sahara, Shahpura, Kotri from Bhilwara district (Hussain, Hussain and Sharma, 2010). While seven hundred fifty-six (73.4%) villages reportedly had fluoride concentrations above 1.0 mg/l, sixty or 5.83% of villages have fluoride concentrations above 5.0 mg/l, with 24 villages belonging to the Shahpura tehsil.

In a separate study undertaken in Pokhran, the fluoride concentration in water samples varied between 0.76–4.74 mg/L with a mean reported value of 2.19 mg/L. It was observed that while 87.50% of the samples exceeded the maximum desirable limit of BIS (Bureau of Indian Standards), nearly 62.5% of the samples exceeded the maximum desirable limit of WHO thresholds (Singh *et al.*, 2011). Hussain et al. studied fluoride concentrations from 121 habitations from Bhilwara tehsil in the district of Bhilwara. With fluoride concentrations varying between 0.5 to 5.8 mg/l, fifty-eight percent of the inhabitants of the villages were under the threat of fluorosis (Hussain et al., 2013). Individuals were found to suffer from dental and skeletal fluorosis.

The problem of fluorosis in the state has been known for a long time. Previous studies corroborate our state-wide data analysis of fluoride toxicity (Agrawal et al., 1997). The maximum summer temperatures reach 48°C in the state, primarily for having a hot and dry

climate, indicating a higher water ingestion rate. A higher water ingestion rate is directly correlated to an increased probability of fluorosis in areas with higher fluoride concentrations. After compiling and evaluating the data from the literature, an urgent need to take ameliorative steps in this region on a war footing to prevent the population, primarily rural, from consuming fluoride-contaminated water is indisputable.

5.6 Water quality analysis of the Hurda block, Bhilwara district

The descriptive statistics of the analyzed water samples are represented in Table 5-3. Table x in Appendix 1 shows the village water quality recorded. The TDS and EC values observed within the researched area ranged from 249 to 1994 mg/l and 470 to 3950 μS/cm, respectively. Only sample V2 had a TDS value exceeding the WHO's permissible value. The average TDS value was 723.9 mg/l, while the average EC value was 1510 μS/cm. EC levels were detected above WHO-prescribed values of 400 μS/cm in 77.78% of the water sample. EC's high readings have been accounted for due to increased applications of agrochemicals, sediment dissolution, and over-exploitation of groundwater resources (Central Ground Water Board, 2013). High conductivity in the groundwater makes the area unsuitable for non-salt tolerance crops.

Recorded Cl^- concentrations ranged from 72.98 mg/l to 1679.48 mg/l, averaging 462.63 mg/l. Cl^- levels were higher than the WHO and BIS tolerance levels of 250 mg/l in 66.67% of the samples analyzed. Excessive industrial and commercial operations, notably textile manufacturing, are to blame for these zones' elevated Cl^- levels (Hussain et al., 2010).

Several academics have used Pearson's correlation analysis to assess the relativeness of different water quality parameters studied. Table 5-4 shows that the data acquired acts as a proportionate measure to depict the relationship between various factors. A weak association indicates a correlation coefficient (r) of less than 0.3. However, if the r-value is between 0.3 and 0.7, the association is deemed moderate, and if it is larger than 0.7, the relationship is termed strong (Xiao et al., 2015). The correlation between TDS, EC, and Cl^- is highly positive. The r values for the EC and TDS, EC and Cl^-, and TDS and Cl^-, respectively, are 0.997, 0.991, and 0.992. Kothari et al. reported a moderate positive correlation between TDS and Cl^- (r – 0.7). The recorded hardness levels ranged from 612 (V3) to 2456 (V2) mg/l. All the studied villages had hardness values beyond the permissible limits. Further, TDS exhibited a significant positive linear correlation with hardness (r – 0.844), similar to a trend reported by Kothari et al. (Kothari et al., 2021).

The observed turbidity ranges from 0 to 5 NTU, with an average of 2.4 NTU. It was observed that V6 had recorded turbidity above the WHO threshold. The pH ranged from 7.9 to 8.9, averaging over 8.48. While 22.22% of samples had pH values over the permissible range of 8.5, 33.33% of samples corresponding to V1, V6, and V9 had pH values well within the permissible upper limit. While turbidity exhibited a modestly good correlation with TDS and EC with r values of 0.363 and 0.343, a negative relationship between turbidity and pH was emphasized by an r-value of -0.405. Except for DO, all factors were inversely linked with pH.

The DO recorded the highest and lowest value at 7.8 and 5.2 mg/l, with a mean of 6.3 mg/l. Though no limits are prescribed for DO concerning human consumption, the reported DO limits are well within the standard prescribed (4 to 6 mg/l).

Figure 5-7 shows the frequency distribution of recorded F^- levels, ranging from 1.6 to 2.6 mg/l. As the prescribed threshold for F^- is 1.5 mg/l according to WHO and BIS allowance, 100% of village samples had recorded F^- concentrations above 1.5 mg/l, highlighting a worrying situation. High F^- levels suggest that inhabitants are at increased risk of fluorosis from continuous water consumption.

F^- exhibited a weak negative relationship with pH and a moderate negative relation with TDS. This study observed an exception, as groundwater with high F^- concentrations are broadly in the pH range of 7.31 – 7.88 (Sun et al., 2019). Telangana had shown a similar tendency of negative correlations between F^- and EC and F^- and TDS (Dasaiah et al., 2020).

Table 5-3 Descriptive statistics of analyzed water samples (Nd = 9 from 9 different locations)

Parameters	Minimum	Maximum	Mean	SD	Q1	Q3	WHO (2017) standards	IS 10500: 2012
pH	7.86	8.93	8.48	0.3	8.3	8.7	6.5 - 8.5	6.5-8.5
TDS (mg/l)	249.0	1994.0	723.9	510.2	481.0	804.5	1000.0	2000.0
Conductivity (µS/cm)	470.0	3950.0	1510.0	336.2	1008.7	995.0	1000.0	800.0
Turbidity (NTU)	0.0	5.0	2.4	1.7	1.0	4.0	5.0	5.0

Hardness (mg/l)	612	2456	1293	583.84	738	1764	500.0	600.0
Chloride (mg/l)	72.98	1679.48	462.63	462.94	174.94	538.83	250.0	250.0
Fluoride (mg/l)	1.6	2.6	2.2	0.3	1.9	2.5	1-1.5	1-1.5
DO (mg/l)	5.2	7.8	6.3	1.0	5.5	7.4	-	-

Table 5-4 Parameter correlation of water quality parameters

	pH	**TDS**	**Conductivity**	**Turbidity**	**Hardness**	**Cl-**	**F-**	**DO**
pH	1							
TDS	-.041	1						
Conductivity	-.026	.997**	1					
Turbidity	-.405	.363	.343	1				
Hardness	-.105	.844**	.858**	.560	1			
Cl-	-.059	.992**	.991**	.358	.872**	1		
F-	-.161	-.414	-.369	-.100	-.343	-.451	1	
DO	.392	.423	.436	-.341	.072	.395	.005	1

****. Correlation is significant at the 0.01 level (2-tailed).**

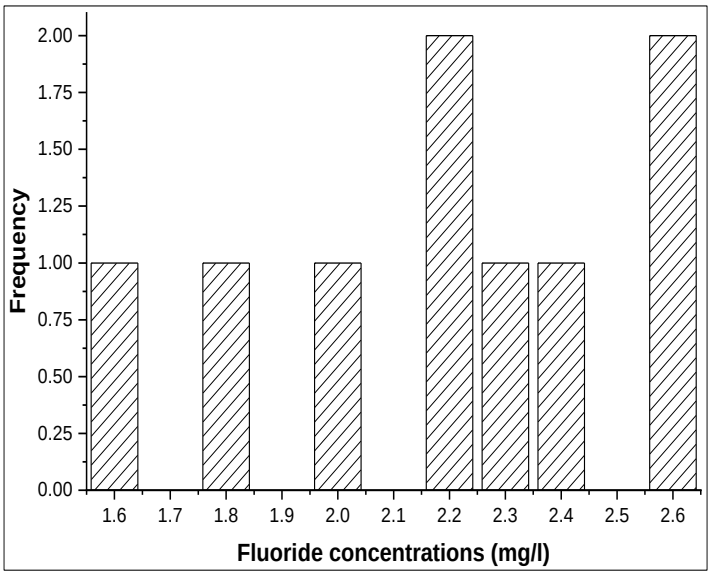

Figure 5-7 Frequency distribution of Fluoride in the study area of Hurda

5.6.1 Fluoride Risk Assessment for Hurda block

The average daily dose (ADD) and ingestion hazard quotient (IHQ) values associated with obtained F^- concentration in the thirteen age classifications were evaluated, integrating the indicators obtained from the US EPA Exposure Factor Handbook (United States Environmental Protection Agency, 2011) and determined F^- concentrations. The mean ADD calculated values are shown in Table 5-5. The mean ADD values for the age group 1 to <2 across the nine villages were 145.93 mg/kg-bw/day, with a standard deviation of 21.42 mg/kg-bw/day. Furthermore, for the age group of 2 to <3 and 3 to <6, the mean and standard deviation of calculated ADD were 136.57 and 20.04 mg/kg-bw/day and 112.86 and 16.56 mg/kg-bw/day, respectively. The mean values of ADD across the remaining age brackets of 6 to < 11, 11 to < 16, 16 to < 21, 21 to < 30, 30 to < 49, 40 to < 50, 50 to < 60, 60 to < 70, 70 to < 80, > 80 were 90.58, 70.18, 54.51, 82.59, 80.13, 77.45, 77.63, 72.34, 78.22, and 87.24 mg/kg-bw/day. Similarly, the SD of the calculated ADD was 13.29, 10.29, 8.0, 12.12, 11.76, 11.36, 11.39, 10.62, 11.48, and 12.8 mg/kg-bw/day over the sampled villages through V1 to V9.

Further observations after computing the IHQ values in Table 5-6 revealed that for the age classification of 1 to <2 years, 100% of the sampled sites were above the permitted threshold as the IHQ values were greater than 1. Similarly, for age brackets 2 to<3, 3 to <6, and 6 to <11, calculated IHQ values exceed 1, as shown in Figure 5-8. The conclusion highlighted that children for ages <11 are more prone to suffer from health complications associated with consuming water laden with high F^- concentrations.

Adults between the ages of 21 and 30 and above 80 had unacceptable IHQ levels for all the studied regions. At the same time, 77.8% of the studied locations had IHQ limits more than 1 for age groups 11 to <16 and 60 to <70, and only 33% of observations for young people aged 16 to 21 had IHQ greater than 1. Approximately 88.9% of the modeled exposures had an IHQ value beyond the permissible range. Despite age classifications 11 to <16, 16 to <21, and 60 to <70 having overall low percentage risks, it was observed that for specific studied locations, higher risks were observed across all age classifications. The positive correlation between higher IHQ values and places with greater F^- concentrations identified the explicit requirement for considerable water treatment.

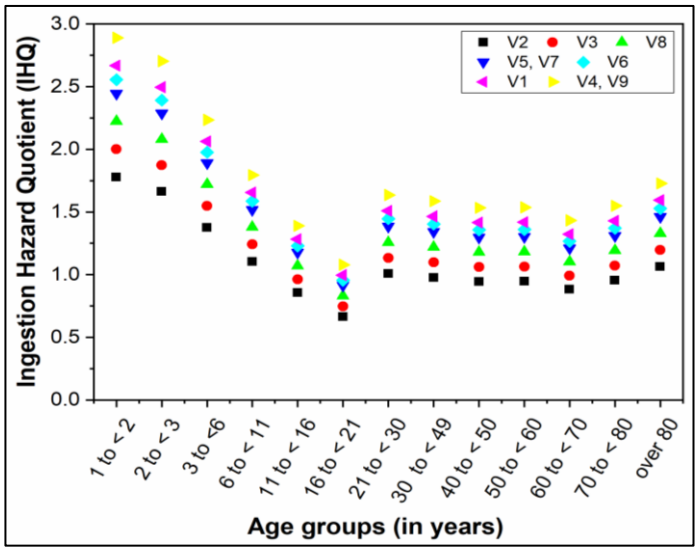

Figure 5-8 IHQ for fluoride values calculated for the study area's inhabitants (Hurda)

Table 5-5 Average daily doses via ingestion pathway (ADD) for different age classification for Hurda block

	Village Id	V1	V2	V3	V4	V5	V6	V7	V8	V9
	1 to < 2	160.00	106.67	120.00	173.33	146.67	153.33	146.67	133.33	173.33
	2 to < 3	149.74	99.83	112.30	162.22	137.26	143.50	137.26	124.78	162.22
	3 to <6	123.74	82.49	92.81	134.05	113.43	118.59	113.43	103.12	134.05
	6 to < 11	99.32	66.21	74.49	107.60	91.04	95.18	91.04	82.77	107.60
	11 to < 16	76.94	51.30	57.71	83.36	70.53	73.74	70.53	64.12	83.36

ADD values for different age groups	16 to < 21	59.77	39.84	44.82	64.75	54.78	57.28	54.78	49.80	64.75
	21 to < 30	90.55	60.37	67.91	98.10	83.01	86.78	83.01	75.46	98.10
	30 to < 49	87.86	58.57	65.90	95.18	80.54	84.20	80.54	73.22	95.18
	40 to < 50	84.92	56.61	63.69	92.00	77.84	81.38	77.84	70.77	92.00
	50 to < 60	85.12	56.75	63.84	92.22	78.03	81.58	78.03	70.94	92.22
	60 to < 70	79.32	52.88	59.49	85.93	72.71	76.02	72.71	66.10	85.93
	70 to < 80	85.76	57.17	64.32	92.91	78.61	82.19	78.61	71.47	92.91
	over 80	95.65	63.77	71.74	103.62	87.68	91.66	87.68	79.71	103.62

Table 5-6 Ingestion hazard quotient (IHQ) via ingestion pathway for different age classification for Hurda block

	Village Id	**V1**	**V2**	**V3**	**V4**	**V5**	**V6**	**V7**	**V8**	**V9**
IHQ values for the different age groups through the ingestion pathway	1 to < 2	2.67	1.78	2.00	2.89	2.44	2.56	2.44	2.22	2.89
	2 to < 3	2.50	1.66	1.87	2.70	2.29	2.39	2.29	2.08	2.70
	3 to <6	2.06	1.37	1.55	2.23	1.89	1.98	1.89	1.72	2.23
	6 to < 11	1.66	1.10	1.24	1.79	1.52	1.59	1.52	1.38	1.79
	11 to < 16	1.28	0.85	0.96	1.39	1.18	1.23	1.18	1.07	1.39
	16 to < 21	1.00	0.66	0.75	1.08	0.91	0.95	0.91	0.83	1.08
	21 to < 30	1.51	1.01	1.13	1.63	1.38	1.45	1.38	1.26	1.63
	30 to < 49	1.46	0.98	1.10	1.59	1.34	1.40	1.34	1.22	1.59
	40 to < 50	1.42	0.94	1.06	1.53	1.30	1.36	1.30	1.18	1.53
	50 to < 60	1.42	0.95	1.06	1.54	1.30	1.36	1.30	1.18	1.54

	60 to < 70	1.32	0.88	0.99	1.43	1.21	1.27	1.21	1.10	1.43
	70 to < 80	1.43	0.95	1.07	1.55	1.31	1.37	1.31	1.19	1.55
	over 80	1.59	1.06	1.20	1.73	1.46	1.53	1.46	1.33	1.73

5.7 Results covering the Preparation of low-cost household water filters for fluoride remediation

This sub-section has reported a detailed discussion regarding the low-cost HWTs' performance. The material composition of the proposed filters, and void ratio calculations, including economic evaluation, have been covered in the subsequent sections.

5.7.1 Total void ratio measurement of the filter plates

The total void ratio for the filter plate was obtained by first determining the difference in weight (W1) of the filter specimen in water and that measured (W2) following air-drying for 24 hours, followed by dividing the difference by the specimen volume (Park & Tia, 2004). The following equation is used to obtain the value.

$$A = 1 - \left(\frac{(W2-W1)/\rho w}{V1}\right) * 100 \quad (5.1)$$

Where, A = total void ratio of the filter plate (in %), W1 = underwater weight of the filter specimen (in gm), W2= weight of filter specimen dried in air for 24 hr. (in gm), V1 = specimen volume (in cm^3), ρw = density of water (g/cm^3). The reported void ratio is tabulated in Table 5-7.

Table 5-7 Void ratio and properties of filter plates extracted from SEM images

Plate Id	Plate 1	Plate 2	Plate 3	Plate 4	Plate 5	Plate 6	Plate 7	Plate 8
Void ratio (%)	17.502	17.949	38.585	32.278	8.922	11.091	14.852	30.892
Porosity (ratio)	0.282	0.189	0.165	0.215	0.157	0.133	0.259	0.245
Average pore radius (micron)	0.712	1.432	0.423	0.132	0.013	0.066	0.298	0.256

Standard deviation of pore size (micron)	0.5849	0.9239	0.265	0.0882	0.0107	0.0683	0.2472	0.1868

Plates 1 to 4 show a higher void ratio value due to the inherent property of the raw material used. However, plates 5 and 6 have a lower void ratio as potato gel was used as the filler material. While plate 6 had 4.2% of sugarcane in addition to potato gel showing a higher percentage, plate 5 had a single filler material. Plates 7 and 8 had a higher ratio due to increased filler material. The discrepancy observed in the void ratio is credited to poor manufacturing.

5.7.2 Pore size distribution of the filter plates

MATLAB analysis estimated the membrane filters' pore size distribution from the SEM images (Figures 5-9 and 5-10). The Watershed algorithm was used for porous space segmenting. It was assumed that the darker spaces on the filter surface represent voids for water filtration in the captured images.

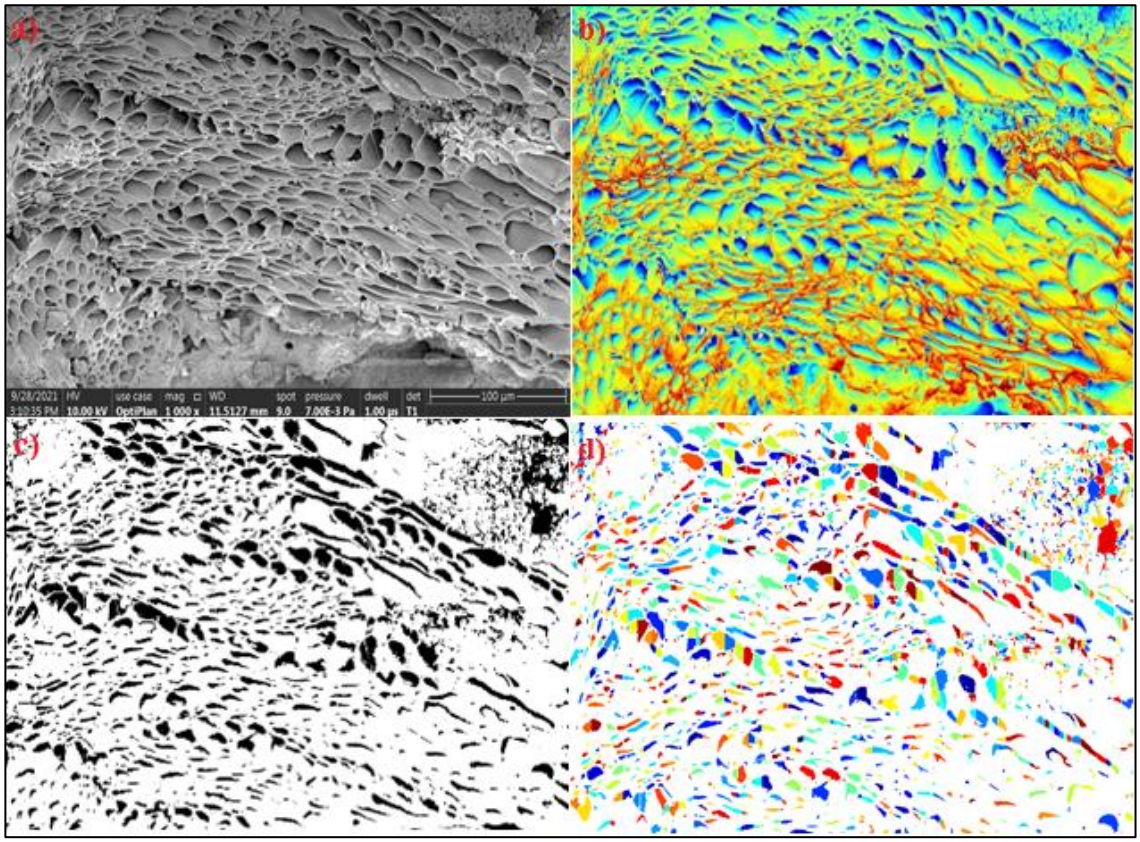

Figure 5-9 Different steps involved in image analysis for detecting and measuring the porous spaces for porous concrete filter plates: a) SEM image of filter plate, b) Intensity map of the image, c) Detected porous space, d) Segmented porous space

After image processing, the average and standard deviation of the pore size and porosity were calculated. The porosity of the filter plate is obtained by dividing the total porous area over the entire filter area, assuming 3-D porosity equals 2-D porosity. Furthermore, it was observed that the average pore size and the standard deviation of the pore size distribution have a linear connection, meaning that the variance of pore sizes is greater for more permeable samples (Rabbani & Salehi, 2017).

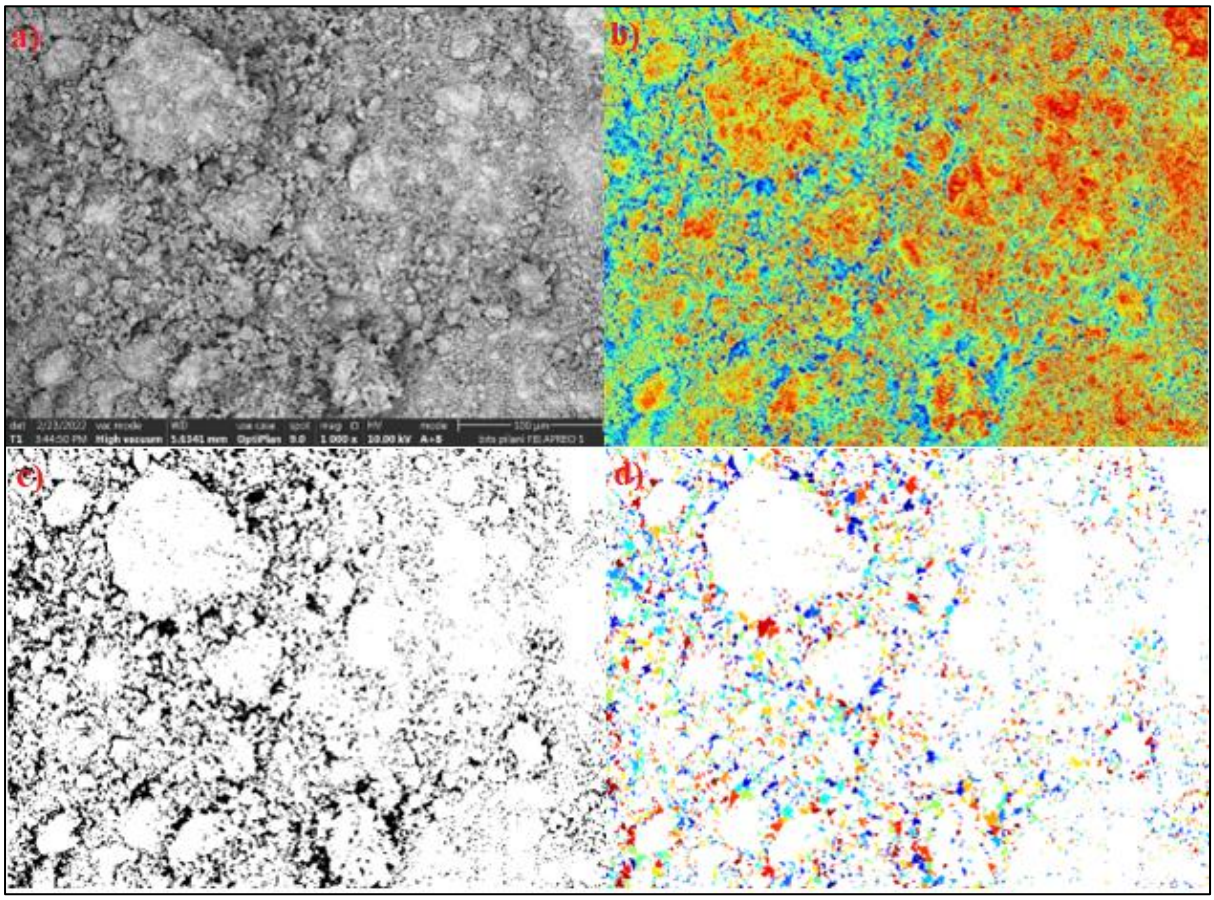

Figure 5-10 Different steps involved in image analysis for detecting and measuring the porous spaces for ceramic filter plates: a) SEM image of filter plate, b) Intensity map of the image, c) Detected porous space, d) Segmented porous space

5.7.3 Performance evaluation of filter plates

A total of 48 filter plates were tested—six plates each of the 8 combinations of raw materials. The filter assemblies were evaluated continuously for 30 days. The water in the testing laboratory was used to evaluate the prepared filter's effectiveness. The quality of the same has been reported in Table 5-8.

Table 5-8 Water quality recorded for the testing waters

Parameters	pH	TDS (mg/l)	EC (µS/cm)	Turbidity (NTU)	Hardness (mg/l)	Cl^- (mg/l)	F^- (mg/l)
Recorded values	8.36	705	1320	0	232	224.93	1.7

The flow rate or discharge is a determining factor when assessing a filter's effectiveness. It is measured by tracking the water passing through the filter plate for a fixed duration. Three liters of water samples were poured into the filter assembly's upper compartment. The water collected in the bottom chamber was volumetrically measured to determine discharge, followed by quality assessment for pH, TDS, EC, Hardness, and Cl^-, the significant being F^-. While few filters showed reduced discharge after 7 to 8 days, others performed effectively for the complete test duration. A possibility for reduced water flow through filters is the accumulation of colloidal particles (Yusuf & Murtala, 2020). The plates were softly washed with clean water and a brush to eliminate salt buildup once the discharge had been reduced significantly. The testing was then resumed, with the filter assembly being refilled with water. Specimens that failed to provide sufficient discharge were discarded. For some combinations, several plates cracked during the experiments. For such occurrences, the entire composite was eliminated if the proportion of fractured plates reached 50% more than those tested per group ($n \geq 4$).

The data curated for the water filters have been compiled from Tables 5-9 to 5-16, each table corresponding to a selected material composition.

For combination 6, 66.67% of plates cracked over the test duration. Therefore, the entire combination was discarded for further evaluation. Although 33.33% ($n = 2$) of the filter disks for combination 7 had fractures, these flaws were insignificant. The combination 8 plate, however, was entirely damaged even though just 16.67% ($n = 1$) of the plate had cracks. The ceramic plate's decreased strength possibly resulted from improper sintering.

The maximum and minimum values for each parameter provided a broad overview of the functionality of the filter plates. The most effectively performing filter was identified by the estimated mean. The best-performing filters were chosen from the observed averages, aiding our study's narrow focus on F- removal. Among the cement filter plates, the mean discharge from plate 3 was 1.17 l/hr, followed by plates 4, 2, and 1 at 0.83, 0.63, and 0.561 l/hr, respectively. The mean recorded discharges from the ceramic plates were lower than the cement filters. Combination 5 had the lowest flow rate among the ceramic filters at 0.034 l/hr.

In the following order, combinations 8, 7, and 6 had discharge at 0.391, 0.131, and 0.103 l/hr, respectively.

With pH values of 11.76 and 11.03, respectively, plates 3 and 4 surpassed the WHO standard. The pH recorded for plates 1 and 2, 8.458 and 8.43, lies within the range of 6.5 to 8.5. On the other hand, the mean recorded values for the ceramic plates lay within the acceptable ranges for all the plates standing at 8.123, 8.125, and 8.095 for plates 5, 7, and 8, respectively.

Plates 1,2,3, and 7 had TDS values well below the permissible limit of Indian standards but higher than the acceptable value by 58.46%, 68.83%, 85.66%, and 86.1%, respectively. The TDS values for Plates 4, 5, and 8 were relatively high (>1000 mg/l). As per standards, EC consistently exceeded the recommended 1000 and 800 μS/cm values for all fabricated specimens. However, Plates 1 and 5 performed better than the remaining plates, with 1620 and 1561.67 μS/cm recorded EC values.

The observed hardness for plate 2 averaged 160 mg/l, which was still well below the permitted limit of 200 mg/l. The hardness value was consistently higher for the remaining plates. While plate 3's maximum and minimum values ranged from 508 to 120 mg/l, plate 1's maximum and minimum values ranged from 460 to 284 mg/l. The maximum hardness value reported for plates 1, 5, 7, and 8 was 460, 376, 380, and 312 mg/l, respectively, below the allowed limit of 600 mg/l as per Indian regulations. With a 76% reduction in hardness throughout the test, combination 3 performed noticeably better.

The Cl^- values for the cement plates were above the acceptable limit of 250 mg/l but much below the permissible limit of 1000 mg/l, indicating that the water was safe to drink. Plate 6 performed substantially better than the other ceramic plates during the test, with Cl^- values averaging 226.1 mg/l and ranging from 196.94 to 242.93 mg/l.

The essential criterion for our investigation, F^-, was effectively eliminated from the test waters for all the plates. The F^- recorded at the end of the experiment day was 0.55, 1.04, 1.5, 1.3, 1.2, 1.16, and 1.2 mg/l for plates 1,2,3,4,5,7, and 8, respectively. Plate 6 performed admirably, but as was already noted, it was rejected. The F^- removal efficiency varied from 67.64% for plate 1 to 23.53% for plate 4. For the remaining combinations, the observed efficiencies were 47.05%, 29.41%, 32.35%, 37.52%, and 29.41%.

Table 5-9 Evaluation of filtering efficiency of Plate 1

Number of Days	Discharge (l/hr)	pH	TDS (mg/l)	EC (µS/cm)	Hardness (mg/l)	Cl- (mg/l)	F- (mg/l)
1	0.682	8.44	820	1580	424	328.89	0.55
3	0.682	8.4	758	1770	460	317.90	1.02
7	0.273	8.66	798	1820	352	263.92	1.03
15	0.364	8.5	789	1420	460	267.92	0.98
21	0.682	8.46	791	1550	284	260.92	1.02
30	0.682	8.29	801	1580	416	265.92	0.55
Max	0.682	8.66	820	1820	460	328.89	1.03
Min	0.273	8.29	758	1420	284	260.92	0.55
Mean	0.561	8.458	792.833	1620.000	399.333	284.25	0.858
Std. Dev	0.190	0.122	20.312	148.728	68.977	30.62	0.239

Table 5-10 Evaluation of filtering efficiency of Plate 2

Number of Days	Discharge (l/hr)	pH	TDS (mg/l)	EC (µS/cm)	Hardness (mg/l)	Cl^- (mg/l)	F^- (mg/l)
1	0.714	8.32	843	2210	176	287.91	1.2
3	0.714	8.33	861	2400	168	296.91	1
7	0.191	8.71	886	2390	172	283.91	1
15	0.714	8.27	802	2420	140	301.91	0.9
21	0.714	8.42	836	2390	124	262.92	1.1
30	0.714	8.55	837	2360	180	306.90	1.04

Max	0.714	8.71	886	2420	180	306.90	1.2
Min	0.0191	8.27	802	2210	124	262.92	0.9
Mean	0.63	8.43	844.17	2361.67	160.00	290.08	1.04
Std. Dev	0.21	0.17	28.04	76.79	22.63	15.81	0.10

Table 5-11 Evaluation of filtering efficiency of Plate 3

Number of Days	Discharge (l/hr)	pH	TDS (mg/l)	EC (µS/cm)	Hardness (mg/l)	Cl- (mg/l)	F- (mg/l)
1	1.083	11.56	1299	2390.00	500	283.91	1.2
3	1.083	11.86	981	2230.00	492	275.91	1.2
7	1.083	11.68	941	2190.00	476	267.92	1.3
15	1.250	11.84	826	2250.00	508	353.89	1.2
21	1.250	11.91	721	1980.00	124	285.91	1.6
30	1.250	11.68	802	2010.00	120	260.92	1.5
Max	1.25	11.91	1299.00	2390.00	508.00	353.89	1.60
Min	1.08	11.56	721.00	1980.00	120.00	260.92	1.20
Mean	1.17	11.76	928.33	2175.00	370.00	288.08	1.33
Std. Dev	0.09	0.14	204.82	155.15	192.40	33.60	0.18

Table 5-12 Evaluation of filtering efficiency of Plate 4

Number of Days	Discharge (l/hr)	pH	TDS (mg/l)	EC (µS/cm)	Hardness (mg/l)	Cl- (mg/l)	F- (mg/l)
1	0.75	10.45	893.00	1400.00	408.00	279.91	1.30
3	1.05	11.36	2371.00	3390.00	388.00	261.92	1.40

7	0.75	10.94	1096.00	1890.00	396.00	281.91	1.40
15	0.75	11.48	856.00	1790.00	376.00	268.92	1.30
21	0.90	11.30	873.00	1810.00	528.00	273.92	1.40
30	0.80	10.67	556.00	1680.00	376.00	384.88	1.30
Max	1.05	11.48	2371.00	3390.00	528.00	384.88	1.40
Min	0.75	10.45	556.00	1400.00	376.00	261.92	1.30
Mean	0.83	11.03	1107.50	1993.33	412.00	291.91	1.35
Std. Dev	0.12	0.41	642.65	705.20	58.13	46.13	0.05

Table 5-13 Evaluation of filtering efficiency of Plate 5

Number of Days	**Discharge (l/hr)**	**pH**	**TDS (mg/l)**	**EC (µS/cm)**	**Hardness (mg/l)**	**Cl- (mg/l)**	**F- (mg/l)**
1	0.021	8.220	1080	1350	376	240.925	1.500
3	0.063	8.100	988	1600	364	289.910	1.350
7	0.050	8.050	928	1400	330	263.118	1.280
15	0.046	8.210	2120	1590	324	271.916	1.220
21	0.011	8.060	1580	1630	336	279.913	1.150
30	0.013	8.100	1200	1800	328	275.914	1.200
Max	0.06	8.22	2120	1800	376	289.91	1.5
Min	0.01	8.05	928	1350	324	240.93	1.15
Mean	0.034	8.1233	1316	1561.6667	343	270.2827	1.2833
Std. Dev	0.02182	0.07394	456.81331	164.12394	21.60555	16.88526	0.1266

Table 5-14 Evaluation of filtering efficiency of Plate 6

Number of Days	Discharge (l/hr)	pH	TDS (mg/l)	EC (µS/cm)	Hardness (mg/l)	Cl- (mg/l)	F- (mg/l)
1	0.083	8.300	951.000	2870.000	360.000	224.930	1.253
3	0.146	8.090	915.000	3050.000	380.000	197.939	1.184
7	0.115	8.180	920.000	2840.000	372.000	220.931	1.233
15	0.088	8.060	912.000	3060.000	360.000	224.930	1.240
21	0.088	8.100	889.000	2993.333	332.000	225.930	0.983
30	**Cracking of plates**						
Max	0.146	8.3	951	3060	380	225.93	1.25
Min	0.083	8.06	889	2840	332	197.94	0.98
Mean	0.10375	8.146	917.4	2962.6667	360.8	218.9321	1.1786
Std. Dev	0.026615	0.09685	22.23286	102.07296	18.1989	11.89169	0.11242

Table 5-15 Evaluation of filtering efficiency of Plate 7

Number of Days	Discharge (l/hr)	pH	TDS (mg/l)	EC (µS/cm)	Hardness (mg/l)	Cl- (mg/l)	F- (mg/l)
1	0.108	8.200	962.000	1980.000	356.000	196.939	1.560
3	0.221	8.150	942.000	2300.000	360.000	217.932	1.062
7	0.083	8.150	936.000	2970.000	380.000	233.927	1.210
15	0.108	8.080	915.000	2970.000	328.000	237.926	1.326
21	0.100	8.120	918.000	2800.000	324.000	226.930	1.150
30	0.167	8.050	910.000	2750.000	320.000	242.925	1.160

Max	0.221	8.2	962	2970	380	242.925	1.56
Min	0.083	8.05	910	1980	320	196.939	1.062
Mean	0.131	8.125	930.500	2628.333	344.667	226.097	1.245
Std. Dev	0.052	0.054	19.857	401.468	24.188	16.745	0.177

Table 5-16 Evaluation of filtering efficiency of Plate 8

Number of Days	Discharge (l/hr)	pH	TDS (mg/l)	EC (µS/cm)	Hardness (mg/l)	Cl- (mg/l)	F- (mg/l)
1	0.129	8.240	2126.000	3000.000	300.000	280.913	1.400
3	0.250	8.110	1987.000	3170.000	306.000	283.912	1.400
7	1.042	8.020	1926.000	2910.000	305.000	291.909	1.400
15	0.417	7.880	1940.000	2840.000	301.000	283.912	1.400
21	0.375	8.220	1768.000	2910.000	312.000	275.914	1.300
30	0.133	8.100	2062.000	2950.000	300.000	267.917	1.200
Max	1.042	8.240	2126.000	3170.000	312.000	291.910	1.400
Min	0.129	7.880	1768.000	2840.000	300.000	267.920	1.200
Mean	0.391	8.095	1968.167	2963.333	304.000	280.746	1.350
Std. Dev	0.341	0.133	123.862	114.134	4.690	8.156	0.084

5.7.4 The performance of filter combination 1 for the sampled Hurda Tehsil water

The current study employed a single measure to assess the effectiveness of the filter plate: F^- removal efficiency. With the highest F^- removal recorded, the Plate 1 combination was selected for further investigation after the initial experiments.

The water samples collected from the villages of the Hurda block were filtered through the PCWF, and the filter's effectiveness in removing F^- was monitored over seven days. The mix

ratios from Plate 1 were used to create two filter plates for each village. Finally, the water samples collected from the nine villages were passed through the PCWF while being monitored for parameters such as discharge (l/hr), pH, TDS (mg/l), hardness (mg/l), and F^- (mg/l). The results averaged over seven days observed for the villages are displayed in Figures 5-11 a to e. The qualitative water parameters recorded over the seven testing days for the villages have been compiled from Tables 5-17 to 5-25.

The final observed discharge value over all the filters ranged from 0.87 to 1.6 l/hr. After filtration, the mean F^- concentration is around 1.235 mg/l, with a documented removal efficiency averaged over 43.477%, with a maximum removal efficiency recorded at 88.55%. Further, 20.63% and 55.56% of filtered samples had F^- concentrations less than 1 and between 1 to 1.5 mg/l, respectively, within the upper tolerance limit of F^- of 1.5 mg/l.

The mean TDS and pH values were recorded at 957.35 mg/l and 8.58, respectively. Though the mean recorded pH value is greater than the threshold value of WHO, maximum samples read a pH of 8.25 to 8.5, safe for consumption. 53.97% of documented samples had a pH in the range of 6.5 to 8.5. The observed high pH values are possibly due to cement usage as a raw material in the preparation of filters. 87.3 % of recorded readings had TDS values above the acceptable value of 500 mg/l but below the permissible limit of 2000 mg/l according to Indian standards. A contributing factor to increased TDS is attributed to alkalinity and calcium concentrations resulting from the weathering of the concrete filter (Mikalsen, 2005). The lowest 7^{th}-day reading was 391 mg/l observed for V3. The recorded hardness value over the 7 days duration varied from 108 mg/l for V9 to 1610 mg/l for V5, with 55.56% of recorded results classified as hard.

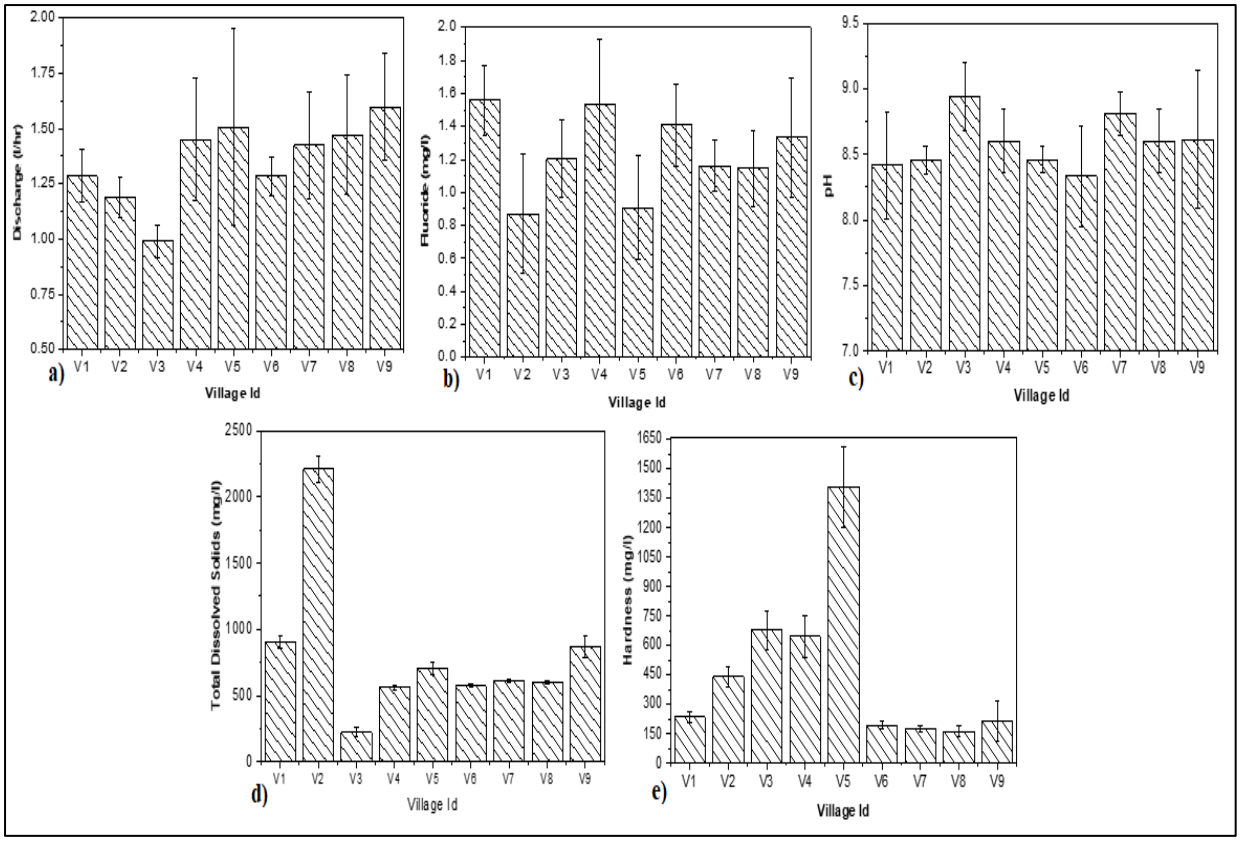

Figure 5-11 (a-e) Average discharge and water quality parameters recorded for the PCWFs over the 7 testing days

Table 5-17 Filtering performance of selected water filter over the seven testing days for Murayla

Test Day	Discharge (l/hr)	pH	TDS (mg/l)	Fluoride(mg/l)
1	1.33	9.40	827.00	1.50
2	1.00	8.36	888.00	1.78
3	1.33	8.19	886.00	1.40
4	1.33	8.14	940.00	1.51
5	1.33	8.17	927.00	1.85
6	1.33	8.33	971.00	1.67
7	1.33	8.33	891.00	1.20

Table 5-18 Filtering performance of selected water filter over the seven testing days for Hajiyas

Test Day	Discharge (l/hr)	pH	TDS (mg/l)	Fluoride(mg/l)
1	1.08	8.47	2300.00	0.95
2	1.08	8.28	2230.00	0.93
3	1.08	8.45	2280.00	1.10
4	1.25	8.44	2210.00	0.55
5	1.25	8.40	2260.00	1.02
6	1.25	8.66	1979.00	1.37
7	1.32	8.50	2200.00	0.18

Table 5-19 Filtering performance of selected water filter over the seven testing days for Patiyon ka Khera

Test Day	Discharge (l/hr)	pH	TDS (mg/l)	Fluoride(mg/l)
1	0.95	8.76	261.50	1.33
2	1.05	9.46	256.00	1.56
3	1.05	8.63	269.50	1.00
4	0.87	8.83	199.00	1.21
5	0.95	8.86	195.50	1.18
6	0.96	9.18	189.00	0.78
7	1.10	8.87	195.50	1.34

Table 5-20 Filtering performance of selected water filter over the seven testing days for Barantiya

Test Day	Discharge (l/hr)	pH	TDS (mg/l)	Fluoride(mg/l)
1	1.82	8.42	584.00	1.70
2	1.85	8.49	566.67	1.96
3	1.55	8.50	570.67	1.72
4	1.37	8.97	540.00	1.63
5	1.24	8.63	558.00	1.43
6	1.08	8.92	544.67	0.63
7	1.25	8.26	566.00	1.66

Table 5-21 Filtering performance of selected water filter over the seven testing days for Phalamada

Test Day	Discharge (l/hr)	pH	TDS (mg/l)	Fluoride(mg/l)
1	2.00	8.44	736.67	0.55
2	1.80	8.40	753.33	1.02
3	1.75	8.66	659.67	1.37
4	2.00	8.50	733.33	1.23
5	1.00	8.46	614.67	1.02
6	1.00	8.29	746.67	0.55
7	1.00	8.46	713.33	0.61

Table 5-22 Filtering performance of selected water filter over the seven testing days for Hurda

Test Day	Discharge (l/hr)	pH	TDS (mg/l)	Fluoride(mg/l)
1	1.33	8.04	589.33	1.84
2	1.33	8.51	583.33	1.60
3	1.33	8.33	570.00	1.16
4	1.25	8.30	579.33	1.33
5	1.33	7.70	579.33	1.43
6	1.33	8.42	558.67	1.03
7	1.08	9.04	550.67	1.46

Table 5-23 Filtering performance of selected water filter over the seven testing days for Balapura

Test Day	Discharge (l/hr)	pH	TDS (mg/l)	Fluoride(mg/l)
1	1.92	8.90	630.77	1.42
2	1.50	9.16	583.08	1.38
3	1.33	8.58	613.85	1.10
4	1.38	8.76	606.92	1.05
5	1.26	8.70	608.46	1.00
6	1.50	8.82	616.15	1.06
7	1.08	8.76	609.23	1.10

Table 5-24 Filtering performance of selected water filter over the seven testing days for Bharliyas

Test Day	Discharge (l/hr)	pH	TDS (mg/l)	Fluoride(mg/l)
1	1.68	8.42	625.71	1.19
2	1.68	8.49	607.14	1.26
3	1.09	8.50	611.43	1.22
4	1.09	8.97	578.57	1.13
5	1.71	8.63	597.86	1.43
6	1.71	8.92	583.57	0.63
7	1.35	8.26	606.43	1.16

Table 5-25 Filtering performance of selected water filter over the seven testing days for Sanodiya

Test Day	Discharge (l/hr)	pH	TDS (mg/l)	Fluoride(mg/l)
1	1.72	8.92	817.00	0.63
2	1.36	8.26	849.00	1.66
3	1.85	7.85	907.00	1.41
4	1.85	8.26	1049.00	1.70
5	1.80	9.60	800.00	1.63
6	1.30	8.61	833.00	1.05
7	1.30	8.79	833.00	1.26

The inability to directly compare the study's findings with those found in the literature was a weakness, which can be attributed to variations in the purification procedures, the raw ingredients used, the test settings, and the quality of the raw water samples. As the filter is

tested locally, significant modifications leading to improvements will ensure a robust HWT model prepared with cement.

5.7.5 Filter cost evaluation

In connection with the filter plate preparation and its characterization, cost analysis is an essential viewpoint to validate its suitability compared to other technologies available in the market. The present work evaluated the filter cost based on the raw material cost, electrical energy consumption during adsorbent preparation, sintering, and water consumption during the filter preparation and curing process. The per-unit price of the consumables is reported in Table 5-26. The study included the transportation charges as and where necessary, including overhead expenses covering handling and preparation charges. However, this outlay did not cover the cost of the stainless filtration container.

Depending on the material composition, the total projected filter plate cost for CWF ranged from INR 805.95 to 1023.90. For PCWF, it went from INR 60.28 to 116.76, as presented in Figure 5-12. It should be emphasized that the entire filter system will be a single-time expenditure, requiring the replacement of the filter plates upon exhaustion.

Table 5-26 Cost of materials used for filter fabrication

Raw Materials	Unit price (Rs /kg)
Cement	4.6
River sand (type 1)	2.2
River sand (type 2)	2.2
Sugarcane bagasse	20
Sawdust	30
Potatoes	43
Activated carbon	290
Clay	50
Ceramic	126.7
Water cost for curing	0.054

Cost of sintering	50
Overhead expenses	5.21

***Rs → INR**

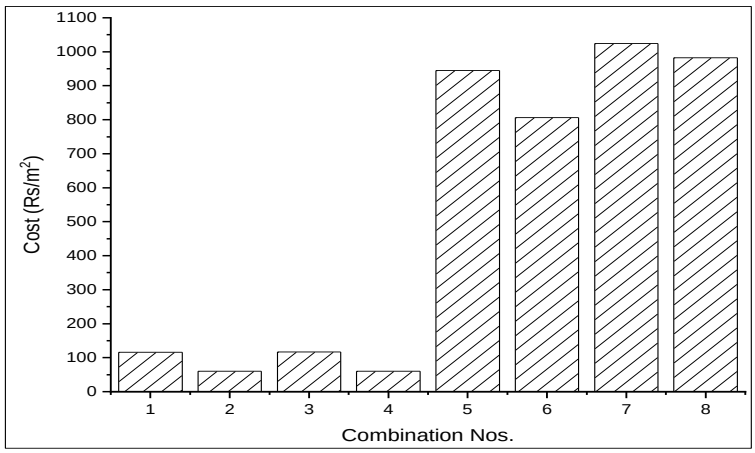

Figure 5-12 Cost (in Rs/m^2) calculated for the filter plates

5.7.6 Maintenance of the filters

Maintenance of the water filters—CWF and PCWF—is carried out after a noticeable decrease in discharge caused by a blockage of the pores by the buildup of contaminants. Clean water and a brush are used to scrub the filter plates' outside surfaces as part of maintenance. However, significant salt deposition has been seen over time on the filter plates because of the high F^- in the relevant water sample. At this stage, removing the exhausted filter plate and replacing it with a new one is necessary.

Chapter Summary

The current chapter's health risk evaluation of fluoride brought to light the severe issue of groundwater contamination. The novelty of a cement water filter that functions well was made possible by new filter construction techniques and materials. The efficiency and effectiveness of cement filters were on par with ceramic filters. The filters' ability to remove fluoride was noticeable.

With the successful filter, the next phase of the study, i.e., field implementation, was carried out.

6 WATER QUALITY ASSESSMENT IN SELECTED VILLAGES OF CHIRAWA TEHSIL AND ON-GROUND PERFORMANCE EVALUATION OF DEVELOPED WATER FILTERS

Chapter Overview

A substantial portion of our work involved implementing lab-scale experiments, prototypes, and models on the field and regularly documenting how well they performed in realistic scenarios. The present chapter covers and goes into great length on the aforementioned goal.

6.1 Selection of study area: Jhunjhunu

For the implementation portion of the study, four villages were selected from the Chirawa tehsil from the Jhunjhunu district in Rajasthan. Jhunjhunu is situated between 27°38′ and 28°31′ north latitudes and 75°02′ and 76°06′ east longitudes (Central Ground Water Board, 2008), falling predominantly under the Sekhawati basin. The climate is particularly semi-arid, characterized by scorching summers and cold winters. Recorded long-term water level data (pre-monsoon, 2001-2015) have highlighted a declining water level ranging from 0.02 to 0.20 m/ year, with the entire district entering the overexploited category (Central Ground Water Board, 2017). The critical water levels necessitate developing a robust rural water management system to offset dwindling groundwater resources and scanty rainfall.

The four villages identified were Jeeni, Kirwana, Dheendhwa aguna, and Ramnath Pura. For the convenience of comprehension, the villages will further be referred to by their initial letters, such as J, K, DA, and RP, throughout the chapter. The principal occupation of the villages is agriculture, comprising small to medium-class farmers. Private and public groundwater wells are the primary water source for the local population's everyday water demands. Figure 6-1 shows the geographical location of the selected villages in Jhunjhunu.

6.2 Water sample collection and analysis from the study area of Jhunjhunu

The water samples analyzed for the study were collected from the community water source and stored in clean polypropylene water storage bottles of 1-liter capacity with necessary precautions and transported to the Public health engineering laboratory of the BITS Pilani campus for further qualitative analysis. In total, 14 water samples (J = 3; K = 3; DA = 4; RP =

4) were collected and assessed for pH, Total dissolved solids (TDS), hardness, and F^-. Essential drinking water physical characteristics, including pH, TDS, and hardness, are markers of significant pollutants detrimental to human health (Sevgili et al., 2021). Given the extensive fluorosis observed over a majority portion of the study region, the ionic concentration of F^- was substantial.

pH and TDS were measured with the Hi-media Soil analysis kit with specified electrodes. The standard colorimetric titration measured the hardness with EDTA solution. The F^- in the water sample was analyzed using Merck's Fluoride test kit. All chemicals used were procured from Merck and used without modifications, and standard laboratory procedures were implemented to accomplish a higher quality assurance. All samples were tested in triplicates, and the mean values were reported.

6.3 Survey of participatory households

Before the commencement of the work, a preliminary survey was conducted in the four villages. The questionnaire was designed to collect information on the annual family income, the land-holding capacity of the family, the size of the family, and access to HWTs, as represented in Figure A7, Appendix 2. The conservation medium was restricted to the local dialects of Marwari and Hindi for user preference. Significant importance was accorded to the inclusion of women participants in the study −−essentially an effort to comprehend women's water problems and provide them with increased overall influence over decision-making regarding clean water. The participants were briefed about the study - installing RWH tanks, fabricating water filters, and subsequent distribution.

6.4 Distribution of fabricated water filters and monitoring of the filter performance

The Plate 1 configuration of the porous cement water filter (PCWF) was selected for the implementation part of the work owing to superior performance. Approximately 130 PCWF were prepared and tested for soundness and fixedness before distribution. The facility water was passed through the contrivances and monitored for flow rates. Set-ups with flow rates ≥ 0.87 l/hr were outfitted for dispatch, with the remaining discarded.

Ninety-nine households from J, K, DA, and RP were identified after the survey. Information sharing on filter handling and maintenance was indispensable during the filter distribution

phase. After demonstrating the know-how and cleaning guidelines, the filters were distributed among the participants.

The real-time filter performance monitoring was ensured by collecting water and evaluating its quality after 3 and 6 months—constant communication with the participants aided in identifying inherent flaws and scope for modification in the water filters.

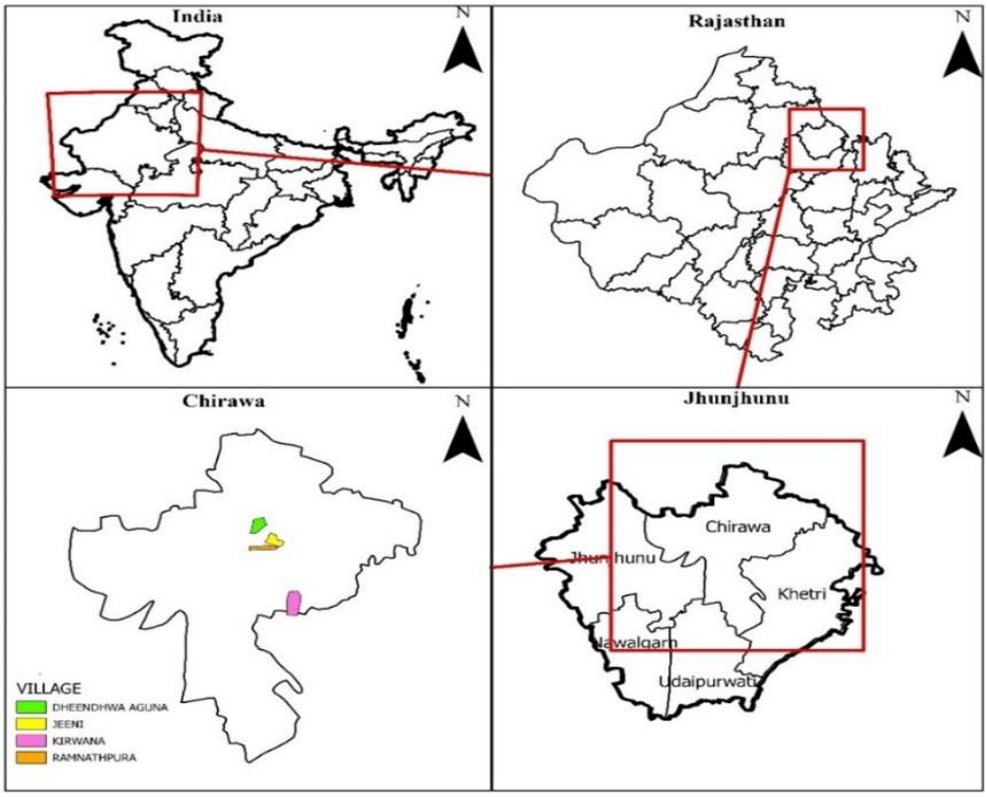

Figure 6-1 Map of the study implementation area in Jhunjhunu

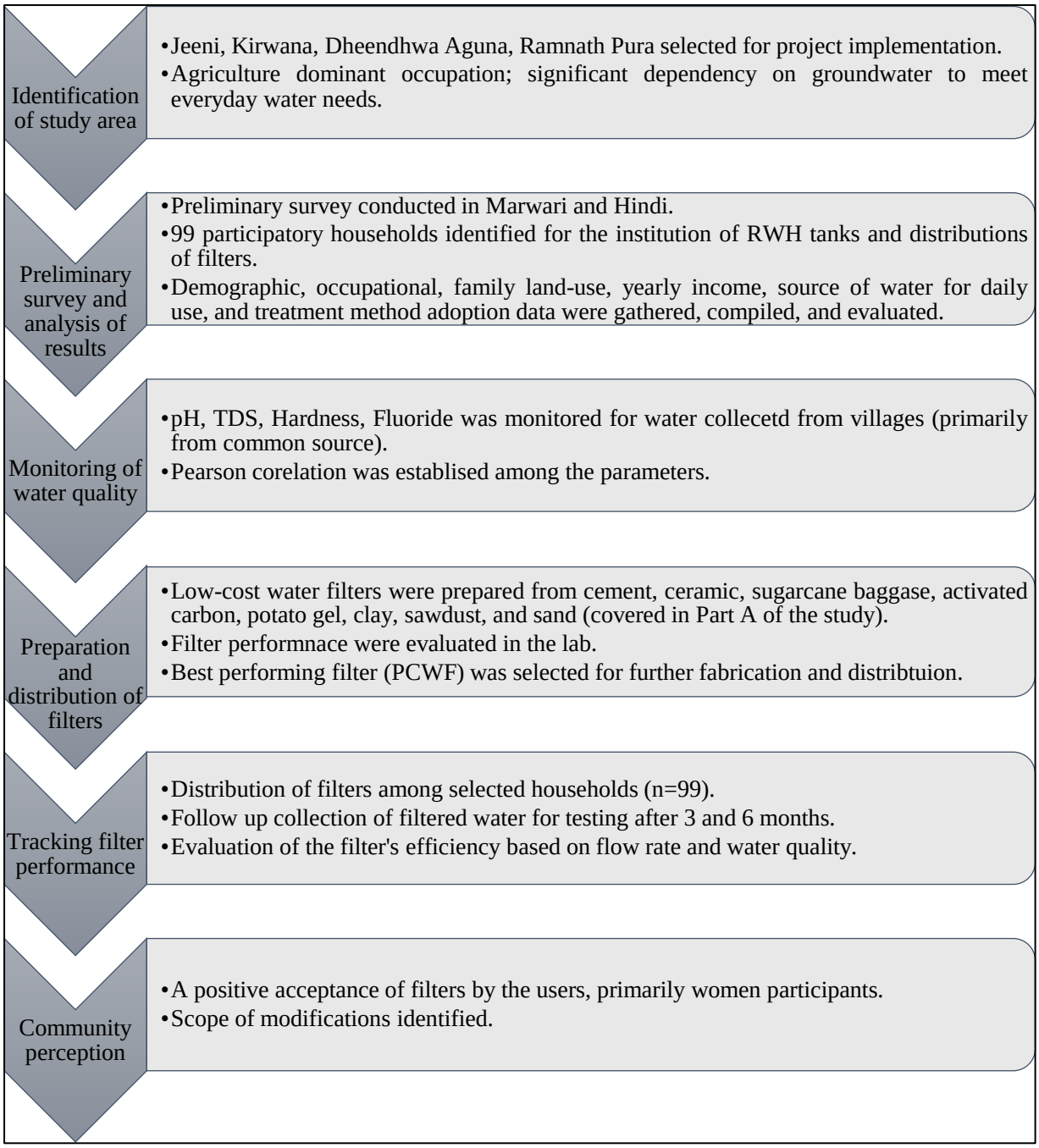

Figure 6-2 An outline of the steps adopted during the distribution study

6.5 Statistical assessment of preliminary data collected

Figure 6-2 outlines the steps followed through the distribution of the water filters and subsequent studies conducted. The survey results for the four villages are depicted in Figures 6-3 a through e. Figure 6-3 a displays the number of participating households and participants. 42.42 % of the 99 families studied collected water from communal village sources, while 57.58 % had access to individual handpumps (Figure 6-3 b). Further information indicates that 46.2 % and 53.8 % of people relied on the village wells and handpumps, respectively.

While 26 households, comprising 138 individuals, had access to advanced water filtration units (such as RO), 73.7 % of households and 78.6 % of individuals had no access to filtration units. These households even lacked inexpensive and accessible physical water treatment equipment. The inhabitants consumed water directly upon collection, as shown in Figure 6-3c.

The population surveyed was split into two groups based on annual income, primarily that earning >1,00,000 and ≤1,00,000 INR (Figure 6-3d). While households having income ≥1,00,000 INR had access to RO units, the remaining households did not. The point-of-use RO units are an efficient water treatment technique generally located directly before tap discharge. A strong and positive correlation value of 1 between annual income and advanced water filters, signified purchasing power, and competence to pay for utilities played a crucial role in adopting HWT units. Additionally, several households, especially those in the low-income bracket, were concerned about water wastage and vacillating electrical power when operating an RO filter. The complete survey data is represented in Table xi in Appendix 1.

6.6 Water Quality Assessment of study area villages

According to the WHO (World Health Organization) and BIS (Bureau of Indian Standards), the observed pH values for J, K, and RP were within the permissible values of 6.5 to 8.5 (BIS, 2012; WHO, 2022). All the monitored water quality are tabulated in Table xii of Appendix 1. However, the pH value for DA exceeded the threshold by 13.9 %. Recorded TDS values for all the villages exceeded the acceptable value of 500 mg/l by 34.4%, 19.6%, 15.6%, and 48%, corresponding to J, K, DA, and RP, respectively. Nevertheless, TDS values were below the permissible limits set by WHO and BIS. Hardness values of 134, 140, 168, and 176 mg/l recorded for J, K, DA, and RP were below 200 mg/l. The acceptable level of F^- for human

consumption is 1 mg/l, with a permissible increase of up to 1.5 mg/l in the absence of alternative sources according to Indian standards. DA had an F^- concentration of 1 mg/l. J, K, and RP exceeded the acceptable limit by 20%, 50%, and 10 %. The monitored water quality data is represented in Figure 6-3 e.

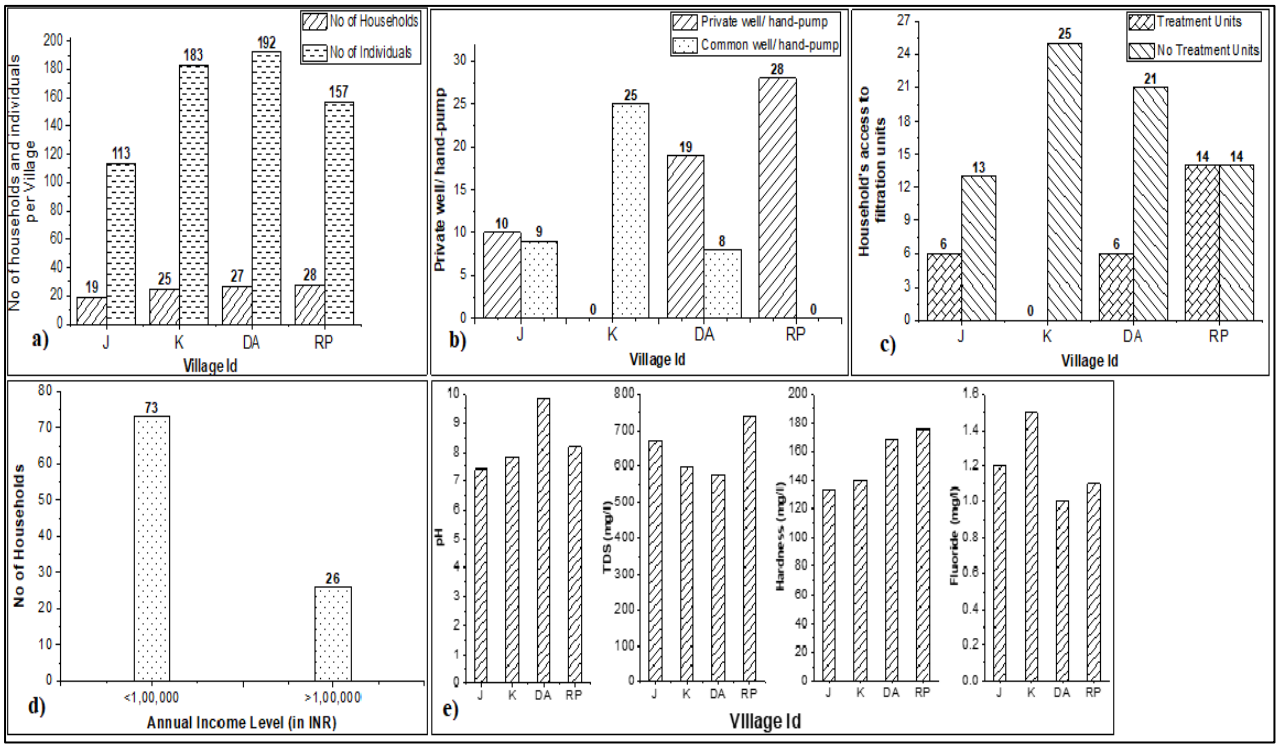

J: Jeeni; K: Kirwana; DA: Dheendhwa Aguna; RP: Ramnath Pura

Figure 6-3 a) Demographic distribution for the studied villages b) Household access to individual and common well/ hand-pump facility c) Household access to treatment units d) Annual income distribution among households broadly classified into two categories e) Average reported village water quality monitored during the preliminary survey

The fourteen village water samples were subjected to a Pearson-coefficient correlation study. The correlation values will provide insight into how the qualitative measures under study are related to one another. The coefficients are presented in Table 6-1.

A favorable positive relation between pH and hardness (r = 0.653) and between hardness and TDS (r = 0.277). Earlier studies reported a significant positive correlation between pH and TH and TDS and TH (Bhandari & Nayal, 2008; Saleem et al., 2012).

F^- has a weak negative relation with TDS (r = -0.213) and a moderate negative association with pH (r = -0.630) and hardness (r = -0.689), respectively. The negative correlation of F^- with pH agreed with studies from Arsanjan, Iran, and Telangana, India (Laxmankumar et al., 2019; Rahmani et al., 2010). A previous Assam, India study showed a clear negative correlation

between F^- and total hardness (r = -0.506) (Das et al., 2003). The data analysis reports a moderately negative relationship between pH and TDS. Tiwari et al. reported a negative correlation between TDS and pH in India's KBNIR region (Tiwari et al., 2017).

Table 6-1 Pearson correlation coefficient (r) between sampled water quality parameters for Jhunjhunu

Qualitative Parameters	pH	TDS	Hardness	F^-
pH	1			
TDS	-.499	1		
Hardness	.653	.277	1	
F^-	-.630	-.213	-.689	1

6.7 Distribution of filters

Figure A8 in Appendix 2 shows the group discussions in the community center of DA followed by PCWF distribution among the participants in the remaining study areas of J, K, and RP. It is advised to clean the outer surface of the filter plate with a scrub and clean water and allow the filter to dry in the sunlight under circumstances of reduced flow to ensure the smooth functioning of the filters. Upon drying, the filter can be re-used.

Users were instructed to totally discard the used filter plate and adequately dispose of it when significant salt accumulation was seen over plates with visibly reduced discharge following the successful cleaning and reoperation of filters. It is deemed reasonable at this time to attach a fresh plate to the filter container.

6.7.1 Follow-up survey for monitoring filter performance after distribution

Subsequent surveys were conducted after 3 and 6 months to supplement data for verifying the on-field performance of the filters and interact with the users to identify potential drawbacks and scope for refinement. Due to strict Covid protocols prevailing in the study area, the authors did not get access to a majority of the participatory households. Nevertheless, the study was

conducted with 25.3% (n= 25) and 28.3% (n=28) accessible households at the end of 3 and 6 months, respectively.

6.7.1.1 Data curated after 3 months of distribution

Of the 25 surveyed units, 5 households highlighted the breakage of filter plates due to mismanagement. For the remaining 20 households, filtered water samples were collected in clean sampling bottles of 1-liter capacity and tested in the campus facility. The remaining data has been represented in Figure 6-4.

For Jeeni, the observed pH levels were increased from 8.51% to 18.24% through all the collected samples. 83.33% of the reported pH values were within the WHO threshold. The variation for TDS was observed to vary from a minimum of 623 mg/l to a maximum reported value of 708 mg/l. In 66.67% of samples, hardness was reportedly reduced between 4.48% to 16.42%.

F^- removal was appreciable for all the samples and ranged from 49.17% to 76.40%, corresponding to values of 0.61 mg/l to 0.28 mg/l, respectively.

A comparable favorable F^- reduction was observed for Kirwana. Compared to the original value of 1.5 mg/l, the reported F^- values were 1.39 and 1.27 mg/l. The reported results, however, exceeded the permissible threshold of 1 mg/l as per Indian norms. As much data could not be collected from Kirwana, it was challenging to provide an appropriate analysis. Of the two collected samples, there was a decrease and increase in pH value to 6.62 and 8.38 from 7.83, respectively. According to the observed values, TDS was reportedly reduced by 26.25% and 33.11%. Additionally, hardness was decreased from 140 mg/l by 40 and 60%.

Water from Dheendwa Aguna that has been collected demonstrated lower pH, hardness, and F^- values. However, TDS showed a declining value in 66.67% of the samples. pH levels dropped from 9.87 to a minimum of 8.17, with efficiency ranging from 12.56 to 17.22%. A higher pH value (> 8) is attributed to cement as the raw filter material. While observed hardness was reduced over a range of 2.38% to 73.81%, F^- removal varied from 35.38% to 95.71%.

For the site of Ramnath Pura, pH showed an increasing trend, unlike TDS, hardness, and F^-. The maximum recorded pH value was 8.46. The maximum reduction observed for TDS, and hardness was 9.73% and 70.45%, respectively. F^- removal efficiency ranged from 56.26% to 77.86% for RP.

The mean value observed for all the filters combined showed appreciable performance. 8.24, 592.76 mg/l, 102.6 mg/l, and 0.47 mg/l were the observed averages for pH, TDS, hardness, and F^-, respectively. All recorded values were within acceptable standards prescribed by the WHO and BIS. F^- removal efficiency peaked at 95.71%, highlighting significant F^- removal over a wide pH range from 3 to 10 (Kagne et al., 2008). For the study, the pH ranged from 6.62 to 8.63.

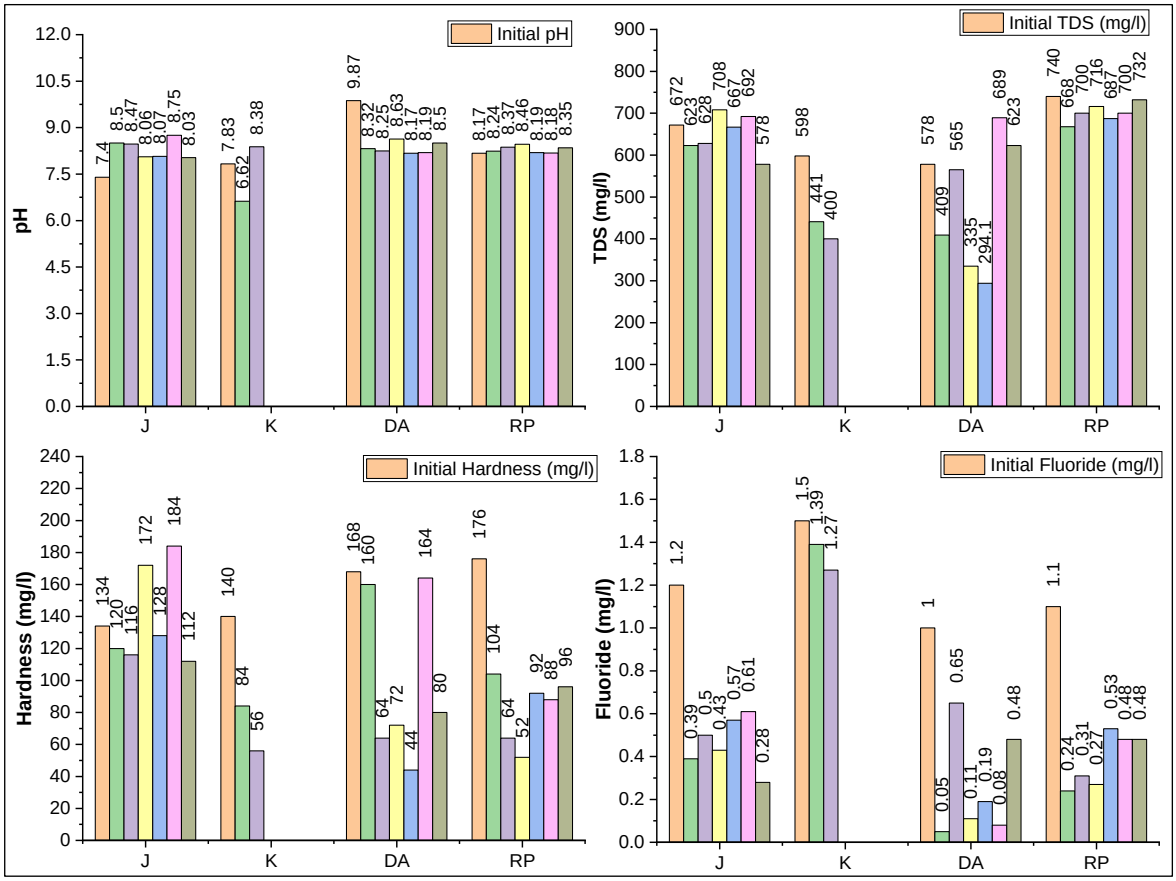

J: Jeeni, K: Kirwana, DA: Dheendhwa Aguna, RP: Ramnath Pura

Figure 6-4 Filter water quality observed after 3 months

Table 6-2 Pearson correlation coefficient (r) between water quality parameters after filtration

Qualitative Parameters	pH	TDS	Hardness	F^-
pH	1			
TDS	0.187	1		

Hardness	0.077	0.347	1	
F^-	-0.535*	-0.124	-0.215	1

***. Correlation is significant at the 0.05 level (2-tailed).**

A Pearson correlation analysis was performed for the collected filtered water to determine the association between the different analyzed parameters, as reported in Table 6-2. A moderate negative relationship between F^- and pH (r = -0.535), and weak negative association between F^- and TDS (r = -0.124), and F^- and hardness (r = -0.215) is reported. A positive and moderate correlation was observed for hardness and TDS (r = 0.347). Additionally, pH had a weak positive affiliation with TDS (r = 0.187) and hardness (r = 0.077).

6.7.1.2 Data curated after 6 months of distribution

During the second survey conducted after 6 months, the authors had access to 28 households, of which 14.28% (n = 4) complained of inadequate filtration rates. Those units were discarded for further qualitative analysis. The data compiled for the remaining filters are presented in Figure 6-5.

The reported pH range for Jeeni was between 7.39 and 8.23, and reported values fell within the WHO and BIS thresholds. TDS was considerably reduced, with variations between 59.23% and 63.84%. From 136 mg/l to 180 mg/l, an upward trend for the reported hardness value was seen. All of the values, however, fell below the acceptable standard values. From an initial value of 1.2 mg/l, F^- removal ranged from 0.54 mg/l to 0.73 mg/l, with the highest removal effectiveness at 54.53%.

A contrary trend was observed for Kirwana as increased F^- levels were observed. The F^- increased significantly as compared to 1.5 ppm. While recontamination of purified water is one explanation for the observation, high F^- values highlighted the need to discard worn plates. Additionally, a rise in the monitored pH value was seen. With a pH value of 9.04, higher than the WHO upper limit, a maximum increase of 15.45% was observed. Similar to J, the recorded TDS values were lower than the initial value by 58.528% to 61.371%. With a single case of decreasing value, an increasing trend in hardness value was observed, ranging from 11.43% to 45.71%.

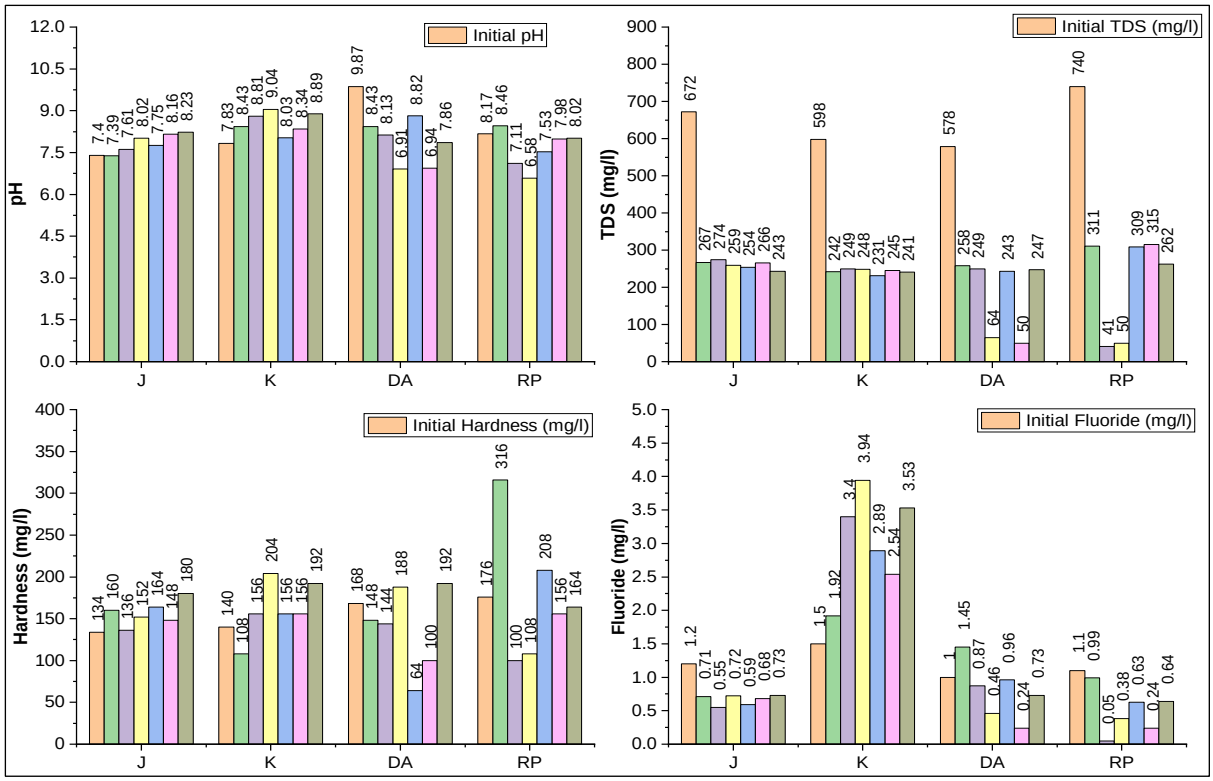

J: Jeeni, K: Kirwana, DA: Dheendhwa Aguna, RP: Ramnath Pura

Figure 6-5 Filter water quality observed after 6 months

For Ramnath Pura, 16.67% (n=1) and 33.33% (n=2) samples had an increased pH and hardness value above the initial values of 8.17 and 176 mg/l. The plates performed satisfactorily in removing F^- with maximum efficiency at 95.28%. All recorded values for TDS showed a positive decrease between 57.43% and 94.46%.

Though a positive decrease in pH value was observed for Dheendhwa Aguna, a single collected sample had a pH of 8.82, higher than the acceptable limits (BIS, 2012). Similarly, while maximum F^- removal efficiency reached 75.56%, an increased value was observed at 1.45 mg/l. 33.33% (n=2) had increased hardness values recorded at 188 mg/l and 192 mg/l. The trend of decreased TDS value was also observed for DA, comparable to the other villages.

After six months, the mean values of pH, TDS, Hardness, and F^- were 7.98, 225.75, 158.33, and 1.24 mg/l, respectively. Despite the investigated values falling within acceptable thresholds, isolated incidents were documented, demonstrating a decline in filter effectiveness, notably in the village of Kirwana, primarily attributable to raw water quality and negligent PCWF handling and maintenance.

Table 6-3 outlines the results of the correlation matrix between the qualitative parameters, wherein a positive correlation among the parameters was recorded. pH showed a weak positive relation with hardness (r = 0.239) and moderate positive relationship with TDS (r = 0.666). While F^- had a strong positive association with pH (r = 0.703), a weak relationship was observed with TDS (r= 0.248) and hardness (r= 0.196).

Table 6-3 Pearson correlation coefficient (r) between water quality parameters after filtration

Qualitative Parameters	pH	TDS	Hardness	F^-
pH	1			
TDS	0.666**	1		
Hardness	0.239	0.436*	1	
F^-	0.703**	0.248	0.196	1

****. Correlation is significant at the 0.01 level (2-tailed).**

***. Correlation is significant at the 0.05 level (2-tailed).**

6.8 Community perception and scope for modification

During the distribution and collection phase of PCWF set-up and filtered water, respectively, one-on-one discourse with the locals was conducted. Reduced flow rates due to filter pore-clogging, rough handling, and participant indifference towards filter maintenance affected the PCWF approbation leading to reduced efficiency. Another stated problem was the filters' brittleness. However, the participant families, especially those with children (under 10 years old) and those who continued to participate in the study, had positive perceptions of the filters and effective suggestions. The suggestions are discussed in depth in the concluding chapter of the thesis.

Chapter Summary

Access to low-cost HWT units plays a significant role in addressing preventable diseases primarily caused by the consumption of contaminated water. The field applicability of the innovative PCWF was examined in the current chapter. User acceptance of a filter and ease of operation and maintenance played a significant role in the mass scalability of lab-tested prototype filters. Continuous monitoring of filters in real scenarios reinforced the performance capability of PCWF. The designed filters performed fairly overall and can be improved as HWTs.

Sustainability means a system's ability to work and achieve desired results for a long time without exhausting or harming essential resources or contributing to environmental damage. A sustainable system balances and preserves its environmental, social, and economic components for future generations, bringing to the final objective of safe disposal of exhausted filter plates/ household sludge generated.

7 EXPERIMENTAL ANALYSIS OF SOIL FLUORIDE CONCENTRATION SUBJECT TO THE DISPOSAL OF EXHAUSTED FILTER PLATES

Chapter Overview

Safe waste disposal is crucial for developing a sustainable water management system. In the same vein, the disposal of exhausted filter plates has been explored in the laboratory and discussed in the current chapter. The soil fluoride concentrations were monitored with increasing time and varying depths. The experimental results were subsequently fitted with machine-learning algorithms to predict soil-fluoride concentrations.

7.1 Design methodology to monitor soil fluoride concentration in lab-scale prototype

For the study, a user-friendly method of disposal of the exhausted filter plates was selected, i.e., soil disposal. The method of disposal was decided upon after taking into consideration the location of the research site. In addition, selecting a simple disposal method will encourage an increased acceptance of HWTs.

A laboratory prototype was designed to emulate the soil disposal conditions –a bucket contraption of 30 cm was designed to monitor the F^- transport through the soil profile as depicted in Figures 7-1a and b. The sand used in the study was collected from the study area. Soil characterization was carried out to determine the particle size analysis, moisture content, and bulk density of sand. The sand replacement method was used to determine bulk density, the falling head method was used to measure hydraulic conductivity, and the mechanical sieve analysis was used to determine the mean grain sizes. The pzc value of the soil was determined following the procedures discussed in Chapter 4 while characterizing Khejri.

As is demonstrated in Figure 7-1c, two pre-determined slots were holed into the bucket. One outlet was holed at a depth of 10 cm from the top, followed by the outlet at the bottom of the bucket at a depth of 29.5 cm. Small pipes 15 cm in length were fixed through the holes to collect the water passing through the soil.

The bucket was then backfilled with the collected sand up to a depth of 19.5 cm. After that, spent PCWFs were placed on the sand. The bucket was re-filled up to the top of the bucket, i.e., the filters are buried at a depth of 10 cm below the top layer of soil. A total of four buckets

were set up. In three sets up, whole plates were buried. However, a broken and powdered plate was buried for the fourth contraption.

Synthetic fluoride solution was allowed to pass through the buried soil and filter plate. After collecting at the outlets at fixed time spacing, the F^- concentration was measured. Zhang and Su designed a similar experimental model to simulate the flow of F^- in the sand (Zhang & Su, 2006). Besides F^- levels, pH and TDS were measured for the soil water. A total of 120 readings were recorded over two months for each parameter. Machine Learning (ML) methods of ANN and ANFIS have been used to model an F^- prediction algorithm, with pH, TDS, depth of observation, and test day duration (in days) as inputs; and measured F^- concentration as the target.

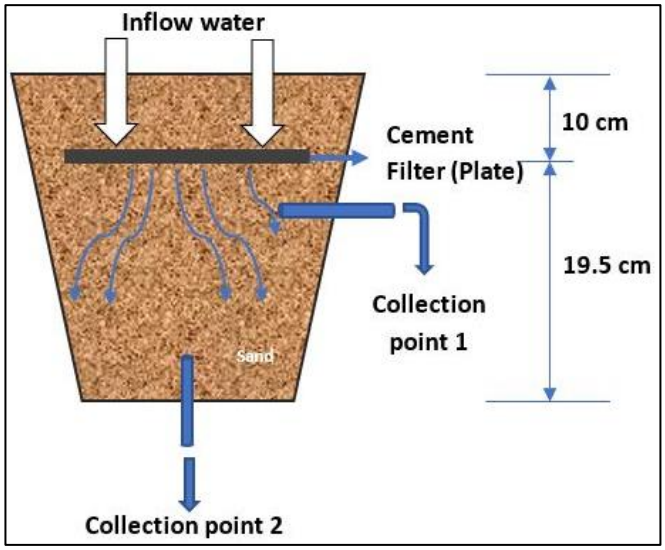

(a)

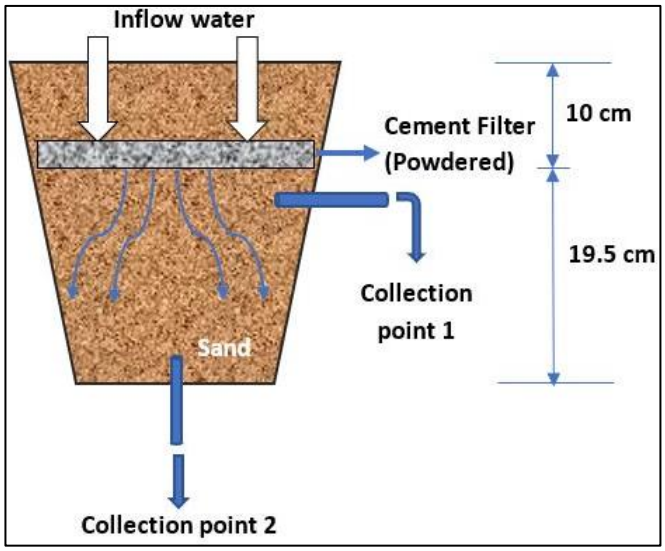

(b)

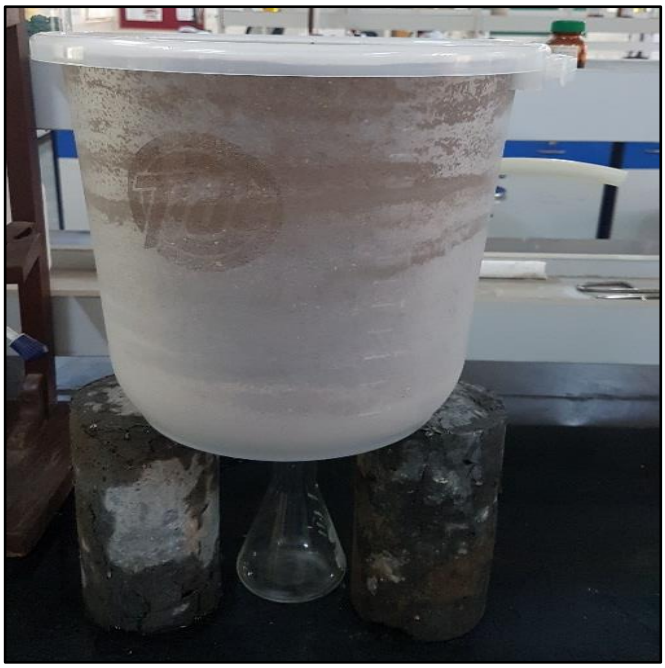

(c)

Figure 7-1 a) and b) Experimental set-up to determine the fluoride levels in the soil at various depths; c) The bucket contraption installed for monitoring water quality parameters at varying depths

[Note: In the initial stages of the experiment, distilled water was allowed to pass through the soil and buried filter plate. However, the extracted F^- concentration was too low to be documented. Therefore, to imitate a pessimistic condition of severe F^- leaching from disposed of plates, synthetic solutions of F^- was passed through the soil profiles to have extractable level contaminant concentration to factor in F^- ion movement through the soil and the self-purifying capacity of the soil.]

The methodology involved in ANN has been discussed in depth in chapter 4. In subsequent sub-sections, discussions covering the working principle of ANFIS have been presented.

7.2 Adaptive Neuro-Fuzzy Inference System (ANFIS)

ANFIS algorithm integrates ANN and FIS (Buragohain & Mahanta, 2008). To map and simulate input-output interactions, ANFIS employs both neural network learning techniques and the fuzzy approach as a multi-layer network. ANFIS employs a Takagi-Sugeno-type Fuzzy Inference System (FIS), with each fuzzy rule's output being a linear combination of input variables plus a constant term. The fuzzy inference approach is based on the if-then principle. ANFIS typically employs two types of learning algorithms: backpropagation and hybrid learning. While backpropagation learning adheres to a methodology similar to ANN, the hybrid

learning approach combines backpropagation with the least squares method. The Least Squares Method (LSM) is applied for forward passing in the ANFIS training process, and Gradient Descent is applied to backpropagation (Loganathan & Girija, 2013). The rules are employed as membership functions (MFs) for a fuzzy decision. However, the FIS can be used as a solid prediction model in complex circumstances where the dataset is highly uncertain. FIS uses the linear equation in subsequent parts, and the least square approach is employed to determine parameter efficiency. The detailed architecture of ANFIS is shown in Figure 7-2.

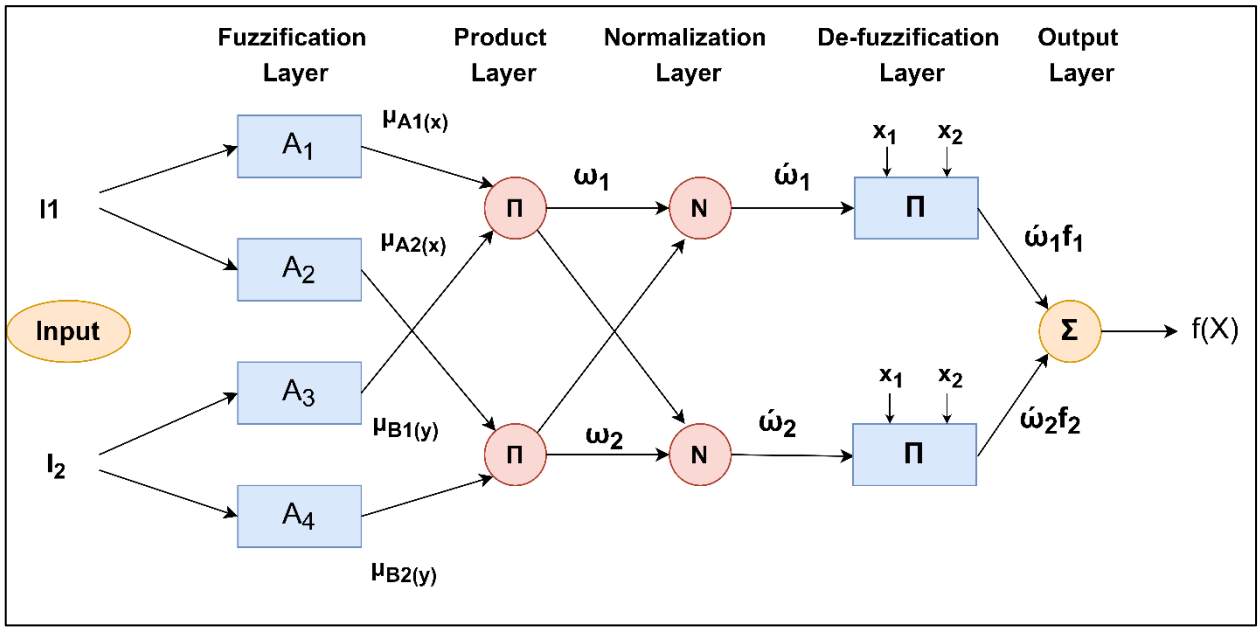

Figure 7-2 The general layout of the Adaptive neuro-fuzzy inference system

R1. If x is A1 and y is B1, then f1 = $p_1 + q_1 + r1$ (7.1)

R2. If x is A2 and y is B2, then f2 = $p_2x + q_2y + r2$ (7.2)

where x and y are inputs, Ai and Bi are membership functions, and pi, qi, and ri are output function variables.

Layer 1: In this layer, inputs have been fuzzified using an appropriate membership function. A node function can represent each node.

$$O_{1,i} = \mu_{Ai}(x) \quad \text{for i= 1,2} \tag{7.3}$$

$$O_{1,i} = \mu_{Bi-2}(y) \text{ for i = 3; 4} \tag{7.4}$$

Where x and y represent input nodes, Ai and Bi represent fuzzy sets, and (x) and (y) represent membership functions. Membership functions exist in various shapes, including general bell, triangular, trapezoidal, and Gaussian.

Layer 2: This layer is called the fire or product layer. It is the preceding component of a fuzzy rule. At this point, each node multiplies the input signals and passes the result to the node of the following layer. As an example (Equation 7.5),

$$w_i = \mu_{Ai}(x)x * \mu_{Bi}(y) \quad for\ i = 1,2 \tag{7.5}$$

Where wi denotes the firing strength of a rule at the i^{th} node.

Layer 3: This phase offers normalized firing strengths. At this step, each node computes the firing strength of the i^{th} rule using the formula below (Equation 7.6):

$$\overline{w_i} = \frac{w_i}{w_1 + w_2}, \quad i = 1,2. \tag{7.6}$$

Layer 4: The defuzzification method has been applied at this layer, sometimes referred to as the normalization layer, to produce the best possible input-output matching. Equation 7.7 represents the process of this layer.

$$Q_i^4 = \overline{w_i} f_i = \overline{w_i}\,(p_i x + q_i y + r) \tag{7.7}$$

where w_i is the previous output and pi, qi, and r are the subsequent parameters.

Layer 5: The overall output from all the signals can be represented in an output layer by Equation 7.8.

$$O_i^5 = \sum \overline{w_i} f_i = \frac{\sum_i w_i f_i}{\sum_i w_i} \tag{7.8}$$

7.3 Sludge Disposal – monitoring the fluoride concentration in the soil

Table 7-1 provides the characteristics of the soil collected from the study region. Figure 7-3 represents the pH_{pzc} curve of the studied soil. The pH_{pzc} was determined to be 8.25.

pH, F^-, and TDS were monitored for two months with an interval of 4 days, i.e., after every four days and complete drying of soil in the bucket, freshly prepared synthetic Fluoride solution was passed through the experimental contraption and physical qualities monitored.

Table 7-1 Properties of the studied sand

Soil media		
Particle size distribution	**D_{10}**	0.215
	C_c	0.811
	C_u	5.1
Void ratio 'e' (%)		13.5
Porosity 'η' (%)		11.89
Moisture content (%)		5.05
Hydraulic conductivity (cm/min)		0.0107
Specific gravity (g/cc)		2.56
Bulk density 'ρ' (g/cc)		2.14

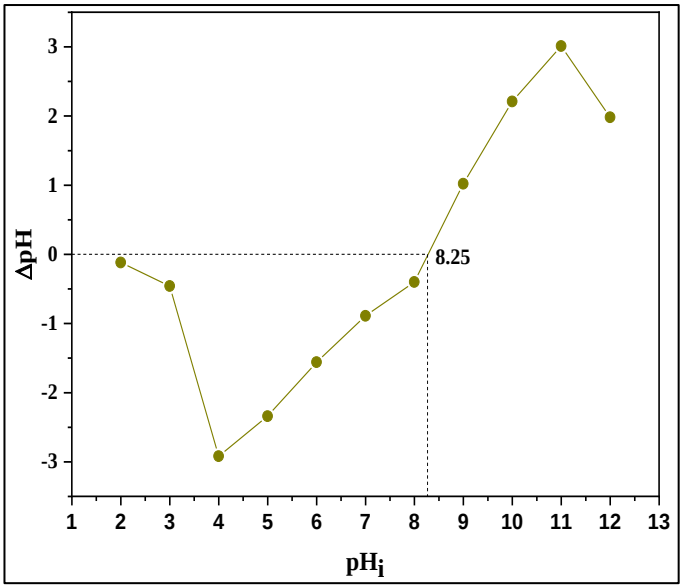

Figure 7-3 The pzc determination curve for the studied soil

The qualitative data measured over the test durations at the pre-selected depths are represented in Figures 7-4 to 7-6. B1, B2, B3, and B4 represent the four experimental setups. Figure 7-4 highlights the observed F^- concentrations. A similar pattern is observed for B1, B2, and B3, with F^- concentrations high at the 10 cm depth and reducing towards the 30 cm depth. As NaF solution is initially injected, the concentration value of F^- is highest at the inlet and gradually decreases with depth. A plausible cause might be the adsorption of F^- ions to the soil surface at the surface level, owing to the self-purifying capacity of the soil (Sharma et al., 2015).

As the depth increased, the detected F^- levels were within the threshold values of 1.5 mg/l. For B3, the F^- levels were not consistent with depth, such that, during the test duration between 10 and 20 days, the concentrations recorded at 29.5 cm were higher than the values detected at 10 cm depth. Since synthetic F^- solutions of strength 2 ppm were added to efficiently monitor contaminants, the concentrations at the 10 cm depth were consistently high.

Figure 7-5 represents the recorded pH over the test duration. No consistent pattern was observed for the set-ups, with the pH values ranging from 7.41 to 9.13. The measured TDS values are represented in Figure 7-6. While for B1 and B2, the TDS values recorded at a depth of 10 cm were higher, the opposite was observed for B3 and B4. A positive outcome was the reduced TDS levels over the test days. The TDS values reduced from 1000 mg/l to 300 mg/l. The recorded experimental values are reported in Table xiii to xv in Appendix 1.

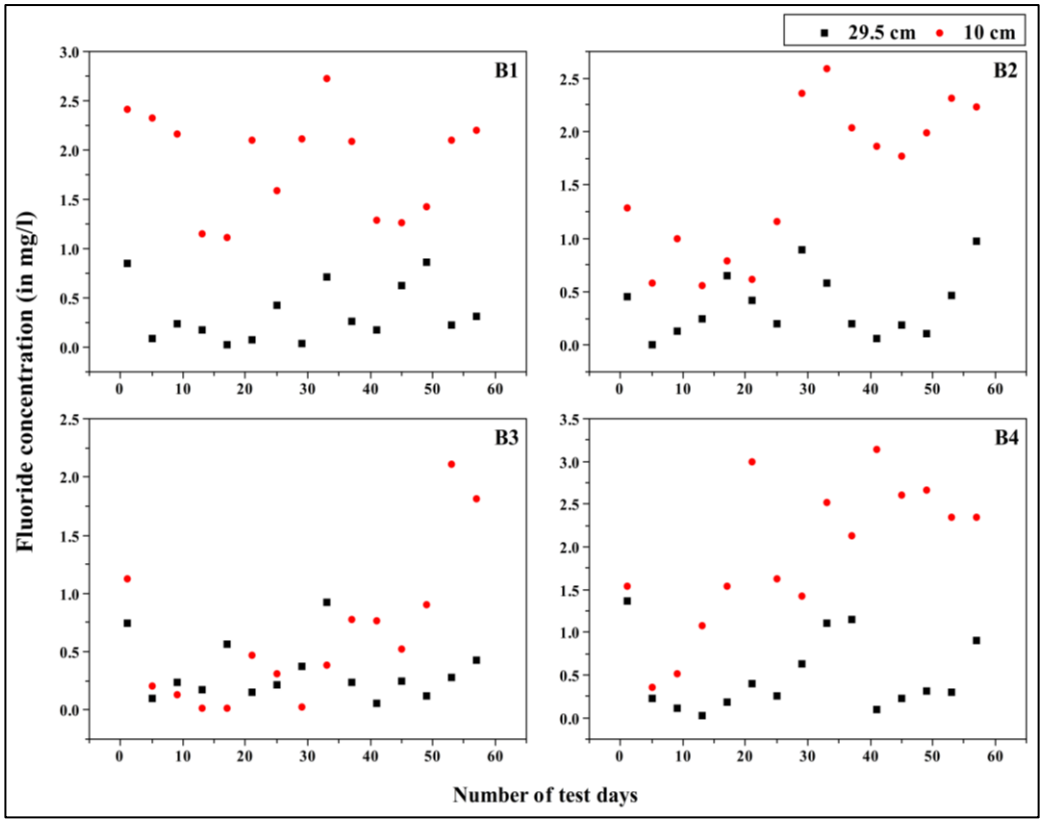

Figure 7-4 Fluoride concentration measured over the test days at varying depths

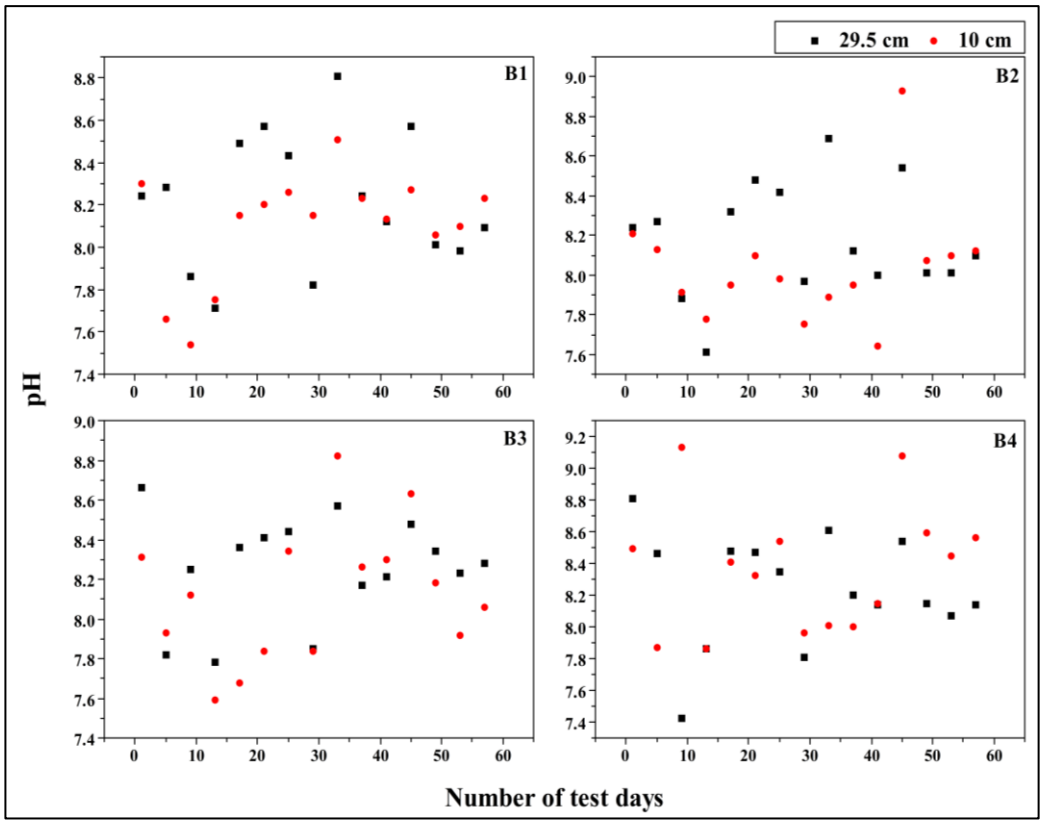

Figure 7-5 pH measured over the test days at varying depths

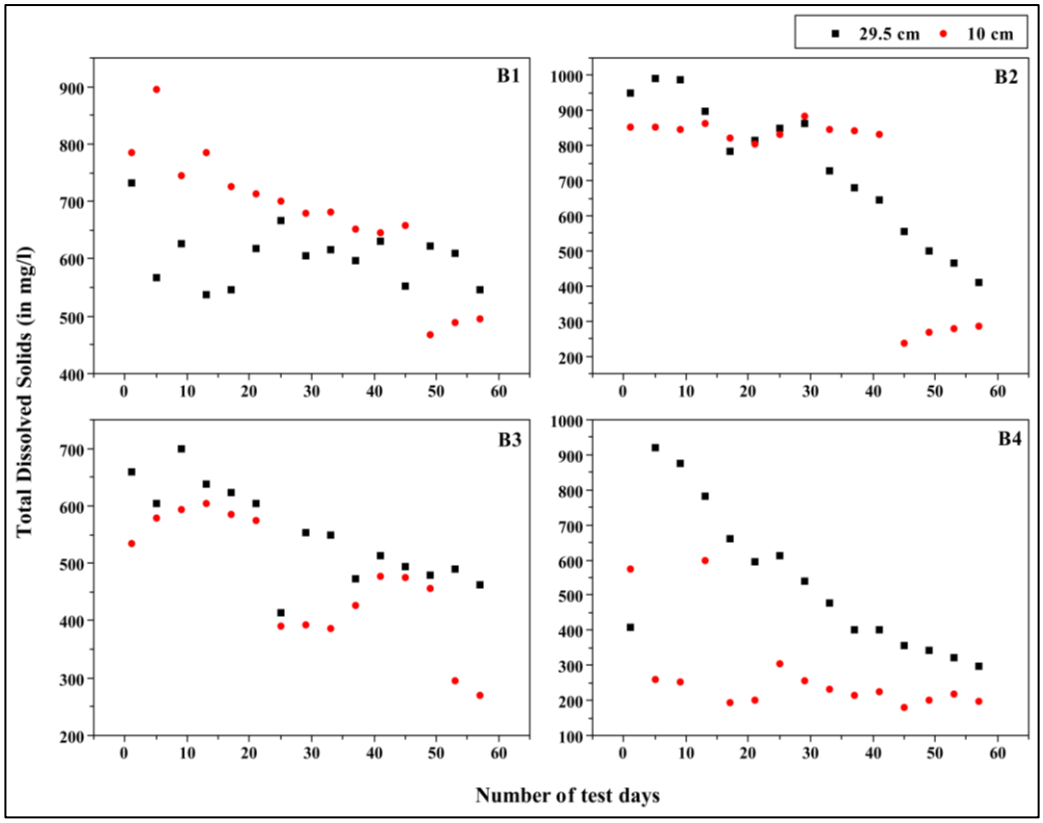

Figure 7-6 Total Dissolved Solids measured over the test days at varying depths

7.3.1 Estimating Fluoride concentration using AI models

Artificial neural network (ANN) and neuro-fuzzy inference system (ANFIS) models were used to estimate F^- concentration in the soil after the exhausted water filter plates were disposed of. Readily measurable parameters like pH and TDS were taken as input parameters. In addition, the depth of measurement and the number of test days were also considered input parameters. The determined F^- concentration was the output variable.

7.3.1.1 ANN model

The neural network toolbox was used to model F^- concentration in the soil. Of the different kinds of ANNs, the feed-forward network has seen wide usage across disciplines. In two studies, monitoring the F^- concentration and soil dispersivity, the MLP network was used (Emamgholizadeh et al., 2017; Nadiri et al., 2013). We used an MLP network with a back-propagation algorithm for the current work.

While the activation function for the hidden layer is typically a continuous and bounded nonlinear transfer function such as sigmoid and log sigmoid functions, the activation function

for the output layer is usually linear. In this study, we select hyperbolic tangent sigmoid (Tansig) for the hidden layer and linear (Purelin) for the output layer. Further, the Levenberg–Marquardt (LM) algorithm was used as a supervised training algorithm due to its superiority to other training algorithms (Daliakopoulos et al., 2005).

In this study, the input layer's four neurons corresponded to the number of test days, depth of measurement, pH, and TDS. A single neuron in the output layer represented the measured F-concentrations. However, choosing the number of neurons in the hidden layer is important to prevent underfitting or overfitting. Considering a network architecture of 4-n-1, the optimum number of neurons in the hidden layer was determined with a higher R^2 value, where R^2 measures the closeness between the data and prediction. Table 7-2 shows that the MSE value decreases with an increase in the number of neurons. However, the error continues to rise when hidden neurons are increased beyond 16. Having the lowest MSE and highest R^2 value, the 4-16-1 network architecture was selected as the optimum network, depicted in Figure 7-7. Figures 7-8a and b highlight the relationship between measured and model-predicted F^- concentrations. While the training data shows an appreciable correlation at an R^2 value of 0.843, the testing data correlates with R^2 at 0.93. The lower value of R^2 in the training stage is plausible because of data scattering (Bazoobandi et al., 2022). R^2 is the measurement of the closeness between the data and prediction. For a perfect fitting, R^2 =1 and RMSE = 0.

The optimum network was then used to simulate experimental input values. Figure 7-8c compares the experimental and predicted F^- concentrations in the soil. Except for some scattered values, i.e., 2.5 to 3 ppm, a reasonable prediction is observed.

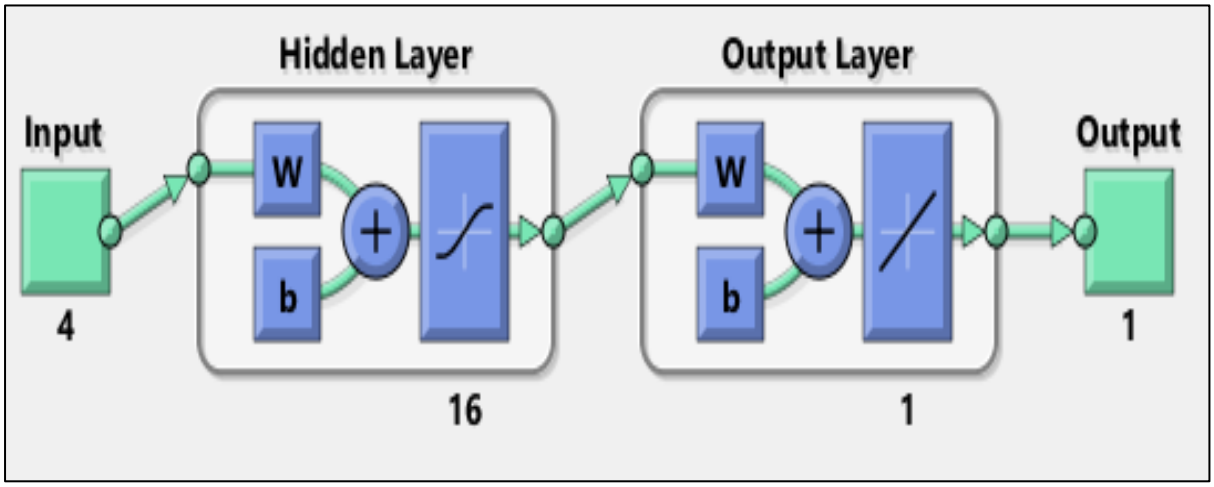

Figure 7-7 Architecture of 4-16-1 Artificial Neural Network

Table 7-2 Comparison of 20 neurons in the hidden layer for modeling Fluoride concentration in soil

Sl No	1 hidden layer Network Architechture	MSE	R^2	Linear Equation
1	4-1-1	0.389	0.732	0.47x+0.48
2	4-2-1	0.413	0.685	0.57x+0.49
3	4-3-1	0.21	0.814	0.72x+0.29
4	4-4-1	0.283	0.712	0.5x+0.42
5	4-5-1	0.18	0.807	0.63x+0.41
6	4-6-1	0.154	0.831	0.71x+0.28
7	4-7-1	0.14	0.74	0.63x+0.42
8	4-8-1	0.0742	0.872	0.78x+0.14
9	4-9-1	0.197	0.689	0.41x+0.46
10	4-10-1	0.0848	0.792	0.64x+0.37
11	4-11-1	0.0511	0.872	0.84x+0.18
12	4-12-1	0.0473	0.917	0.9x+0.093
13	4-13-1	0.0884	0.78	0.62x+0.33
14	4-14-1	0.0771	0.864	0.72x+0.42
15	4-15-1	0.0978	0.659	0.39x+0.58
16	**4-16-1**	0.00511	0.92	0.84x+0.11
17	4-17-1	0.0271	0.818	0.7x+0.3

18	4-18-1	0.0516	0.829	0.8x+0.24
19	4-19-1	0.0306	0.87	0.72x+0.28
20	4-20-1	0.0369	0.854	0.68x+0.24

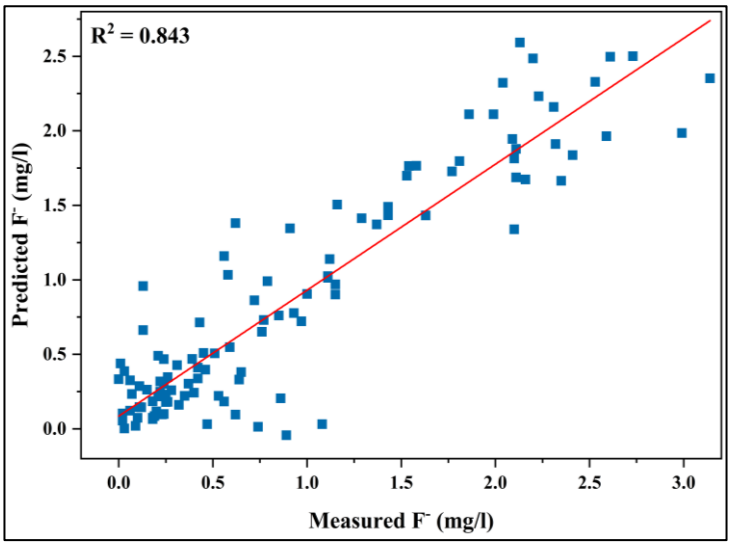

(a)

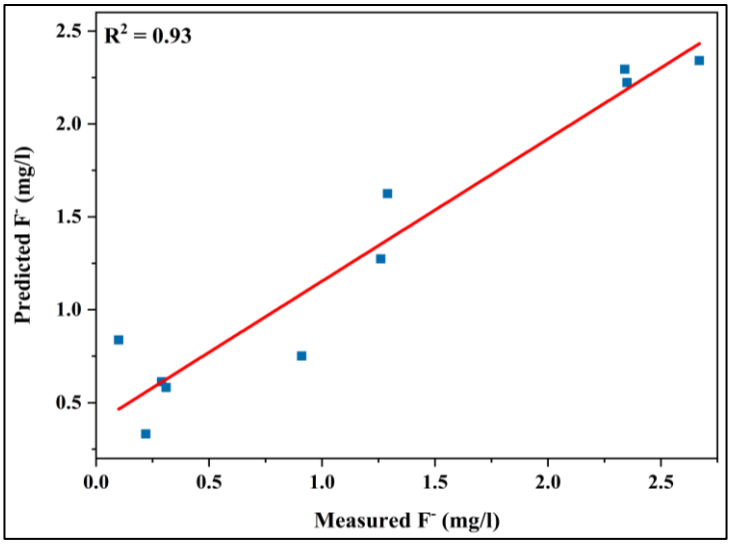

(b)

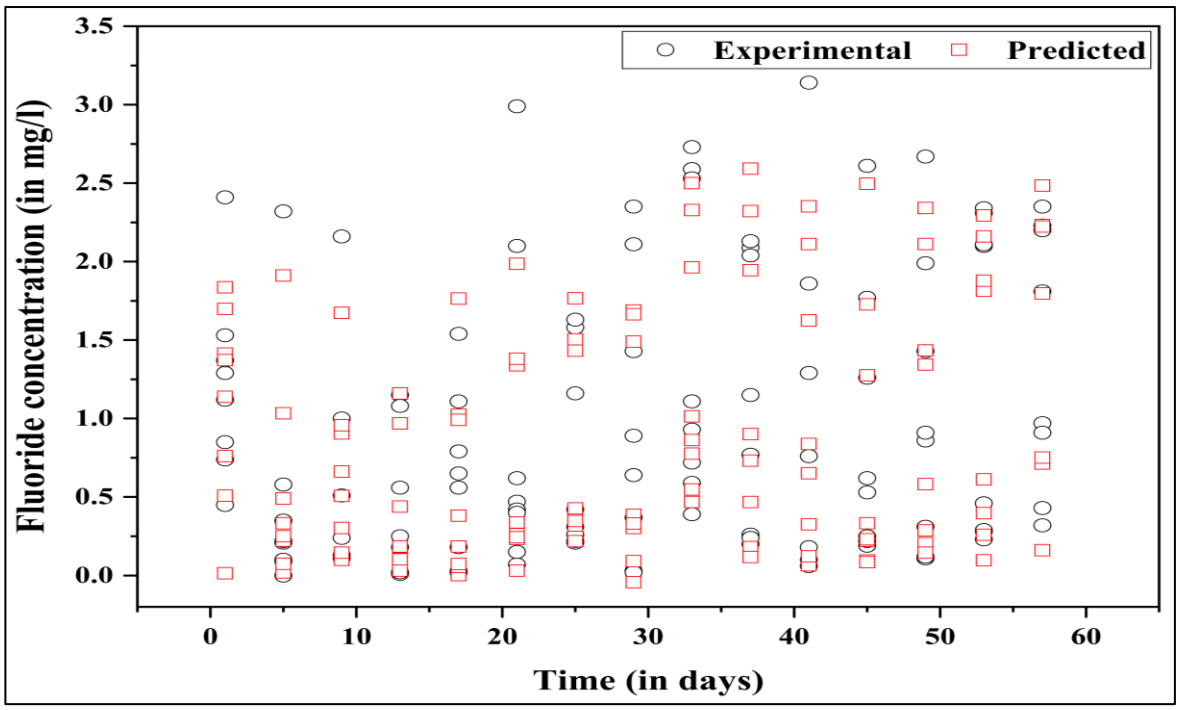

(c)

Figure 7-8 Comparison of the measured fluoride concentration to predicted fluoride concentration by ANN model in a) training step and b) test step and c) variation in observed Fluoride levels

7.3.1.2 ANFIS model

Both the constant and linear functions were tried for the output MF. 3 and 4 membership functions were evaluated for the MF types. By the trial and error method, results showed that the best configuration of the ANFIS model ran with the Triangular function, 4 MF, hybrid learning method, constant output MFs, and 20 epochs (Table 7-3). Compared to other training MFs, the triangular type performed well, considering the training and test steps' correlation coefficient and RMSE values (Kaveh et al., 2018). The structure of the Sugeno-type FIS generated by the Grid partition approach is shown in Figure 7-9.

After the optimum neuro-fuzzy model was derived, the F^- concentration was simulated. Figures 7-10a and b highlight the correlation between measured and predicted data for training and testing. The recorded R^2 was reduced for the test dataset in all observed cases attributed to data scattering. Figure 7-10c represents the simulated and experimental F^- concentrations over the test days. In comparison, the ANFIS model fared better than the ANN model in the training stage. The reverse trend was observed for the testing stage, where ANN had a higher correlation than the ANFIS model, with R^2 values at 0.93 and 0.885, respectively. The primary strength of

ANFIS is achieving minimum error by enhancing fuzzy controllers with a self-learning capability. Predicted F^- values beyond the test days of 50 are very high – 4 mg/l and above.

The computed values for F^- concentration at various depths are comparable to the experimental results, indicating that the established prediction models and parameters may adequately explain the F^- concentration and transport. Comparing Figures 7-8c and 7-10c, the ANFIS model has a greater capacity to predict the observed outcomes. Nonetheless, there are discrepancies between the experimental and predicted values for both models, which are primarily attributable to the mechanisms involved, such as adsorption, desorption, and chemical reactions during the movement of F^- with water.

Table 7-3 Results of application of different MFs in the ANFIS model

Number of MFs	MF Type	Step	Learning method	R^2	RMSE
4 4 4 4	Triangular	Train	HYBRID	0.9809	0.116
		Test		0.8851	2.946
	Trapezoidal	Train		0.9246	0.229
		Test		0.7238	42.517
	Bell-shaped	Train		0.9925	0.0726
		Test		0.3801	5.914
	Gaussian	Train		0.9915	0.077
		Test		0.7646	16.771
	Pi	Train		0.9161	0.242
		Test		0.3464	2.793
	Dsig	Train		0.9798	0.119
		Test		0.7198	16.995
	psig	Train		0.9862	0.098
		Test		0.8112	27.51

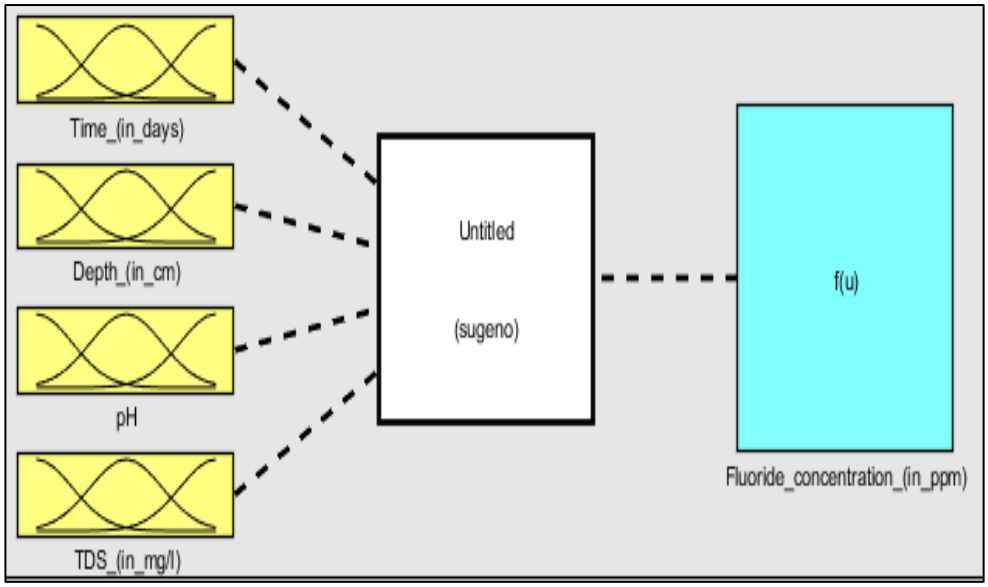

Figure 7-9 ANFIS Sugeno type structure

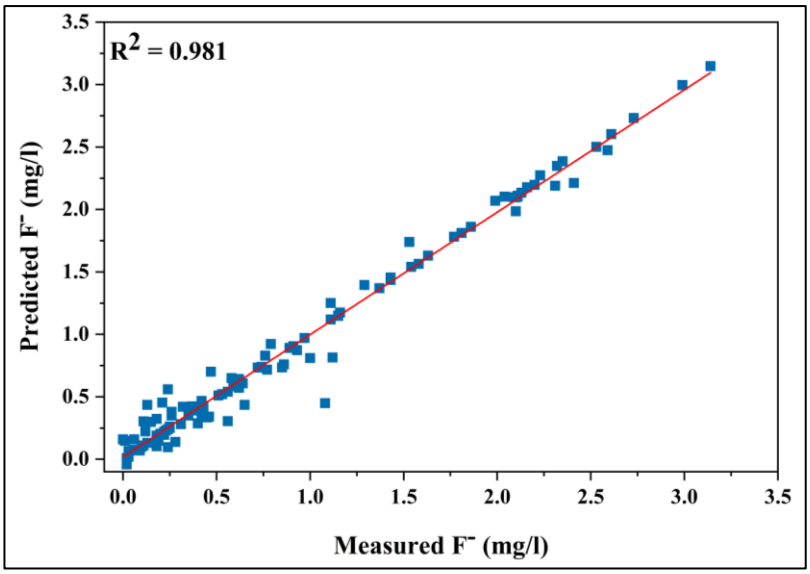

(a)

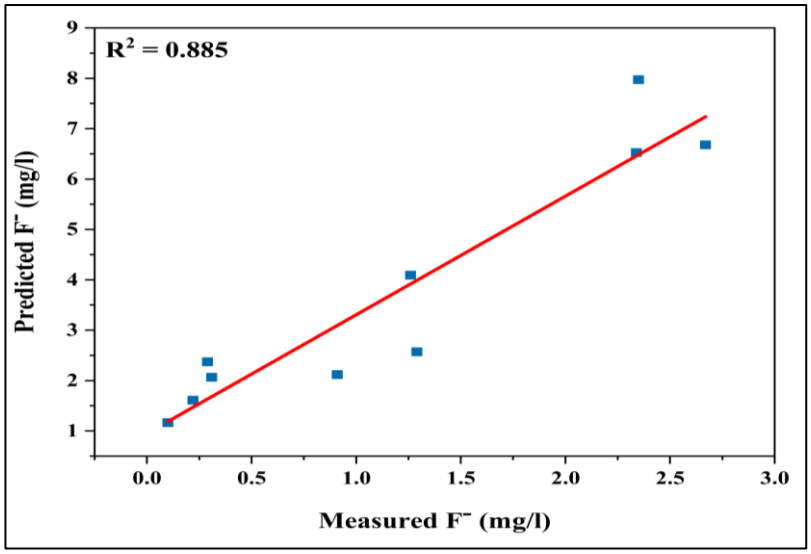

(b)

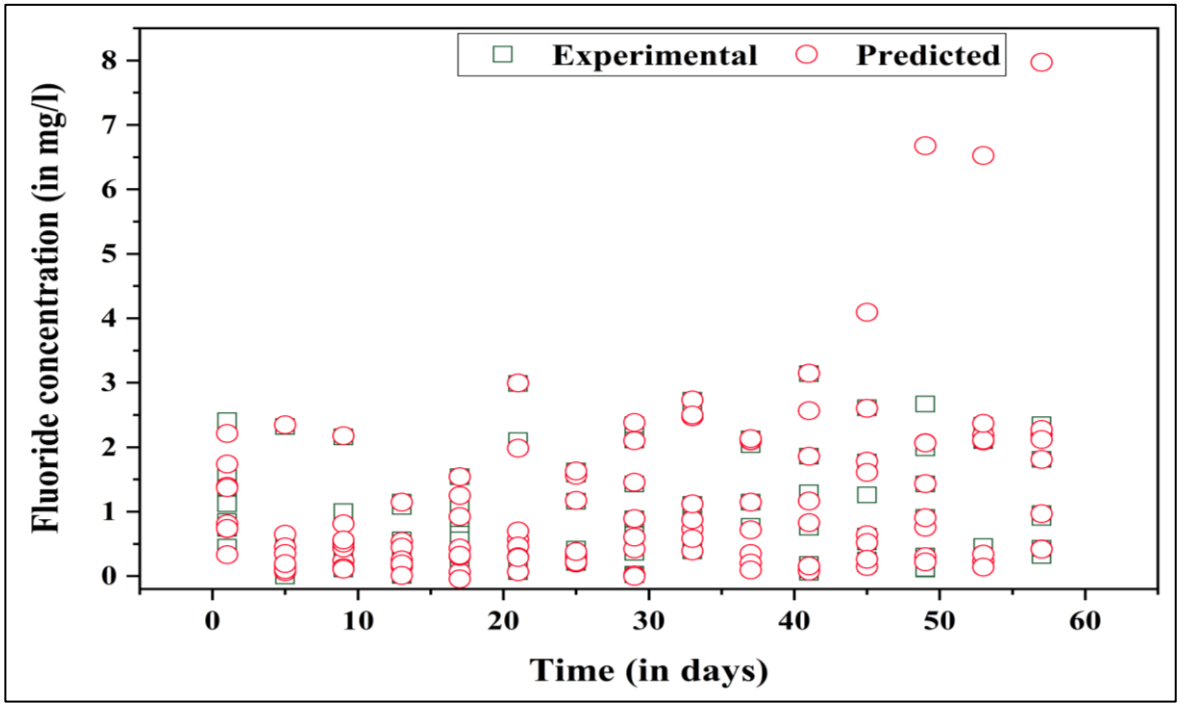

(c)

Figure 7-10 Comparison of the measured fluoride concentration to predicted fluoride concentration by ANFIS model in a) training step and b) test step and c) variation in observed Fluoride levels

Even though both models performed and can be used to monitor and predict the F^- concentrations in the test soils, more data sets will improve both models' performance. Several studies have shown the influence of multiple factors on the transportation and transformation of F^- in pore media. Since all factors have not been examined through the experimental study, leading to errors between computed and measured values (Ji-cheng, 1988).

With overall F^- concentrations reducing over the disposed soil depth, a conclusion in affirmation can be derived towards the suggested filter plate disposal method.

Chapter Summary

An experimental setup was prepared to study the variation of Fluoride concentrations in the soil profile through the increased duration of monitoring. It was noticed that the F^- concentration reduced as soil depth increased, providing insights into the soil's absorption capacity. Even with increasing test days, the F^- concentration monitored at the bottom of the test apparatus remained below the 1 mg/l threshold –an optimistic nod toward the disposal methodology selected for filter plates (in an introductory level of study). The data curated over the duration of the test fitted well with two ML algorithms: ANN and ANFIS. The models were successful in predicting the soil-fluoride concentrations.

8 CONCLUSION

A significant portion of the world's population lacks convenient access to potable water, and obtaining water requires substantial time and effort for those without access to water sources near their homes. With the advent of piped water, fetching water has only lately become entirely irrelevant in many locations from a historical standpoint. In most cases, wells and pure surface water were so close that obtaining them was not an issue. However, population increase, sustenance migration, weather fluctuations, and socioeconomic upheavals have made the everyday task of transporting water an essential public health issue for many, particularly women, in the world's poorest regions and classes.

Women and children are known to be the most common water carriers spending considerable time supplying water to their households. To and fro movements between the household and the water source can take more than an hour depending on factors such as distance to the source, the volume of water required to meet everyday demands, seasons, and household incomes.

Apart from time consumption, which is only one indicator of the price of obtaining water, caloric expenditures, factors affecting general health and quality of life, and endangering the lives of women and girls must be included when calculating the total cost of fetching water. The synergy of all factors is essential when measuring progress towards Millennium Development Goals --- increasing access to potable water and working to eradicate poverty.

This concluding chapter offers a comprehensive discussion of the conclusions derived from the preceding chapters covering the study's objectives. The chapter culminates with the investigation's limitations, followed by the intended future scope of the entire study presented in the dissertation. The current work started with the hypothesis of providing a sustainable water infrastructure system comprising water storage, treatment, and sludge disposal at a household level. A rural background was selected as the study area for the lack of sturdy water infrastructure.

The central themes identified for this research are: the experimentation and implementation of household rainwater harvesting infrastructure, the development of a novel adsorbent for fluoride remediation, low-cost filter fabrication and distribution, and subsequent disposal of sludge generated, represented sequentially in the following sections.

1. To reduce the dependence upon groundwater, alternative water resources like rainwater harvesting are a sustainable and conspicuous step toward meeting water demands. RWH is

achieved at a household level through access to a high-capacity and secure on-site water holding facility, positively favoring the lives of residents, pre-eminently women, and fostering gender equality. However, the social acceptance of RWH is sometimes impeded by financial feasibility and investment profitability. Though conventional water tanks are available for this study, suggestions and qualitative evaluations of a jute fiber-reinforced polymer (JFRP) water tank edges the research toward a green path. However, problems faced during the fabrication stage of a full-size JFRP tank shifted the sight to exploring Glass fiber-reinforced polymer as tank material. The tanks were solar-powered to advocate sustainability at the nexus of water storage and energy. The experimental analysis of the water tanks justified the performance of storage structures at par with a traditional concrete structure. Installation of an RWH structure is warranted for water demand during drier periods but would not completely eradicate dependence upon groundwater sources.

2. The study's second phase evaluates fluoride toxicity in the studied region and develops adsorbent and low-cost water filters for F^- remediation.

   The study commenced with the initial stage of identifying the water woes in the state of Rajasthan. Besides literary evidence highlighting the problem of high fluoride concentrations in groundwater and its associated toxicity, water samples from the selected study area, Hurda block in Bhilwara district, were evaluated in the public health engineering laboratory at the Birla Institute of Technology and Sciences university campus. All the water samples collected had F^- concentrations beyond the acceptable threshold of Bureau of Indian Standards, i.e., 1 mg/l. The experimental values were used to determine the Ingestion hazard quotient for F^- consumption among the inhabitants by classifying the population into age brackets with varying body weights and water ingestion rates. With an IHQ > 1, a grim situation was highlighted for all the studied villages. Further, it was observed that the group comprising young adults, primarily in the age bracket ≤ 21 years old, was more susceptible to F^- toxicity. The senior class in the age bracket ≥ 65 was equally affected by F^- toxicity.

   a. With the study area of Hurda and Chirawa Tehsil falling under the arid and semi-arid zones, the region witnesses harsh summers accompanied by low rainfall. Lack of piped water supply, intermittent power supply, and absence of robust household water infrastructure forces the inhabitants to walk great distances to collect water.
   b. The economically advantaged have the means to own private bore wells, depending upon F^- contaminated water. Upon public interaction among the villages of Jeeni, Kidwana, Dheendwa Aguna, and Ramnath Pura, from the Chirawa tehsil of District

Jhunjhunu, the problem of water scarcity was discussed. A particular issue highlighted by the habitants was the wastage of water produced by the RO units.

3. The local fauna of Rajasthan, Khejri, with immense adaptability in the region and among the residents, was deliberated to develop an adsorbent. Characterization and mechanism followed for F^- adsorption were studied through experimentations. Calcium-rich biomass, Khejri, showed removal efficiency in the ranges of 79% for synthetic conditions and between 79 to 87% for real-groundwater samples. A predictive model was developed by fitting the ML algorithms to the experimental data. Sensitivity analysis highlighted the input parameter having the highest effect on removal efficiency, i.e., adsorbent dosage.
4. The significance and usage of cement (PCWF) and ceramic (CWF) household water filters were evaluated in the following objective dealing with the fabrication of low-cost water filters. Sugarcane bagasse, potato gel, and activated carbon were used to develop novel water filters with cement and ceramic. The F- removal efficiency achieved by the filters is fair. The PCWF achieved removal efficiency of up to 88%. Further, the pore size calculated is satisfactory in removing waterborne pathogens. Manufacturing the filters is an easy process, the knowledge for which can be imparted to the local inhabitants of an area, thereby increasing public participation and reducing costs. This pilot study establishes the viability of ceramic and cement filters, PCWF in particular, as efficient HWT units.
5. The next phase of the study covers the distribution of the novel and performing PCWF. With guided instructions concerning the operation and maintenance of the PCWF, continuous dialogues with the villagers highlighted areas of development for improved application in the field. After three and six months, follow-up surveys highlighted the appreciable performance of the distributed filters.
6. Disposing the water filter plates consequent to exhaustion is a significant step towards ensuring a sustainable water system. At the initial stages of development and implementation, soil disposal was chosen as a viable option, considering the study area location. Before field implementation, soil monitoring was achieved through lab-scale experiments. Modeling F^- movement was an essential component of the study to ensure no contamination of existing groundwater resources near habitation areas. The application of ANN and ANFIS gave a well-fitted predictive model for soil-fluoride concentration.

Water security matters the most to vulnerable individuals, households, communities, and nations. Improving water infrastructure at the ground level and community participation is a milestone step toward improving water security. Engagement of local self-help groups,

awareness, and education regarding handling HWTs brings a sense of ownership among people belonging to low-income strata of society. Inclusion encourages using HWT systems to improve water quality, ultimately reducing preventable waterborne diseases and deaths, improving social lives, and empowering women and girls with increased decision-making power.

Figure 8-1 Gaps identified and methodology adopted to achieve a sustainable drinking water scheme

Limitations of the present work

The study's primary objective was to develop eco-friendly and reproducible components to enable an efficient water system while leaving a small environmental footprint. Though the thesis's multi-component approach, including the household water treatment, rainwater harvesting system, and on-site sludge disposal, was highly appreciated and accepted by the participants in the study area, limitations were highlighted with continuous dialogue during the study.

1. The water quality analysis was restricted to GFRP, JFRP, and concrete RWH. Evaluation of water quality for an extended time used for RWH construction is required.
2. Construction limitations encountered during the fabrication of the JFRP tank.
3. Using statistical models to plan experiments will reduce the number of unnecessary tests and help identify the optimal operating conditions. Co-ion interference is a factor to consider when determining an adsorbent's effectiveness.
4. A robust design will prevent breakage and damage to the designed HWTs. In-field soil-fluoride concentration measurements for disposal studies will provide insight into ground reality for fluoride transmission.

Future scope of the study

1. Microbial analysis of the water quality of the study area will ensure a comprehensive database to lay down effective policies concerning treatment.
2. Only the physicochemical analysis of the JFRP and GFRP tank water has been conducted in the study. A detailed microbial analysis of the stored water aided with forecasting models will guide to predicting the water quality for an extended time.
3. A more durable filter construction, simplicity of cleaning, and a higher discharge rate were some areas noted during the distribution and follow-up survey rounds. Effective fabrication, industrialized manufacturing, and testing can be adopted to overcome the mentioned issue.
4. By introducing novel ML and optimization methods and hybridizing existing ones, more accurate and efficient prediction models for effectual decision-making can be achieved.

REFERENCES

Aayog, N. I. T. I. (2018). Composite water management index: a tool for water management.

Abliz, D., Duan, Y., Steuernagel, L., Xie, L., Li, D., & Ziegmann, G. (2013). Curing methods for advanced polymer composites-a review. Polymers and Polymer Composites, 21(6), 341-348.

Agensi, A., Tibyangye, J., Tamale, A., Agwu, E., & Amongi, C. (2019). Contamination potentials of household water handling and storage practices in kirundo subcounty, kisoro district, Uganda. Journal of Environmental and Public Health, 2019.

Agrawal, V. K., & Bhalwar, R. (2009). Household water purification: low-cost interventions. Medical Journal Armed Forces India, 65(3), 260-263.

Agrawal, V., Vaish, A. K., & Vaish, P. (1997). Groundwater quality: focus on fluoride and fluorosis in Rajasthan. Current Science, 73(9), 743-746.

Ahmad, T., Ahmad, K., & Alam, M. (2016). Characterization of water treatment plant's sludge and its safe disposal options. Procedia Environmental Sciences, 35, 950-955.

Akkurt, S., Tayfur, G., & Can, S. (2004). Fuzzy logic model for the prediction of cement compressive strength. Cement and concrete research, 34(8), 1429-1433.

Al-Bahry, S. N., Elshafie, A. E., Victor, R., Mahmoud, I. Y., & Al-Hinai, J. A. (2011). Opportunistic pathogens relative to physicochemical factors in water storage tanks. Journal of water and health, 9(2), 382-393.

American Water Works Association. (2002). Finished Water Storage Facilities.

Ankidawa, B. A., & Tope, A. A. (2017). Design of slow sand filter technology for rural water treatment in Girei, Adamawa State, North Eastern Nigeria. Asian J Environ Ecol, 3(3), 1-7.

Antwi, E., Bensah, E. C., & Ahiekpor, J. C. (2011). Use of solar water distiller for treatment of fluoride-contaminated water: the case of Bongo district of Ghana. Desalination, 278(1-3), 333-336.

Arnold, R. D., & Wade, J. P. (2015). A definition of systems thinking: A systems approach. Procedia computer science, 44, 669-678.

Asgher, M., & Bhatti, H. N. (2012). Removal of reactive blue 19 and reactive blue 49 textile dyes by citrus waste biomass from aqueous solution: equilibrium and kinetic study. The Canadian Journal of Chemical Engineering, 90(2), 412-419.

Ayub, A., Raza, Z. A., Majeed, M. I., Tariq, M. R., & Irfan, A. (2020). Development of sustainable magnetic chitosan biosorbent beads for kinetic remediation of arsenic contaminated water. International journal of biological macromolecules, 163, 603-617.

Babu, A. N., Reddy, D. S., Kumar, G. S., Ravindhranath, K., & Mohan, G. K. (2018). Removal of lead and fluoride from contaminated water using exhausted coffee grounds based bio-sorbent. Journal of Environmental Management, 218, 602-612.

Baker, R. W. (2012). Membrane Technology and Applications (3rd ed.). Wiley.

Bashir, M., Salmiaton, A., Nourouzi, M., Azni, I., & Harun, R. (2015). Fluoride removal by chemical modification of palm kernel shell-based adsorbent: A novel agricultural waste utilization approach. Asian J. of Microbial. Biotech. Env. Sc, 17(3), 533-542.

Bazoobandi, A., Emamgholizadeh, S., & Ghorbani, H. (2022). Estimating the amount of cadmium and lead in the polluted soil using artificial intelligence models. European Journal of Environmental and Civil Engineering, 26(3), 933-951.

Benlalla, A., Elmoussaouiti, M., Cherkaoui, M., Ait Hsain, L., & Assafi, M. (2015). Characterization and valorization of drinking water sludges applied to agricultural spreading. Journal of Materials and Environmental Science, 6(6), 1692-1698.

Bhandari, N. S., & Nayal, K. (2008). Correlation study on physico-chemical parameters and quality assessment of Kosi river water, Uttarakhand. E-Journal of Chemistry, 5(2), 342-346.

Bhaumik, R., & Mondal, N. K. (2015). Adsorption of fluoride from aqueous solution by a new low-cost adsorbent: thermally and chemically activated coconut fibre dust. Clean Technologies and Environmental Policy, 17(8), 2157-2172.

Bhaumik, R., & Mondal, N. K. (2016). Optimizing adsorption of fluoride from water by modified banana peel dust using response surface modelling approach. Applied Water Science, 6(2), 115-135.

Bilgili, M., & Sahin, B. (2010). Comparative analysis of regression and artificial neural network models for wind speed prediction. Meteorology and atmospheric physics, 109(1), 61-72.

Bitew, B. D., Gete, Y. K., Biks, G. A., & Adafrie, T. T. (2018). The effect of SODIS water treatment intervention at the household level in reducing diarrheal incidence among children under 5 years of age: a cluster randomized controlled trial in Dabat district, northwest Ethiopia. Trials, 19(1), 1-15.

Bitew, B. D., Gete, Y. K., Biks, G. A., & Adafrie, T. T. (2020). Barriers and Enabling Factors Associated with the Implementation of Household Solar Water Disinfection: A Qualitative Study in Northwest Ethiopia. The American Journal of Tropical Medicine and Hygiene, 102(2), 458.

Borde, P., Elmusharaf, K., McGuigan, K. G., & Keogh, M. B. (2016). Community challenges when using large plastic bottles for Solar Energy Disinfection of Water (SODIS). BMC public health, 16(1), 1-8.

Bourgeois, J. C., Walsh, M. E., & Gagnon, G. A. (2004). Treatment of drinking water residuals: comparing sedimentation and dissolved air flotation performance with optimal cation ratios. Water Research, 38(5), 1173-1182.

Braga, R. A., & Magalhaes Jr, P. A. A. (2015). Analysis of the mechanical and thermal properties of jute and glass fiber as reinforcement epoxy hybrid composites. Materials science and engineering: C, 56, 269-273.

Brunner, N., Starkl, M., Sakthivel, P., Elango, L., Amirthalingam, S., Pratap, C. E., ... & Parimalarenganayaki, S. (2014). Policy preferences about managed aquifer recharge for securing sustainable water supply to Chennai city, India. Water, 6(12), 3739-3757.

Buragohain, M., & Mahanta, C. (2008). A novel approach for ANFIS modelling based on full factorial design. Applied soft computing, 8(1), 609-625.

Cankaya, S. (2009). A comparative study of some estimation methods for parameters and effects of outliers in simple regression model for research on small ruminants. Tropical animal health and production, 41(1), 35-41.

Carbas, R. J. C., Marques, E. A. S., Da Silva, L. F. M., & Lopes, A. M. (2014). Effect of cure temperature on the glass transition temperature and mechanical properties of epoxy adhesives. The Journal of Adhesion, 90(1), 104-119.

Çengeloğlu, Y., Kır, E., & Ersöz, M. (2002). Removal of fluoride from aqueous solution by using red mud. Separation and purification Technology, 28(1), 81-86.

Central Ground Water Board. (2010). Ground Water Quality in Shallow Aquifers of India. Ministry of Water Resources, Government of India.

Central Ground Water Board. (2013). Ground Water Scenario, Bhilwara District, Rajasthan. Retrieved from http://www.cgwb.gov.in/District_Profile/Rajasthan/Bhilwara.pdf

Central Ground Water Board. (2020). Groundwater Year Book- India 2019-20. Ministry of Jal Shakti, Department of Water Resources, River Development and Ganga Rejuvenation Government of India.

Cevik, A. (2007). Unified formulation for web crippling strength of cold-formed steel sheeting using stepwise regression. Journal of Constructional Steel Research, 63(10), 1305-1316.

Chakrabarty, S., & Sarma, H. P. (2012). Defluoridation of contaminated drinking water using neem charcoal adsorbent: kinetics and equilibrium studies. International Journal of ChemTech Research, 4(2), 511-516.

Chalchisa, D., Megersa, M., & Beyene, A. (2018). Assessment of the quality of drinking water in storage tanks and its implication on the safety of urban water supply in developing countries. Environmental Systems Research, 6(1), 1-6.

Chandramohan, D., Murali, B., Vasantha-Srinivasan, P., & Dinesh Kumar, S. (2019). Mechanical, moisture absorption, and abrasion resistance properties of bamboo–jute–glass fiber composites. Journal of Bio-and Tribo-Corrosion, 5(3), 66.

Chaney, R. L. (2012). Food safety issues for mineral and organic fertilizers. Advances in Agronomy, 117, 51-116.

Chen, M., He, F., Hu, D., Bao, C., & Huang, Q. (2020). Broadened operating pH range for adsorption/reduction of aqueous Cr (VI) using biochar from directly treated jute (Corchorus capsularis L.) fibers by H3PO4. Chemical Engineering Journal, 381, 122739.

Chia, A. M., Oniye, S. J., & Swanta, A. A. (2013). Domestic water quality assessment: microalgal and cyanobacterial contamination of stored water in plastic tanks in Zaria, Nigeria. European Journal of Scientific Research, 110(4), 501-510.

Choi, M. Y., Lee, C. G., & Park, S. J. (2022). Conversion of organic waste to novel adsorbent for fluoride removal: Efficacy and mechanism of fluoride adsorption by calcined Venerupis philippinarum Shells. Water, Air, & Soil Pollution, 233(7), 1-18.

Choubisa, S. L. (2001). Endemic fluorosis in southern Rajasthan, India. Fluoride, 34(1), 61-70.

Choubisa, S. L. (2018). Fluoride distribution in drinking groundwater in Rajasthan, India. Current Science, 1851-1857.

Chowdhury, S., Misra, R., Kushwaha, P., & Das, P. (2011). Optimum sorption isotherm by linear and nonlinear methods for safranin onto alkali-treated rice husk. Bioremediation Journal, 15(2), 77-89.

Clasen, T. F., & Cairncross, S. (2004). Household water management: refining the dominant paradigm. Tropical Medicine & International Health, 9(2), 187-191.

Clasen, T. F., Thao, D. H., Boisson, S., & Shipin, O. (2008). Microbiological effectiveness and cost of boiling to disinfect drinking water in rural Vietnam. Environmental science & technology, 42(12), 4255-4260.

Clasen, T., McLaughlin, C., Nayaar, N., Boisson, S., Gupta, R., Desai, D., & Shah, N. (2008). Microbiological effectiveness and cost of disinfecting water by boiling in semi-urban India. The American journal of tropical medicine and hygiene, 79(3), 407-413.

Conroy, R. M., Meegan, M. E., Joyce, T., McGuigan, K., & Barnes, J. (1999). Solar disinfection of water reduces diarrhoeal disease: an update. Archives of disease in childhood, 81(4), 337-338.

Cosgrove, W. J., & Loucks, D. P. (2015). Water management: Current and future challenges and research directions. Water Resources Research, 51(6), 4823-4839.

Dahhou, M., El Moussaouiti, M., El Morhit, M., Gamouh, S., & Moustahsine, S. (2017). Drinking water sludge of the Moroccan capital: statistical analysis of its environmental aspects. Journal of Taibah University for Science, 11(5), 749-758.

Daliakopoulos, I. N., Coulibaly, P., & Tsanis, I. K. (2005). Groundwater level forecasting using artificial neural networks. Journal of hydrology, 309(1-4), 229-240.

Das, B., Talukdar, J., Sarma, S., Gohain, B., Dutta, R. K., Das, H. B., & Das, S. C. (2003). Fluoride and other inorganic constituents in groundwater of Guwahati, Assam, India. Current Science, 657-661.

Dasaiah, S., Kurakalva, R. M., & Pindi, P. K. (2020). Data on fluoride concentration profile in groundwater of rural habitats in Mahabubnagar district, Telangana, India. Data in brief, 32, 106165.

Dehghani, M. H., Gholami, S., Karri, R. R., Lima, E. C., Mahvi, A. H., Nazmara, S., & Fazlzadeh, M. (2021). Process modeling, characterization, optimization, and mechanisms of fluoride adsorption using magnetic agro-based adsorbent. Journal of Environmental Management, 286, 112173.

Demelash, H., Beyene, A., Abebe, Z., & Melese, A. (2019). Fluoride concentration in ground water and prevalence of dental fluorosis in Ethiopian Rift Valley: systematic review and meta-analysis. BMC Public Health, 19(1), 1-9.

Dickin, S., Segnestam, L., & Sou Dakouré, M. (2021). Women's vulnerability to climate-related risks to household water security in Centre-East, Burkina Faso. Climate and Development, 13(5), 443-453.

Domènech, L., & Saurí, D. (2011). A comparative appraisal of the use of rainwater harvesting in single and multi-family buildings of the Metropolitan Area of Barcelona (Spain): social experience, drinking water savings and economic costs. Journal of Cleaner production, 19(6-7), 598-608.

Duhan, A., Chauhan, B. M., & Punia, D. (1992). Nutritional value of some non-conventional plant foods of India. Plant foods for human nutrition, 42(3), 193-200.

Duran, C., Ozdes, D., Gundogdu, A., & Senturk, H. B. (2011). Kinetics and isotherm analysis of basic dyes adsorption onto almond shell (Prunus dulcis) as a low cost adsorbent. Journal of Chemical & Engineering Data, 56(5), 2136-2147.

Dutta, S., & Gupta, J. P. (2010). PVT correlations for Indian crude using artificial neural networks. Journal of Petroleum Science and Engineering, 72(1-2), 93-109.

Emamgholizadeh, S., Bahman, K., Bateni, S. M., Ghorbani, H., Marofpoor, I., & Nielson, J. R. (2017). Estimation of soil dispersivity using soft computing approaches. Neural Computing and Applications, 28(1), 207-216.

Eshraghi, F., Motavassel, M., Roozbehani, B., & Fard, N. J. H. (2016). Cadmium Removal from Aqueous Solution by Prosopis Cineraria Leaf Ash (PCLA). American Journal of Oil and Chemical Technologies: Volume, 4(4).

Evison, L., & Sunna, N. (2001). Microbial regrowth in household water storage tanks. Journal-American Water Works Association, 93(9), 85-94.

Fan, M., Hu, J., Cao, R., Xiong, K., & Wei, X. (2017). Modeling and prediction of copper removal from aqueous solutions by nZVI/rGO magnetic nanocomposites using ANN-GA and ANN-PSO. Scientific reports, 7(1), 1-14.

Fan, M., Li, T., Hu, J., Cao, R., Wei, X., Shi, X., & Ruan, W. (2017). Artificial neural network modeling and genetic algorithm optimization for cadmium removal from aqueous solutions by reduced graphene oxide-supported nanoscale zero-valent iron (nZVI/rGO) composites. Materials, 10(5), 544.

Farrow, C., McBean, E., Huang, G., Yang, A., Wu, Y., Liu, Z., ... & Li, Y. (2018). Ceramic water filters: a point-of-use water treatment technology to remove bacteria from drinking water in Longhai City, Fujian Province, China. Journal of Environmental Informatics, 32(2), 63-68.

Freni, G., & Liuzzo, L. (2019). Effectiveness of rainwater harvesting systems for flood reduction in residential urban areas. Water, 11(7), 1389.

Gadgil, A. (1998). Drinking water in developing countries. Annual review of energy and the environment, 23(1), 253-286.

García-Ávila, F., Zhindón-Arévalo, C., Valdiviezo-Gonzales, L., Cadme-Galabay, M., Gutiérrez-Ortega, H., & del Pino, L. F. (2022). A comparative study of water quality using two quality indices and a risk index in a drinking water distribution network. Environmental Technology Reviews, 11(1), 49-61.

Garg, V. K., Kumar, R., & Gupta, R. (2004). Removal of malachite green dye from aqueous solution by adsorption using agro-industry waste: a case study of Prosopis cineraria. Dyes and pigments, 62(1), 1-10.

Gebrewold, B. D., Kijjanapanich, P., Rene, E. R., Lens, P. N. L., & Annachhatre, A. P. (2019). Fluoride removal from groundwater using chemically modified rice husk and corn cob activated carbon. Environmental Technology, 40(22), 2913–2927.

Getachew, T., Hussen, A., & Rao, V. M. (2015). Defluoridation of water by activated carbon prepared from banana (Musa paradisiaca) peel and coffee (Coffea arabica) husk. International Journal of Environmental Science and Technology, 12(6), 1857-1866.

Gevrey, M., Dimopoulos, I., & Lek, S. (2003). Review and comparison of methods to study the contribution of variables in artificial neural network models. Ecological modelling, 160(3), 249-264.

Ghaedi, A. M., Ghaedi, M., Pouranfard, A. R., Ansari, A., Avazzadeh, Z., Vafaei, A., ... & Gupta, V. K. (2016). Adsorption of Triamterene on multi-walled and single-walled carbon nanotubes: Artificial neural network modeling and genetic algorithm optimization. Journal of Molecular Liquids, 216, 654-665.

GhaffarianHoseini, A., Tookey, J., GhaffarianHoseini, A., Yusoff, S. M., & Hassan, N. B. (2016). State of the art of rainwater harvesting systems towards promoting green built environments: a review. Desalination and Water Treatment, 57(1), 95-104.

Ghisi, E., Montibeller, A., & Schmidt, R. W. (2006). Potential for potable water savings by using rainwater: An analysis over 62 cities in southern Brazil. Building and Environment, 41(2), 204-210.

Ghorai, S., & Pant, K. K. (2005). Equilibrium, kinetics and breakthrough studies for adsorption of fluoride on activated alumina. Separation and purification technology, 42(3), 265-271.

Ghosal, P. S., & Gupta, A. K. (2016). Enhanced efficiency of ANN using non-linear regression for modeling adsorptive removal of fluoride by calcined Ca-Al-(NO3)-LDH. Journal of Molecular Liquids, 222, 564-570.

Ghosh, D., Sinha, M. K., & Purkait, M. K. (2013). A comparative analysis of low-cost ceramic membrane preparation for effective fluoride removal using hybrid technique. Desalination, 327, 2-13.

Goh, A. T. (1995). Back-propagation neural networks for modeling complex systems. Artificial intelligence in engineering, 9(3), 143-151.

Goyal, M. K., & Surampalli, R. Y. (2018). Impact of climate change on water resources in India. Journal of Environmental Engineering, 144(7), 04018054.

Graham, J. P., & VanDerslice, J. (2007). The effectiveness of large household water storage tanks for protecting the quality of drinking water. Journal of Water and Health, 5(2), 307-313.

Graham, J. P., Hirai, M., & Kim, S. S. (2016). An analysis of water collection labor among women and children in 24 sub-Saharan African countries. PloS one, 11(6), e0155981.

Granbohm, H., Kulmala, K., Iyer, A., Ge, Y., & Hannula, S. P. (2017). Preparation and photocatalytic activity of quaternary GO/TiO2/Ag/AgCl nanocomposites. Water, Air, & Soil Pollution, 228(4), 1-16.

Gray, N. F. (2014). Filtration methods. In Microbiology of Waterborne Diseases (pp. 631-650). Academic Press.

Grey, D., Garrick, D., Blackmore, D., Kelman, J., Muller, M., & Sadoff, C. (2013). Water security in one blue planet: twenty-first century policy challenges for science. Philosophical Transactions of the Royal Society A: Mathematical, Physical and Engineering Sciences, 371(2002), 20120406.

Gupta, M. K., Srivastava, R. K., & Bisaria, H. (2015). Potential of jute fibre reinforced polymer composites: a review. Int. J. Fiber Text. Res, 5(3), 30-38.

Gupta, R. (2020). Water Purifying Bio-concrete. Advanced Materials Letters, 11(7), 1-5.

Hardis, R. (2012). Cure kinetics characterization and monitoring of an epoxy resin for thick composite structures (Doctoral dissertation, Iowa State University).

Hardis, R., Jessop, J. L., Peters, F. E., & Kessler, M. R. (2013). Cure kinetics characterization and monitoring of an epoxy resin using DSC, Raman spectroscopy, and DEA. Composites Part A: Applied Science and Manufacturing, 49, 100-108.

Haykin, S. (1994). Neural networks. A comprehensive foundation.

Heil, D. M., & Barbarick, K. A. (1990). Water Treatment Sludge Influence on the Growth of Sorghum-Sudangrass. Journal of Environmental Quality, 19(1), 161-161.

Hou, D., Wang, J., Zhao, C., Wang, B., Luan, Z., & Sun, X. (2010). Fluoride removal from brackish groundwater by direct contact membrane distillation. Journal of Environmental Sciences, 22(12), 1860-1867.

Huang, G., & Sun, H. (2007). Effect of water absorption on the mechanical properties of glass/polyester composites. Materials & design, 28(5), 1647-1650.

Hussain, J., Husain, I., & Arif, M. (2013). Fluoride contamination in groundwater of central Rajasthan, India and its toxicity in rural habitants. Toxicological & Environmental Chemistry, 95(6), 1048-1055.

Hussain, J., Hussain, I., & Sharma, K. C. (2010). Fluoride and health hazards: community perception in a fluorotic area of central Rajasthan (India): an arid environment. Environmental monitoring and assessment, 162(1), 1-14.

Huston, R., Chan, Y. C., Gardner, T., Shaw, G., & Chapman, H. (2009). Characterisation of atmospheric deposition as a source of contaminants in urban rainwater tanks. Water research, 43(6), 1630-1640.

Indana, M. K., Gangapuram, B. R., Dadigala, R., Bandi, R., & Guttena, V. (2016). A novel green synthesis and characterization of silver nanoparticles using gum tragacanth and evaluation of their potential catalytic reduction activities with methylene blue and Congo red dyes. Journal of Analytical Science and Technology, 7(1), 1-9.

IS10500, B. I. S. (2012). Indian standard drinking water–specification (second revision). Bureau of Indian Standards (BIS), New Delhi.

Islam, M., & Patel, R. (2011). Thermal activation of basic oxygen furnace slag and evaluation of its fluoride removal efficiency. Chemical engineering journal, 169(1-3), 68-77.

Izquierdo-Vega, J. A., Sánchez-Gutiérrez, M., & Del Razo, L. M. (2008). Decreased in vitro fertility in male rats exposed to fluoride-induced oxidative stress damage and mitochondrial transmembrane potential loss. Toxicology and applied pharmacology, 230(3), 352-357.

Jagtap, S., Yenkie, M. K., Labhsetwar, N., & Rayalu, S. (2012). Fluoride in drinking water and defluoridation of water. Chemical reviews, 112(4), 2454-2466.

Jana, S., Saikia, A., Purkait, M. K., & Mohanty, K. (2011). Chitosan based ceramic ultrafiltration membrane: Preparation, characterization and application to remove Hg (II) and As (III) using polymer enhanced ultrafiltration. Chemical engineering journal, 170(1), 209-219.

Jha, B. M., & Sinha, S. K. (2009). Towards better management of ground water resources in India. QJ, 24(4), 1-20.

Jha, S. K., Mishra, V. K., Sharma, D. K., & Damodaran, T. (2011). Fluoride in the environment and its metabolism in humans. Reviews of Environmental Contamination and Toxicology Volume 211, 121-142.

Ji-cheng, Z. H. U. (1988). Preliminary study on transport and transformation of fluorine pollution in groundwater,[J]. Environmental Chemistry, 7(3), 62-66.

Joglekar, A. M., & May, A. T. (1987). Product excellence through design of experiments. Cereal foods world, 32(12), 857.

Johnke, B. (1992). Waste incineration—an important element of the integrated waste management system in Germany. Waste management & research, 10(4), 303-315.

Joo, S. H., & Tansel, B. (2015). Novel technologies for reverse osmosis concentrate treatment: A review. Journal of Environmental Management, 150, 322-335.

Kabir, A. E., Chakraborty, T. K., & Ghosh, G. C. (2016). Bio-Sand Filter (BSF): A simple water treatment device for safe drinking water supply and to promote health in Hazard prone hard-to-reach coastal areas of Bangladesh. American Journal of Environmental Protection, 5(5), 107-112.

Kabir, M. M., Wang, H., Lau, K. T., & Cardona, F. (2012). Chemical treatments on plant-based natural fibre reinforced polymer composites: An overview. Composites Part B: Engineering, 43(7), 2883-2892.

Kagne, S., Jagtap, S., Dhawade, P., Kamble, S. P., Devotta, S., & Rayalu, S. S. (2008). Hydrated cement: a promising adsorbent for the removal of fluoride from aqueous solution. Journal of hazardous materials, 154(1-3), 88-95.

Kaoud, H., & Kalifa, B. (2010). Effect of fluoride, cadmium and arsenic intoxication on brain and learning–memory ability in rats. Toxicology Letters, (196), S53.

Kaushal, A., & Singh, S. K. (2017). Critical analysis of adsorption data statistically. Applied Water Science, 7(6), 3191-3196.

Kaveh, M., Sharabiani, V. R., Chayjan, R. A., Taghinezhad, E., Abbaspour-Gilandeh, Y., & Golpour, I. (2018). ANFIS and ANNs model for prediction of moisture diffusivity and specific energy consumption potato, garlic and cantaloupe drying under convective hot air dryer. Information Processing in Agriculture, 5(3), 372-387.

Khan, M. M. R., Arif, R. B., Siddique, M. A. B., & Oishe, M. R. (2018, September). Study and observation of the variation of accuracies of KNN, SVM, LMNN, ENN algorithms on eleven different datasets from UCI machine learning repository. In 2018 4th International Conference on Electrical Engineering and Information & Communication Technology (iCEEiCT) (pp. 124-129). IEEE.

Khandare, A. L., Validandi, V., Rajendran, A., Singh, T. G., Thingnganing, L., Kurella, S., ... & Maddela, Y. (2020). Health risk assessment of heavy metals and strontium in

groundwater used for drinking and cooking in 58 villages of Prakasam district, Andhra Pradesh, India. Environmental Geochemistry and Health, 42(11), 3675-3701.

Kim, H. G., Park, C., Yang, J., Lee, B., Kim, S. S., & Kim, S. (2007). Optimization of backflushing conditions for ceramic ultrafiltration membrane of disperse dye solutions. Desalination, 202(1-3), 150-155.

King, P., Rakesh, N., Beenalahari, S., Kumar, Y. P., & Prasad, V. S. R. K. (2007). Removal of lead from aqueous solution using Syzygium cumini L.: equilibrium and kinetic studies. Journal of Hazardous Materials, 142(1-2), 340-347.

Kline, P. (2009). How Can We Dispose of Membrane Waste?. Opflow, 35(4), 6-7.

Kongparakul, S., Kornprasert, S., Suriya, P., Le, D., Samart, C., Chantarasiri, N., ... & Guan, G. (2017). Self-healing hybrid nanocomposite anticorrosive coating from epoxy/modified nanosilica/perfluorooctyl triethoxysilane. Progress in Organic Coatings, 104, 173-179.

Kothari, C. R. (2004). Research methodology: Methods and techniques. New Age International.

Kothari, V., Vij, S., Sharma, S., & Gupta, N. (2021). Correlation of various water quality parameters and water quality index of districts of Uttarakhand. Environmental and Sustainability Indicators, 9, 100093.

Krauss, G., Kindangen, J. I., & Depecker, P. (1997). Using artificial neural networks to predict interior velocity coefficients. Building and environment, 32(4), 295-303.

Krishnan, P. R., & Jindal, S. K. (2015). Khejri, the king of Indian Thar desert is under phenophase change. Current Science, 108(11), 1987-1990.

Kumar, M. D., Ghosh, S., Patel, A., Singh, O. P., & Ravindranath, R. (2006). Rainwater harvesting in India: some critical issues for basin planning and research. Land Use and Water Resources Research, 6(1732-2016-140267).

Kumar, M., Goswami, R., Patel, A. K., Srivastava, M., & Das, N. (2020). Scenario, perspectives and mechanism of arsenic and fluoride co-occurrence in the groundwater: a review. Chemosphere, 249, 126126.

Kumar, R., Singh, R. D., & Sharma, K. D. (2005). Water resources of India. Current science, 794-811.

Kurmi, O., & Ayres, J. (2010). Indoor air pollution in developing countries. Environmental Medicine, 191.

Lantagne, D. S., Quick, R., & Mintz, E. D. (2006). Household water treatment and safe: storage options in developing countries. Navig, 99, 17-38.

Lawler, W., Bradford-Hartke, Z., Cran, M. J., Duke, M., Leslie, G., Ladewig, B. P., & Le-Clech, P. (2012). Towards new opportunities for reuse, recycling and disposal of used reverse osmosis membranes. Desalination, 299, 103-112.

Laxmankumar, D., Satyanarayana, E., Dhakate, R., & Saxena, P. R. (2019). Hydrogeochemical characteristics with respect to fluoride contamination in groundwater of Maheshwarm mandal, RR district, Telangana state, India. Groundwater for Sustainable Development, 8, 474-483.

Lee, J. I., Kang, J. K., Hong, S. H., Lee, C. G., Jeong, S., & Park, S. J. (2021). Thermally treated Mytilus coruscus shells for fluoride removal and their adsorption mechanism. Chemosphere, 263, 128328.

Leman, Z., Sapuan, S. M., Saifol, A. M., Maleque, M. A., & Ahmad, M. M. H. M. (2008). Moisture absorption behavior of sugar palm fiber reinforced epoxy composites. Materials & Design, 29(8), 1666-1670.

Li, X., Tabil, L. G., & Panigrahi, S. (2007). Chemical treatments of natural fiber for use in natural fiber-reinforced composites: a review. Journal of Polymers and the Environment, 15(1), 25-33.

Loganathan, C., & Girija, K. V. (2013). Cancer classification using adaptive neuro fuzzy inference system with runge kutta learning. International Journal of Computer Applications, 79(4).

Luby, S. E., Syed, A. H., Atiullah, N., Faizan, M. K., & Fisher-Hoch, S. (2000). Limited effectiveness of home drinking water purification efforts in Karachi, Pakistan. International Journal of Infectious Diseases, 4(1), 3-7.

Lupia, F., & Pulighe, G. (2015). Water use and urban agriculture: Estimation and water saving scenarios for residential kitchen gardens. Agriculture and agricultural science procedia, 4, 50-58.

Madaeni, S. S., Hasankiadeh, N. T., & Tavakolian, H. R. (2012). Modeling and optimization of membrane chemical cleaning by artificial neural network, fuzzy logic, and genetic algorithm. Chemical Engineering Communications, 199(3), 399-416.

Madhav, S., Ahamad, A., Singh, A. K., Kushawaha, J., Chauhan, J. S., Sharma, S., & Singh, P. (2020). Water pollutants: sources and impact on the environment and human health. Sensors in Water Pollutants Monitoring: Role of Material, 43-62.

Maguire, A. (2014). ADA clinical recommendations on topical fluoride for caries prevention. Evidence-based dentistry, 15(2), 38-39.

Maheshwari, R. C. (2006). Fluoride in drinking water and its removal. Journal of Hazardous materials, 137(1), 456-463.

Mahramanlioglu, M. E. H. M. E. T., Kizilcikli, I., & Bicer, I. O. (2002). Adsorption of fluoride from aqueous solution by acid treated spent bleaching earth. Journal of Fluorine Chemistry, 115(1), 41-47.

Mala, R. (2009). Nutrient content of important fruit trees from arid zone of Rajasthan. Journal of Horticulture and Forestry, 1(7), 103-108.

Manahan, S. E. (2002). Toxicological chemistry and biochemistry. CRC Press.

Manga, M., Ngobi, T. G., Okeny, L., Acheng, P., Namakula, H., Kyaterekera, E., ... & Kibwami, N. (2021). The effect of household storage tanks/vessels and user practices on the quality of water: a systematic review of literature. Environmental Systems Research, 10(1), 1-26.

Mathur, V. K. (2006). Composite materials from local resources. Construction and Building materials, 20(7), 470-477.

McCulloch, W. S., & Pitts, W. (1943). A logical calculus of the ideas immanent in nervous activity. The bulletin of mathematical biophysics, 5, 115-133.

Meadows, D. H. (2008). Thinking in Systems Overview. Retrieved from https://www.cdc.gov/policy/polaris/tis/index.html

Melidis, P., Akratos, C. S., Tsihrintzis, V. A., & Trikilidou, E. (2007). Characterization of rain and roof drainage water quality in Xanthi, Greece. Environmental monitoring and assessment, 127(1), 15-27.

Melville-Shreeve, P., Ward, S., & Butler, D. (2016). Rainwater harvesting typologies for UK houses: a multi criteria analysis of system configurations. Water, 8(4), 129.

Meng, X., Korfiatis, G. P., Christodoulatos, C., & Bang, S. (2001). Treatment of arsenic in Bangladesh well water using a household co-precipitation and filtration system. Water research, 35(12), 2805-2810.

Mikalsen, T. (2005). Causes of increased total dissolved solids and conductivity levels in urban streams in Georgia. Georgia Institute of Technology.

Milly, P. C., Betancourt, J., Falkenmark, M., Hirsch, R. M., Kundzewicz, Z. W., Lettenmaier, D. P., & Stouffer, R. J. (2008). Stationarity is dead: Whither water management?. Science, 319(5863), 573-574.

Mohamed, H. M., & Benmokrane, B. (2014). Design and performance of reinforced concrete water chlorination tank totally reinforced with GFRP bars: Case study. Journal of Composites for Construction, 18(1), 05013001.

Mohammed, L., Ansari, M. N., Pua, G., Jawaid, M., & Islam, M. S. (2015). A review on natural fiber reinforced polymer composite and its applications. International journal of polymer science, 2015.

Mohanan, N., Manju, E., & Sonia, J. (2017). The effect of different types of storage vessels on water quality. International Journal of Innovative Research in Science, Engineering and Technology, 6(10), 20362-20368.

Mondal, N. K., Bhaumik, R., Baur, T., Das, B., Roy, P., & Datta, J. K. (2012). Studies on defluoridation of water by tea ash: an unconventional biosorbent. Chemical Science Transactions, 1(2), 239-256.

Mondal, N. K., Bhaumik, R., Sen, K., & Debnath, P. (2022). Adsorption of fluoride in aqueous solutions using saline water algae (Rhodophyta sp.): an insight into isotherm, kinetics, thermodynamics and optimization studies. Modeling Earth Systems and Environment, 8(3), 3507-3521.

Moran Ayala, L. I., Paquet, M., Janowska, K., Jamard, P., Quist-Jensen, C. A., Bosio, G. N., ... & Boffa, V. (2018). Water defluoridation: nanofiltration vs membrane distillation. Industrial & Engineering Chemistry Research, 57(43), 14740-14748.

Mueller, B., Dangol, B., Ngai, T. K., & Hug, S. J. (2021). Kanchan arsenic filters in the lowlands of Nepal: mode of operation, arsenic removal, and future improvements. Environmental Geochemistry and Health, 43(1), 375-389.

Muralidharan, D., Nair, A. P., & Sathyanarayana, U. (2002). Fluoride in shallow aquifers in Rajgarh Tehsil of Churu District, Rajasthan–an arid environment. Current Science, 83(6), 699-702.

Musz-Pomorska, A., Widomski, M. K., & Gołębiowska, J. (2020). Financial sustainability of selected rain water harvesting systems for single-family house under conditions of eastern Poland. Sustainability, 12(12), 4853.

Mutemi, S., Hoko, Z., & Makurira, H. (2020). Investigating feasibility of use of bio-sand filters for household water treatment in Epworth, Zimbabwe. Physics and Chemistry of the Earth, Parts A/b/c, 117, 102864.

Mutsvangwa, C., & Matope, E. (2017). Use of an external organic carbon source in the removal of nitrates in bio-sand filters (BSFs). Drinking Water Engineering and Science, 10(2), 119-127.

Naddeo, V., Scannapieco, D., & Belgiorno, V. (2013). Enhanced drinking water supply through harvested rainwater treatment. Journal of hydrology, 498, 287-291.

Nadiri, A. A., Fijani, E., Tsai, F. T. C., & Asghari Moghaddam, A. (2013). Supervised committee machine with artificial intelligence for prediction of fluoride concentration. Journal of Hydroinformatics, 15(4), 1474-1490.

Naik, R. G., Dodamani, A. S., Vishwakarma, P., Jadhav, H. C., Khairnar, M. R., Deshmukh, M. A., & Wadgave, U. (2017). Level of fluoride in soil, grain and water in Jalgaon district, Maharashtra, India. Journal of Clinical and Diagnostic Research: JCDR, 11(2), ZC05.

Nanseu-Njiki, C. P., Gwenzi, W., Pengou, M., Rahman, M. A., & Noubactep, C. (2019). Fe0/H2O filtration systems for decentralized safe drinking water: Where to from here?. Water, 11(3), 429.

Natarajan, R., & Manivasagan, R. (2020). Effect of operating parameters on dye wastewater treatment using Prosopis cineraria and kinetic modeling. Environmental Engineering Research, 25(5), 788-793.

National Research Council. (1983). Risk assessment in the federal government: Managing the process. Washington, DC: National Academy Press.

Nayak, S., & Mohanty, J. R. (2019). Influence of chemical treatment on tensile strength, water absorption, surface morphology, and thermal analysis of areca sheath fibers. Journal of Natural Fibers, 16(4), 589-599.

Nethaji, S., & Sivasamy, A. (2014). Removal of hexavalent chromium from aqueous solution using activated carbon prepared from walnut shell biomass through alkali impregnation processes. Clean Technologies and Environmental Policy, 16(2), 361-368.

Newberry, A. L., & Putri, G. (2005). World's largest FRP acid storage tanks. Reinforced plastics, 49(10), 26-29.

Ngai, T. K., Shrestha, R. R., Dangol, B., Maharjan, M., & Murcott, S. E. (2007). Design for sustainable development—Household drinking water filter for arsenic and pathogen treatment in Nepal. Journal of Environmental Science and Health, Part A, 42(12), 1879-1888.

Nguyen, L., Hoa, T. M., Bashir, M., Eppe, G., Avti, P., & Nguyen, T. T. (2021). Removal of phosphate from wastewater using coal slag. International Journal of Environmental Analytical Chemistry, 101(15).

Nie, S., Zhong, X., Song, J., Tu, G., & Chen, C. (2022). Experimental study on hydraulic fracturing in clayey-silty hydrate-bearing sediments and fracability evaluation based on multilayer perceptron-analytic hierarchy process. Journal of Natural Gas Science and Engineering, 106, 104735.

Nnaji, C. C., Nnaji, I. V., & Ekwule, R. O. (2019). Storage-induced deterioration of domestic water quality. Journal of Water, Sanitation and Hygiene for Development, 9(2), 329-337.

Noori, R., Karbassi, A. R., Mehdizadeh, H., Vesali-Naseh, M., & Sabahi, M. S. (2011). A framework development for predicting the longitudinal dispersion coefficient in natural streams using an artificial neural network. Environmental Progress & Sustainable Energy, 30(3), 439-449.

Novak Babič, M., & Gunde-Cimerman, N. (2021). Water-transmitted fungi are involved in degradation of concrete drinking water storage tanks. Microorganisms, 9(1), 160.

Nuño Martínez, N., Muela Ribera, J., Hausmann-Muela, S., Cevallos, M., Hartinger, S. M., Christen, A., & Maeusezahl, D. (2020). The meanings of water: socio-cultural

perceptions of solar disinfected (SODIS) drinking water in Bolivia and implications for its uptake. Water, 12(2), 442.

Nur, T., Loganathan, P., Nguyen, T. C., Vigneswaran, S., Singh, G., & Kandasamy, J. (2014). Batch and column adsorption and desorption of fluoride using hydrous ferric oxide: Solution chemistry and modeling. Chemical Engineering Journal, 247, 93-102.

Olden, J. D., & Jackson, D. A. (2002). Illuminating the "black box": a randomization approach for understanding variable contributions in artificial neural networks. Ecological modelling, 154(1-2), 135-150.

Olden, J. D., Joy, M. K., & Death, R. G. (2004). An accurate comparison of methods for quantifying variable importance in artificial neural networks using simulated data. Ecological modelling, 178(3-4), 389-397.

Olorunnisola, A. O., & Alaka, A. C. (2018). Production and evaluation of composite rainwater storage tanks from recycled materials Part 2: stored water quality assessment. Recycling, 3(2), 25.

Onu, C. E., Nwabanne, J. T., Ohale, P. E., & Asadu, C. O. (2021). Comparative analysis of RSM, ANN and ANFIS and the mechanistic modeling in eriochrome black-T dye adsorption using modified clay. South African Journal of Chemical Engineering, 36, 24-42.

Oskouei, A. V., Bazli, M., Ashrafi, H., & Imani, M. (2018). Flexural and web crippling properties of GFRP pultruded profiles subjected to wetting and drying cycles in different sea water conditions. Polymer Testing, 69, 417-430.

Panneerselvam, B., Karuppannan, S., & Muniraj, K. (2020). Evaluation of drinking and irrigation suitability of groundwater with special emphasizing the health risk posed by nitrate contamination using nitrate pollution index (NPI) and human health risk assessment (HHRA). Human and Ecological Risk Assessment: An International Journal, 27(5), 1324-1348.

Parashar, D., & Gandhimathi, R. (2022). Zinc Ions adsorption from aqueous solution using raw and acid-modified orange peels: Kinetics, Isotherm, Thermodynamics, and Adsorption mechanism. Water, Air, & Soil Pollution, 233(10), 1-21.

Park, S. B., & Tia, M. (2004). An experimental study on the water-purification properties of porous concrete. Cement and concrete research, 34(2), 177-184.

Pinar, E., Seckin, G., Sahin, B., Akilli, H., Cobaner, M., Canpolat, C., ... & Kocaman, S. (2011). ANN approaches for the prediction of bridge backwater using both field and experimental data. Intl. J. River Basin Management, 9(1), 53-62.

Planning Commission. (2002). India assessment 2002: Water supply and sanitation. Planning Commission, Government of India.

Podgorski, J. E., Labhasetwar, P., Saha, D., & Berg, M. (2018). Prediction modeling and mapping of groundwater fluoride contamination throughout India. Environmental science & technology, 52(17), 9889-9898.

Pouretedal, H. R., & Sadegh, N. (2014). Effective removal of amoxicillin, cephalexin, tetracycline and penicillin G from aqueous solutions using activated carbon nanoparticles prepared from vine wood. Journal of Water Process Engineering, 1, 64-73.

Pourhashem, S., Rashidi, A., Vaezi, M. R., & Bagherzadeh, M. R. (2017). Excellent corrosion protection performance of epoxy composite coatings filled with amino-silane functionalized graphene oxide. Surface and Coatings Technology, 317, 1-9.

Purohit, U., Mehar, S. K., & Sundaramoorthy, S. (2002). Role of Prosopis cineraria on the ecology of soil fungi in Indian desert. Journal of arid environments, 52(1), 17-27.

Pyrgaki, K., Messini, P., & Zotiadis, V. (2018). Adsorption of Pb and Cu from aqueous solutions by raw and heat-treated attapulgite clay. Geosciences, 8(5), 157.

Quick, R. E., Venczel, L. V., Mintz, E. D., Soleto, L., Aparicio, J., Gironaz, M., ... & Tauxe, R. V. (1999). Diarrhoea prevention in Bolivia through point-of-use water treatment and safe storage: a promising new strategy. Epidemiology & Infection, 122(1), 83-90.

Rabbani, A., & Salehi, S. (2017). Dynamic modeling of the formation damage and mud cake deposition using filtration theories coupled with SEM image processing. Journal of Natural Gas Science and Engineering, 42, 157-168.

Rahman, S., Khan, M. T. R., Akib, S., Din, N. B. C., Biswas, S. K., & Shirazi, S. M. (2014). Sustainability of rainwater harvesting system in terms of water quality. The Scientific World Journal, 2014.

Rahmani, A., Rahmani, K., Dobaradaran, S., Mahvi, A. H., Mohamadjani, R., & Rahmani, H. (2010). Child dental caries in relation to fluoride and some inorganic constituents in drinking water in Arsanjan, Iran. Fluoride, 43(4), 179-186.

Ramanaiah, S. V., Mohan, S. V., & Sarma, P. N. (2007). Adsorptive removal of fluoride from aqueous phase using waste fungus (Pleurotus ostreatus 1804) biosorbent: Kinetics evaluation. ecological engineering, 31(1), 47-56.

Ramasamy, V., Anand, P., & Suresh, G. (2018). Synthesis and characterization of polymer-mediated CaCO3 nanoparticles using limestone: a novel approach. Advanced Powder Technology, 29(3), 818-834.

Rani, B., Singh, U., Sharma, R., GUPTA, A. A., Dhawan, N. G., Sharma, A. K., ... & Maheshwari, R. K. (2013). Prosopis cineraria (L) Druce: a desert tree to brace livelihood in Rajasthan. Asian Journal of Pharmaceutical Research and Health Care, 5(2).

Rasool, A., Farooqi, A., Xiao, T., Ali, W., Noor, S., Abiola, O., ... & Nasim, W. (2018). A review of global outlook on fluoride contamination in groundwater with prominence on the Pakistan current situation. Environmental geochemistry and health, 40(4), 1265-1281.

Rathore, M. (2009). Nutrient content of important fruit trees from arid zone of Rajasthan. Journal of Horticulture and Forestry, 1(7), 103-108.

Ray, C., Roy, P. K., Majumder, A., & Roy, M. B. (2020). Performance analysis of some low-cost and locally available adsorbents that remove excess fluoride ion from raw water to develop a filter for the rural population. Journal of The Institution of Engineers (India): Series E, 101(2), 149-160.

Ray, D., Sarkar, B. K., Rana, A. K., & Bose, N. R. (2001). The mechanical properties of vinylester resin matrix composites reinforced with alkali-treated jute fibres. Composites Part A: applied science and manufacturing, 32(1), 119-127.

Rehfuess, E., Mehta, S., & Prüss-Üstün, A. (2006). Assessing household solid fuel use: multiple implications for the Millennium Development Goals. Environmental health perspectives, 114(3), 373-378.

Richards, S., Rao, L., Connelly, S., Raj, A., Raveendran, L., Shirin, S., ... & Helliwell, R. (2021). Sustainable water resources through harvesting rainwater and the effectiveness of a low-cost water treatment. Journal of Environmental Management, 286, 112223.

Rosa, G., & Clasen, T. (2010). Estimating the scope of household water treatment in low-and medium-income countries. The American journal of tropical medicine and hygiene, 82(2), 289-300.

Saha, D., Shekhar, S., Ali, S., Vittala, S. S., & Raju, N. J. (2016). Recent hydrogeological research in India. In Proc. Indian Natl. Sci. Acad, 82(3), 787–803.

Sahu, S., Yadav, M. K., Gupta, A. K., Uddameri, V., Toppo, A. N., Maheedhar, B., & Ghosal, P. S. (2022). Modeling defluoridation of real-life groundwater by a green adsorbent aluminum/olivine composite: Isotherm, kinetics, thermodynamics and novel framework based on artificial neural network and support vector machine. Journal of Environmental Management, 302, 113965.

Saleem, A., Dandigi, M. N., & Kumar, K. V. (2012). Correlation-regression model for physico-chemical quality of groundwater in the South Indian city of Gulbarga. African Journal of Environmental Science and Technology, 6(9), 353-364.

Sangiorgio, V., Uva, G., Adam, J. M., & Scarcelli, L. (2020). Failure analysis of reinforced concrete elevated storage tanks. Engineering failure analysis, 115, 104637.

Schafer, C. A. (2010). Impact of tank material on water quality in household water storage systems in Cochabamba, Bolivia. University of South Florida.

Schafer, C. A., & Mihelcic, J. R. (2012). Effect of storage tank material and maintenance on household water quality. Journal-American Water Works Association, 104(9), E521-E529.

Sehn, P. (2008). Fluoride removal with extra low energy reverse osmosis membranes: three years of large scale field experience in Finland. Desalination, 223(1-3), 73-84.

Sepehri, M., Malekinezhad, H., Ilderomi, A. R., Talebi, A., & Hosseini, S. Z. (2018). Studying the effect of rain water harvesting from roof surfaces on runoff and household consumption reduction. Sustainable Cities and Society, 43, 317-324.

Sevgili, İ., Dilmaç, Ö. F., & Şimşek, B. (2021). An environmentally sustainable way for effective water purification by adsorptive red mud cementitious composite cubes modified with bentonite and activated carbon. Separation and Purification Technology, 274, 119115.

Shahmaleki, A. A., Motevassel, M., Isari, A. A., & Anvaripour, B. (2020). An effective approach for the adsorptive removal of lead from an aqueous medium using nano Prosopis Cineraria leaf ash (NPCLA): characterization, operational effects, and recyclability. Modeling Earth Systems and Environment, 6(1), 139-149.

Sharma, P. K., Ojha, C. S. P., Abegaze, T. A., Swami, D., & Yadav, A. (2015). Simulation of Fluoride Transport through Fine Sand Column Experiments. Journal of Hydrogeology & Hydrologic Engineering, 4: 2.

Shen, J., Mkongo, G., Abbt-Braun, G., Ceppi, S. L., Richards, B. S., & Schäfer, A. I. (2015). Renewable energy powered membrane technology: Fluoride removal in a rural community in northern Tanzania. Separation and Purification Technology, 149, 349-361.

Shenvi, S. S., Isloor, A. M., & Ismail, A. F. (2015). A review on RO membrane technology: Developments and challenges. Desalination, 368, 10-26.

Shivaprakash, P. K., Ohri, K., & Noorani, H. (2011). Relation between dental fluorosis and intelligence quotient in school children of Bagalkot district. Journal of Indian Society of Pedodontics and Preventive Dentistry, 29(2), 117.

Shyamal, D. S., & Ghosh, P. K. (2019). Efficiency of Portland Pozzolana Cement as an adsorbent in removing excess fluoride from groundwater. Groundwater for Sustainable Development, 9, 100248.

Silva, C. M., Sousa, V., & Carvalho, N. V. (2015). Evaluation of rainwater harvesting in Portugal: Application to single-family residences. Resources, Conservation and Recycling, 94, 21-34.

Simões, C. L., Vasconcelos, M., Nunes, J. P., & Bernardo, C. A. (2016). Using a glass-fibre reinforced polymer composite in the production of sustainable water storage tanks. International Journal of Materials and Product Technology, 52(1-2), 162-175.

Singh, C. K., Rina, K., Singh, R. P., Shashtri, S., Kamal, V., & Mukherjee, S. (2011). Geochemical modeling of high fluoride concentration in groundwater of Pokhran area of Rajasthan, India. Bulletin of Environmental Contamination and Toxicology, 86(2), 152-158.

Singh, K., Lataye, D. H., & Wasewar, K. L. (2016). Removal of fluoride from aqueous solution by using low-cost sugarcane bagasse: kinetic study and equilibrium isotherm analyses. Journal of Hazardous, Toxic, and Radioactive Waste, 20(3), 04015024.

Singh, R., Raghuvanshi, S. P., & Kaushik, C. P. (2008). Defluoridation of drinking water using brick powder as an adsorbent. Asian Journal of Chemistry, 20(8), 5818.

Singhal, A., Gupta, R., & Singh, A. (2019). Sustainable Bio-Adsorbent for Treatment of Nitrate, Fluoride and TDS in Groundwater. International Research Journal of Pure and Applied Chemistry, 1–11.

Sivasankar, V., Rajkumar, S., Murugesh, S., & Darchen, A. (2012). Tamarind (Tamarindus indica) fruit shell carbon: a calcium-rich promising adsorbent for fluoride removal from groundwater. Journal of hazardous materials, 225, 164-172.

Slavik, I., Oliveira, K. R., Cheung, P. B., & Uhl, W. (2020). Water quality aspects related to domestic drinking water storage tanks and consideration in current standards and guidelines throughout the world–a review. Journal of water and health, 18(4), 439-463.

Sobsey, M. D., Handzel, T., & Venczel, L. (2003). Chlorination and safe storage of household drinking water in developing countries to reduce waterborne disease. Water science and Technology, 47(3), 221-228.

Suditu, G. D., Piuleac, C. G., Bulgariu, L., & Curteanu, S. (2013). Application of a neuro-genetic technique in the optimization of heavy metals removal from wastewaters for environmental risk reduction. Environmental Engineering & Management Journal, 12(1).

Sun, Q., & Yang, L. (2003). The adsorption of basic dyes from aqueous solution on modified peat–resin particle. Water research, 37(7), 1535-1544.

Sun, Y., Liang, X., Xiao, C., Wang, G., & Meng, F. (2019). Hydrogeochemical characteristics of fluoride in the groundwater of Shuangliao City, China. In E3S Web of Conferences (Vol. 98, p. 09028). EDP Sciences.

Suthar, S., Garg, V. K., Jangir, S., Kaur, S., Goswami, N., & Singh, S. (2008). Fluoride contamination in drinking water in rural habitations of Northern Rajasthan, India. Environmental Monitoring and Assessment, 145(1), 1-6.

Taghizadeh, M. M., Torabian, A., Borghei, M., & Hassani, A. H. (2007). Feasibility study of water purification using vertical porous concrete filter. International Journal of Environmental Science & Technology, 4(4), 505-512.

Tahaikt, M., El Habbani, R., Haddou, A. A., Achary, I., Amor, Z., Taky, M., ... & Elmidaoui, A. (2007). Fluoride removal from groundwater by nanofiltration. Desalination, 212(1-3), 46-53.

Tamaddun, K., Kalra, A., & Ahmad, S. (2018). Potential of rooftop rainwater harvesting to meet outdoor water demand in arid regions. Journal of Arid Land, 10(1), 68-83.

Tamas, A., & Mosler, H. J. (2011). Why do people stop treating contaminated drinking water with solar water disinfection (SODIS)?. Health education & behavior, 38(4), 357-366.

Tang, G., Ren, T., Yan, Z., Ma, L., Pan, X., Liu, J., ... & Huang, X. (2019). Corrosion resistance of a self-curing waterborne epoxy resin coating. Journal of Coatings Technology and Research, 16(3), 895-904.

Tanji, Y., Sakai, R., Miyanaga, K., & Unno, H. (2006). Estimation of the self-purification capacity of biofilm formed in domestic sewer pipes. Biochemical engineering journal, 31(1), 96-101.

Tchobanoglous, G., Burton, F. L., & Stensel, H. D. (2003). Wastewater Engineering: Treatment and Reuse (Fourth Edition). Metcalf and Eddy Inc. New York: McGraw- Hill Book Company.

Tchomgui-Kamga, E., Ngameni, E., & Darchen, A. (2010). Evaluation of removal efficiency of fluoride from aqueous solution using new charcoals that contain calcium compounds. Journal of Colloid and Interface Science, 346(2), 494-499.

Te, B., Wichitsathian, B., Yossapol, C., & Wonglertarak, W. (2018). Enhancing the quality of arsenic-contaminated groundwater using a bio-sand filter with iron-mixed clay pellets. Water Practice & Technology, 13(2), 285-294.

Tenza-Abril, A. J., Villacampa, Y., Solak, A. M., & Baeza-Brotons, F. (2018). Prediction and sensitivity analysis of compressive strength in segregated lightweight concrete based on artificial neural network using ultrasonic pulse velocity. Construction and Building Materials, 189, 1173-1183.

Thole, B. (2013). Ground water contamination with fluoride and potential fluoride removal technologies for East and Southern Africa. Perspectives in water pollution, 65-95.

Titshall, L. W., & Hughes, J. C. (2005). Characterisation of some South African water treatment residues and implications for land application. Water Sa, 31(3), 299-308.

Tiwari, K., Goyal, R., & Sarkar, A. (2017). GIS-based spatial distribution of groundwater quality and regional suitability evaluation for drinking water. Environmental Processes, 4(3), 645-662.

Tor, A., Danaoglu, N., Arslan, G., & Cengeloglu, Y. (2009). Removal of fluoride from water by using granular red mud: batch and column studies. Journal of hazardous materials, 164(1), 271-278.

Tripathy, S. S., Bersillon, J. L., & Gopal, K. (2006). Removal of fluoride from drinking water by adsorption onto alum-impregnated activated alumina. Separation and purification technology, 50(3), 310-317.

Tüzün, I., Bayramoğlu, G., Yalçın, E., Başaran, G., Celik, G., & Arıca, M. Y. (2005). Equilibrium and kinetic studies on biosorption of Hg (II), Cd (II) and Pb (II) ions onto microalgae Chlamydomonas reinhardtii. Journal of Environmental Management, 77(2), 85-92.

United States Environmental Protection Agency. (2011). Exposure Factors Handbook: 2011 Edition (Vol. EPA/600/R-).

Vaheddoost, B., Guan, Y., & Mohammadi, B. (2020). Application of hybrid ANN-whale optimization model in evaluation of the field capacity and the permanent wilting point of the soils. Environmental Science and Pollution Research, 27(12), 13131-13141.

Van Halem, D., Heijman, S. G. J., Soppe, A. I. A., Van Dijk, J. C., & Amy, G. L. (2007). Ceramic silver-impregnated pot filters for household drinking water treatment in developing countries: material characterization and performance study. Water science and technology: Water Supply, 7(5-6), 9-17.

Vialle, C., Busset, G., Tanfin, L., Montrejaud-Vignoles, M., Huau, M. C., & Sablayrolles, C. (2015). Environmental analysis of a domestic rainwater harvesting system: A case study in France. Resources, Conservation and Recycling, 102, 178-184.

Villela-Martínez, D. E., Leyva-Ramos, R., Aragón-Piña, A., & Navarro-Tovar, R. (2020). Arsenic elimination from water solutions by adsorption on bone char. Effect of operating conditions and removal from actual drinking water. Water, Air, & Soil Pollution, 231(5), 1-13.

Walters, J. P. (2015). *A systems approach to sustainable rural water infrastructure in developing countries* (Doctoral dissertation, University of Colorado at Boulder).

Wang, B., Li, D., Xian, G., & Li, C. (2021). Effect of Immersion in water or alkali solution on the structures and properties of epoxy resin. Polymers, 13(12), 1902.

Wei, Y., & Hadigheh, S. A. (2022). Cost benefit and life cycle analysis of CFRP and GFRP waste treatment methods. Construction and Building Materials, 348, 128654.

Whittington, D., Davis, J., Prokopy, L., Komives, K., Thorsten, R., Lukacs, H., ... & Wakeman, W. (2009). How well is the demand-driven, community management model for rural water supply systems doing? Evidence from Bolivia, Peru and Ghana. *Water Policy*, *11*(6), 696-718.

World Health Organization. (2022). Guidelines for drinking water quality: incorporating the first and second addenda.

Wright, J., Gundry, S., & Conroy, R. (2004). Household drinking water in developing countries: a systematic review of microbiological contamination between source and point-of-use. Tropical medicine & international health, 9(1), 106-117.

Xiao, J., Jin, Z., & Zhang, F. (2015). Geochemical controls on fluoride concentrations in natural waters from the middle Loess Plateau, China. Journal of Geochemical Exploration, 159, 252-261.

Yadav, A. K., Abbassi, R., Gupta, A., & Dadashzadeh, M. (2013). Removal of fluoride from aqueous solution and groundwater by wheat straw, sawdust and activated bagasse carbon of sugarcane. Ecological engineering, 52, 211-218.

Yao, J., Teng, N., Poh, H. L., & Tan, C. L. (1998). Forecasting and analysis of marketing data using neural networks. J. Inf. Sci. Eng., 14(4), 843-862.

Yetilmezsoy, K., & Demirel, S. (2008). Artificial neural network (ANN) approach for modeling of Pb (II) adsorption from aqueous solution by Antep pistachio (Pistacia Vera L.) shells. Journal of hazardous materials, 153(3), 1288-1300.

Yousefi Kebria, D., Ghavami, M., Javadi, S., & Goharimanesh, M. (2018). Combining an experimental study and ANFIS modeling to predict landfill leachate transport in underlying soil—a case study in north of Iran. Environmental monitoring and assessment, 190(1), 1-17.

Yu, Z., Di, H., Ma, Y., Lv, L., Pan, Y., Zhang, C., & He, Y. (2015). Fabrication of graphene oxide–alumina hybrids to reinforce the anti-corrosion performance of composite epoxy coatings. Applied Surface Science, 351, 986-996.

Yusoff, M. Z. M., Salit, M. S., Ismail, N., & Wirawan, R. (2010). Mechanical properties of short random oil palm fibre reinforced epoxy composites. Sains Malaysiana, 39(1), 87-92.

Yusuf, K. O., & Murtala, M. O. (2020). Development and performance evaluation of a portable household ceramic water filter with activated carbon and magnetic treatment unit. International Journal of Environmental Science and Technology, 17(9), 4009-4018.

Zhang, H. M., & Su, B. Y. (2006). Experimental study and numerical simulation of fluoride in sand. Journal of Hydrodynamics, 18(6), 748-751.

LIST OF PUBLICATIONS

Patent

1. Jute Fiber Water Tank: An Eco-Friendly Water Storage Method, India Provisional Patent Application No.: 201911045423 Inventors: Soumya Kar, Raya Raghavendra Kumar, Rajiv Gupta, Dated: November 4, 2019; Status: Awaited
2. Adsorbent material and process for Preparation thereof; Soumya Kar, Rajiv Gupta, Application No: 202011011674; TEMP/E-1/12578/2020-DEL; Filed on 18.3.2020; India; Status: Awaited

Research papers

Published/ Accepted

1. Kar, S., & Gupta, R. (2020). Water and Sanitation Management: During and after COVID-19 Pandemic. Advanced Materials Letters, 11(11), 1-6. https://doi.org/10.5185/amlett.2020.111570
2. Kar, S., & Gupta, R. (2022). Fluoride Toxicity in Rajasthan, India: Water Filter Distribution, Monitoring and User Perception. Water Conservation Science and Engineering, 7, 561-572. https://doi.org/10.1007/s41101-022-00163-y
3. Kar, S., & Gupta, R. (2023). Fluoride toxicity in Rajasthan, India: Human health risk assessment, low-cost water filter preparation, and contaminant remediation. Water Conservation Science and Engineering, 8(1), 3. https://doi.org/10.1007/s41101-023-00175-2
4. Kar, S., & Gupta, R. (2023). Efficiency of a glass fiber-reinforced polymer (GFRP) tank in pursuit of reliable water resources through rainwater harvesting. Environmental Engineering & Management Journal (EEMJ), 22(1). http://doi.org/10.30638/eemj.2023.008
5. Patil, D., Kar, S., Shastri, V., & Gupta, R. (2023). Qualitative and health risk assessment of water using a novel weight-integrated health hazard and fuzzy-derived indices. Sustainable Water Resources Management, 9(2), 55. https://doi.org/10.1007/s40899-023-00832-3

6. Patil, D., Kar, S., & Gupta, R. (2023). Classification and Prediction of Developed Water Quality Indexes Using Soft Computing Tools. Water Conservation Science and Engineering, 8(1), 16. https://doi.org/10.1007/s41101-023-00190-3

Conferences

1. Kar, S., & Gupta, R. (2018). A Study on the Disposal and Efficient Re-use of Water Treatment Sludge Generated in a Household: A Review. In 8th Annual International Conference on Civil Engineering, 25-28 June 2018, Athens, Greece (pp. 33) [Abstract book]
2. Kar, S. & Mohapatra, S. (2022). A Preliminary Study Exploring the Rooftop Rainwater Harvesting Potential of Bhubaneswar: Scope, Optimization, and Economic Viability. In: Das, B.B., Hettiarachchi, H., Sahu, P.K., Nanda, S. (eds) Recent Developments in Sustainable Infrastructure (ICRDSI-2020)—GEO-TRA-ENV-WRM. Lecture Notes in Civil Engineering, vol 207, pp. 483-493. doi:10.1007/978-981-16-7509-6_37
3. Raya, R, K., Kar, S., Kumar, D., & Gupta, R. (2022). A Sustainable Integrated Rural Water Management with emphasis on Network Prioritization, Household Water Treatment and Real-Time Feedback. In 2022 IEEE Conference on Technologies for Sustainability (SusTech), Corona, CA, USA, 2022, pp. 144-149. doi: 10.1109/SusTech53338.2022.9794202.
4. Patil, D., Kar, S., & Gupta, R. (2023). An efficient urban water management practice based on optimum LPCD estimated using the MLR-GA optimization approach- A case study for Jaipur, Rajasthan (India). In 2023 IEEE Conference on Technologies for Sustainability (SusTech), Portland, OR, USA, 2023, pp. 275-279. doi: 10.1109/SusTech57309.2023.10129533.
5. Kar, S., and Gupta, R. (2023). Studying the potential of a novel jute fiber-reinforced polymer water storage tank. In CSCE Annual Conference 2023 – Moncton, NB.
6. Kar, S., Gupta, R., & Chen, Z. (2023). Characterization and field application assessment of Prosopis cineraria (l.) for fluoride sequestration: a preliminary investigation. In RTESE Annual Conference 2023, pp. 142-1-142-8. doi: 10.11159/rtese23.142

Book Chapter

1. Gupta, R., and Kar, S. (2021). Disaster Preparedness for Standing Crops and Irrigation Water during Drought Spells. In Fourth WCDM: Vol. 2 Hardcover.

Popular Student Magazine Article

1. Kar, S. (2022, October). Water scarcity: An impending pandemic. Science Horizon, Odisha Bigyan Academy, 9-13.

APPENDIX 1

Table i: Calculated ADD for Days 15, 60, and 180 (µg/kg-bw/day)

Average Age	Days 15			Days 60			Days 180		
	S2	S3	S4	S2	S3	S4	S2	S3	S4
6 to ≤9	0	0.08 (0.051)	0.01 (0.004)	0.07 (0.043)	0.12 (0.034)	0.12 (0.036)	0.35 (0.24)	0.15 (0.034)	0.84 (0.135)
≤9 to ≤12	0	0.07 (0.041)	0.01 (0.003)	0.06 (0.035)	0.10 (0.027)	0.10 (0.029)	0.29 (0.194)	0.12 (0.028)	0.67 (0.109)
≤12 to ≤18	0	0.07 (0.041)	0.01 (0.003)	0.06 (0.035)	0.10 (0.027)	0.10 (0.029)	0.28 (0.192)	0.12 (0.027)	0.67 (0.108)
≤18 to ≤21	0	0.06 (0.04)	0.01 (0.003)	0.06 (0.034)	0.10 (0.027)	0.10 (0.028)	0.28 (0.188)	0.12 (0.027)	0.65 (0.105)
≥21	0	0.08 (0.053)	0.01 (0.004)	0.08 (0.044)	0.13 (0.035)	0.13 (0.037)	0.36 (0.247)	0.15 (0.035)	0.86 (0.138)
≥65	0	0.09 (0.054)	0.01 (0.004)	0.08 (0.045)	0.13 (0.036)	0.13 (0.038)	0.37 (0.252)	0.16 (0.036)	0.88 (0.141)

Note: ADD (±S.D.)

Table ii: Median ADD for Days 15, 60, and 180 (µg/kg-bw/day)

Average Age Groups	**Days 15**			**Days 60**			**Days 180**		
	S2	**S3**	**S4**	**S2**	**S3**	**S4**	**S2**	**S3**	**S4**
6 to ≤9	0	0.09	0.01	0.10	0.13	0.14	0.51	0.17	0.81
≤9 to ≤12	0	0.07	0.01	0.08	0.10	0.11	0.41	0.13	0.65

≤12 to ≤18	0	0.07	0.01	0.08	0.10	0.11	0.41	0.13	0.65
≤18 to ≤21	0	0.07	0.01	0.08	0.10	0.11	0.40	0.13	0.63
≥21	0	0.09	0.01	0.11	0.13	0.14	0.52	0.17	0.83
≥65	0	0.10	0.01	0.11	0.13	0.85	0.54	0.18	0.85

Table iii: Age-specific and specimen-specific calculated IHQ values for test Days 15

Age Groups	**R_fD = 50 (µg/kg/day)**			**R_fD = 25 (µg/kg/day)**			**R_fD = 4 (µg/kg/day)**		
	S2	**S3**	**S4**	**S2**	**S3**	**S4**	**S2**	**S3**	**S4**
6 to ≤9	0.0000	0.0016	0.0003	0.0000	0.0033	0.0005	0.0000	0.0205	0.0032
≤9 to ≤12	0.0000	0.0013	0.0002	0.0000	0.0026	0.0004	0.0000	0.0165	0.0026
≤12 to ≤18	0.0000	0.0013	0.0002	0.0000	0.0026	0.0004	0.0000	0.0164	0.0026
≤18 to ≤21	0.0000	0.0013	0.0002	0.0000	0.0026	0.0004	0.0000	0.0160	0.0025
≥21	0.0000	0.0017	0.0003	0.0000	0.0034	0.0005	0.0000	0.0211	0.0033
≥65	0.0000	0.0017	0.0003	0.0000	0.0034	0.0005	0.0000	0.0215	0.0034

Table iv: Age-specific and specimen-specific calculated IHQ values for test Days 60

Age Groups	**R_fD = 50 (µg/kg/day)**			**R_fD = 25 (µg/kg/day)**			**R_fD = 4 (µg/kg/day)**		
	S2	**S3**	**S4**	**S2**	**S3**	**S4**	**S2**	**S3**	**S4**
6 to ≤9	0.0015	0.0025	0.0025	0.0030	0.0049	0.0050	0.0186	0.0307	0.0312
≤9 to ≤12	0.0012	0.0020	0.0020	0.0024	0.0040	0.0040	0.0150	0.0248	0.0252

≤12 to ≤18	0.0012	0.0020	0.0020	0.0024	0.0039	0.0040	0.0149	0.0246	0.0250
≤18 to ≤21	0.0012	0.0019	0.0020	0.0023	0.0039	0.0039	0.0146	0.0241	0.0245
≥21	0.0015	0.0025	0.0026	0.0031	0.0051	0.0051	0.0191	0.0316	0.0322
≥65	0.0016	0.0026	0.0026	0.0031	0.0052	0.0053	0.0195	0.0323	0.0328

Table v: Recorded thickness levels in the GFRP specimen panels

Sampling Point	**Specimen 1**	**Specimen 2**	**Specimen 3**	**Sampling Point**	**Specimen 1**	**Specimen 2**	**Specimen 3**
1	4.88	4.71	4.51	**19**	5.12	4.39	4.88
2	4.20	4.68	4.55	**20**	4.68	4.39	4.63
3	4.85	4.90	4.80	**21**	4.82	4.39	4.66
4	4.95	4.90	4.46	**22**	4.95	5.49	4.87
5	4.12	4.90	4.71	**23**	4.82	4.39	4.83
6	4.56	4.78	4.45	**24**	4.81	4.39	4.73
7	4.68	4.63	4.48	**25**	4.66	4.39	4.85
8	4.52	4.66	4.78	**26**	4.86	4.39	4.96
9	4.83	4.87	4.59	**27**	4.733	4.39	4.67

10	4.33	4.83	4.83	**28**	4.53	5.83	4.87
11	5.12	4.73	4.33	**29**	4.46	4.39	4.88
12	4.68	4.85	5.08	**30**	4.71	4.39	4.95
13	4.82	4.93	4.68	**31**	4.68	4.69	4.80
14	4.91	4.67	4.82	**32**	4.9	4.39	4.68
15	4.82	4.87	4.95	**33**	4.9	4.59	4.82
16	4.81	4.88	4.82	**34**	4.87	4.44	4.94
17	4.66	4.92	4.81	**35**	4.9	4.23	4.71
18	4.86	4.80	4.60	**36**	4.63	4.39	4.68

Table vi: Machine learning predictive models

S/N	**Experimental removal %**	**Model Predictions (%)**					
		Simple LR	**Step-wise LR**	**Simple NLR**	**Step-wise NLR**	**ANN**	**FIS**
1	40.20	44.15	42.65	21.06	18.57	39.20	53.00
2	41.30	3.08	2.33	6.52	6.25	37.83	44.00
3	26.70	1.00	-1.08	3.14	5.34	33.51	29.43
4	75.82	24.66	20.97	16.46	16.38	79.88	76.50
5	15.33	5.55	-0.54	3.78	8.07	18.87	19.43
6	20.20	1.06	0.68	4.34	4.25	26.38	22.20

7	20.50	24.39	20.70	16.78	16.38	23.81	12.57
8	76.91	21.91	20.70	13.86	12.63	75.27	68.86
9	49.31	3.92	3.14	6.25	6.25	40.84	41.25
10	76.91	34.41	31.95	19.17	17.63	76.44	76.50
11	31.50	3.36	2.60	6.44	6.25	33.73	36.14
12	77.91	24.79	20.97	16.13	16.38	79.12	72.91
13	26.80	1.34	0.95	4.27	4.25	25.54	31.80
14	13.73	7.11	1.22	6.92	10.80	22.37	23.43
15	79.33	24.66	20.97	16.46	16.38	79.88	76.50
16	31.50	21.07	19.89	14.47	12.63	32.56	33.75
17	98.45	49.89	42.65	25.04	24.08	94.15	92.03
18	50.43	21.89	20.43	13.92	12.63	51.14	58.86
19	45.00	49.83	41.84	24.54	24.08	36.79	42.19
20	38.80	0.50	0.14	4.46	4.25	39.91	33.86
21	28.15	34.64	31.41	18.65	17.63	34.46	29.45
22	6.33	0.05	-0.54	2.29	3.18	12.34	10.43
23	45.75	15.31	3.14	10.02	15.87	51.85	53.00
24	92.52	44.16	42.92	21.36	18.57	83.19	88.55
25	76.95	31.17	20.70	18.12	21.24	78.39	58.22
26	31.20	50.11	42.11	24.24	24.08	32.34	38.22
27	30.34	1.28	-0.81	3.09	5.34	33.18	39.02
28	8.85	1.55	-0.54	3.03	5.34	13.11	19.43
29	30.34	49.61	42.38	25.45	24.08	37.59	29.43
30	75.82	8.95	7.53	9.21	9.19	74.72	59.84

31	31.50	5.64	2.87	7.93	9.44	34.16	37.28
32	28.15	0.72	-1.35	3.18	5.34	28.10	38.88
33	28.80	28.08	31.14	12.19	6.94	26.30	21.59
34	37.80	3.64	2.87	6.35	6.25	29.36	47.14
35	92.52	44.16	42.92	21.36	18.57	88.30	86.50
36	48.00	15.05	3.14	10.19	15.87	46.63	43.00
37	29.25	8.39	6.99	9.49	9.19	27.80	22.15
38	29.30	3.56	0.68	6.24	8.33	31.13	34.33
39	7.77	0.55	-0.54	2.63	4.12	12.49	12.76
40	71.20	25.44	20.97	15.46	16.38	72.74	58.86
41	23.78	1.83	-0.27	2.96	5.34	24.62	17.23
42	76.80	19.21	7.53	13.00	18.00	71.46	53.00
43	38.37	1.55	-0.54	3.03	5.34	13.11	49.43
44	73.60	25.18	20.97	15.64	16.38	72.39	65.37
45	33.60	34.36	31.14	18.91	17.63	28.19	22.86
46	9.94	2.55	-0.54	3.29	6.22	14.14	19.43
47	30.30	8.67	7.26	9.36	9.19	37.67	27.30
48	25.46	12.97	0.95	7.96	14.00	25.29	29.50
49	44.60	34.08	30.87	19.15	17.63	39.91	57.93
50	30.34	0.44	-1.62	3.22	5.34	38.51	37.64
51	44.60	9.67	7.26	10.16	10.70	42.64	39.68
52	92.80	50.02	42.65	24.55	24.08	89.55	96.71
53	26.80	9.06	3.41	8.99	12.24	27.66	41.25
54	85.25	40.14	31.68	22.48	22.86	68.02	76.52

55	15.50	11.55	-0.54	4.35	10.46	9.71	17.57
56	74.86	24.92	20.97	15.92	16.38	75.66	77.68
57	23.80	21.63	20.43	14.09	12.63	30.17	32.86
58	29.30	8.11	6.72	9.61	9.19	29.61	29.44
59	31.50	21.35	20.16	14.29	12.63	33.41	21.86
60	49.31	3.92	3.14	6.25	6.25	46.38	47.13
61	40.20	19.47	7.53	12.84	18.00	36.76	49.00
62	30.00	34.27	31.68	19.15	17.63	37.07	36.00
63	27.30	13.10	0.95	7.85	14.00	33.33	29.50

Table vii: Relative importance of input variables

Inputs	**Connection weight approach**	**Garson's Algorithm**	**Perturbation method**	
			MSE	**MSE**
			5%	**10%**
pH	3.93	23.69	38.29	51.17
Contact Time (in minutes)	5.76	21.83	40.01	56.37
Initial Fluoride Concentration (mg/l)	43.43	24.69	36.77	44.06
Adsorbent Dosage (g)	46.89	29.79	45.54	78.03

Table viii: Limitations imposed on the GA simulations

pH	**Contact Time (in minutes)**	**Adsorbent dosage (in gm)**
6 to 8.5	90 to 240	60 to 100

Table ix: ADD and IHQ values calculated for districts in Rajasthan

Districts	ADD[+]			IHQ[*]		
	Age Groups					
	<= 21	<=65	>=65	<= 21	<=65	>=65
Ajmer	0.16	0.13	0.09	2.63	2.22	1.54
Alwar	0.28	0.24	0.17	4.70	3.98	2.76
Banswara	0.16	0.13	0.09	2.64	2.23	1.55
Baran	0.04	0.03	0.02	0.68	0.58	0.40
Barmer	0.16	0.14	0.09	2.66	2.25	1.57
Bharatpur district	0.09	0.08	0.05	1.55	1.31	0.91
Bhilwara district	0.29	0.24	0.17	4.77	4.03	2.81
Bikaner	0.15	0.12	0.09	2.43	2.06	1.43
Bundi	0.06	0.05	0.03	0.97	0.82	0.57
Chittorgarh	0.05	0.04	0.03	0.78	0.66	0.46
Churu	0.13	0.11	0.08	2.20	1.86	1.29
Dausa	0.53	0.45	0.31	8.92	7.54	5.24
Dholpur	0.22	0.19	0.13	3.71	3.13	2.18
Dungarpur	0.25	0.21	0.15	4.20	3.55	2.47
Hanumangarh	0.30	0.25	0.17	4.96	4.19	2.92
Jaipur	0.13	0.11	0.08	2.14	1.81	1.26
Jaisalmer	0.12	0.10	0.07	1.97	1.66	1.16

Jalore	0.17	0.14	0.10	2.78	2.35	1.63
Jhalawar	0.09	0.08	0.05	1.51	1.27	0.88
Jhunjhunu	0.33	0.28	0.20	5.53	4.68	3.25
Jodhpur	0.17	0.14	0.10	2.78	2.35	1.63
Karauli	0.19	0.16	0.11	3.18	2.69	1.87
Kota	0.07	0.06	0.04	1.10	0.93	0.65
Nagaur	0.32	0.27	0.19	5.33	4.50	3.13
Pali	0.12	0.10	0.07	2.01	1.70	1.18
Pratapgarh	0.17	0.14	0.10	2.79	2.36	1.64
Rajsamand	0.07	0.06	0.04	1.15	0.97	0.67
Sawai Madhopur	0.42	0.35	0.25	6.95	5.87	4.08
Sikar	0.04	0.03	0.02	0.62	0.52	0.36
Sirohi	0.06	0.05	0.04	1.00	0.85	0.59
Sri Ganganagar	0.18	0.15	0.10	2.95	2.50	1.74
Tonk	0.11	0.09	0.06	1.81	1.53	1.06
Udaipur	0.21	0.18	0.13	3.57	3.01	2.10

+ ADD: Average daily dose (µg/kg-bw/day); * IHQ: Ingestion Hazard Quotient

Table x: Water qualitative parameters collected from village Hurda, Bhilwara district, Rajasthan

Parameters	**V1**	**V2**	**V3**	**V4**	**V5**	**V6**	**V7**	**V8**	**V9**
pH	8.34	8.49	8.56	8.89	8.46	7.86	8.53	8.93	8.26

TDS (mg/l)	575	1994	249	541	671	446	585	516	938
Conductivity (µS/cm)	1.27	3.95	0.47	1.15	1.43	0.86	1.28	1.13	2.05
Turbidity (NTU)	0	4	1	2	1	5	4	2	3
Hardness (mg/l)	21.3	61.4	15.3	15.6	27.3	26.3	40.1	35.5	48.1
Chloride (mg/l)	35.8	168	7.3	17.8	33.1	17.2	36.2	29.5	71.6
Fluoride (mg/l)	2.4	1.6	1.8	2.6	2.2	2.3	2.2	2	2.6
DO (mg/l)	7.8	7.4	5.4	7.3	5.9	5.2	5.9	6.3	5.6

*** V1: Murayla, V2: Hajiyas, V3: Patiyon ka Khera, V4: Barantiya; V5: Phalamada; V6: Hurda; V7: Balapura; V8: Bharliyas; V9: Sanodiya**

Table xi: Basic details of participatory households collected from Study villages

Participatory household Identification No	Number of family members/ household	Source of water	Present household water treatment facility	Annual Income (in INR)/Household
K1	14	Common village source	No treatment	< 1,00,000
K2	10	Common village source	No treatment	< 1,00,000
K3	5	Common village source	No treatment	< 1,00,000
K4	5	Common village source	No treatment	< 1,00,000
K5	7	Common village source	No treatment	< 1,00,000
K6	10	Common village source	No treatment	< 1,00,000
K7	5	Common village source	No treatment	< 1,00,000
K8	8	Common village source	No treatment	< 1,00,000
K9	7	Common village source	No treatment	< 1,00,000

K10	11	Common village source	No treatment	< 1,00,000
K11	4	Common village source	No treatment	< 1,00,000
K12	5	Common village source	No treatment	< 1,00,000
K13	7	Common village source	No treatment	< 1,00,000
K14	7	Common village source	No treatment	< 1,00,000
K15	6	Common village source	No treatment	< 1,00,000
K16	6	Common village source	No treatment	< 1,00,000
K17	9	Common village source	No treatment	< 1,00,000
K18	6	Common village source	No treatment	< 1,00,000
K19	13	Common village source	No treatment	< 1,00,000
K20	6	Common village source	No treatment	< 1,00,000
K21	5	Common village source	No treatment	< 1,00,000
K22	5	Common village source	No treatment	< 1,00,000
K23	8	Common village source	No treatment	< 1,00,000
K24	8	Common village source	No treatment	< 1,00,000
K25	6	Common village source	No treatment	< 1,00,000
DA1	8	Individual tube/ bore-well	RO technology	>1,00,000
DA2	9	Individual tube/ bore-well	RO technology	>1,00,000
DA3	11	Individual tube/ bore-well	RO technology	>1,00,000
DA4	4	Individual tube/ bore-well	RO technology	>1,00,000
DA5	10	Individual tube/ bore-well	No treatment	< 1,00,000

DA6	3	Individual tube/ bore-well	RO technology	>1,00,000
DA7	5	Individual tube/ bore-well	No treatment	< 1,00,000
DA8	12	Individual tube/ bore-well	No treatment	< 1,00,000
DA9	9	Individual tube/ bore-well	No treatment	< 1,00,000
DA10	4	Individual tube/ bore-well	RO technology	>1,00,000
DA11	6	Individual tube/ bore-well	No treatment	< 1,00,000
DA12	13	Individual tube/ bore-well	No treatment	< 1,00,000
DA13	5	Individual tube/ bore-well	No treatment	< 1,00,000
DA14	6	Individual tube/ bore-well	No treatment	< 1,00,000
DA15	6	Individual tube/ bore-well	No treatment	< 1,00,000
DA16	5	Individual tube/ bore-well	No treatment	< 1,00,000
DA17	10	Individual tube/ bore-well	No treatment	< 1,00,000
DA18	13	Individual tube/ bore-well	No treatment	< 1,00,000
DA19	6	Individual tube/ bore-well	No treatment	< 1,00,000
DA20	8	Common village source	No treatment	< 1,00,000
DA21	8	Common village source	No treatment	< 1,00,000
DA22	6	Common village source	No treatment	< 1,00,000
DA23	5	Common village source	No treatment	< 1,00,000
DA24	4	Common village source	No treatment	< 1,00,000
DA25	5	Common village source	No treatment	< 1,00,000
DA26	7	Common village source	No treatment	< 1,00,000

DA27	4	Common village source	No treatment	< 1,00,000
J1	5	Individual tube/ bore-well	RO technology	>1,00,000
J2	4	Individual tube/ bore-well	RO technology	>1,00,000
J3	2	Individual tube/ bore-well	RO technology	>1,00,000
J4	4	Individual tube/ bore-well	RO technology	>1,00,000
J5	4	Individual tube/ bore-well	RO technology	>1,00,000
J6	4	Individual tube/ bore-well	RO technology	>1,00,000
J7	7	Individual tube/ bore-well	No treatment	< 1,00,000
J8	4	Individual tube/ bore-well	No treatment	< 1,00,000
J9	5	Individual tube/ bore-well	No treatment	< 1,00,000
J10	6	Individual tube/ bore-well	No treatment	< 1,00,000
J11	10	Common village source	No treatment	< 1,00,000
J12	5	Common village source	No treatment	< 1,00,000
J13	7	Common village source	No treatment	< 1,00,000
J14	6	Common village source	No treatment	< 1,00,000
J15	9	Common village source	No treatment	< 1,00,000
J16	9	Common village source	No treatment	< 1,00,000
J17	3	Common village source	No treatment	< 1,00,000
J18	10	Common village source	No treatment	< 1,00,000
J19	9	Common village source	No treatment	< 1,00,000
R1	6	Individual tube/ bore-well	RO technology	>1,00,000

R2	5	Individual tube/ bore-well	RO technology	>1,00,000
R3	8	Individual tube/ bore-well	RO technology	>1,00,000
R4	4	Individual tube/ bore-well	RO technology	>1,00,000
R5	4	Individual tube/ bore-well	RO technology	>1,00,000
R6	4	Individual tube/ bore-well	RO technology	>1,00,000
R7	4	Individual tube/ bore-well	RO technology	>1,00,000
R8	6	Individual tube/ bore-well	RO technology	>1,00,000
R9	6	Individual tube/ bore-well	RO technology	>1,00,000
R10	8	Individual tube/ bore-well	RO technology	>1,00,000
R11	4	Individual tube/ bore-well	RO technology	>1,00,000
R12	5	Individual tube/ bore-well	RO technology	>1,00,000
R13	5	Individual tube/ bore-well	RO technology	>1,00,000
R14	7	Individual tube/ bore-well	RO technology	>1,00,000
R15	6	Individual tube/ bore-well	No treatment	< 1,00,000
R16	6	Individual tube/ bore-well	No treatment	< 1,00,000
R17	4	Individual tube/ bore-well	No treatment	< 1,00,000
R18	4	Individual tube/ bore-well	No treatment	< 1,00,000
R19	10	Individual tube/ bore-well	No treatment	< 1,00,000
R20	6	Individual tube/ bore-well	No treatment	< 1,00,000
R21	9	Individual tube/ bore-well	No treatment	< 1,00,000
R22	10	Individual tube/ bore-well	No treatment	< 1,00,000

R23	4	Individual tube/ bore-well	No treatment	< 1,00,000
R24	4	Individual tube/ bore-well	No treatment	< 1,00,000
R25	4	Individual tube/ bore-well	No treatment	< 1,00,000
R26	4	Individual tube/ bore-well	No treatment	< 1,00,000
R27	5	Individual tube/ bore-well	No treatment	< 1,00,000
R28	5	Individual tube/ bore-well	No treatment	< 1,00,000

K: Kidwana, DA: Dheendwa Aguna, RP: RamnathPura, J: Jeeni

Table xii: Water qualitative parameters collected from villages selected for study implementation in Jhunjhunu district, Rajasthan

Parameters	Jeeni	Kidwana	Dheendwa Aguna	Ramnath Pura
pH	7.4	7.83	9.87	8.17
TDS (mg/l)	672	598	578	740
Hardness (mg/l)	134	140	168	176
Fluoride (mg/l)	1.2	1.5	1	1.1

Table xiii: Recorded fluoride levels in the experimental set-up

Test Days	B1 (10 cm)	B1 (29.5 cm)	B2 (10 cm)	B2 (29.5 cm)	B3 (10 cm)	B3 (29.5 cm)	B4 (10 cm)	B4 (29.5 cm)
1	2.41	0.85	1.29	0.45	1.12	0.74	1.53	1.37
5	2.32	0.09	0.58	0.00	0.21	0.10	0.35	0.22
9	2.16	0.24	1.00	0.13	0.13	0.24	0.51	0.11
13	1.15	0.18	0.56	0.25	0.01	0.18	1.08	0.02

17	1.11	0.03	0.79	0.65	0.02	0.56	1.54	0.18
21	2.10	0.07	0.62	0.42	0.47	0.15	2.99	0.40
25	1.58	0.42	1.16	0.21	0.31	0.22	1.63	0.26
29	2.11	0.03	2.35	0.89	0.02	0.37	1.43	0.64
33	2.73	0.72	2.59	0.59	0.39	0.93	2.53	1.11
37	2.09	0.26	2.04	0.20	0.77	0.24	2.13	1.15
41	1.29	0.18	1.86	0.06	0.76	0.06	3.14	0.10
45	1.26	0.62	1.77	0.19	0.53	0.25	2.61	0.22
49	1.43	0.86	1.99	0.11	0.91	0.12	2.67	0.31
53	2.10	0.23	2.31	0.46	2.11	0.28	2.34	0.29
57	2.20	0.32	2.23	0.97	1.81	0.43	2.35	0.91

Table xiv: Recorded pH levels in the experimental set-up

Test Days	**B1 (10 cm)**	**B1 (29.5 cm)**	**B2 (10 cm)**	**B2 (29.5 cm)**	**B3 (10 cm)**	**B3 (29.5 cm)**	**B4 (10 cm)**	**B4 (29.5 cm)**
1	8.3	8.24	8.21	8.24	8.31	8.66	8.49	8.81
5	7.66	8.28	8.13	8.27	7.93	7.82	7.87	8.46
9	7.54	7.86	7.91	7.88	8.12	8.25	9.13	7.42
13	7.75	7.71	7.78	7.61	7.59	7.78	7.86	7.86
17	8.15	8.49	7.95	8.32	7.68	8.36	8.41	8.48
21	8.2	8.57	8.1	8.48	7.84	8.41	8.32	8.47
25	8.26	8.43	7.98	8.42	8.34	8.44	8.54	8.35
29	8.15	7.82	7.75	7.97	7.84	7.85	7.96	7.81
33	8.51	8.81	7.89	8.69	8.82	8.57	8.01	8.61
37	8.23	8.24	7.95	8.12	8.26	8.17	8	8.2

41	8.13	8.12	7.64	8	8.3	8.21	8.15	8.14
45	8.27	8.57	8.93	8.54	8.63	8.48	9.08	8.54
49	8.06	8.01	8.07	8.01	8.18	8.34	8.59	8.15
53	8.1	7.98	8.1	8.01	7.92	8.23	8.45	8.07
57	8.23	8.09	8.12	8.1	8.06	8.28	8.56	8.14

Table xv: Recorded TDS levels in the experimental set-up

Test Days	**B1 (10 cm)**	**B1 (29.5 cm)**	**B2 (10 cm)**	**B2 (29.5 cm)**	**B3 (10 cm)**	**B3 (29.5 cm)**	**B4 (10 cm)**	**B4 (29.5 cm)**
1	785	733	854	949	535	658	573	407
5	895	568	854	990	578	604	259	919
9	745	626	845	988	594	699	251	875
13	786	538	863	896	603	637	597	782
17	726	545	821	782	585	624	194	662
21	713	617	805	816	574	605	202	596
25	701	667	831	849	390	414	303	613
29	679	606	884.1	862	393	553	256	540
33	681	615	845	729	387	549	231	477
37	652	597	841	681	426	473	215	400
41	645	631	832	646	477	513	223	402
45	658	552	236	556	476	495	178	357
49	468	622	268	501	455	480	200	344
53	489	609	277	464	296	490	217	321
57	495	545	285	408	270	463	198	297

APPENDIX 2

In Appendix 2, the results of selected experiments carried out as preliminary studies have been documented and represented.

Glass fiber-reinforced polymer composites

Before the commencement of experiments dealing with selecting appropriate resins and hardeners for the composite, a water quality analysis was performed between epoxy and polyester resins subsequent to pure sample curing, i.e., no embedded fibers. As is observed from the recorded water quality, an acidic pH was observed for the polyester resin. After that, epoxy resin was chosen for further experiments.

Table i: Water quality observed for the different resins

Parameters	Facility Water	Polyester Resin	Epoxy Resin
pH	7.58	4.26	8
TDS (ppm)	211	250	680
Hardness (ppm)	160	160	167

Following the fabrication of the GFRP specimens, the specimens were cut into sizes specified in the standards and immersed in distilled and rainwater to observe the deteriorating effects on the samples. After fixed test days, the samples were tested for tensile and compressive strength. Following lab-scale experiments, panels were fabricated for assembling the proposed GFRP water storage tanks.

a) 

b) 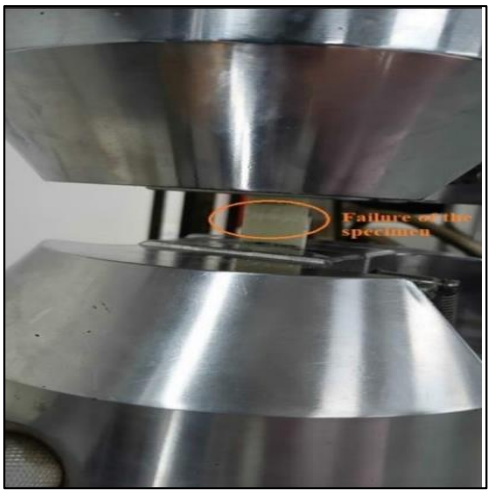

c) 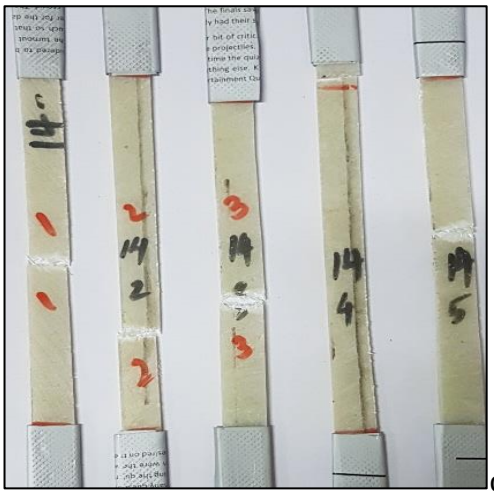 d) 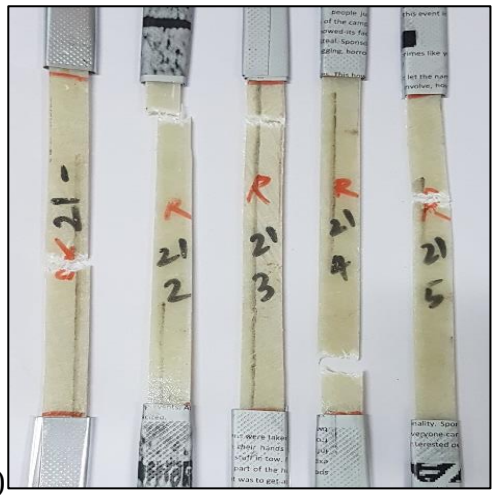

Figure A1: a) Tensile and b) compressive strength test of the three-layered GRP specimen; c) and d) Tested specimens after 14 and 21 days immersion in rainwater sample

(a)

(b)

(c)

Figure A2: a) Application of glass fiber mats on dye frame along with the application of epoxy resin-hardener; b) GRP panels set for curing; and c) Multiple GRP panels set for curing before assembling and installation

<u>The casting of PCWF and CWF water filters</u>

a)  b) 

c)  d) 

Figure A3: a) and b) Casting of PCWF and assembled filters; c) and d) A ceramic filter plate after sintering and assembling with filter unit

Experimental data for filter pellets

Apart from plates, filters in the form of pellets were also fabricated and tested. The pellets were prepared from sugarcane bagasse and clay. Neem adsorbent and clay pellets were also tested to observe the effect on Fluoride removal efficiency.

In the initial phase, sugarcane pellets' performance in fluoride removal was observed with an initial pH = 8.65, TDS = 2920 mg/l, and F^- concentration = 6.15 mg/l.

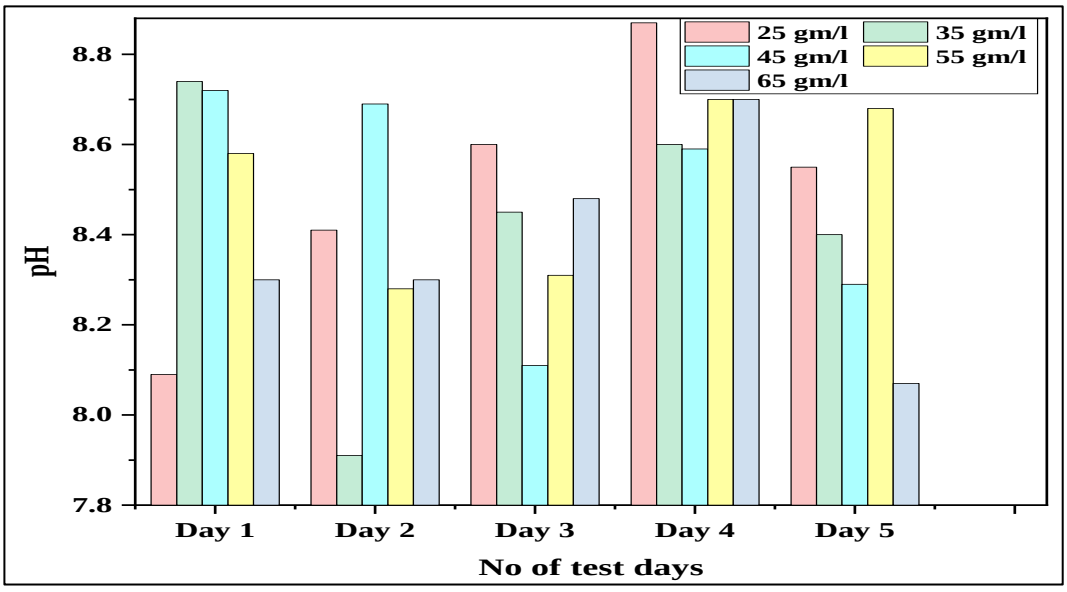

(a)

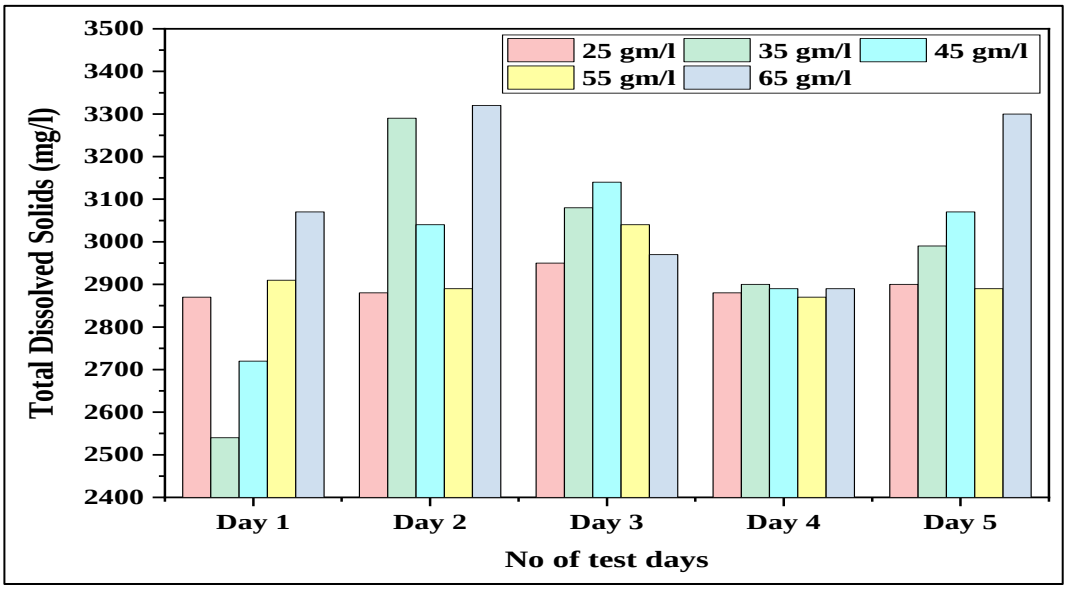

(b)

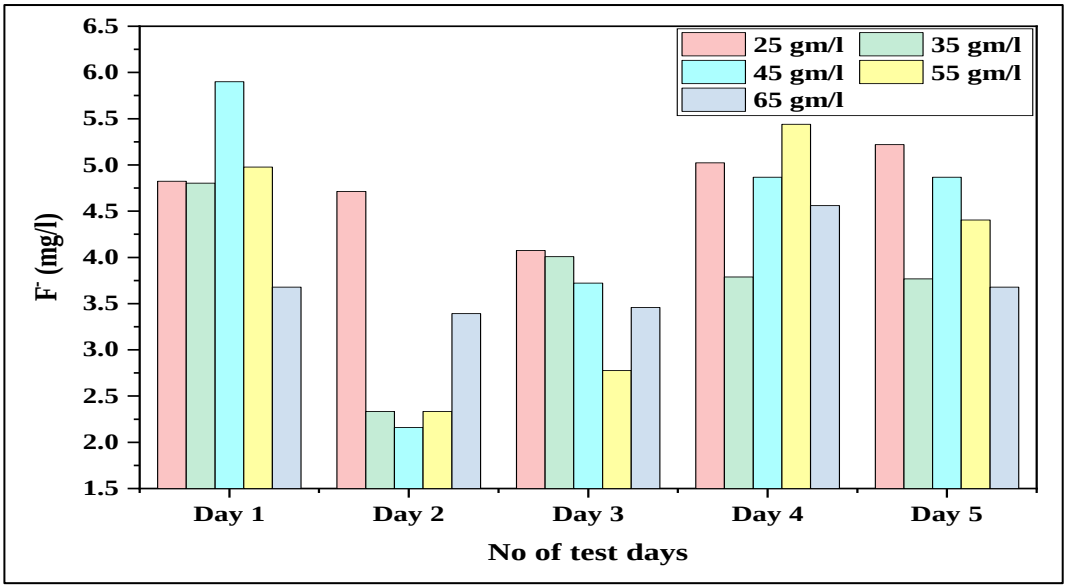

(c)

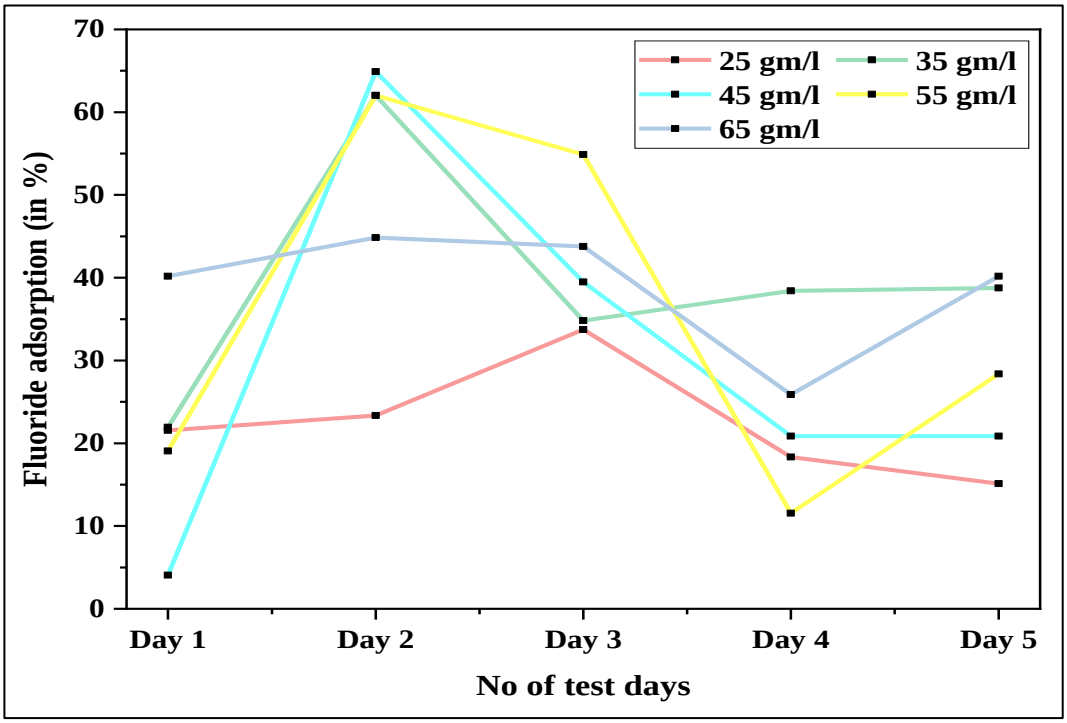

(d)

Figure A4: Observed water quality observed over the test days a) pH, b) TDS, and c) F^-, d) F^- adsorption

The sugarcane filters in the form of pellets did not generate noticeable results, as observed in Figure A4 c, possibly due to the less surface area available for the adsorption of F^-.

In the subsequent phase, neem and sugarcane pellets were also tested with an initial pH = 8.53, TDS = 785 mg/l, and F^- concentration = 3.7 mg/l; the results are represented in Figure A5. Therefore, a plate filter was selected for further study.

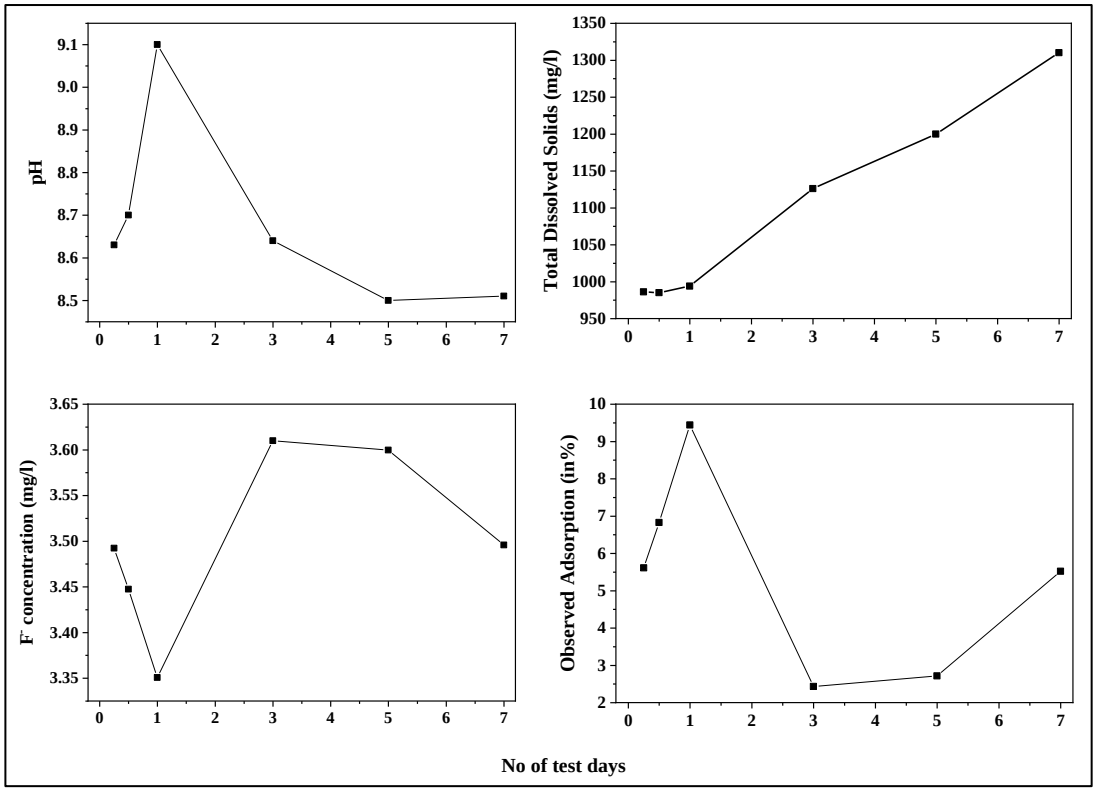

Figure A5: Observed parameters for the neem pellet

Experimental set-up for sludge disposal study

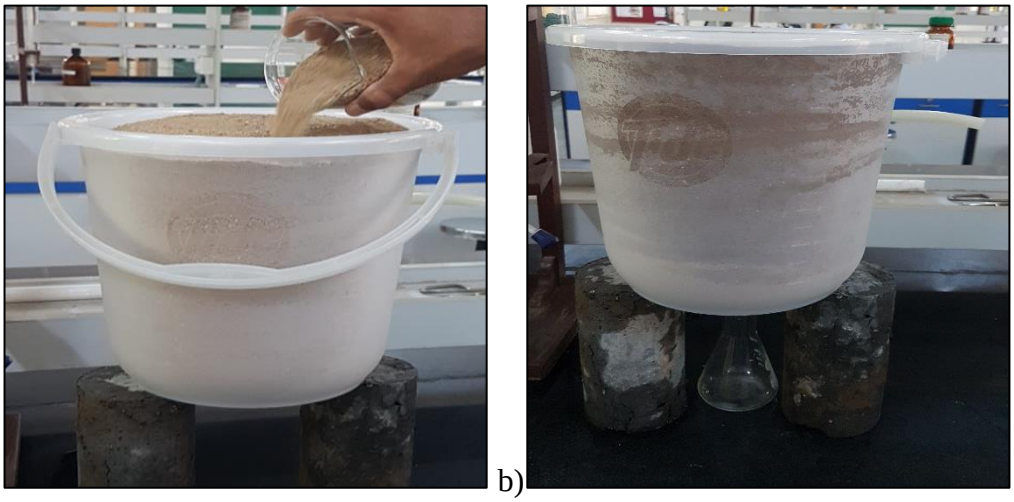

Figure A6: a) Filling of the bucket with sand; b) Fully saturated sand during experimentation

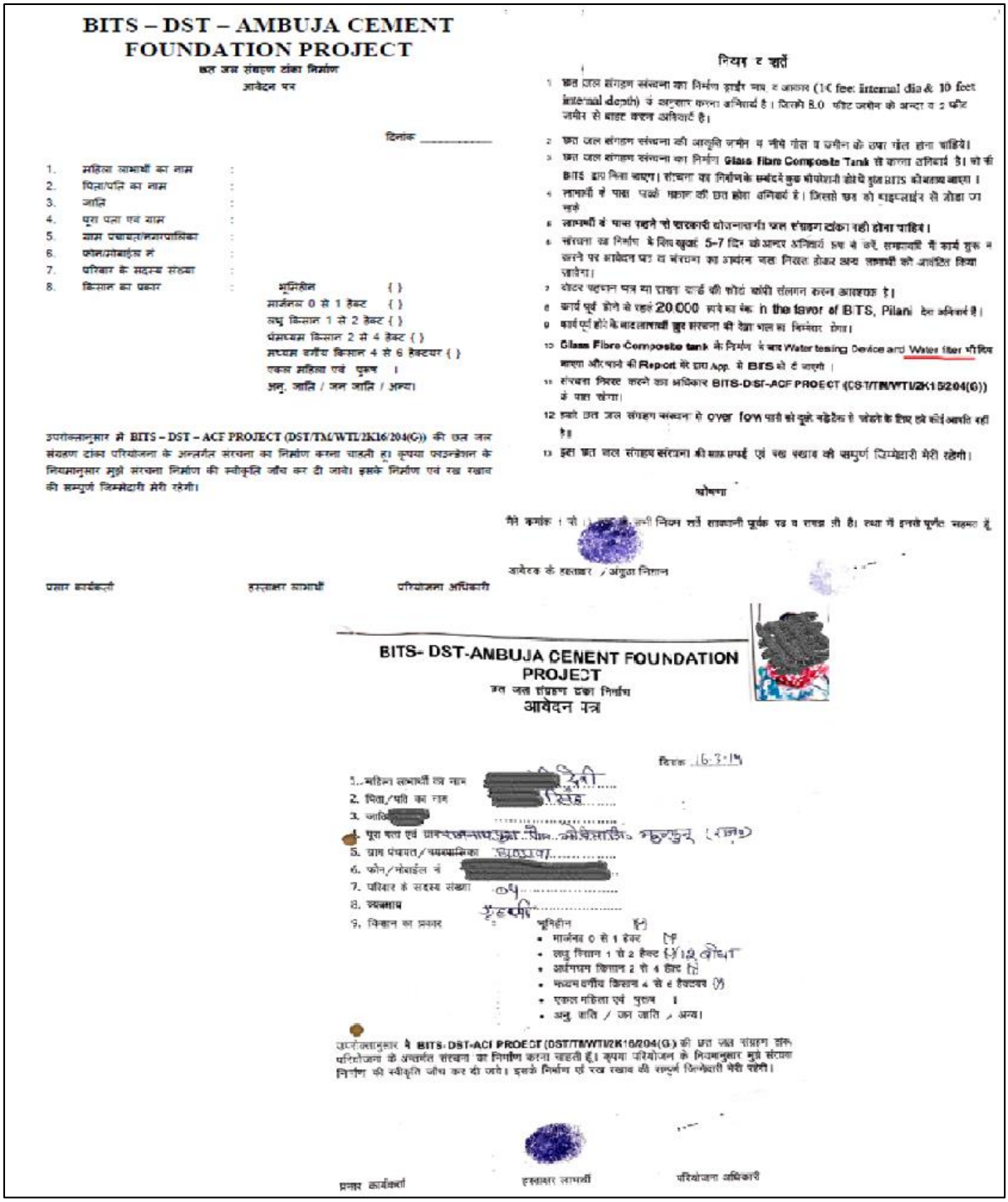

BITS – DST – AMBUJA CEMENT FOUNDATION PROJECT

छत जल संग्रहण टांका निर्माण

आवेदन पत्र

दिनांक _____

1. महिला लाभार्थी का नाम :
2. पिता/पति का नाम :
3. जाति :
4. पूरा पता एवं ग्राम :
5. ग्राम पंचायत/नगरपालिका :
6. फोन/मोबाईल नं :
7. परिवार के सदस्य संख्या :
8. किसान का प्रकार :

भूमिहीन { }
मार्जनल 0 से 1 हेक्टर { }
लघु किसान 1 से 2 हेक्टर { }
अर्धमध्यम किसान 2 से 4 हेक्टर { }
मध्यम वर्गीय किसान 4 से 6 हेक्टयर { }
एकल महिला एवं पुरुष ।
अनु. जाति / जन जाति / अन्य।

उपरोक्तानुसार मैं BITS – DST – ACF PROJECT (DST/TM/WTI/2K16/204(G)) की छत जल संग्रहण टांका परियोजना के अन्तर्गत संरचना का निर्माण करना चाहती हूं। कृपया फाउन्डेशन के नियमानुसार मुझे संरचना निर्माण की स्वीकृति जाँच कर दी जावे। इसके निर्माण एवं रख रखाव की सम्पूर्ण जिम्मेदारी मेरी रहेगी।

प्रसार कार्यकर्ता हस्ताक्षर लाभार्थी परियोजना अधिकारी

नियम व शर्तें

1. छत जल संग्रहण संरचना का निर्माण डाईं मात्र ए आकार (10 feet internal dia & 10 feet internal depth) के अनुसार करना अनिवार्य है। जिसमें 8.0 फीट जमीन के अन्दर व 2 फीट जमीन से बाहर रहना अनिवार्य है।
2. छत जल संग्रहण संरचना की आकृति जमीन व नीचे गोल व जमीन के ऊपर चौकोर होना चाहिये।
3. छत जल संग्रहण संरचना का निर्माण **Glass Fibre Composite Tank** से करना अनिवार्य है। जो की BITS द्वारा किया जाएगा। सीमेन्ट का निर्माण के स्थान पर कुछ सीमेन्टी होगा पूरा BITS को बताना होगा।
4. लाभार्थी के पास पक्की मकान की छत होना अनिवार्य है। जिससे छत को पाइपलाईन से जोड़ा जा सके
5. **लाभार्थी के पास रहने की सरकारी योजनान्तर्गत जल संग्रहण टांका नहीं होना चाहिये।**
6. संरचना के निर्माण के लिये खुदाई 5-7 दिन के अन्दर अनिवार्य रूप से करें, समयावधि में कार्य शुरू न करने पर आवेदन पत्र व संरचना का आवंटन स्वतः निरस्त होकर अन्य लाभार्थी को आवंटित किया जावेगा।
7. फोटो पहचान पत्र या राशन कार्ड की फोटो कॉपी संलग्न करना आवश्यक है।
8. कार्य पूर्व होने से पहले 20,000 रुपये का चेक in the favor of BITS, Pilani देना अनिवार्य है।
9. कार्य पूर्ण होने के बाद लाभार्थी छत संरचना की देखा भाल का जिम्मेवार होगा।
10. **Glass Fibre Composite tank** के निर्माण के बाद Water testing Device and Water filter मशीन लगाना और पानी की **Report** मेरे द्वारा App. से **BITS** को दे जाएगी।
11. संरचना निरक्षण करने का अधिकार **BITS-DST-ACF PROECT (DST/TM/WTI/2K15/204(G))** के पास रहेगा।
12. इसी छत जल संग्रहण संरचना से **OVER FOW** पानी को दूसरे गड्ढे/टैंक से जोड़ने के लिए हमें कोई आपत्ति नहीं है।
13. इस छत जल संग्रहण संरचना की साफ सफाई एवं रख रखाव की सम्पूर्ण जिम्मेदारी मेरी रहेगी।

घोषणा

मैंने क्रमांक 1 से [redacted] सभी नियम शर्तें सावधानी पूर्वक पढ़ व समझ ली है। तथा मैं इनसे पूर्णतः सहमत हूं

आवेदक के हस्ताक्षर / अंगूठा निशान

BITS- DST-AMBUJA CEMENT FOUNDATION PROJECT

छत जल संग्रहण टांका निर्माण

आवेदन पत्र

दिनांक 16-3-19

1. महिला लाभार्थी का नाम [redacted]
2. पिता/पति का नाम [redacted]
3. जाति [redacted]
4. पूरा पता एवं ग्राम [redacted]
5. ग्राम पंचायत/नगरपालिका [redacted]
6. फोन/मोबाईल नं [redacted]
7. परिवार के सदस्य संख्या 04
8. व्यवसाय [redacted]
9. किसान का प्रकार

भूमिहीन ( )
- मार्जनल 0 से 1 हेक्टर ( )
- लघु किसान 1 से 2 हेक्टर ( )
- अर्धमध्यम किसान 2 से 4 हेक्टर ( )
- मध्यम वर्गीय किसान 4 से 6 हेक्टयर ( )
- एकल महिला एवं पुरुष ।
- अनु. जाति / जन जाति / अन्य।

उपरोक्तानुसार मैं BITS-DST-ACF PROECT (DST/TM/WTI/2K16/204(G)) की छत जल संग्रहण टांका परियोजना के अन्तर्गत संरचना का निर्माण करना चाहती हूं। कृपया परियोजना के नियमानुसार मुझे संरचना निर्माण की स्वीकृति जाँच कर दी जावे। इसके निर्माण एवं रख रखाव की सम्पूर्ण जिम्मेदारी मेरी रहेगी।

प्रसार कार्यकर्ता हस्ताक्षर लाभार्थी परियोजना अधिकारी

Figure A7: Survey forms for permission and rules and conditions for implementing the study on the field and survey forms distributed in participating villages to collect basic details of the stakeholders (face, names, and contact numbers have been obscured to maintain anonymity)

Figure A8: Filter distribution in Dheendwa Aguna, Jeeni, Kidwana, and Ramnath Pura

BRIEF BIOGRAPHY OF THE CANDIDATE

Ms. Soumya Kar is a Research Scholar in the Department of Civil Engineering, Birla Institute of Technology and Science, Pilani, Rajasthan, India. She received her Bachelor's degree in Civil Engineering from Kalinga Institute of Industrial Technology, Bhubaneswar, Odisha, India, in 2014. She received her Master's in Infrastructure Engineering and Management from the Birla Institute of Technology and Science in 2016. She was involved as a Junior Research Fellow in the Department of Science and Technology (DST), India funded project titled "Conjunctive use of Rainwater and Groundwater to provide safe drinking water with the intervention of Advanced Technology" during her Ph.D. tenure in BITS Pilani.

BRIEF BIOGRAPHY OF THE SUPERVISOR

Prof. Rajiv Gupta is currently a Senior Professor in the Department of Civil Engineering at Birla Institute of Technology and Science, Pilani, Rajasthan, India, with more than 35 years of teaching experience. He has been involved in active research for the last 30 years and has published around 70 papers in refereed journals and 120 conference papers and reviewed around 160 papers for reputed journals. He has executed and is executing sponsored projects worth more than Rs. 1000 lacs and guided and is guiding 16 Doctoral candidates, 30 dissertations/M.E. projects, and 150 undergraduate students. He has authored and co-authored 3 books and other lecture materials. He won grant funding of $1,96,000 at the Global Development Marketplace organized by World Bank in Washington in 2006. He has been actively involved in Water management systems in rural areas for the last 10 years, appreciated by all, mainly villagers and Rajasthan Government. He has more than 15 years of experience in institutional development and decision-making. He worked as a Deans (ESD, EHD), Assistant Unit Chief (Maintenance), and Group Leader of various groups in BITS Pilani. He was involved in construction work for more than 250 crores, implemented rainwater harvesting and green architecture, and campus development of BITS Pilani.